

"Jaszowiec 2021"

49th International School & Conference on the Physics of Semiconductors



1-10 September 2021, Online only

www.jaszowiec.edu.pl

Organized by:

Institute of Physics, Polish Academy of Sciences

Faculty of Physics, University of Warsaw, Institutes of Experimental and Theoretical Physics

Institute of High Pressure Physics, Polish Academy of Sciences

Divisions of Experimental and Theoretical Physics, Wrocław University of Science and Technology

Institute of Microelectronics and Photonics, Łukasiewicz Research Network

Polish Academy of Sciences



Program committee

Johannes Binder - ***Chair of the Tutorial Session***

Piotr Bogusławski

Michał Borysiewicz

Andrzej Golnik

Grzegorz Grabecki

Joanna Jadczak

Maria Kamińska

Bogdan Kowalski

Stanisław Krukowski

Ewa Płaczek-Popko

Hanka Przybylińska

Czesław Skierbiszewski - ***Chairman***

Tomasz Story

Jan Suffczyński

Henryk Turski - ***Secretary***

Jakub Tworzydło

Piotr Wojnar

Agnieszka Wołoś

Arkadiusz Wójs

Advisory committee

Günther Bauer, *Linz*

Laurence Eaves, *Nottingham*

Jonathan Finley, *Munich*

Jacek K. Furdyna, *Notre Dame*

David Gershoni, *Haifa*

Paweł Hawrylak, *Ottawa*

Hideo Ohno, *Sendai*

Marek Potemski, *Grenoble*

Maurice S. Skolnick, *Sheffield*

Luis Vina, *Madrid*

Dmitri Yakovlev, *Dortmund*

Organizing committee

Anna Reszka - ***Organizing Committee Chair***

Zbigniew Adamus

Johannes Binder

Czesław Skierbiszewski

Piotr Sybilski

Jacek Szczepkowski

Henryk Turski

Sponsoring organizations:

- Polish Academy of Sciences
- US Army Combat Capabilities Development Command



Sponsoring companies:

- Dr. Eberl MBE Komponenten
- EDVAC
- LabSoft
- Nextnano



EDVAC

TECHNIKA PRÓŻNIOWA



LABSOFT®

nextnano
Software for semiconductor nanodevices

INTRODUCTION

The 49th International School and Conference on the Physics of Semiconductors “Jaszowiec 2021” is held online for the first time. The Conference follows a nearly half century long tradition of gathering members of the semiconductor community from all over the world to present their recent achievements, to be inspired by new ideas, and to find the answers to relevant scientific questions.

The intention of the Organizers is to cover important topics in semiconductor physics. However, given the present width of the field, this mission is difficult. The Conference mainly covers the following areas: growth and characterization of structures and devices, topological insulators, quantum computing, graphene and other two-dimensional systems. As always, an important theme is also applications, and several lectures outside of these main themes will be presented as well. Selected papers will be published in Acta Physica Polonica A. The Conference is traditionally preceded by the School, i.e., a three-day tutorial session which targets primarily undergraduate and postgraduate students, during which five outstanding teachers and scientists introduce some of the hot topics relevant to modern semiconductor physics. Together with all School lecturers also its Chairman – Johannes Binder, truly deserves our special acknowledgment.

It is a privilege and pleasure to thank the members of the Program and Advisory Committees who took the responsibility of shaping the scientific program of Jaszowiec 2021. I also wish to acknowledge the tremendous effort put forward by the Organizing Committee: Secretary of the Conference – Henryk Turski, as well as Anna Reszka, Zbigniew Adamus, Piotr Sybilski and Jacek Szczepkowski, who made this conference possible. Finally, I wish to express my deepest gratitude to the organizing institutions and our local and overseas sponsors for the crucial financial support of Jaszowiec 2021.



Czesław Skierbiszewski

Conference Chairman



- Versatile MBE system for R&D
- Applications: III-V, II-VI or oxide semiconductors, topological insulators
- Up to 10 source ports
- Wide range of source options
- Horizontal substrates up to 3"
- Adaptable UHV pumping system, base pressure $< 5 \times 10^{-11}$ mbar
- Variety of in-situ monitoring tools

EDVAC

TECHNIKA PRÓŻNIOWA



Laboratoryjne pompy próżniowe



turbomolekularne



bezelejowe „scroll”



jonowe



rotacyjne olejowe



oleje, filtry, czujniki, zawory, przyłącza próżniowe

SERWIS - DYSRITYBUCJA

www.edvac.pl

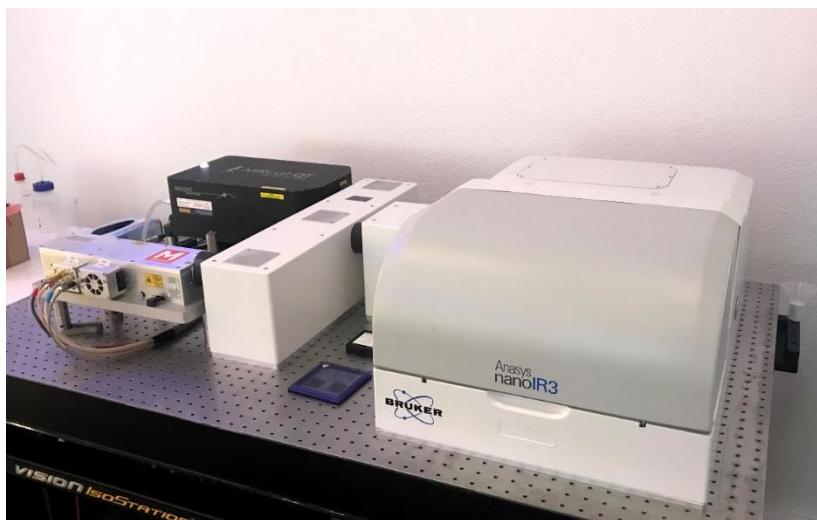
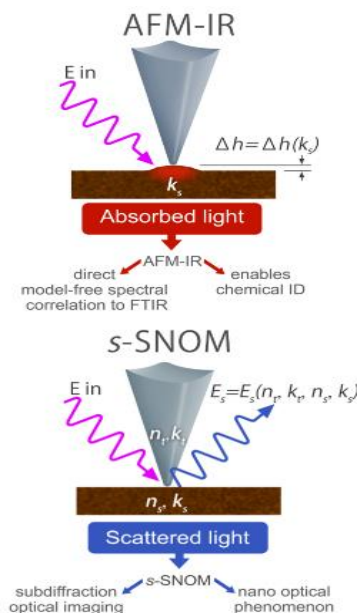
EDVAC Sp. z o.o.

ul. Lotnicza 27, 05-090 Raszyn

tel.: 22 490 41 81, e-mail: biuro@edvac.pl

Firma **LABSOFT** jest wieloletnim, uznanym dostawcą urządzeń badawczych, aparatury pomiarowej i technologicznej renomowanych producentów, w tym Brukera oraz Thermo Fisher Scientific. Oferowane przez nas urządzenia takiej jak mikroskopy sił atomowych, mikroskopy elektronowe, elipsometry, znajdują zastosowanie w ogólnie pojętej nanotechnologii, inżynierii materiałowej, naukach fizycznych czy chemicznych.

Najnowszy system Brukera **nanoIR3-s** to jedyny na świecie układ obrazowania umożliwiający zastosowanie skaningowej mikroskopii optycznej pola bliskiego **s-SNOM** oraz zjawiska fototermalnie indukowanego rezonansu **AFM-IR** na jednej platformie badawczej. Technika AFM-IR łączy mikroskopię sił atomowych oraz spektroskopię w podczerwieni z transformacją Fouriera FTIR. Takie połączenie pozwala osiągnąć rozdzielczość przestrzenną obrazowania mikroskopowego w podczerwieni w skali nano, nawet do wartości **8 nm**.

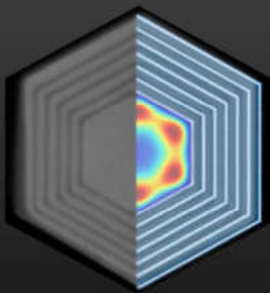
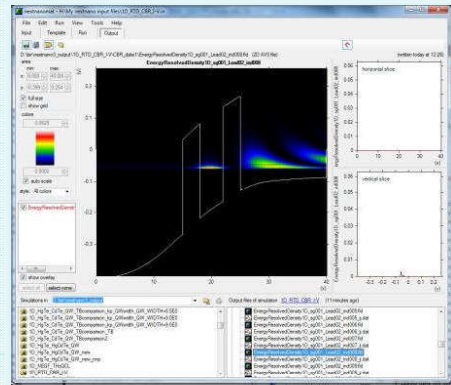


Zastosowania obrazowania nanoIR oraz s-SNOM:

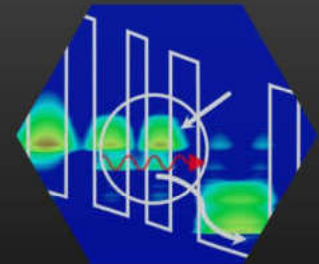
- Nano-technologie, np. nano-włókna i nano-rurki, nano-kompozyty, monowarstwy
- Perowskity i fotowoltaika
- Techniki półprzewodnikowe
- Polimery/kopolimery/biopolimery

Software for the simulation of electronic and optoelectronic semiconductor nanodevices

- Quantum Cascade Lasers, RTDs
- LEDs, μ -LEDs
- Semiconductor Laser Diodes, VCSELs
- Nanotransistors, HEMTs
- Photodetectors, Solar Cells
- Nanowires, Quantum Dots
- Quantum Computing: Qubits
- Biosensors



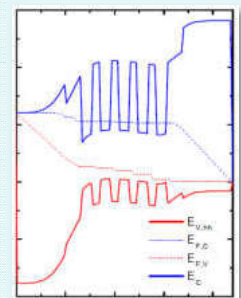
```
# AlGaAs Shell
region{
  hexagon{
    center{ x = 0.0
    corner{ x = $barrier
  }
  ternary_constant{
    name = "Al(x)Ga(
    alloy_x = 0.15
  }
}
```



- Schrödinger-Poisson-Current solver in 1D, 2D & 3D
- Effective-mass, 8-band k·p, Quantum transport (NEGF)
- Strain, Piezo- & Pyroelectricity
- Materials: Group IV, III-V, II-VI (Zinc blende & Wurtzite)

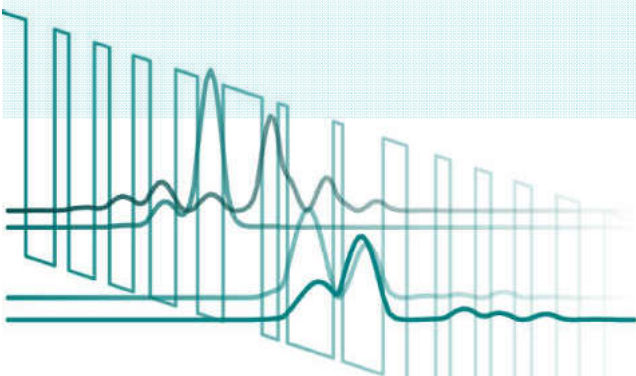
Try our new Python package: github.com/nextnanopy

Download trial version: www.nextnano.com/download



nextnano GmbH – Munich – Germany
Dr. Stefan Birner, stefan.birner@nextnano.com

nextnano Lab SAS – Grenoble – France
Dr. Thomas Grange, thomas.grange@nextnano.com



Program of the 49th International School & Conference on the Physics of Semiconductors
1 - 10 September 2021

School - Special Tutorial Session

Wednesday, 1 September 2021

12:45 - 13:00 Johannes Binder – *Opening*

13:00 - 14:30 Philip Moll (EPFL Lausanne, Switzerland)
Focused Ion Beam fabrication of crystalline devices: from topology to correlations
– **S1**

Thursday, 2 September 2021

13:00 - 14:30 Michał Zieliński (Nicolaus Copernicus University, Toruń, Poland)
Atomistic and Phenomenological Models of Quantum Dots and Quantum Dot
Molecules – **S2**

Break

15:00 - 16:30 Gregory Fuchs (Cornell University, USA)
Defect Centers in Hexagonal Boron Nitride: Optical, Spin Properties and
Applications – **S3**

Friday, 3 September 2021

9:00 - 10:30 Alberto Morpurgo (University of Geneva, Switzerland)
Ionic gating of 2D materials – **S4**

Break

15:00 - 16:30: Alexandre Blais (Université de Sherbrooke, Canada)
Towards Quantum Information Processing with Superconducting Circuits – **S5**

16:30 - 16:45 Johannes Binder – *Closing*

Conference

Monday, 6 September 2021

8:45 - 9:00 **Czesław Skierbiszewski** – *Opening*

Chair: Piotr Kossacki

9:00 - 9:45 **Takashi Taniguchi** (National Institute for Materials Science (NIMS), Tsukuba, Japan)
Single Crystalline Hexagonal Boron Nitride for 2D Opto-Electric Devices – **MoI1**

9:45 - 10:00 **K. Ludwiczak**, A.K. Dąbrowska, J. Binder, M. Tokarczyk, J. Iwański, G. Kowalski, R. Bożek, R. Stępniewski, W. Pacuski, A. Wysmołek
Optical properties of MoSe₂ layers grown on 2" h-BN templates - a combined MBE/MOVPE approach – **MoO1**

10:00 - 10:15 **W. Pacuski**, M. Grzeszczyk, K. Nogajewski, A. Bogucki, K. Oreszczuk, A. Rodek, K.E. Połczyńska, B. Seredyński, R. Bożek, S. Kret, T. Taniguchi, K. Watanabe, J. Sadowski, T. Kazimierzczuk, M. Potemski, P. Kossacki
Narrow excitonic lines and large-scale homogeneity of transition metal dichalcogenide monolayers grown by MBE on hBN – **MoO2**

10:15 - 10:30 **P. Tatarczak**, A.K. Dąbrowska, J. Iwański, J. Binder, G. Kowalski, M. Tokarczyk, R. Stępniewski, A. Wysmołek
Raman spectroscopy of epitaxial h-BN layers grown by MOVPE – role of anharmonic processes and interaction with the substrate – **MoO3**

10:30 - 11:00 **Coffee Break**

Chair: Michał Borysiewicz

11:00 - 11:45 **Elvira Fortunato** (Universidade Nova de Lisboa, Portugal)
E. Fortunato, E. Carlos, R. Branquinho, P. Barquinha, R. Martins
Transparent electronics based on oxide transistors – **MoI2**

11:45 - 12:00 **J. Kierdaszuk**, E. Rozbiegała, K. Piętaś, S. Złotnik, A. Przewłoka, A. Krajewska, W. Kaszub, M. Gryglas-Borysiewicz, A. Wysmołek, J. Binder, A. Drabińska
Highly effective gating of graphene on GaN – **MoO4**

12:00 - 12:15 **J. Rogoża**, J. Binder, L. Tkachenko, I. Pasternak, J. Sitek, W. Strupiński, M. Zdrojek, J. Baranowski, R. Stępniewski, A. Wysmołek
Selective local etching of germanium via photocorrosion and creation of graphene micro-membranes – **MoO5**

12:15 - 12:30 **A. Opala**, R. Panico, D. Ballarini, D. Sanvitto, M. Matuszewski
Feed-forward exciton-polariton neural network – **MoO6**

12:30 - 14:00 Lunch Break

14:00 – 16:00 MONDAY POSTER SESSIONS

Chair: Jerzy Łusakowski

- 16:00 – 16:45** Zbigniew Wasilewski (University of Waterloo, Canada)
Towards room temperature, compact sources of coherent terahertz radiation
– **MoI3**
- 16:45 - 17:00** **J.A. Delgado-Notario**, V. Clericò, J. Salvador-Sánchez, J.E. Velázquez-Pérez, J. Calvo-Gallego, E. Diez, T. Taniguchi, K. Watanabe, T. Otsuji, Y.M. Meziani, W. Knap
Enhancement of THz detection by using an Asymmetric-Dual-Grating-Gate Graphene FET – **MoO7**
- 17:00 - 17:15** **M. Dub**, P. Sai, D. But, M. Sakowicz, A. Przewłoka, A. Krajewska, P. Prystawko, I. Pasternak, M. Haras, G. Cywiński, W. Knap, S. Rumyantsev
Graphene/AlGaIn/GaN FETs for sub-THz detection – **MoO8**
- 17:15 – 17:30** **J. Sadowski**, P. Dziawa, W. Zajkowska, S. Dad, B. Seredynski, W. Pacuski, S. Kret
Hybrid Nanowires Comprising III-V Semiconductor Cores and Narrow Bandgap IV-VI Semiconductor Shells – **MoO9**

Tuesday, 7 September 2021

Chair: *Agata Kamińska*

- 9:00 - 9:45** **F. Tuomisto** (University of Helsinki, Finland)
Point Defect Related Phenomena in Semiconductors with Low Symmetry:
Examples of β -Ga₂O₃, Nitride Alloys, and Nitride Devices – **Tu11**
- 9:45 - 10:00** **E. Przezdziecka**, A. Wierzbička, P. Dłuzewski, A. Lysak, P. Sybilski, I. Sankowska, P. Strak, K. Morawiec, R. Jakiela, M.A. Pietrzyk, A. Kozanecki
CdO/MgO cubic superlattices grown by MBE on sapphire – **Tu01**
- 10:00 - 10:15** V. Yurgens, J.A. Zuber, S. Flågan, M. de Luca, B. Shields, I. Zardo, P. Maletinsky, R.J. Warburton, **T. Jakubczyk**
Low charge-noise nitrogen-vacancy centers in diamond created using laser writing with a solid-immersion lens – **Tu02**

10:15 - 10:45 Coffee Break

Chair: *Andrzej Golnik*

- 10:45 - 11:30** **Thorsten Deilmann** (Universitaet Münster, Germany)
Monolayer Transition Metal Dichalcogenides in Magnetic Fields – **Tu12**
- 11:30 - 11:45** **M. Goryca**, J. Li, A.V. Stier, T. Taniguchi, K. Watanabe, E. Courtade, S. Shree, C. Robert, B. Urbaszek, X. Marie, S.A. Crooker
Revealing exciton masses and dielectric properties of monolayer semiconductors with high magnetic fields – **Tu03**
- 11:45 - 12:00** **M. Szotła**, D. Yavorskiy, Y. Ivonyak, M. Haras, J. Przybytek, I. Yahniuk, D.B. But, N.N. Mikhailov, S. Dvoretzky, G. Cywiński, J. Łusakowski, F. Teppe, S.S. Krishtopenko, W. Knap
Magnetospectroscopy of Kane Electrons in HgCdTe Alloys – **Tu04**
- 12:00 - 12:15** **A. Łusakowski**, P. Bogusławski, T. Story
Mn-driven Weyl semimetal phase of PbSnMnTe – **Tu05**

12:15 - 13:45 Lunch Break

13:45 – 15:45 TUESDAY POSTER SESSIONS

Chair: *Jan Suffczyński*

- 15:45 – 16:30** **Hui Deng** (University of Michigan, USA)
Excitons and Polaritons in van der Waals Hetero-bilayers – **Tu13**
- 16:30 – 16:45** **M. Furman**, R. Mirek, A. Opala, K. Tyszka, M. Król, P. Stawicki, B. Seredyński, W. Pacuski, J. Suffczyński, M. Matuszewski, J. Szczytko, B. Piętko

Time-delayed nonlinear phenomena in exciton-polariton condensate – **TuO6**

16:45 - 17:00 **R. Mirek**, A. Opala, P. Comaron, M. Furman, M. Król, K. Tyszka, B. Seredyński,
D. Ballarini, D. Sanvitto, T.C. Liew, W. Pacuski, J. Suffczyński, J. Szczytko, M.
Matuszewski, B. Piętka

Neuromorphic binarized polariton networks – **TuO7**

17:00 - 17:15 **D. Biegańska**, M. Pieczarka, H. Suchomel, C. Schneider, S. Klemmt, S. Höfling,
M. Sypererek
Condensation and ballistic propagation of exciton polaritons in AlGaAs microcavity
at high temperatures – **TuO8**

Wednesday, 8 September 2021

Chair: Tomasz Story

- 9:00 - 9:45** **Lukasz Plucinski** (Peter Grünberg Institut, Forschungszentrum Jülich, Germany)
Band Structure Engineering in 3D Topological Insulators – **We1**
- 9:45 - 10:00** **K.M. Fijalkowski**, M. Hartl, M. Winnerlein, P. Mandal, N. Liu, S. Schreyeck,
K. Brunner, C. Gould, L.W. Molenkamp
Coexistence of Surface and Bulk Ferromagnetism in a Topological Insulator
– **We01**
- 10:00 - 10:15** **A. Kazakov**, W. Brzezicki, T. Hyart, B. Turowski, J. Polaczynski, Z. Adamus,
M. Aleszkiewicz, T. Wojciechowski, J. Domagala, A. Varykhalov, G. Springholz,
T. Wojtowicz, V.V. Volobuev, T. Dietl
Dephasing by Mirror-Symmetry Breaking with Resulting Magnetoresistance across
the Topological Transition in Pb_{1-x}Sn_xSe – **We02**
- 10:15 - 10:30** **R. Rechciński**, M. Galicka, M. Simma, V.V. Volobuev, O. Caha, J. Sánchez-Barriga,
P.S. Mandal, E. Golias, A. Varykhalov, O. Rader, G. Bauer, P. Kacman, R. Buczko,
G. Springholz
Rashba Effect in Topological PbSnSe/PbEuSe Quantum Wells – **We03**

10:30 – 11:00 Coffee Break

Chair: Bogdan Kowalski

- 11:00 - 11:45** **Jacek Szczytko** (University of Warsaw, Poland)
Synthetic Hamiltonians in optical cavities: "solid-state physics" of "massive
photons with spin" – **We12**
- 11:45 - 12:00** **K. Rechcińska**, M. Król, P. Oliwa, R. Mazur, P. Morawiak, P. Kula, W. Piecek, P.G.
Lagoudakis, W. Bardyszewski, M. Matuszewski, B. Piętko, J. Szczytko
Optical persistent spin helix phenomenon in liquid crystal microcavities – **We04**
- 12:00 - 12:15** **K. Łempicka**, M. Król, A. Wincukiewicz, P. Morawiak, R. Mazur, W. Piecek, P. Kula,
T. Stefaniuk, M. Kamińska, L.De. Marco, D. Ballarini, D. Sanvitto, M. Matuszewski,
J. Szczytko, B. Piętko
Light-matter interaction in birefringent microcavity with two-dimensional hybrid
perovskite at room temperature – **We05**
- 12:15 - 12:30** **M. Pieczarka**, E. Estrecho, S. Ghosh, M. Wurdack, M. Steger, D.W. Snoke, K. West,
L.N. Pfeiffer, T. Liew, A.G. Truscott, E.A. Ostrovskaya
Topological phase transition in an all-optical exciton-polariton Su-Schrieffer-
Heeger lattice – **We06**

12:30 - 14:00 Lunch Break

14:00 - 16:00 WEDNESDAY POSTER SESSIONS

Chair: Maria Kamińska

- 16:00 - 16:45** Jacek Jasinski (University of Louisville, USA)
Fabrication, Characterization and Property Tuning of Phosphorene, Chromium Trihalides and Related 2D Materials – **WeI3**
- 16:45 - 17:00** **N. Zawadzka**, Ł. Kipczak, T. Woźniak, M. Grzeszczyk, A. Babiński, M.R. Molas
Highly anisotropic optical response of GeS – **WeO7**
- 17:00 - 17:15** **T. Hahn**, A. Rodek, J. Kasprzak, T. Kazimierczuk, K. Nogajewski, K. Polczyńska, K. Watanabe, T. Taniguchi, M. Potemski, P. Kossacki, T. Kuhn, P. Machnikowski, D. Wigger
Influence of the local field effect on nonlinear spectroscopy signals from 2D semiconductors – **WeO8**
- 17:15 - 17:30** **A. Rodek**, K. Oreszczuk, T. Kazimierczuk, J. Howarth, T. Taniguchi, K. Watanabe, M. Potemski, P. Kossacki
Exciton-exciton interactions in MoSe₂ probed by nonlinear spectroscopy in charge-tunable device – **WeO9**

Thursday, 9 September 2021

Chair: Tomasz Dietl

- 9:00 - 9:45** **Karel Vyborný** (FZU - Institute of Physics, ASCR, Czech Republic)
Two examples of Mn-based antiferromagnetic semiconductors – **Th11**
- 9:45 - 10:00** **K. Gas**, A. Królicka, S. Kret, K. Dybko, T. Story, M. Sawicki
Magnetic Constitution of Thermoelectric PbTe:Cr – **Th01**
- 10:00 - 10:15** **M. Birowska**, P.E. Faria Junior, J. Fabian, J. Kunstmann
Large exciton binding energies in vdW layered magnet MnPS3 and related systems – **Th02**

10:15 – 10:45 Coffee Break

Chair: Stanisław Krukowski

- 10:45 - 11:30** **Nicolas Grandjean** (École polytechnique fédérale de Lausanne, Switzerland)
Efficiency of blue LEDs: impact of Point defects and GaN growth temperature – **Th12**
- 11:30 - 11:45** **A. Kafar**, A. Sakaki, R. Ishii, S. Stanczyk, K. Gibasiewicz, Y. Matsuda, D. Schiavon, S. Grzanka, T. Suski, P. Perlin, M. Funato, Y. Kawakami
Influence of substrate misorientation on emission and waveguiding properties of blue (In,Al,Ga)N laser-like structure studied by synchrotron radiation microbeam X-ray diffraction – **Th03**
- 11:45 - 12:00** **M. Chlipala**, H. Turski, M. Siekacz, G. Muziol, K. Nowakowski-Szkudlarek, A. Feduniewicz-Żmuda, C. Skierbiszewski
Toward single photon emitters – new concepts in nitride optoelectronic devices – **Th04**
- 12:00 - 12:15** **L. van Deurzen**, R. Page, K. Nomoto, J. Encomendero, M. Gong, H.G. Xing, D. Jena
Towards Deep-UV Laser Diodes by MBE – **Th05**

12:15 - 13:30 Lunch Break

13:30 - 15:30 THURSDAY POSTER SESSIONS

Chair: Krzysztof Korona

- 15:30 - 16:15** **Agata Kaminska** (Cardinal Stefan Wyszyński University and Institute of Physics of the Polish Academy of Sciences, Warsaw, Poland)
Instantaneous decay rate analysis of time resolved photoluminescence: application to nitride layers and heterostructures – **Th13**
- 16:15 - 16:30** **E. Rogowicz**, J. Kopaczek, J. Kutrowska-Girzycka, M. Myronov, R. Kudrawiec,

M. Syperek

Carrier Dynamics in Thin Germanium-Tin Epilayers: The Issue of Below Bandgap States – **ThO6**

16:30 - 17:15 **Eli Sutter**

Nanoscale Optoelectronics of Layered Crystals, Heterostructures and van der Waals Nanowires – **ThI4**

17:15 - 17:30 **T. Woźniak**, P.E. Faria Junior, G. Seifert, A. Chaves, J. Kunstmann

Exciton g-factors of van der Waals heterostructures from first principles calculations – **ThO7**

Friday, 10 September 2021

Chair: Ewa Popko

- 9:00 - 9:45** **Maciej Molas** (University of Warsaw, Poland)
Excitonic complexes in monolayers of transition metal dichalcogenides – **FrI1**
- 9:45 - 10:00** **M. Bhatnagar**, N. N. Zawadzka, Ł. Kipczak, M. Grzeszczyk, K. Watanabe, T. Taniguchi, A. Babiński, M. Molas
Fine structure of K-excitons in multilayers of MoS₂ and MoSe₂ – **FrO1**
- 10:00 - 10:15** **P. Kapuściński**, A. Delhomme, D. Vaclavkova, A.O. Slobodeniuk, M. Grzeszczyk, M. Bartos, K. Watanabe, T. Taniguchi, C. Faugeras, M. Potemski
Rydberg series of dark excitons and spin-orbit splitting of the conduction band in WSe₂ monolayer – **FrO2**
- 10:15 - 10:30** **L. Bryja**, J. Kutrowska- Girzycka, M. Majak, J. Lubczyński, Ch.H. Ho, J. Jadcak
Upconversion photoluminescence processes in monolayer WSe₂ and MoSe₂ – **FrO3**
- 10:30 - 11:00** **Coffee Break**
- Chair: Adam Babiński*
- 11:00 - 11:15** **P. Holewa**, A. Sakanas, U.M. Gür, P. Mrowiński, A. Musiał, N. Gregersen, E. Semenova, M. Syperek
Bright Quantum Dot Single-Photon Emitters at Telecom Bands Heterogeneously Integrated with Si – **FrO4**
- 11:15 - 11:30** **M.V. Rakhlin**, S.V. Sorokin, D.R. Kazanov, I.V. Sedova, T.V. Shubina, S.V. Ivanov, V.Yu. Mikhailovskii, A.A. Toropov
Bright Single-Photon Emitters with a CdSe Quantum Dot and Multimode Tapered Nanoantenna for the Visible Spectral Range – **FrO5**
- 11:30 - 11:45** **D. Wigger**, M. Weiß, M. Lienhart, M. Nägele, K. Müller, J.J. Finley, T. Kuhn, H.J. Krenner, P. Machnikowski
Controlling the energy and timing of single photons by acoustic modulation of a quantum dot – **FrO6**
- 11:45 - 12:00** N. Srocka, **P. Mrowiński**, J. Grosse, M. von Helversen, M. Schmidt, T. Heindel, S. Rodt, S. Reitzenstein
Deterministically fabricated and tunable quantum dot single-photon source emitting in the telecom O-band – **FrO7**
- 12:00 - 12:15** **K.E. Połczyńska**, T. Kazimierzczuk, P. Kossacki, W. Pacuski
Magneto-optical properties of a single CdTe Quantum Dot with a single ion of Vanadium – **FrO8**

12:15 - 13:45 Lunch Break

Chair: *Jakub Tworzydło*

13:45 - 14:30 **Paweł Kowalczyk** (University of Lodz, Poland)

P.J. Kowalczyk, L. Lutsyk, D.A. Kowalczyk, M. Rogala, P. Dabrowski, P. Krukowski, M. Piskorski, W. Kozłowski, E.M. Lacinska, A. Wyszomolek, R. Stepniewski, J. Binder, R. Udovyt'ska, J. Jung, J. Ulanski, J. Baranowski, S.A. Brown, G. Bian, Z. Klusek
2D materials and their hybrids: pathway toward new phenomena – **FrI2**

14:30 - 14:45 **M. Krajewski**, P. Piotrowski, W. Mech, K.P. Korona, J. Wojtkiewicz, M. Pilch, A. Kaim, A. Drabińska, M. Kamińska
Charge Separation in Blends of Newly Synthesized C60 Fullerene Derivatives and P3HT – **FrO9**

14:45 - 15:00 P. Holewa, P. Wyborski, Ł. Dusanowski, R. Stühler, A. Consiglio, D. Di Sante, W. Hanke, C. Schneider, S. Höfling, R. Claessen, **M. Sypererek**
Optical spectroscopy of excitons in the atomically thin topological insulator Bismuthene – **FrO10**

15:00 - 16:30 **Leonard Sosnowski Prize Ceremony**

Best Poster Award Ceremony

16:30 - 16:45 **Czesław Skierbiszewski** – *Closing*

MONDAY POSTER SESSIONS

14:00-15:00 SHORT PRESENTATIONS (parallel sessions in 4 Zoom Rooms)

15:00-16:00 POSTERS DISCUSSIONS (each poster could be discussed in separate Zoom Room)

MoP1 – Optical emitters

Chair: Michał Szot

- MoP1.1** **R.A. Bogaczewicz**, P. Machnikowski
Resonance Fluorescence of Noisy Systems
- MoP1.2** **I. Bragar**, Ł. Cywiński
Limitations on Maximal Level of Entanglement of Two Singlet-Triplet Qubit States in GaAs Gated Quantum Dots
- MoP1.3** **M. Wasiluk**, M. Mikulicz, A. Musiał, A. Kors, J.P. Reithmaier, G. Sęk, M. Benyoucef
Thermal stability of emission from single symmetric InAs/InP quantum dots emitting in the telecom C-band
- MoP1.4** **A. Zielińska**, A. Musiał, T. Heuser, N. Srocka, D. Quandt, A. Strittmatter, S. Rodt, S. Reitzenstein, G. Sęk
Single-photon emission from InGaAs/GaAs quantum dots in 1.3 μm telecommunication range
- MoP1.5** **P. Baranowski**, P. Wojnar, M. Szymura, J. Płachta, S. Chusnutdinow, G. Karczewski, T. Wojtowicz
Carrier separation effects in type-II Cd(Se,Te)/ZnTe self-assembled QDs
- MoP1.6** A. Łopion, A. Bogucki, **W. Kraśnicki**, K.E. Połczyńska, W. Pacuski, P. Kossacki, A. Golnik
ODMR studies of interfaces of (Cd,Mn)Te/(Cd,Mg)Te QWs
- MoP1.7** **K.E. Połczyńska**, A. Rodek, K. Oreszczuk, Ł. Zinkiewicz, T. Kazimierczuk, Z. Ogorzałek, P. Kossacki, W. Pacuski
Manipulation of the electric state of QDs with single magnetic dopants
- MoP1.8** **M. Burakowski**, P. Holewa, A. Musiał, N. Srocka, D. Quandt, A. Strittmatter, S. Rodt, S. Reitzenstein, G. Sęk
Thermal Stability and Single-Photon Emission from GaAs-based Quantum Dots emitting at 1.3 μm
- MoP1.9** **P. Wyborski**, P.A. Wroński, A. Musiał, P. Podemski, F. Jabeen, S. Höfling, G. Sęk
InAs quantum dots grown on metamorphic buffer layer as single-photon sources at third telecommunication window
- MoP1.10** J. Płachta, **P. Wojnar**, T. Kazimierczuk, P. Kossacki, G. Karczewski, T. Wojtowicz, J. Kossut
Optical emission from ultra-thin CdTe nanowires

MoP2 – Oxides

Chair: Anna Kafar

- MoP2.1** **A. Adhikari**, E. Przewdziecka, S. Mishra, P. Sybilski, J. Sajkowski, E. Guzewicz
Optical Properties of ZnO Deposited by Atomic Layer Deposition on Sapphire:
A Comparison of Thin and Thick Films
- MoP2.2** **M. Stachowicz**, A. Wierzbicka, J.M. Sajkowski, M.A. Pietrzyk, P. Dłuzewski, E. Dynowska,
S. Magalhaes, E. Alves, A. Kozanecki
Structural and excitonic analysis of the ZnO/MgO superlattices on a-polar ZnO substrates
grown by MBE
- MoP2.3** **A. Ciechan**, P. Bogusławski
s,p-d coupling in ZnO doped with 3d transition metal impurities
- MoP2.4** **S. Mishra**, E. Przewdziecka, W. Wozniak, A. Adhikari, R. Jakiela, W. Paszkowicz, A. Sulich,
M. Ożga, K. Kopalko, E. Guzewicz
Structural properties of thin ZnO films grown by ALD under O-rich and Zn-rich growth
conditions and their relationship to electrical parameters
- MoP2.5** **A.V. Chernyadiev**, D.B. But, C. Kołaciński, K. Ikamas, A. Lisauskas
Investigation of the electromagnetic interaction between the vertically coupled
split-ring-based metasurface and antenna
- MoP2.6** **E. Zielony**, A. Wierzbicka, R. Szymon, M.A. Pietrzyk, E. Popko
Investigation of micro-strain in ZnO/CdO and ZnO/ZnCdO multiple quantum well
nanowires grown on Si by PA-MBE
- MoP2.7** **R. Lewandków**
Properties of MgO insulating layers on 6H-SiC and GaN: Photoelectron studies
- MoP2.8** **E. Guzewicz**, O. Volnianska, I.N. Demchenko, P. Zeller, M. Amatti, L. Gregoratti
Local electronic structure of thin p-type ZnO films doped with nitrogen
- MoP2.9** **J. Gosk**, R. Puźniak, A. Lynnyk
Defects and Magnetism in Heavy Ion Implanted Monocrystalline ZnO

MoP3 – Topological effects

Chair: Natalia Olszowska

- MoP3.1** **A. Khaliq**, M. Arciszewska, A. Avdonin, B. Brodowska, V.E. Slynko, E.I. Slynko, L. Kilanski
Magnetic Ordering and Frustration in GeSnMnTe Multiferroic Crystals
- MoP3.2** **S. Prem**, M. Wysokinski, M. Trif
Non-Abelian Berry phases of electrically driven hole-spin qubits in waveguide QED
- MoP3.3** **G. Hussain**, G. Cuono, A. Lau, C. Autieri
Electronic Properties and Structural Stability of thin SnTe and PbTe Nanowires

- MoP3.4** **A.S. Wadge**, G. Grabecki, B.J. Kowalski, C. Autieri, K. Dybko, P. Iwanowski, A. Hruban, A. Łusakowski, R. Diduszko, M. Rosmus, N. Olszowska, J. Kołodziej, A. Wiśniewski
Electron transport and ARPES study on topological semimetal: TaAs₂
- MoP3.5** **W. Wołkanowicz**, M. Szot, J. Polaczyński, K. Karpińska, L. Kowalczyk, P. Dziawa, T. Taliasvili, M. Zięba, R. Minikayev, E. Łusakowska, A. Reszka, K. Dybko, A.M. Witowski, T. Wojtowicz, T. Story
Plasma reflectivity of Pb_{1-x}Sn_xTe/CdTe/GaAs epitaxial layer in the band inversion region
- MoP3.6** **R. Islam**, B. Ghosh, G. Cuono, A. Agarwal, B. Singh, A. Bansil, C. Autieri, T. Dietl
Robust Weyl and nodal line semimetal phases in 3D superlattice of Hg-based chalcogenides: ab initio studies
- MoP3.7** **W.K. Pasek**, M. Kupczyński
Properties of fractal lattices with higher Chern number
- MoP3.8** T. Andrearczyk, J. Sadowski, J. Wróbel, T. Figielski, **T. Wosiński**
Tunable Planar Hall Effect in (Ga,Mn)(Bi,As) Epitaxial Layers

MoP4 – Optical cavities and devices

Chair: Marta Sawicka

- MoP4.1** **I. Perlikowski**, E. Zielony, T. Özdağ, H. Kavak
Electrical and Structural Properties of CZTS-Based Structures for Thin Film Photovoltaic Cells
- MoP4.2** **A. Singh**, Md. K. Shamim, S. Sharma, L. Reissig
Utilizing Ferroelectric Materials to Tune the Performance of Organic Differential Photodetectors
- MoP4.3** **R. Rudniewski**, W. Zaleszczyk, Z. Adamus, D. Śnieżek, P. Ungier, T. Wojciechowski, J. Wróbel, T. Wojtowicz
Quantum constrictions and inner Corbino contacts in Cd_{1-x}Mn_xTe microdevices
- MoP4.4** **A. Wójcicka**, K. Piskorski, A. Taube, M.A. Borysiewicz
Comparison of Ir-Si-O and Ru-Si-O as Schottky barrier electrodes to amorphous In-Ga-Zn-O
- MoP4.5** **P. Oliwa**, W. Bardyszewski, B. Piętka, J. Szczytko
Light modes in microcavity with anisotropic and gyrotropic medium
- MoP4.6** **M. Muszyński**, E. Otón, M. Król, M. Kędziora, P. Morawiak, R. Mazur, P. Kula, W. Piecek, B. Piętka, J. Szczytko
Optical properties of dye-doped monocrystalline free-standing blue phase liquid crystal
- MoP4.7** **S. Piotrowska**, M. Król, K. Rechcińska, P. Oliwa, R. Mazur, P. Morawiak, P. Kula, W. Piecek, B. Piętka, J. Szczytko
The optical tomography of cavity modes in a tunable liquid crystal cavity

- MoP4.8** **D. Biegańska**, M. Pieczarka, E. Estrecho, M. Steger, D.W. Snoke, K. West, L.N. Pfeiffer, M. Syperek, A.G. Truscott, E.A. Ostrovskaya
Direct measurement of the anisotropic elementary excitations in an exciton-polariton condensate in a synthetic gauge field
- MoP4.9** **A. Bohdan**, A. Wincukiewicz, M. Tokarczyk, K.P. Korona, E. Kwiatkowska, M. Skompska, M. Kaminska
Positive Impact of Camphorsulfonic Acid on Perovskite Solar Cell Performance
- MoP4.10** **K. Sawicki**, M. Ściesiek, W. Pacuski, J. Suffczyński
Bose-Einstein condensation of exciton-polaritons triggered by magnetic field in coupled planar microcavities

TUESDAY POSTER SESSIONS

13:45-14:45 SHORT PRESENTATIONS (parallel sessions in 4 Zoom Rooms)

14:45-15:45 POSTERS DISCUSSIONS (each poster could be discussed in separate Zoom Room)

TuP1 – 2D materials

Chair: Marta Gryglas-Borysiewicz

- TuP1.1** **A. Rehman**, A. Krajewska, B. Stonio, S. Smirnov, D.B. But, M. Filipiak, K. Pavlov, J. Smulko, G. Cywinski, D. Lioubtchenko, W. Knap, S. Rumyantsev
Low-Frequency Noise in Carbon Nanotube Networks
- TuP1.2** M. Grzeszczyk, **K. Olkowska-Pucko**, K. Watanabe, T. Taniguchi, P. Kossacki, A. Babiński, M.R. Molas
Carrier density in monolayer MoS₂ govern by hBN encapsulation - unraveling the fine structure of the negative trion
- TuP1.3** **J. Iwański**, P. Tatarczak, M. Tokarczyk, J. Binder, A.K. Dąbrowska, G. Kowalski, R. Stępniewski, A. Wymołek
Characterization of Epitaxial Boron Nitride Layers With Fourier-transform Infrared Spectroscopy
- TuP1.4** **M. Sokołowski**, M. Marchwiany, A.M. Jastrzębska, M. Birowska
Structural search and stability prediction of new MxB_{1-x} phases based on ab initio calculations and Machine Learning Methods
- TuP1.5** **A. Wania Rodrigues**, Y. Saleem, M. Bieniek, P. Hawrylak
Synthetic correlated electron system with twisted bilayer graphene quantum dots
- TuP1.6** **K. Oreszczuk**, A. Rodek, M. Goryca, T. Kazimierczuk, J. Howarth, T. Taniguchi, K. Watanabe, M. Potemski, P. Kossacki
Effective electron g-factors in electrically gated MoSe₂
- TuP1.7** **B. Tronowicz**, J. Kucharek, W. Pacuski
ZnSe as an epitaxial protection of MBE grown MoSe₂/hBN
- TuP1.8** **Ł. Zinkiewicz**, M. Grzeszczyk, J. Sławińska, A. Rodek, K. Watanabe, T. Taniguchi, M. Potemski, C. Skierbiszewski, P. Kossacki
Narrow Excitonic Lines Of Monolayer Transition Metal Dichalcogenides Deposited Directly On AlGa_N Substrate
- TuP1.9** **J. Jastrzębski**, A. Wania Rodrigues, K. Sadecka, J. Pawłowski, M. Bieniek
Effect of intrinsic and Rashba spin-orbit coupling on DOS in twisted bilayer graphene
- TuP1.10** **J. Kołodziejczyk**, J.A. Majewski
Stability and Electronic Structure of Functionalized 2D Molybdenum Nitrides – MXenes

TuP2 – Nitrides

Chair: Eunika Zielony

- TuP2.1** **E.B. Rozbiegała**, K. Piętak, S. Złotnik, J. Gaca, K.P. Korona, J.M. Baranowski
The origin of red light emission in GaN:B alloys
- TuP2.2** **P.A. Drózdź**, V.Yu. Kachorovskii, P. Prystawko, M. Słowikowski, M. Filipiak, D. Yavorski, M. Szoła, W. Knap
Physical structure for observation of inverse Faraday effect enhanced by twisted plasmon modes.
- TuP2.3** **N. Fiuczek**, M. Sawicka, P. Wolny, H. Turski, A. Feduniewicz-Żmuda, K. Nowakowski-Szkudlarek, M. Siekacz, C. Skierbiszewski
Revealing 3D nanoscale inhomogeneities of Si and Ge dopants incorporation into GaN by electrochemical etching
- TuP2.4** S.P. Łepkowski, **A.R. Anwar**
Biaxial Relaxation Coefficient in Group-III Nitride Quantum Wells and Thin Films
- TuP2.5** **Y.K. Edathumkandy**, K. Das, D. Sztenkiel
Comparative study of magnetic properties of Mn³⁺ magnetic clusters in GaN using classical and quantum mechanical approach.
- TuP2.6** **D. Majchrzak**, M. Grodzicki, P.P. Michałowski, K. Moszak, W. Olszewski, D. Hommel
Reduction of Al incorporation into AlGa_N layers grown by molecular beam epitaxy in Ga-droplet regime
- TuP2.7** A. Tkachuk, A. Sukach, **V. Tetyorkin**, O. Porada, A. Kozak, V. Ivaschenko
Band and Defect States in Amorphous SiCN
- TuP2.8** **P. Sai**, K. Stelmaszczyk, M. Sakowicz, M. Filipiak, M. Słowikowski, D.B. But, P. Prystawko, G. Cywiński, S. Rumyantsev, W. Knap
Terahertz spectroscopy of 2D-plasmons in AlGa_N/Ga_N heterostructures
- TuP2.9** E. Zielony, **R. Szymon**, A. Wierzbicka, A. Reszka, W. Perwez, M. Sobanska, Z.R. Zytkeiwicz
Strain and lattice vibration mechanisms in GaN-AlGa_N core-shell nanowires on Si substrate
- TuP2.10** **K. Gas**, P. Wiśniewski, D. Sztenkiel, A. Grochot, M. Iwinska, T. Sochacki, H. Przybylinska, M. Bockowski, M. Sawicki
Magnetization steps in dilute bulk GaN:Mn

TuP3 – Topological effects

Chair: Joanna Jadczak

- TuP3.1** **T. Sobol**, J. Szade
Quantum well states in Bi₂Te₃ upon deposition of ultrathin Fe cap layer

- TuP3.2** **M. Lis**, J. Tworzydło
Berry Curvature Dipol in Monolayers of Transition Metal Dichalcogenides
- TuP3.3** **J. Polaczyński**, A. Kazakov, R. Rudniewski, B. Turowski, Z. Adamus, T. Wojtowicz, V.V. Volobuev
Signature of Chiral Anomaly and Magnetotransport in (001) Strained "Grey" Tin
- TuP3.4** **M. Kupczyński**, B. Jaworowski
An interaction-driven transition between the Wigner crystal and the Fractional Chern insulator in topological bands
- TuP3.5** **B. Turowski**, R. Rudniewski, M. Rosmus, M. Aleszkiewicz, T. Wojciechowski, W. Zaleszczyk, Z. Muhammad, N. Olszowska, T. Wojtowicz, V.V. Volobuev
Growth of Gray Tin epilayers on insulating (001)-CdTe/GaAs substrates and its Angular Resolved Photoemission Spectroscopy studies
- TuP3.6** **J. Sitnicka**, K. Sobczak, P. Skupiński, A. Reszka, I. Fedorchenko, K. Graszka, N. Olszowska, J. Kołodziej, M. Tokarczyk, Z. Adamus, B.J. Kowalski, H. Deng, K. Park, M. Konczykowski, L. Krusin-Elbaum, A. Wołoś
Magnetic disorder in intrinsic topological magnets MnBi₂Te₄/(Bi₂Te₃)_n
- TuP3.7** **A. Mishra**, P. Simon, T. Hyart, M. Trif
Yu-Shiba-Rusinov qubit
- TuP3.8** **N. Olszowska**, M. Rosmus, J.J. Kołodziej
UARPEs - Beamline in Polish Synchrotron for the measurements of solids band structure

TuP4 – Growth and optical effects

Chair: Ramon Schifano

- TuP4.1** **M. Pawlak**, N. Jukam, A. Ludwig, T. Kruck, N. Spitzer, D. Dziczek, A. Shafiq, A. Wieck
A novel method for thermal characterization of superlattice sample
- TuP4.2** **M. Kędziora**, K. Kołtáj, R. Ambroziak, J. Krajczewski, A. Kudelski
Bifunctional Nanocomposites with Plasmonic and Magnetic Properties as Substrates for Surface-enhanced Raman Scattering (SERS) Measurements.
- TuP4.3** **P.S. Avdienko**, I.V. Sedova, D.A. Kirilenko, D.D. Firsov, O.S. Komkov, S.V. Sorokin
Temperature induced polymorphic transition in GaTe/GaAs(001) layers grown by molecular beam epitaxy
- TuP4.4** K. Karpińska, G. Karczewski, A. Witowski, J. Polaczyński, J. Korczak, S. Schreyeck, S. Chusnutdinov, T. Story, **M. Szot**
CdTe/PbTe periodic structures as photonic crystals
- TuP4.5** **P. Skupiński**, K. Sobczak, G. Graszka, A. Reszka, A. Avdonin, Z. Adamus, A. Arciszewska, J. Sitnicka, A. Wołoś
Growth mechanism of MnBi₂Te₄/(Bi₂Te₃)_n self-assembling superlattices

- TuP4.6** **D. Pashnev**, J. Jorudas, R. Balagula, A. Urbanowicz, I. Kašalynas
Modeling transmission spectra for a thin conductive layer on a semi-insulating substrate
- TuP4.7** **P. Wojnar**, M. Muszyński, P. Baranowski, M. Wójcik, S. Kret, G. Karczewski, T. Wojtowicz
Optical emission from highly strained CdTe/(Zn,Mg)Te nanowires
- TuP4.8** **D. Yavorskiy**, M. Szota, T. Tarkowski, W. Knap, V. Umansky, P. Nowicki, J. Wróbel,
J. Łusakowski
THz emission from GaAs/GaAlAs heterostructure
- TuP4.9** **I. Yahniuk**
THz ratchet effect in HgTe-based interdigitated structures

WEDNESDAY POSTER SESSIONS

14:00-15:00 SHORT PRESENTATIONS (parallel sessions in 4 Zoom Rooms)

15:00-16:00 POSTERS DISCUSSIONS (each poster could be discussed in separate Zoom Room)

WeP1 – 2D Materials

Chair: Anna Ciechan

- WeP1.1** **A.K. Dąbrowska**, M. Tokarczyk, J. Iwański, G. Kowalski, R. Bożek, J. Binder, R. Stępniewski, A. Wyszomółek
The Influence of the Buffer Layer on the Properties of Two Stage Epitaxial Boron Nitride Samples
- WeP1.2** **A. Wójcik**, A.K. Dąbrowska, S. Kozdra, J. Binder, A. Wyszomółek, P.P. Michałowski
Filtering Properties of Epitaxial Boron Nitride
- WeP1.3** **Ł. Kipczak**, M. Grzeszczyk, K. Olkowska-Pucko, A. Babiński, M.R. Molas
The optical signature of few-layer ReSe₂
- WeP1.4** **K. Kotur**, M. Birowska
The influence of the magnetic ordering on the electronic properties of bilayer NiPS₃/FePS₃ – an ab initio study of vdW heterostructure.
- WeP1.5** **K. Szałowski**, M. Gmitra, D. Kochan
Proximity spin-orbit coupling in graphene/1T-TaS₂ heterostructure and its sensitivity to charge density wave ordering: Density Functional Theory calculations
- WeP1.6** **K. Oreszczuk**, W. Pacuski, A. Rodek, T. Kazimierczuk, K. Nogajewski, T. Taniguchi, K. Watanabe, M. Potemski, P. Kossacki
Magneto-optical properties of monolayer MoSe₂ grown by molecular beam epitaxy on hexagonal boron nitride
- WeP1.7** **J. Rogoża**, J. Binder, A.K. Dąbrowska, R. Stępniewski, A. Wyszomółek
Photoconductivity of hexagonal boron nitride grown by MOVPE
- WeP1.8** **J. Kucharek**, R. Bożek, M. Goryca, W. Pacuski
Toward Magnetic – Semiconductor Van der Waals Heterostructures Grown by Molecular Beam Epitaxy
- WeP1.9** **P. Jureczko**, M. Kurpas
Intrinsic and extrinsic spin-orbit coupling in monolayer nitrogene.
- WeP1.10** **M. Karpińska**, M. Liang, R. Kempt, K. Finzel, M. Kamminga, N. Zhang, M. Dyksik, D.K. Maude, J. Jasiński, J. Ziegler, A. Surrente, M. Baranowski, J. Ye, A. Chernikov, A. Kuc, Ł. Kłopotowski, P. Plochocka
Electronic coupling in hybrid monolayer transition metal dichalcogenide/2D perovskite heterostructures

WeP2 – Oxides

Chair: Ewa Przeździecka

- WeP2.1** **A. Adhikari**, A. Lysak, A. Wierzbicka, P. Sybilski, B. Witkowski, E. Przeździecka
Plasma-assisted MBE growth of CdMgO Random alloys on Al₂O₃ substrate
- WeP2.2** **M. Stachowicz**, E. Przeździecka, J.M. Sajkowski, M.A. Pietrzyk, A. Pieniążek, S. Magalhaes, D. Faye, E. Alves, A. Kozanecki
RBS based structural investigation of ZnO/ZnCdO structures grown on Al₂O₃ a- and r-oriented substrates by MBE
- WeP2.3** **A. Lysak**, E. Przeździecka, K.M. Paradowska, A. Wierzbicka, P. Sybilski, J. Sajkowski, R. Jakiela, E. Placzek-Popko, A. Kozanecki
Influence of As Doping on the Properties of MBE Grown Nonpolar ZnO Thin Films
- WeP2.4** **M. Ozga**, B.S. Witkowski, P. Sybilski, M. Godlewski
CuO thin films obtained by hydrothermal method – growth technology, properties and applications
- WeP2.5** **A. Wójcicka**, I. Cora, J. Lábár, Z. Fogarassy, A. Rácz, T. Kravchuk, M.A. Borysiewicz
Multifactorial investigations of the deposition process - material property relationships of ZnO:Al thin films deposited by magnetron sputtering in DC, pulsed DC and RF modes using different targets
- WeP2.6** **J.A. Mathew**, A. Lysak, J.M. Sajkowski, R. Jakiela, Y. Zhydashchuk, M. Stachowicz, E. Przeździecka, A. Kozanecki
Luminescence Properties of ZnO:Eu³⁺ Thin Film Grown by Plasma Assisted Molecular Beam Epitaxy on a-Al₂O₃
- WeP2.7** **M. Sarwar**, B.S. Witkowski, E. Guziewicz
Low-temperature Cathodoluminescence of Nitrogen-doped ZnO Films Deposited at Low-temperature by Atomic Layer Deposition
- WeP2.8** **R. Schifano**, T.A. Krajewski, P. Dłużewski, W. Zajkowska, B. Kurowska, G. Łuka, K. Kopalko, E. Guziewicz, P.S. Smertenko
Schottky contacts to ALD-ZnO: transport mechanisms and effects of the H₂O₂ functionalization
- WeP2.9** **S.M. Faraz**, Z. Tajwar, Q. ul Wahab, V. Khranovskyy, A. Ulyashin, R. Yakimova
Voltage and Frequency Dependent Electrical Characteristics and Interface State Density of Ni/ZnO Schottky Diodes

WeP3 – Topological effects

Chair: Katarzyna Gas

- WeP3.1** **G. Grabecki**, P. Iwanowski, A. Dąbrowski, A. Hruban, K. Dybko, A. Łusakowski, T. Wojtowicz, T. Wojciechowski, R. Jakiela, A. Wiśniewski

Experimental studies of electron transmission through conventional superconductor/type-I Weyl semimetal junctions

- WeP3.2 S. Samadi**, R. Rechciński, R. Buczek
One-dimensional Dirac modes of a pentagonal topological crystalline insulator nanowires
- WeP3.3 W. Brzezicki**
Topological effects in SnTe-class multilayers and nanowires
- WeP3.4 P. Sidorczak**, W. Wołkanowicz, R. Minikayev, S. Kret, Z. Ogorzałek, T. Wojtowicz, D. Wasik, M. Gryglas-Borysiewicz, K. Dybko
Soft Point Contact Spectroscopy Studies of PbTe/SnTe Multi-Layered System
- WeP3.5 Z. Ogorzałek**, B. Seredyński, S. Kret, W. Zajkowska, R. Bożek, M. Tokarczyk, M. Baj, W. Pacuski, J. Sadowski, M. Gryglas-Borysiewicz
Magnetotransport properties of MBE-grown NiTe₂ - a new candidate for Dirac fermion studies.
- WeP3.6 M. Zięba**, B. Turowski, V.V. Volobuev, B.J. Kowalski, N. Olszowska, M. Rosmus, J. Kołodziej, A. Kazakov, T. Wojciechowski, M. Aleszkiewicz, K. Gas, M. Sawicki, A. Łusakowski, T. Wojtowicz, T. Story
Electronic structure of Sn_{1-x}Mn_xTe thin films studied by ARPES
- WeP3.7 N. Nguyen Minh**, T. Hyart, W. Brzezicki
Topological states in SnTe nanowires

WeP4 – Optical characterization

Chair: Tomasz Jakubczyk

- WeP4.1 A. Królicka**, K. Gas, M. Sawicki, J. Korczak, R. Minikayev, A. Reszka, A. Kwiatkowski, M. Gryglas-Borysiewicz, T. Story, K. Dybko
Temperature effect on the location of the resonant Cr^{2+/3+} level in PbTe:Cr
- WeP4.2 P. Baranowski**, P. Wojnar, M. Szymura, R. Georgiev, S. Chusnutdinov, G. Karczewski, T. Wojtowicz
Growth and optical properties of type II ZnTe/ZnSe core/shell nanowire quantum dots
- WeP4.3 S.M. Gheewala**, P.N. Patel, R. Dhavse
Macro Porous Structure Silicon Capacitive Sensor for Aqueous Methyl Alcohol
- WeP4.4 Z. Yu**, J. Grendysa, R. Rudniewski, J. Polaczyński, V.V. Volobuev, A. Kazakov, D. Jarosz, W. Zaleszczyk, T. Wojciechowski, M. Aleszkiewicz, T. Wojtowicz, M. Marchewka
MBE Growth of HgTe-based Structures on (001)-CdTe/GaAs Hybrid Substrates and their Transport Studies
- WeP4.5 A. Łopion**, A. Bogucki, K.E. Połczyńska, W. Pacuski, T. Kazimierzuk, P. Kossacki, A. Golnik
Charged exciton dissociation energy in (Cd,Mn)Te quantum wells with variable disorder and carrier density

- WeP4.6** T. Fąs, A.K. Budniak, Y. Amouyal, E. Lifshitz, J. Suffczyński
Raman magnetospectroscopy of CrPS4
- WeP4.7** M. Grzeszczyk, J. Gawraczyński, T. Woźniak, J. Inabez-Insa, M.R. Molas, A. Babiński
Pressure driven phase transitions in bulk HfS2
- WeP4.8** B.A. Orlowski, K. Gwozdz, K. Goscinski, S. Chusnutdinov, M. Galicka, E. Guzewicz,
B.J. Kowalski
Open circuit voltage spectra influenced by extended and local defects
- WeP4.9** K. Kulinowski, M. Radecka, B.J. Spisak
Influence of dimensionality on electrical properties of TiO2 thin films

THURSDAY POSTER SESSIONS

13:30-14:30 SHORT PRESENTATIONS (parallel sessions in 3 Zoom Rooms)

14:30-15:30 POSTERS DISCUSSIONS (each poster could be discussed in separate Zoom Room)

ThP1 – 2D Materials

Chair: Piotr Wojnar

- ThP1.1** **A.K. Dąbrowska**, K. Pakuła, M. Tokarczyk, J. Binder, R. Stępniewski, A. Wyszomółek
Classical Huang-Rhys Description of Luminescence for a Carbon Related Defect in BN
- ThP1.2** **K.P. Korona**, K. Pakuła, A.K. Dąbrowska, J. Binder, R. Stępniewski, A. Wyszomółek
Deep UV Photoluminescence of MOCVD grown Boron Nitride
- ThP1.3** **E. Zięba**, J. Kutrowska-Girzycka, P. Mrowiński, M. Florian, C. Gies, S. Tongay, K. Watanabe,
T. Taniguchi, C. Schneider, M. Syperek
Detailed studies on the influence of dielectric environment on exciton and trion
properties in monolayer and bilayer MoTe₂
- ThP1.4** **A. Skolasińska**, M. Birowska
Dielectric properties of transition metal trichalcogenides MPX₃
- ThP1.5** **M. Zinkiewicz**, A.O. Slobodeniuk, T. Kazimierzczuk, P. Kapuściński, K. Oreszczuk,
M. Grzeszczyk, M. Bartoš, K. Nogajewski, K. Watanabe, T. Taniguchi, C. Faugeras,
P. Kossacki, M. Potemski, A. Babiński, M.R. Molas
Dark Excitons In Monolayer WS₂
- ThP1.6** **K. Sadecka**, M. Bieniek, A. Wójs, P. Hawrylak
Excitons in Transition Metal Dichalcogenide Heterostructures
- ThP1.7** **Z. Ogorzałek**, B. Seredyński, S. Kret, A. Kwiatkowski, K. Korona, M. Grzeszczyk,
J. Mierzejewski, D. Wasik, W. Pacuski, J. Sadowski, M. Gryglas-Borysiewicz
Charge Transport in MBE-grown MoTe₂ Bilayers With Enhanced Stability Provided
by AlO_x Capping
- ThP1.8** **V.G. Nair**, K. Kotur, A.M. Jastrzębska, M. Birowska
Exploring Electronic Properties of Functionalized 2D MBenes -Graphene Like 2D Boron
Sheets
- ThP1.9** **M. Rybak**, M. Birowska
Optical properties of transition metal trichalcogenides MPX₃: a first principle study of 2D
magnets

ThP2 – Nitrides

Chair: Piotr Drózd

- ThP2.1** **R.M. Balagula**, L. Subačius, J. Jorudas, P. Prystawko, I. Kašalynas
Electric Field Modulation of GaN Transmittance in Terahertz Range
- ThP2.2** **J. Jorudas**, P. Prystawko, M. Dub, A. Selskis, M. Skapas, P. Sai, M. Sakowicz,
S. Rumyantsev, W. Knap, I. Kašalynas
Structural and electrical analysis of the "buffer-free" AlGa_N/Ga_N on SiC heterostructure
- ThP2.3** **K. Moszak**, W. Olszewski, D. Majchrzak, D. Pucicki, J. Osiecki, J. Serafińczuk, D. Hommel
AlGa_N composition correction under variable ammonia flow and pressure conditions
in MOVPE reactor
- ThP2.4** **R. Hrytsak**
DFT based modeling of point defect diffusion across the In_{0.125}Ga_{0.875}N/GaN
and In_{0.25}Ga_{0.75}N/GaN interfaces
- ThP2.5** **M. Żak**, H. Turski, G. Muziol, M. Siekacz, K. Nowakowski-Szkudlarek, M. Chlipała,
C. Skierbiszewski
Tunnel junction for III-Nitride devices with inverted polarization
- ThP2.6** **J. Slawinska**, C. Skierbiszewski, M. Siekacz, G. Muzioł, K. Nowakowski-Szkudlarek,
A. Feduniewicz-Żmuda, M. Żak, M. Hajdel
Size dependence of Internal Quantum Efficiency (IQE) in nitride micro-LEDs with tunnel
junction grown by PAMBE
- ThP2.7** **M. Sawicka**, N. Fiuczek, G. Muzioł, M. Hajdel, A. Feduniewicz-Żmuda, K. Nowakowski-
Szkudlarek, M. Żak, P. Wolny, H. Turski, M. Siekacz, C. Skierbiszewski
Porous GaN for cladding layers in nitride edge emitting laser diodes

ThP3 – Theoretical studies

Chair: Maciej Molas

- ThP3.1** **I. Bragar**
Retardation of Quantum Correlation Decay of Two Spin Qubits by Quantum
Measurements
- ThP3.2** **J.A. Krzywda**, Ł. Cywiński
Interplay of charge noise and coupling to phonons in adiabatic electron transfer between
quantum dots
- ThP3.3** **M. Krzykowski**, P. Machnikowski
Multi-band envelope-function theory of fine structure splitting in semiconductor
nanostructures
- ThP3.4** **K. Kawa**, P. Machnikowski
Spread of Correlations in Highly Disordered System with Long-Range Coupling

- ThP3.5** **T.JF. Verstijnen**, D. Tjeertes, A. Rice, K. Alberi, M.E. Flatté, P.M. Koenraad
An atomic scale study of isoelectronic dopant pairs in GaAs using X-STM and DFT
- ThP3.6** **K. Bilińska**, M.J. Winiarski
A search for potentially valuable thermoelectric materials over 18-electron half-Heusler alloys
- ThP3.7** **A. Koshevarnikov**, T. Ketolainen, J.A. Majewski
The magnetic properties of the iron phthalocyanine molecule on the Ti2C MXenes layer
- ThP3.8** **M. Patera**, P.T. Róžański, M. Zieliński
Self-consistent and External Electric Field Calculations for Crystal Phase Quantum Dots
- ThP3.9** **B. Rzepkowski**, M. Kupczyński, P. Potasz, A. Wójs
DMRG and Monte Carlo Studies of CrI3 Phase Transitions
- ThP3.10** **G.V. Budkin**, S.A. Tarasenko
Shift electric current induced by energy relaxation of hot carriers in quantum wells

Focused Ion Beam fabrication of crystalline devices: from topology to correlations

Philip J.W. Moll^{1,2}

¹ *Laboratory of Quantum Materials (QMAT), Institute of Materials (IMX), Ecole Polytechnique Federale de Lausanne (EPFL), CH-1015 Lausanne, Switzerland*

² *Microstructured Quantum Matter Department, Max-Planck-Institute for the Structure and Dynamics of Matter (MPSD), D-22761 Hamburg, Germany*

"Form follows function" as a motto ranges from philosophy to architecture to biology. Unsurprisingly, it explicitly manifests itself in quantum mechanics via the boundary conditions set by the form of a physical object – that dictates the wave equations and the quantum mechanical behavior in it. These ideas of finite size effects are regularly encountered when critical dimensions are constrained, such as in quantum wells or quantum dot structures which are usually fabricated from traditional metals and semi-conductors.

If one aspires to tackle similar questions in chemically and physically more complex compound crystals, such as topological semi-metals or superconductors, one needs to go new ways to define the boundary for 3D electronic systems without the luxury of lithography in 2D. To this end, my research group has been using Focused Ion Beam (FIB) machining to carve from as-grown single crystallites intricate structures on the micron- and sub-micron scale.

I will first introduce you to the technique and workflows, highlighting both the advantages and caveats of FIB machining of quantum materials. Then we will review some of the prominent works in the field, in which advanced functionality has been achieved by precision shape control.

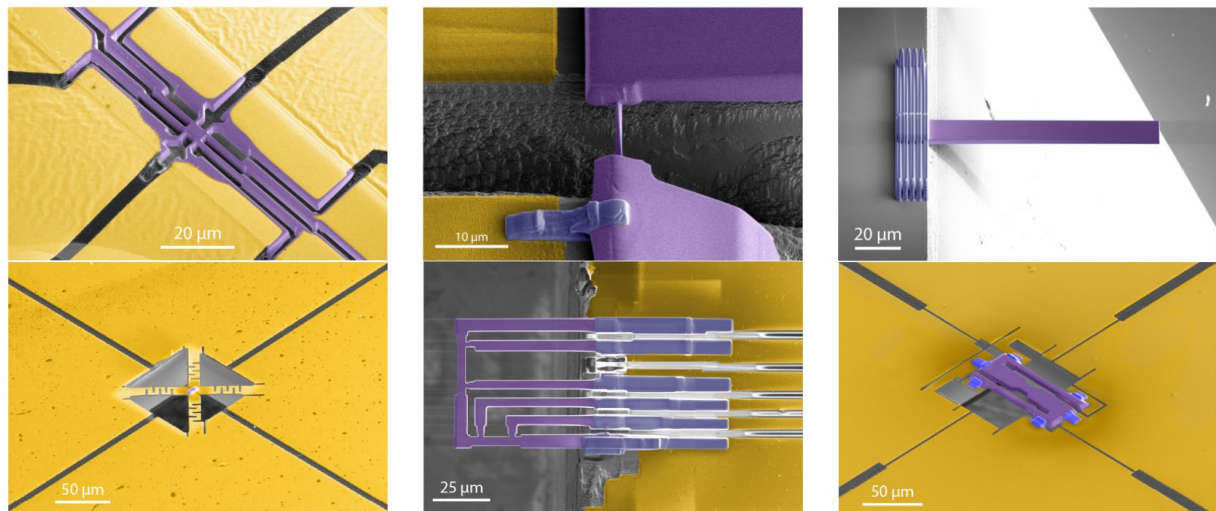


Fig. 1: Examples of FIB-prepared 3D single crystal transport structures from heavy Fermion superconductors and topological semi-metals

- [1] C. Putzke et al., *Science* **368**, 1234 (2020).
- [2] M.D. Bachmann et al., *Nat. Comm.* **10**:5081 (2019)
- [3] P.J.W. Moll, *Ann. Rev. Cond. Mat. Phys.* **9**:147 (2018)

Atomistic and Phenomenological Models of Quantum Dots and Quantum Dot Molecules

Michał Zieliński¹

¹ *Institute of Physics, Faculty of Physics, Astronomy and Informatics, Nicolaus Copernicus University, Grudziadzka 5, 87-100 Torun, Poland*

Atomically sharp interfaces, low lattice symmetry, or disorder due to alloy randomness frequently occur in various nanostructures. From a theory point of view, they are often best treated by atomistic approaches, i.e., where one defines systems on an atom-by-atom basis. Atomistic methods benefit tremendously from the computational power [1] of modern multi-core computer clusters. However, atomistic calculations remain nonetheless very demanding, and their results may sometimes be challenging to understand. Thus, it often makes sense to augment time-consuming, numerical calculations with computationally much simpler, phenomenological models where one uses, e.g., 4x4 Hamiltonians. In this lecture, I will present several cases where it is beneficial to combine atomistic and phenomenological treatments, including the optical activity of dark excitons in self-assembled and alloyed quantum dots [2-4], fine structure splitting in highly-elongated nanostructures [5], and excitonic spectra of artificial quantum dot molecules embedded in nanowires [6].

- [1] P. Róžański, and M. Zieliński, *Comput. Phys. Commun.* **238**, 254 (2020).
- [2] M. Zieliński, Y. Don, and D. Gershoni, *Phys. Rev. B* **91**, 085403 (2015).
- [3] M. Zieliński, *Phys. Rev. B* **102**, 245423 (2020).
- [4] M. Zieliński, *Phys. Rev. B* **103**, 155418 (2021).
- [5] M. Zieliński, *Sci. Rep.* **10**, 13542 (2020) (2020).
- [6] M. Świdorski, and M. Zieliński, *Phys. Rev. B* **100**, 235417 (2019).

Defect Centers in Hexagonal Boron Nitride: Optical, Spin Properties and Applications

Gregory D. Fuchs¹

¹*Cornell University, Ithaca, NY, USA*

Defect centers in wide bandgap materials have emerged as a powerful platform for quantum information science and technology, with applications ranging from quantum sensing to quantum networking. Although the most mature materials hosting 'quantum defects' are three dimensional materials like diamond and silicon carbide, defect centers in a two dimensional insulator, hexagonal boron nitride (hBN), have recently been isolated and studied. In this school lecture, I will discuss the phenomenology and applications of hBN defect centers, including a presentation of the Huang-Rhys model that describes the interaction between the electronic transitions of a defect and its local phonons. Additionally, I will present materials considerations, what we know about the optical coherence of hBN defect quantum emission, and what we can deduce about the structure of hBN defects that have been observed. Finally, I will discuss the recent discovery of optically accessible spin from hBN defects, which is a promising platform for quantum sensing at surfaces and interfaces due to the two dimensional nature of the hBN host material.

Ionic gating of 2D materials

Alberto Morpurgo¹

¹ *DQMP, University of Geneva, quai Ernest-Ansermet 24, CH1200 Geneva, Switzerland*

The idea of gating materials using electrolytes is very old as it first appeared already in the early days of semiconductor physics, at the time when transistors were first developed. In more recent times, different practical strategies have been attempted to implement the idea in practice, corresponding to the use of different types of electrolytes and of materials to be gated. This early work showed both the potential and possible problems of the technique. Over the last decade, the use of ionic liquids as electrolytes has allowed most problems to be eliminated when using selected classes of materials, leading to a number of very interesting results in different research areas.

In this lecture I will attempt to illustrate the current status in the field in a pedagogical way through an overview of our research on ionic liquid gated transistors based on 2D materials, mostly consisting of semiconducting transition metal dichalcogenides. After explaining the key technical ideas and the most common possible problems in its application I will discuss the use of ionic liquid gating in the context of semiconductor physics, as well as in relation to the study of gate induced superconductivity.

In the context of semiconducting physics, the aspect that is particularly important is the very large gate capacitance of the devices. This large capacitance enables both electrons and holes to be accumulated on a 2D material on a same device, just by properly varying the bias conditions. The corresponding ambipolar transport regime can be used to realize different kind of devices, such as light emitting transistors. It also allows a new form of energy spectroscopy that appears to be one of the most convenient ways to determine quantitatively the band gap of 2D semiconducting materials, as well as the energetics of their band alignment in heterostructures. I will also discuss recent ongoing developments, such as the realization of double ionic gated devices to apply extremely large electric fields perpendicular to a 2D material.

As for gate induced superconductivity I will outline the main results in the field, try to explain the status of what is understood, and discuss experiments that can possibly provide information about the mechanism responsible for the formation of Cooper pairs (which remains to be established).

Towards Quantum Information Processing with Superconducting Circuits

Alexandre Blais¹

¹*Institut Quantique and Département de Physique, Université de Sherbrooke,
Sherbrooke, Québec, J1K 2R1, Canada*

By exploiting effects such as quantum superpositions and entanglement, quantum computers could solve problems that are intractable on standard, classical, computers. While building a full-scale quantum computer capable of rivaling with today's supercomputers remains a challenge, the last few years have seen tremendous improvements in our ability to build small superconducting quantum processors and run simple algorithms on these processors. In this talk, I will review some of the basic concepts that could allow quantum computers to outperform their classical counterparts. With an emphasis on superconducting quantum processors, I will also discuss recent developments of the field and outline some of the challenges that lie ahead [1,2].

[1] A. Blais, S. M. Girvin and W. D. Oliver, Quantum information processing and quantum optics with circuit quantum electrodynamics, *Nature Physics* **16**, 247 (2020)

[2] A. Blais, A.L. Grimsmo, S.M. Girvin and A. Wallraff, Circuit quantum electrodynamics, *Rev. Mod. Phys.* **93**, 025005 (2021).

Single Crystalline Hexagonal Boron Nitride for 2D Opto-Electric Devices

Takashi Taniguchi

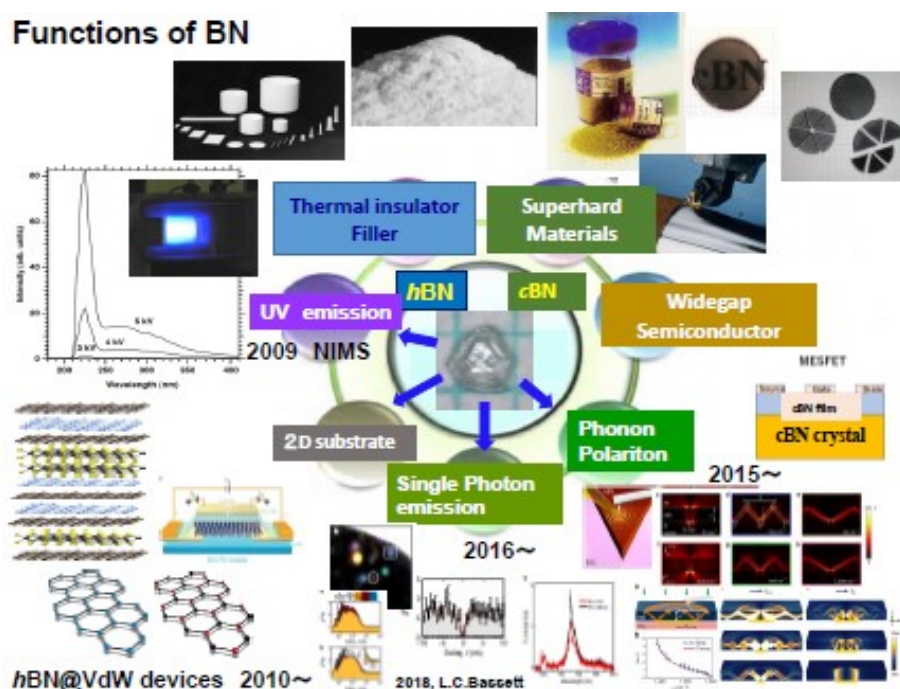
National Institute for Materials Science, 1-1 Namiki Tsukuba Ibaraki 305-0044 Japan

Hexagonal boron nitride BN (hBN) and cubic BN (cBN) are known as the representative crystal structures of BN. The former is chemically and thermally stable, and has been widely used as an electrical insulator and heat-resistant materials. The latter, which is a high-density phase, is a super-hard material second only to diamond.

Some progresses in the synthesis of high purity boron nitride (BN) crystals were achieved by using Ba-BN as a growth solvent material at high pressure (HP) of 5.5GPa [1]. Band-edge natures (cBN $E_g=6.2\text{eV}$ and hBN $E_g=6.4\text{eV}$) were characterized by their optical properties. The key issue to obtain high purity crystals is to reduce oxygen and carbon contamination in the HP growth circumstances. Then an attractive potential of hBN as a deep ultraviolet (DUV) light emitter [2] and also superior properties as substrate of graphene devices [3] were realized.

Also, controlling of boron and nitrogen isotope ratio (^{10}B , ^{11}B and ^{15}N) in hBN and cBN crystals can be now carried out by metathesis reaction under HPHT [4]. The newly developed functions can be realized by using high purity BN single crystals as shown in figure.

In this paper, recent studies on residual impurity control for BN single crystals obtained at high pressure with respect to impurity / isotope controls and their functionalization will be reported.



References

- [1] T. Taniguchi, K. Watanabe, J. Cryst. Growth, **303** 525 7 (2007).
- [2] K. Watanabe, T. Taniguchi and H. Kanda, Nature Materials, **3**, 404 (2004).
- [3] C.R. Dean, T. Taniguchi, P. Kim, et. al Nat. Nanotechnol., **5** 722, (2010).
- [4] K. Chen, T. Taniguchi, et. al., Science, **367**, 555 (2020).

Transparent electronics based on oxide transistors

Elvira Fortunato, Emanuel Carlos, Rita Branquinho, Pedro Barquinha and Rodrigo Martins

CENIMAT/i3N, Department of Materials Science, NOVA School of Science and Technology (FCT-NOVA) and CEMOP/UNINOVA, NOVA University Lisbon, Campus de Caparica, 2829-516 Caparica, Portugal; emf@fct.unl.pt

Transparent electronics has gained special attention during the last decade and is today well established as one of the key technologies for a wide range of device applications and is one of the most promising technologies for new electronic products with high added value, away from the traditional silicon technology.

The key components are sustainable abundant and non-toxic materials based on metal oxides (like zinc oxide) of different origins and play an important role, not only as passive components but also as active components, similar to what is observed in conventional semiconductors like silicon. The viability of this technology depends to a large extent on the performance, reproducibility, reliability and cost of the metal oxide based thin film transistors (TFTs). Transistors are the key components in most modern electronic circuits, and are commonly used to amplify or to switch electronic analog and digital signals. The best known application of TFTs is in flat panel displays.

TFTs have been fabricated in a wide variety of materials, but hydrogenated amorphous silicon has been the enabling technology for the active matrix liquid crystal display (AMLCD), common place in portable and desktop computers, high resolution TVs, tablets and smartphones. However, due to low cost of production, low-temperature processing and high resolution, AMLCD technology is gradually shifting towards metal oxide based TFT. Beside higher resolution, one of the advantages of this technology is that it can use existing manufacturing infrastructure which was developed for amorphous-Si TFT. The metal oxide was already adopted by the industry and is based on IGZO (Indium-Galium-Zinc-Oxide) and it was a breakthrough in display technology since it delivers high-resolution, ultra-low power, and slim product profiles, plus exceptionally detailed touch panel capabilities (see Fig. 1). IGZO is a driving force behind new developments in a variety of fields, enabling LCDs, as well as OLED, and MEMS displays, with new levels of performance.

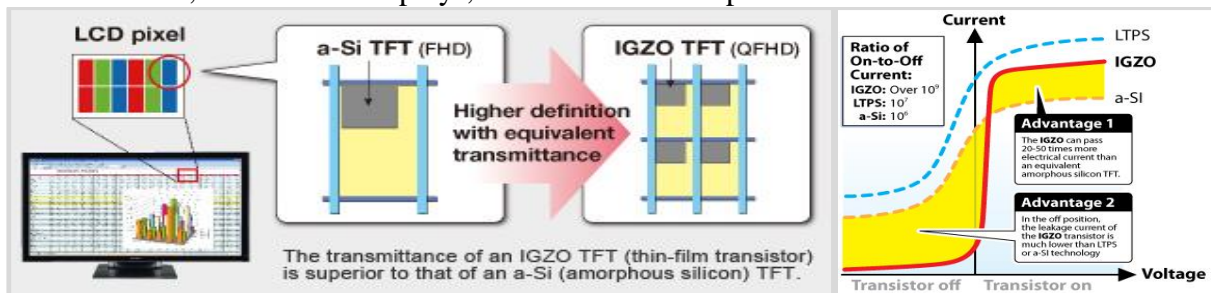


Fig. 1 – Comparison of active matrix backplanes using amorphous silicon with the IGZO technology (Adapted from SHARP).

As it was projected by some forecast reports, transparent electronics market was valued at USD 1000 million in 2019 and is expected to reach USD 3800 million by 2025, at a CAGR of 25% over the forecast period 2020 - 2025. These numbers justify a real need as well as a scientific and social commitment in order to keep/increase the level of development but in a responsible way in terms of our planet in accordance with the green deal. We start it 10 years ago!. Besides that and by adding electronics to the rest of the 95% of objects surrounding us but do not have electronics yet, the market of electronics will growth at least 10 times.

Towards room temperature, compact sources of coherent terahertz radiation

Z. R. Wasilewski

Department of Electrical and Computer Engineering

Department of Physics and Astronomy

Waterloo Institute for Nanotechnology

Institute for Quantum Computing

University of Waterloo, 200 University Avenue West, Waterloo, Ontario N2L 3G1, Canada

The so-called terahertz gap ($\sim 1\text{--}10$ THz) has received much attention over the last two decades because of many potential applications waiting for compact, portable terahertz radiation sources. The report of the first [1] terahertz quantum cascade laser (QCL) in 2002 brought much hope to the community. However, the possibility of ever reaching room temperature operation was considered unlikely by many. Indeed, after a slow ascent of the maximum operating temperature to 200 K in 2012, [2] the progress in the field stalled for close to a decade. However, the recent demonstration of GaAs/AlGaAs THz QCL lasing up to 250 K, [3] brought back the vigor to these pursuits. Indeed, with the current understanding, no hard physical obstacles would preclude achieving lasing action at still higher temperatures.

Nevertheless, the prolonged stagnation in terahertz QCL progress inspired many to look for alternatives. Our research group has embarked on a parallel pursuit of a coherent terahertz light source based on a very different principle, namely the polariton lasing mechanism – more analogous to Bose-Einstein condensation than conventional lasing, but with a similar end result – in arrays of AlGaAs parabolic quantum wells. [4] Albeit demonstration of coherent terahertz radiation at 300 K from such quantum systems may be still years away, the research has already produced important results furthering understanding of plasmons and evidence of polariton formation up to 200 K in the dispersive cavities necessary for polariton scattering.

This presentation will outline the physics behind both types of terahertz sources, show the current status of research in these projects, and discuss the key challenges ahead.

- [1] R. Kohler, A. Tredicucci, F. Beltram, H. E. Beere, E. H. Linfield, A. G. Davies, D. A. Ritchie, R. C. Iotti, and F. Rossi, "Terahertz semiconductor-heterostructure laser", *Nature* 417, 156-159 (2002).
- [2] S. Fatholouloumi, E. Dupont, C. W. I. Chan, Z. R. Wasilewski, S. R. Laframboise, D. Ban, A. Mátyás, C. Jirauschek, Q. Hu, and H. C. Liu, "Terahertz quantum cascade lasers operating up to ~ 200 K with optimized oscillator strength and improved injection tunneling", *Opt. Express* 20, 3866-3876 (2012).
- [3] A. Khalatpour, A. K. Paulsen, C. Deimert, Z. R. Wasilewski, and Q. Hu, "High power portable terahertz laser systems", *Nature Photonics* 15, 16-20 (2020).
- [4] C. Deimert, P. Goulain, J. M. Manceau, W. Pasek, T. Yoon, A. Bousseksou, N. Y. Kim, R. Colombelli, and Z. R. Wasilewski, "Realization of Harmonic Oscillator Arrays with Graded Semiconductor Quantum Wells", *Phys. Rev. Lett.* 125, 097403 (2020).

Optical properties of MoSe₂ layers grown on 2" h-BN templates - a combined MBE/MOVPE approach

Katarzyna Ludwiczak, Aleksandra Krystyna Dąbrowska, Johannes Binder, Mateusz Tokarczyk, Jakub Iwański, Grzegorz Kowalski, Rafał Bożek, Roman Stępniewski, Wojciech Pacuski and Andrzej Wysmolek

Faculty of Physics, University of Warsaw, Pasteura 5, 02-093 Warsaw, Poland

Transition metal dichalcogenides (TMD) – representatives of 2D materials - have recently emerged as a promising candidates for next-generation optoelectronic devices. Present-day realizations requires however a time-consuming mechanical exfoliation process which allows to prepare flakes only tens of micrometers in size with properties that vary flake-by flake. For any future application it is important to develop a large-area and high quality sample synthesis technique.

In this work, we present a novel, heteroepitaxial approach. Our method starts with the growth of hexagonal boron nitride (h-BN) using Metalorganic Vapour Phase Epitaxy (MOVPE) on 2" sapphire wafers [1]. Subsequently, we deposit a single atomic layer of MoSe₂ using Molecular Beam Epitaxy [2]. We discuss the impact of various h-BN thicknesses on the properties of the TMD layer and optimize the growth parameters.

The presented method allows to uniformly cover the whole 2" wafer with monolayer MoSe₂ (fig. 1a). Optical studies (Raman and photoluminescence spectroscopy) unveil an exceptional homogeneity of the material and proves that it is indeed a single layer (fig. 1b). Photoluminescence spectra measured at low temperatures are also great indicators of the optical quality of the sample. The observed excitonic lines are narrow and allow to resolve two components corresponding to the neutral exciton A and charged trion (fig. 1c). The obtained peak widths are however not as narrow as those observed for the material grown on an exfoliated hBN flakes [2], but significantly better than for the material grown directly on silicon dioxide (fig. 1d). We believe that a further optimization of MOVPE and MBE growth processes will result in a significant improvement of the optical quality of the produced samples.

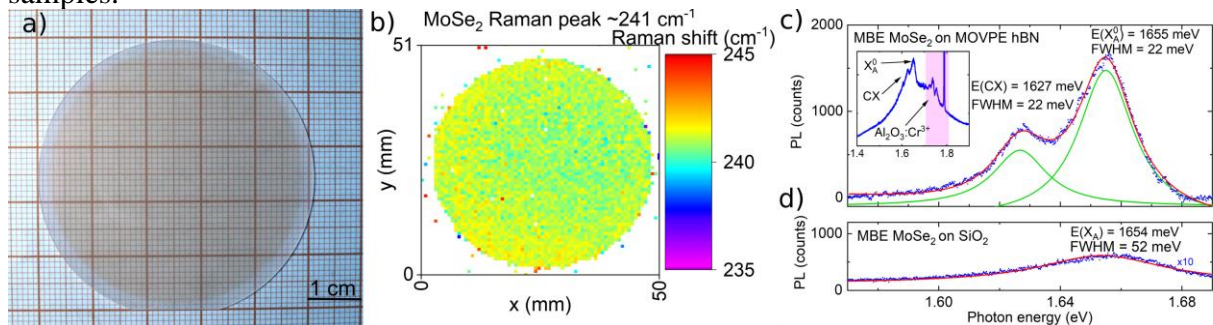


Fig. 1. a) A photo of a 2" wafer. The darker, brownish area corresponds to the MoSe₂ monolayer. b) Results of Raman mapping of the whole sample. The slight variation of the MoSe₂ phonon related peak position indicates homogeneous growth of the monolayer material on the whole sample. c) Low-temperature photoluminescence measurements of a typical point on the sample. Excitonic peaks are narrow and well-resolved in contrast to d) MoSe₂ grown on a silicon dioxide, for which a broad peak was obtained.

Our heteroepitaxial growth method constitutes a step towards the fabrication of large-area uniform layers of various 2D materials. It allows to produce samples of high optical quality with reproducible properties which is crucial for many future applications.

This work was supported by the National Science Centre grant OPUS 17 (2019/33/B/ST5/02766)

[1] A.K. Dąbrowska et.al., *2D Mater.* **8**, 015017 (2021), [2] W. Pacuski et.al., *Nano Lett.* **20**, 3058–3066 (2020)

Narrow excitonic lines and large-scale homogeneity of transition metal dichalcogenide monolayers grown by MBE on hBN

W. Pacuski¹, M. Grzeszczyk¹, K. Nogajewski¹, A. Bogucki¹, K. Oreszczuk¹,
A. Rodek¹, J. Kucharek¹, K.E. Polczyńska¹, B. Seredyński¹, R. Bożek¹, S. Kret²,
T. Taniguchi³, K. Watanabe³, J. Sadowski^{1,2,4}, T. Kazimierzczuk¹, M. Potemski^{1,5},
P. Kossacki¹

¹ *Institute of Experimental Physics, Faculty of Physics, University of Warsaw, Pasteura St. 5, 02-093 Warsaw, Poland,*

² *Institute of Physics, Polish Academy of Sciences, al. Lotników 32/46, 02-668 Warsaw, Poland,*

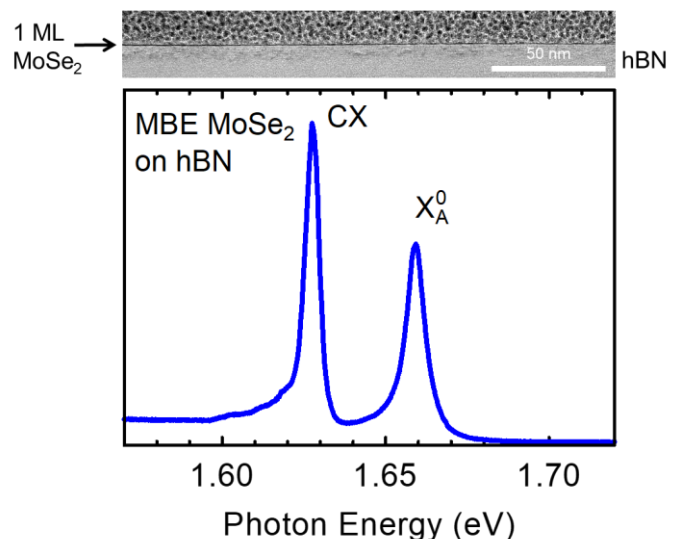
³ *National Institute for Materials Science, Tsukuba, 305-0047, Ibaraki, Japan,*

⁴ *Department of Physics and Electrical Engineering, Linnaeus University, Kalmar, Sweden,*

⁵ *Laboratoire National des Champs Magnétiques Intenses, CNRS-UJF-UPS-INSA, 25, avenue des Martyrs, 38042 Grenoble, France*

Monolayer transition metal dichalcogenides (TMDs) are two-dimensional materials with exceptional optical properties such as high oscillator strength, valley related excitonic physics, efficient photoluminescence, and several narrow excitonic resonances. However, above effects have been so far explored only for structures produced by techniques involving mechanical exfoliation and encapsulation in hBN inevitably inducing considerable large-scale inhomogeneity. On the other hand, techniques which are essentially free from this disadvantage, such as molecular beam epitaxy (MBE), have to date yielded only structures characterized by considerable spectral broadening, which hinders most of interesting optical effects.

We report for the first time on the MBE-grown TMD exhibiting narrow and fully resolved spectral lines of neutral and charged exciton (see Figure). Moreover, our MBE-grown TMD exhibits unprecedented high spatial homogeneity of optical properties, with variation of the exciton energy as small as 0.16 meV over a distance of tens of micrometers. Our recipe for MBE growth [1] is presented for MoSe₂ and includes extremely slow growth rate, the use of atomically flat hexagonal boron nitride (hBN) substrate and the annealing at very high temperature. Importantly, good optical properties are achieved for as-grown sample, without any post growth exfoliation and encapsulation in hBN. This novel recipe opens a possibility of MBE growth of TMD and their heterostructures with optical quality, dimensions and homogeneity required for optoelectronic applications.



[1] W. Pacuski, M. Grzeszczyk, K. Nogajewski, A. Bogucki, K. Oreszczuk, J. Kucharek, K.E. Polczyńska, B. Seredyński, A. Rodek, R. Bożek, T. Taniguchi, K. Watanabe, S. Kret, J. Sadowski, T. Kazimierzczuk, M. Potemski, P. Kossacki, Nano Letters 20, 3058 (2020).

Raman spectroscopy of epitaxial h-BN layers grown by MOVPE – role of anharmonic processes and interaction with the substrate

P. Tatarczak, A. K. Dąbrowska, J. Iwański, J. Binder, G. Kowalski, M. Tokarczyk,
R. Stępniewski and A. Wysmolek

Faculty of Physics, University of Warsaw, Pasteura 5, 02-093 Warsaw, Poland

Hexagonal boron nitride (h-BN) can contribute greatly to the development of van der Waals heterostructures and deep UV optoelectronic devices. In order to realize this idea the growth of wafer-scale epitaxial h-BN using Metal Organic Vapor Phase Epitaxy (MOVPE) can be employed [1]. As far as technological applications are concerned, the quality of the h-BN layers is of key importance. Raman spectroscopy is a well-established method providing information about the quality of epitaxial layers and a perfect tool for studying the interaction of grown layers with the substrate, including effects resulting from their different thermal expansion [2]. Temperature dependent Raman studies of epitaxial h-BN were so far limited to temperatures of about 400K-500K, mainly due to defect-related luminescence which hinders the observation of the Raman signal [3]. However, we have found that this luminescence can be successively quenched by annealing in nitrogen atmosphere in the 1000-1100 K temperature range (Fig. 1.). In this report we present detailed Raman scattering studies of the in-plane E_{2g}^{high} phonon mode in the temperature range from 300 K up to 1200 K (Fig. 2.). The collected experimental data allows us to compare anharmonic processes [4,5] in the bulk material and h-BN epilayers in a broad temperature range that has never been presented before. It was found that the E_{2g}^{high} mode energies are slightly higher for epitaxial material, probably due to internal strain induced during the growth. A significant difference between results for as-grown samples and delaminated h-BN films [6] transferred to silicon substrates indicates the crucial role of the layer-substrate interaction. The role of intrinsic and extrinsic factors on the crystal quality and thermal properties are discussed.

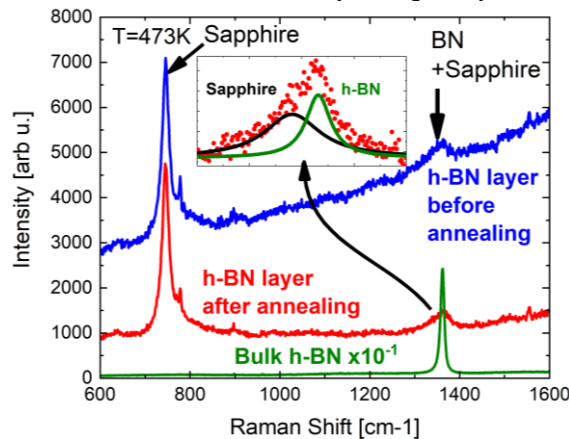


Fig. 1. Raman spectra at 473K of bulk h-BN and epitaxial h-BN before and after annealing to 1100K.

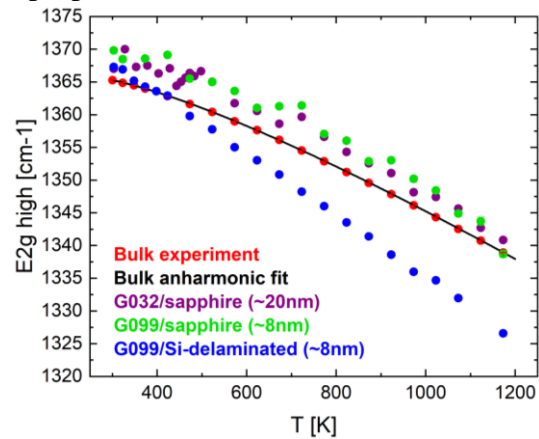


Fig. 2. The energy of E_{2g}^{high} mode as a function of temperature for h-BN layers of different thickness.

Acknowledgement: This work has been partially supported by the National Science Centre under grant no. 2019/33/B/ST5/02766.

- [1] A. K. Dąbrowska et al., *2D Mater.* **8**, 015017 (2021).
- [2] S. Linas et al., *Phys. Rev. B* **91**, 075426 (2015).
- [3] K. Bera et al., *Nanotechnology* **32**, 075702 (2021).
- [4] R. Cuscó et al., *Phys. Rev. B* **94**, 155435 (2016).
- [5] M. Balkanski, R. F. Wallis, and E. Haro, *Phys. Rev. B* **28**, 1928 (1983).
- [6] J. Iwański et al., *Acta Phys. Pol. A* **139**, 4 (2021).

Highly effective gating of graphene on GaN

Jakub Kierdaszuk¹, Ewelina Rozbiegała^{2,3}, Karolina Piętak^{2,4}, Sebastian Złotnik^{2,5}, Aleksandra Przewłoka^{2,6,7}, Aleksandra Krajewska^{2,6}, Wawrzyniec Kaszub², Marta Gryglas-Borysiewicz¹, Andrzej Wysmolek¹, Johannes Binder¹, Aneta Drabińska¹

¹ Faculty of Physics, University of Warsaw, Poland

² Łukasiewicz - Institute of Microelectronics and Photonics, Warsaw, Poland

³ Warsaw University of Technology, Faculty of Materials Science and Engineering,

⁴ Warsaw University of Technology, Faculty of Chemistry, Poland

⁵ Institute of Applied Physics, Military University of Technology, Warsaw, Poland

⁶ CENTERA Laboratories, Institute of High Pressure Physics PAS, Warsaw, Poland

⁷ Institute of Optoelectronics, Military University of Technology, Warsaw, Poland

By applied graphene/GaN Schottky diode with an undoped GaN spacer, we studied potential of this structure for efficient graphene gating [1]. A layer of undoped GaN (100 nm) preceded by a 1.3 μm thick layer of highly conductive (n-doped) GaN were grown on a sapphire substrate by MOCVD (Metalorganic Chemical Vapour Deposition). Four-layer graphene (4-LGr) with turbostratic layer stacking was transferred by a polymer frame method to form a top contact to GaN. Current-voltage characteristics of the sample exhibit a Schottky-like behavior (Fig. 1a). Raman measurements of graphene layers subjected to external bias showed three different types of spectra with G-band splitting into one, two, or three subbands. No splitting of the 2D band was observed. The presence of G band splitting is therefore related to different carrier concentrations of subsequent graphene layers in the turbostratic 4-LGr structure. A redshift of the G bands as a function of gate bias was observed which suggests n-doping of graphene (Fig. 1b). Interestingly, the most significant G band energy shift of up to 8.5 cm^{-1} occurs for the lowest bias, in the range between 1 V and -1 V (Fig. 1c). A further G band energy shift of up to 1.4 cm^{-1} was observed in the range between -1 V and -5 V. Capacitance-voltage (CV), as well as electroreflectance (ER) measurements together with a band alignment analysis, showed that the undoped GaN spacer behaves like a capacitor (Fig. 1d) at reverse bias. A rapid decrease of electron concentration in graphene and a vanishing G band splitting occurs at forward bias. A comparison with solution-gated graphene suggests, that the strong gating effect at forward bias occurs on graphene/GaN interface, which is promising for the fabrication of sensitive detectors based on tracing the G band splitting [2].

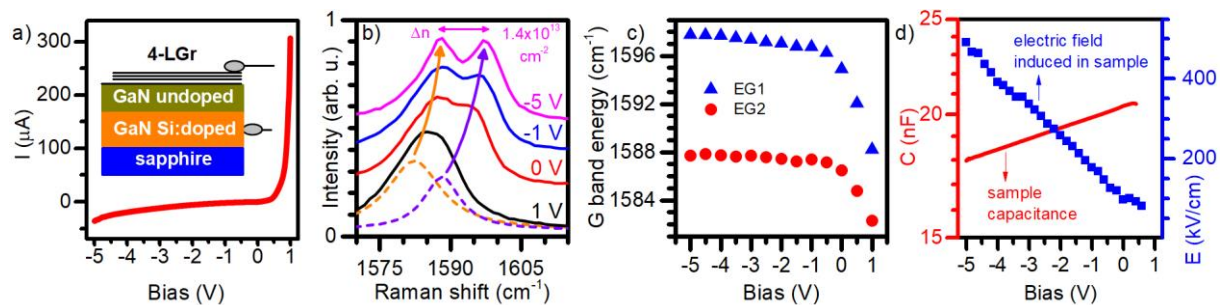


Fig. 1. a) IV characteristics; inset: sample scheme, b) G band evolution as a function of bias, c) dependence of G band energy on bias, d) CV& ER results.

REFERENCES

- [1] J. Kierdaszuk, et al., Applied Surface Science, journal pre-proof 149939 (2021).
- [2] J. Binder, et al., Nanotechnology 27, 045704 (2016).

Selective local etching of germanium via photocorrosion and creation of graphene micro-membranes

J.Rogoża¹, J.Binder¹, L.Tkachenko¹, I.Pasternak², J.Sitek², W.Strupiński²,
M.Zdrojek², J.Baranowski³, R.Stępniewski¹, A.Wysmolek¹

¹Faculty of Physics, University of Warsaw, Pasteura 5, 02 – 093 Warsaw, Poland

²Faculty of Physics, Warsaw University of Technology, Koszykowa 75, 00-662 Warsaw, Poland

³Łukasiewicz – Institute of Microelectronics and Photonics, al. Lotników 32/46, 02-668 Warsaw, Poland

Graphene is the first and one of the most extensively studied members of the 2D materials family. Despite its astonishing properties, widespread graphene-based electronics are still not in sight. One of the reasons for this may be the fact, that most of the substrates for graphene growth are incompatible with CMOS (complementary metal-oxide semiconductor) technology. A substrate that is compatible with CMOS technology and at the same time allows for growth of high-quality graphene on germanium.

In this communication we present results of selective local etching via laser-induced photocorrosion of germanium and the creation of graphene micro-membranes on GR/Ge/Si samples [1]. Our newly developed method allows to selectively etch germanium without damaging the covering graphene layer, which directly results in a graphene membrane. A schematical illustration of the process is shown in Fig. 1 (a) and a SEM image of a graphene membrane fabricated by this method is shown in Fig 1 (b). The graphene sample was grown on a (100) germanium epilayer on silicon using the CVD method. 2D and 3D structures in the Ge/Si sample were directly etched in deionized water. In-situ Raman measurements were performed to determine how graphene and germanium behave during this etching process. Raman maps of free-standing graphene membranes were measured and show a dramatic increase of the Raman signal on the suspended areas. The origin of this enhanced Raman signal and the change in strain and carrier concentration upon etching will be discussed in this communication.

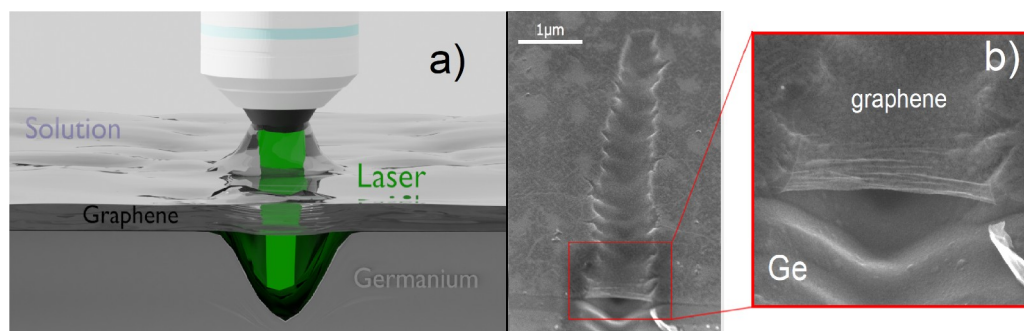


Fig 1. a) Visualisation of the employed experimental setup. b) Photoetched graphene membrane on a germanium epilayer [1].

The obtained results describe a cheap and straightforward method of processing germanium with micrometer precision. This method also allows for the creation of thin, high quality graphene membranes that in the future may be used in NEMS devices or other types of electronics

[1] J. Binder, J. Rogoża, et al. 2D Materials 2021 in press, <https://doi.org/10.1088/2053-1583/abfedcdoi>

Feed-forward exciton-polariton neural network

A. Opala¹, R. Panico², D. Ballarini², D. Sanvitto², M. Matuszewski¹

¹ Institute of Physics, Polish Academy of Sciences, Al. Lotników 32/46, PL-02-668 Warsaw, Poland

² CNR NANOTEC–Institute of Nanotechnology, Via Monteroni, 73100 Lecce, Italy

Technological solutions based on the CMOS technology reach the physical limits imposed by quantum effects. Progress in computing and communication enforces the necessity to process large data sets in an ever shorter time. Unfortunately, the performance of commonly used computers based on the von Neumann architecture reaches its limit. This limitation results in the von Neumann bottleneck. Physical limits of the miniaturisation of integrated circuits make it impossible to solve this problem traditionally. Arguably, the best solution to avoid the technological impasse is using an optoelectronic system with architecture inspired by the structure of a brain. The features which are crucial for a so-called neuromorphic computing system are: the non-linearity of the active medium, the possibility of precise input state manipulation, scalability, energy efficiency and speed of operation. All of the above criteria are fulfilled by exciton-polariton quantum fluids of light [1,2,3]. This work demonstrates the first experimental realisation of a feed-forward exciton-polariton neural network optimised using a backpropagation algorithm, see Fig. 1 [4]. The backpropagation algorithm allows a significant improvement of the neural network performance. The presented method enables effective applications of polariton networks that contain only several neurons.

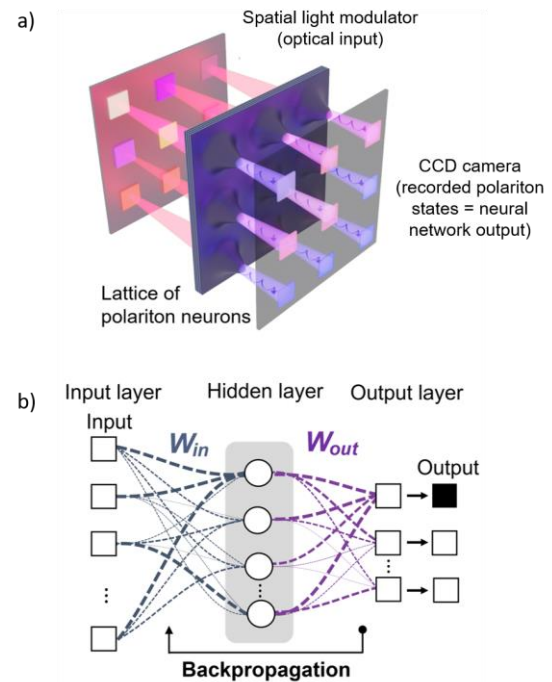


Fig.1 a) Scheme of the experimental configuration, b) schematic model of the considered exciton-polariton neural network.

- [1] D. Ballarini, A. Gianfrate, R. Panico, A. Opala et al. Nano Lett, 20, 5, 3506–3512 (2020)
- [2] R. Mirek, A. Opala, P. Comaron, M. Furman et al. Nano Lett. (2021)
- [3] A. Opala, S. Ghosh, T. C. H. Liew and M. Matuszewski, "Neuromorphic computing in Ginzburg-Landau lattice systems", Phys. Rev. Applied 11, 064029, (2019)
- [4] "Teaching a neural network with non-tunable exciton-polariton nodes" (in preparation)

Enhancement of THz detection by using an Asymmetric-Dual-Grating-Gate Graphene FET

Juan A. Delgado-Notario ^{1,2}, Vito Clericò ², Juan Salvador-Sanchez ², Jesús E. Velázquez-Pérez ², Jaime Calvo-Gallego ², Enrique Diez ², Takashi Taniguchi ³, Kenji Watanabe ³, Taiichi Otsuji ⁴, Yahya M. Meziani ² and Wojciech Knap ^{1,4,5}

¹CENTERA Laboratories, Institute of High-Pressure Physics PAS, Warsaw 01-142, Poland

²Nanolab, Universidad de Salamanca, Plaza de la Merced, Edificio Trilingüe, 37008, Salamanca, Spain

³National Institute of Material Sciences, 1-1 Namiki, Tsukuba, Ibaraki 305-0044, Japan

⁴Research Institute of Electrical Communication, Tohoku University, Sendai 980-8577, Japan

⁵Laboratory Charles Coulomb, University of Montpellier and CNRS, Montpellier F-34095, France

The unique optical and electronic properties of graphene based heterostructures open the way for the development of new graphene-based devices. Indeed, new hybrid graphene-based devices operating in the terahertz (THz) range are appealing since it is one of the least explored frequency regions [1,2] and their applications hold potential to revolutionize different fields like security, medical imaging, or high-speed wireless communication [3]. In this work, we report on an enhancement of the detection of terahertz radiation by using a graphene-based FETs with asymmetric dual grating gates (ADGG-GFET) and a few-layers thick of graphite as back gate. The device was fabricated with a stack of h-BN/Graphene/h-BN/Graphite on a standard SiO₂/Si substrate (Figure 1 (a)). The device was illuminated under 0.3 THz radiation from 4K up to room temperature and a clear photocurrent was measured while biasing with the top gate. Moreover, when a positive (or negative) voltage was applied on the few-layers graphite back-gate, we observed a clear enhancement of the measured photocurrent under illumination of the 0.3 THz radiation (Figure 1 (b)-(c)).

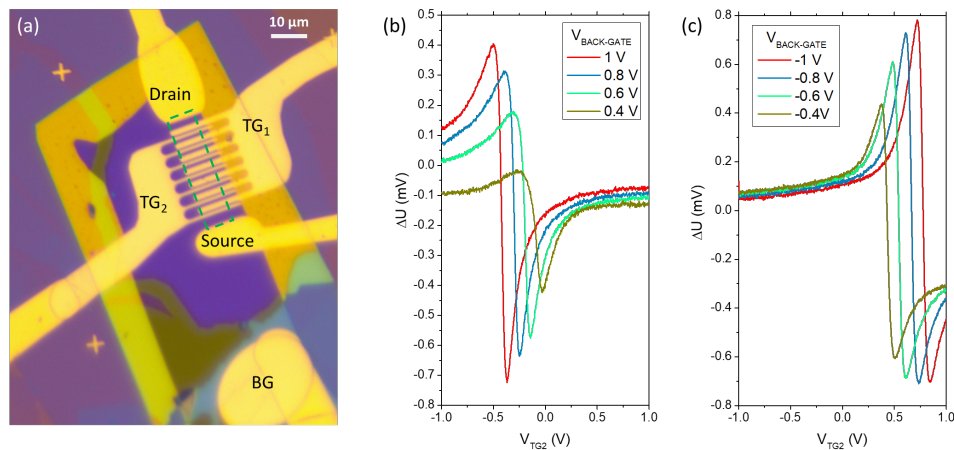


Figure 1. Optical image of the ADGG-GFET where the graphene sheet has been highlighted with a green dashed line (a) and the THz photoresponse as a function of the Top Gate 2 (TG₂) voltage for different positive (b) and negative (c) back-gate voltages under 0.3 THz. T = 77K.

- [1] J. A. Delgado-Notario, V. Clericò, E. Diez, J. E. Velázquez-Pérez, T. Taniguchi, K. Watanabe, T. Otsuji, and Y. M. Meziani, *APL Photonics* **5**, 066102 (2020).
- [2] S. Boubanga-Tombet, W. Knap, D. Yadav, A. Satou, D. B. But, V. V. Popov, I. V. Gorbenko, V. Kachorovskii, and T. Otsuji, *Phys. Rev. X* **10**, 031004 (2020).
- [3] M. Wang and E. H. Yang, *Nano-Structures and Nano-Objects* **15**, 107 (2018).

Graphene/AlGaIn/GaN FETs for sub-THz detection

M. Dub^{1,2,3}, P. Sai^{1,3,4}, D. B. But^{1,3,4}, M. Sakowicz², A. Przewłoka^{1,5}, A. Krajewska¹, P. Prystawko², I. Pasternak⁶, M. Haras^{1,4}, G. Cywiński¹, W. Knap^{1,4} and S. Rumyantsev¹

¹ CENTERA Laboratories, Institute of High Pressure Physics PAS, st. Sokolowska 29/37, Warsaw, Poland

² Institute of High Pressure Physics PAS, st. Sokolowska 29/37, Warsaw, Poland

³ Institute of Semiconductor Physics, NAS of Ukraine, pr. Nauki 41, Kyiv, Ukraine

⁴ CEZAMAT, Warsaw University of Technology, st. Poleczki 19, Warsaw, Poland

⁵ Institute of Optoelectronics, Military University of Technology, st. Sylwester Kaliskiego 2, Warsaw, Poland

⁶ Faculty of Physics, Warsaw University of Technology, ul. Koszykowa 75, Warsaw, Poland

Graphene (GR) is transparent for electromagnetic radiation in the very wide spectral range, including sub-terahertz and terahertz frequency ranges. Particularly, at frequency of 1 THz, graphene transmittance is ~ 96 percent [1]. This makes graphene very promising for such applications like opto-transistors and terahertz devices with transparent electrodes.

We report on GaN/AlGaIn fin-shaped field-effect transistors (FinFETs) with GR gate. Small gate area and narrow channel make this transistors promising for terahertz applications. FinFETs structures were fabricated using the technology described in details in Ref. [2]. GR gates were formed by high-speed electrochemical delamination method on pre-deposited metal pads which were used as the contacts to GR. Barrier height and ideality factor of GR/AlGaIn Schottky barrier found from current-voltage characteristics were $\phi_b = (1.0 - 1.26)$ eV and $(1.7 - 2.5)$, respectively.

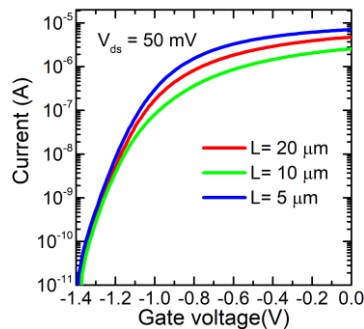


Fig. 1. Transfer characteristics of FinFETs with GR gate, channel width $W = 4 \mu\text{m}$ and gate length $L = 5, 10, 20 \mu\text{m}$

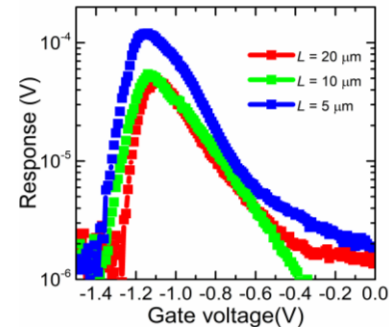


Fig. 2. Response of the same as in Fig. 1 GR/AlGaIn/GaN FinFETs to $f = 120 \text{ GHz}$ radiation at room temperature.

Characteristics of GaN/AlGaIn FinFETs with GR gate are shown in Fig. 1. The devices were characterized by 6 order of magnitude on/off ratio and subthreshold slope ~ 1.1 . Aging during 6 months did not indicate noticeable change in the current voltage characteristics. Measurements of the low frequency noise allowed us to extract the effective trap density responsible for noise, which was similar as for Ni/Au gate FinFETs. Results of detection at the frequency $f = 120 \text{ GHz}$ by FinFET with GR gate at room temperature are shown in Fig. 2. The signal peaks are located near the threshold voltage of investigated FinFETs.

To summarize, we have demonstrated that GR works well as a gate for AlGaIn/GaN transistors and can be used in multiple device configurations with transparent gate electrode. Particularly, studied in this work GR-gate FinFETs demonstrated good DC characteristics and effective detection at sub-terahertz frequencies. Combined properties of high transmittance in THz frequency range of GR, high sheet density of two-dimensional electron gas in GaN/AlGaIn, and fin shape of these devices make them promising for plasmonic THz detection.

[1] Choi, Hyun Joo, et al., Scientific Reports **7**, 42833 (2017)

[2] P. Sai, et al., Semicond. Sci. Technol. **34** 024002 (2019)

Hybrid Nanowires Comprising III-V Semiconductor Cores and Narrow Bandgap IV-VI Semiconductor Shells

J. Sadowski^{1,2}, P. Dziawa¹, W. Zajkowska¹, S. Dad¹, B. Seredyński³, W. Pacuski³, S. Kret¹

¹ Institute of Physics, Polish Academy of Sciences, Aleja Lotnikow 32/46, Warsaw, Poland

² Department of Physics and Electrical Engineering, Linnaeus University, Kalmar, Sweden

³ Faculty of Physics, University of Warsaw, Pasteura 5, Warsaw, Poland

Due to the nanoscale dimensions nanowire (NW) heterostructures enable combination of dissimilar materials without generation of misfit dislocations at their interfaces [1]. Here we exploit the possibility of obtaining tubular nanostructures consisting of thin IV-VI narrow bandgap semiconductor shells deposited by molecular beam epitaxy (MBE) on the sidewalls of III-V (Ga,In)As NW cores. As IV-VI shell material we have chosen $\text{Pb}_{1-x}\text{Sn}_x\text{Te}$ solid solution, which in the composition range $0.32 < x \leq 1$ has an inverted energy gap (at 4 K) and belongs to the family of topological crystalline insulators (TCI) [2]. $\text{Pb}_{1-x}\text{Sn}_x\text{Te}$ shells are deposited on the (1-210) sidewalls of wurtzite (WZ) (Ga,In)As NWs, grown in a separate III-V MBE system. The III-V NWs have been transferred (in air) to the IV-VI MBE system. Before the deposition of IV-VI shells the native oxide was thermally desorbed from III-V NW sidewalls by heating the samples to 590 °C in ultrahigh vacuum. The IV-VI shells were deposited at much lower temperatures (below 450 °C). We have grown the IV-VI shells with different compositions spanning from binary PbTe, through $\text{Pb}_{1-x}\text{Sn}_x\text{Te}$ solid solution with Sn content (x) increasing from 0.35, 0.55 up to 1 (binary SnTe). The samples are characterized by scanning electron transmission microscopy (STEM). The best quality of IV-VI shells has been obtained for binary PbTe, with the best lattice matching to WZ GaAs(1-210). The PbTe shells grow with (010) crystallographic planes parallel to (1-210) III-V NW sidewalls, with the following azimuthal orientations: $[001]_{\text{PbTe}} \parallel [0001]_{\text{GaAs}}$ III-V NW axis, $[100]_{\text{PbTe}} \parallel [-1010]_{\text{GaAs}}$ as shown Fig.1. In such configuration the lattice matching between PbTe shells and GaAs NW cores along the NW axis is quite good. The distances (d) between corresponding lattice planes of PbTe shells and GaAs cores are similar i.e., ($d_{(002)/\text{PbTe}} = 3.23 \text{ \AA}$, $d_{(0002)/\text{GaAs}} = 3.26 \text{ \AA}$); ($d_{(020)/\text{PbTe}} = 3.23 \text{ \AA}$, $d_{(-1010)/\text{GaAs}} = 3.44 \text{ \AA}$). This indicates that PbTe shells are under biaxial tensile strain. Such configuration can extend the composition range of IV-VI semiconductors with TCI properties, since recently, topological phase of ultrathin PbTe layers under tensile strain has been theoretically predicted [3].

This work has been supported by the National Science Centre Poland, through projects No: 2019/35/B/ST3/03381 and 2019/35/B/ST5/03434.

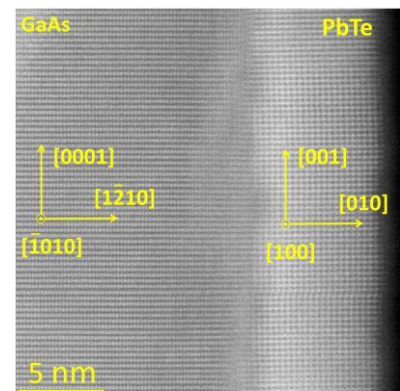


Fig. 1. STEM image of the outer part of GaAs[0001]NW with PbTe[001] shell.

[1] Elif Ertekin, P. A. Greaney, D. C. Chrzan, and Timothy D. Sands, *J. Appl. Phys.* **97**, 114325 (2005).

[2] Su-Yang Xu, et. al., and M.Z. Hasan, *Nat. Commun.* **3**, 1192 (2012).

[3] Yi-zhen Jia, et. al., *Phys. Chem. Chem. Phys.* **19**, 29647 (2017).

Resonance Fluorescence of Noisy Systems

Rafał A. Bogaczewicz, Paweł Machnikowski

*Department of Theoretical Physics, Wrocław University of Technology, Wybrzeże
Wyspiańskiego 27 50-370, Wrocław, Poland*

Resonance fluorescence (RF), originally studied in atomic systems, can also be observed in semiconductor quantum dots (QDs) [1]. It can be used e.g. for reading out quantum states of spins confined in QDs [2]. In this contribution we consider the spectrum of low-excitation RF for a single two - level QD, perturbed by fluctuating electrostatic environment (e. g. - charging and discharging traps in the vicinity of the QD) that randomly shifts the transition energy $\hbar\omega_0$. We consider the case of the telegraph noise (TN), when the detuning $\Delta = \omega_L - \omega_0$ (ω_L is a laser frequency) takes two possible values, $\Delta_h = \bar{\Delta} + \frac{\Delta_0}{2}$ and $\Delta_l = \bar{\Delta} - \frac{\Delta_0}{2}$. The rates of transitions $\Delta_l \rightarrow \Delta_h$ and $\Delta_h \rightarrow \Delta_l$ are defined, respectively by β_\uparrow and β_\downarrow . The spectrum of scattered light is transmitted by a Lorentzian filter. We present results for both symmetric (STN) (where $\beta_\uparrow = \beta_\downarrow = \beta$) and assymetric TN (ATN) cases with different $\bar{\Delta}$ values. Moreover, dependence between spectrum intensity and $\bar{\Delta}$ is shown.

We iteratively solve the equations of motion for the density matrix of a two-level system driven by a weak, classical light field. Then, the two-time correlation function for any time-dependent detuning $\Delta(t)$ is found with the quantum regression theorem. The RF spectrum $F(\omega)$ is obtained in the standard way as its Fourier transform. The observed spectrum, $\tilde{F}(\omega)$, is a convolution of $F(\omega)$ with the filter function.

For the case of STN with $\bar{\Delta} = 0$, we show that the spectrum evolves as a function of β from a single sharp (as compared to the exciton life time) line for small β , via a triplet of broadened lines for β comparable with the life time, back to a sharp line for a large β . This demonstrates that the time scales of environmental fluctuations are reflected in the qualitative features of the RF spectrum for a single emitter. When $\bar{\Delta} \neq 0$, two side peaks (for $\beta \leq \frac{\Delta_0}{2}$) or a merged peak (for $\beta \geq \frac{\Delta_0}{2}$) are shifted from the central peak (responsible for a RF) to the left by $\bar{\Delta}$. We show that the total scattering intensity I_{tot} qualitatively depends on β . In the quasi-static state (low β), the scattering is efficient whenever the laser is resonant with one of the two transition energies between which the system is switching. In contrast, for fast switching, there is only one I_{tot} maximum as a function of the laser frequency, corresponding to the averaged transition energy.

We also extended our considerations to the ATN case.

- [1] A. N. Vamivakas *et al.*, *Nat. Phys.* **5**, 198 (2009).
- [2] A. Delteil *et al.*, *Phys. Rev. Lett.* **112**, 116802 (2014).

Limitations on Maximal Level of Entanglement of Two Singlet-Triplet Qubit States in GaAs Gated Quantum Dots

Igor Bragar and Łukasz Cywiński

Institute of Physics, Polish Academy of Sciences, al. Lotników 32/46, Warszawa, Poland

Singlet-triplet qubits created by electric gates in an GaAs-AlGaAs heterostructure can be initialised, entangled and read out [1, 2], and therefore they are a promising physical realisation of a quantum-information hardware in a solid-state system.

We have analysed in detail a procedure of entangling of two singlet-triplet qubits (labeled with $i = 1, 2$) that were operated in a regime when energy associated with magnetic field gradient $\Delta B_{z,i}$ is an order of magnitude smaller than exchange energy between singlet and triplet states J_i [1]. We consider the impact of fluctuating J_1, J_2 on the resulting two-qubit state and its degree of entanglement. Although direct impact of the quasistatic fluctuations of J_1, J_2 on the resulting two-qubit state can be completely removed by utilising a proper desing of entangling procedure (simultaneous Hahn echo sequence on each qubit), the entangling interaction between qubits, which is determined by two-qubit interaction energy $J_{12} \propto J_1 J_2$, remains sensitive to the fluctuations, so the efficiency of the entangling procedure decreases with increasing its duration τ (see Fig. 1). Moreover, it is known that for the experimental device the spectrum of charge noise, which drives dynamical fluctuations of J_1, J_2 , is described by a power law function $1/f^\beta$ with $\beta \approx 0.7$ [2]. In connection to that we have studied the impact of correlated and uncorrelated charge noises on the two-qubit state. It turned out that the level of correlation of charge noises as well as their exact functional form (value of parameter β) translates in a distinctive manner on the shape of decay of two-qubit entanglement as a function of procedure duration τ (see Fig. 2, 3). Comparison of experimental data with our theoretical estimates points out that the case of uncorrelated charge noise in the qubits is realised in the experiment. We can also conclude that the main reason of decreased level of entanglement of the resulted two-qubit state is infidelity of single-qubit operations, whereas contribution of non-ideal two-qubit gate is negligible in considered entangling procedure.

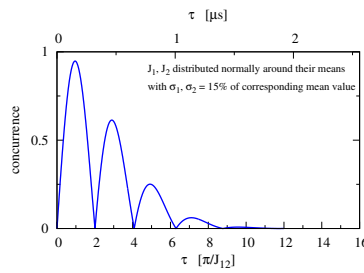


Figure 1: Case of quasi-statically fluctuating J_1, J_2 .

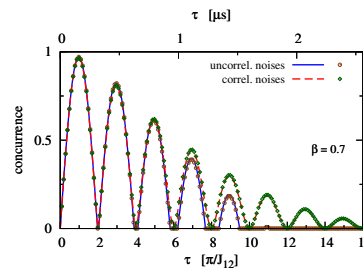


Figure 2: Case of dynamically fluctuating J_1, J_2 with spectral density $1/f^{0.7}$.

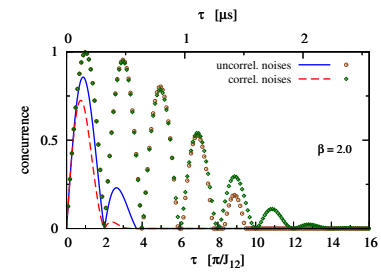


Figure 3: Case of dynamically fluctuating J_1, J_2 with spectral density $1/f^{2.0}$.

This research has been supported by Polish National Science Centre (NCN), grant no. DEC-2012/07/B/ST3/03616.

[1] M. D. Shulman, O. E. Dial, S. P. Harvey, H. Bluhm, V. Umansky, and A. Yacoby, *Science* **336**, 202 (2012).

[2] O. E. Dial, M. D. Shulman, S. P. Harvey, H. Bluhm, V. Umansky, and A. Yacoby, *Phys. Rev. Lett.* **110**, 146804 (2013).

Thermal stability of emission from single symmetric InAs/InP quantum dots emitting in the telecom C-band

Maja Wasiluk¹, Monika Mikulicz¹, Anna Musiał¹, Andrei Kors²,
Johann P. Reithmaier², Grzegorz Sęk¹, Mohamed Benyoucef²

1 - Laboratory for Optical Spectroscopy of Nanostructures, Department of Experimental Physics,
Wrocław University of Science and Technology, Wybrzeże Wyspiańskiego 27, Wrocław, Poland

2 - Institute of Nanostructure Technologies and Analytics, Center for Interdisciplinary Nanostructure
Science and Technology, University of Kassel, Heinrich-Plett-Str. 40, Kassel, Germany

Self-assembled semiconductor quantum dots (QDs) considered as potential emitters in non-classical light sources are extensively investigated for the last decades [1] and have proven being advantageous in comparison to other approaches in terms of single-photon purity [2, 3]. For long-distance communication and ultra-secure quantum communication using standard telecom fibers, emission in the C-band (1.55 μm) is required, therefore the appliance of InAs/InP QDs is considered. Likewise, room temperature operation is desirable for practical use. This requirement is hard to fulfill in III-V QDs emitting at telecom wavelengths due the limited depth of confining potential, but it is important to investigate thermal stability of their emission to identify the main photoluminescence (PL) quenching channels which could possibly be engineered.

In this contribution we experimentally study the temperature dependence of (micro)PL emission from single QDs as well as the QDs' ensemble of highly symmetric low-density InAs/InP QDs emitting in the 3rd telecommunication window. These nanostructures are grown by applying the ripening process [4, 5] during the epitaxial growth (MBE) resulting in QDs featuring a negligible fine-structure splitting, which makes them suitable for sources of entangled photon pairs [6, 7]. The emission from single QDs was visible up to a temperature of 150K, which is promising for use of these structures at elevated temperatures and thus allows for cheaper cooling methods. Besides, the possible mechanism of emission quenching and interaction between excitons confined in quantum dots and phonons in the surrounding bulk material were studied and quantitatively analyzed. The main PL quenching mechanism was identified to be carrier promotion to higher energy QD states with activation energies in the single meV range related to the escape of holes and around 20 meV related to the escape of electrons. For single cases PL intensity increases in low temperature range which can be associated with thermal activation of carriers from a reservoir (defects/charge traps in the QDs' vicinity) and their re-capture by the QDs [8]. Activation energies for this process were in the range (21–65) meV. This initial increase in emission intensity was observed also for QDs' ensemble together with decrease in intensity of emission band observed at approx. 1350 nm (possibly from defects in bulk material) coinciding in the temperature range. This relative intensity change leads to the conclusion about the possible transfer of carriers between QD and the surrounding semiconductor matrix.

- [1] Y. Arakawa et al., *Appl. Phys. Rev.* **7**, 021309 (2020).
- [2] L. Schweickert et al., *Appl. Phys. Lett.* **112**, 093106 (2018).
- [3] T. Miyazawa et al., *Appl. Phys. Lett.* **109**, 132106 (2016).
- [4] M. Yacob et al., *Appl. Phys. Lett.* **104**, 022113 (2014).
- [5] M. Benyoucef et al., *Appl. Phys. Lett.* **103**, 162101 (2013).
- [6] A. Musiał et al., *Adv. Quantum Technol.* **3**, 1900082 (2019).
- [7] A. Kors et al., *Appl. Phys. Lett.* **112**, 172102 (2018).
- [8] F. Olbrich et al., *J. Appl. Phys.* **121**, 184302 (2017).

Single-photon emission from InGaAs/GaAs quantum dots in 1.3 μm telecommunication range

Agata Zielińska¹, Anna Musiał¹, Tobias Heuser³, Nicole Srocka², David Quandt²,
André Strittmatter^{2†}, Sven Rodt², Stephan Reitzenstein², and Grzegorz Sęk¹

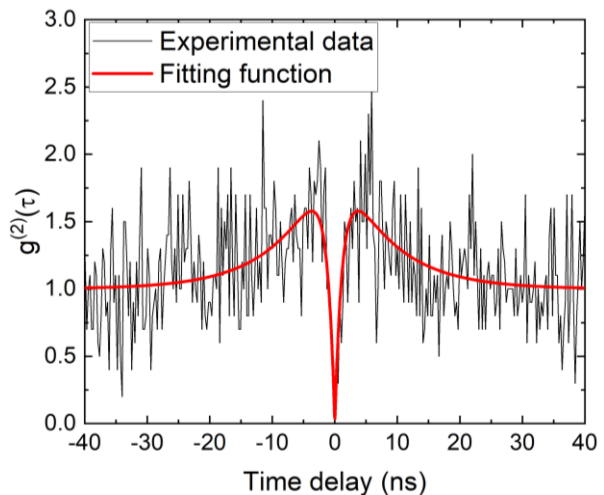
¹ Department of Experimental Physics, Wrocław University of Science and Technology,
Wybrzeże Wyspiańskiego 27, 50-370 Wrocław, Poland

² Institute of Solid State Physics, Technical University of Berlin, Hardenbergstraße 36, D-
10623 Berlin, Germany

[†] Present address: Institute of Experimental Physics, Otto von Guericke University
Magdeburg, D-39106 Magdeburg, Germany.

Epitaxial quantum dots (QDs) based single-photon sources are of great significance for developing secure quantum communication networks [1]. They offer the highest single-photon purity [2,3], are compatible with semiconductor technology and with currently existing fiber networks if a proper material system is selected, so the source operates at telecommunication wavelengths. Telecom O-band (1260-1360 nm) is highly desirable for local quantum networks and offer lack of distortion of optical signal (no dispersion).

We report an experimental study of optical properties of self-assembled $\text{In}_{0.75}\text{Ga}_{0.25}\text{As}$ QDs on GaAs substrate grown in Stranski-Krastanow mode by metal-organic chemical vapor deposition [4]. QDs are covered by an $\text{In}_{0.2}\text{Ga}_{0.8}\text{As}$ strain reducing layer for redshifting the emission to 1.3 μm . Nondeterministic cylindrical mesa structures of diameters in the range of (300–2100) nm and 670 nm height are fabricated on the sample surface using electron-beam lithography and reactive ion etching (ICP-RIE). Preliminary optical characterization of single QDs was carried out by means of microphotoluminescence (μPL) in order to find the best candidates for single-photon sources - single high-intensity emission lines well spectrally-separated and with low background emission level. Spectral resolution of used μPL setup was about 50 μeV . All measurements were carried out in temperature of 5K and under continuous wave nonresonant excitation. Selected emission lines were further investigated by excitation power-dependent and polarization-resolved μPL for excitonic complexes identification. Single-photon emission purity was determined by second-order correlation function - $g^{(2)}(\tau)$, measurements (autocorrelation) in Hanbury-Brown and Twiss fiber setup with a pair of superconducting NbN nanowire single-photon detectors preceded by 0.32 m focal-length monochromator used as spectral filter. In the best case antibunching with $g^{(2)}(0)=0.1$ is visible and proves single-photon emission (figure 1). Bunching observed for longer time delays can be caused by metastable states taking part in the dynamics.



- [1] P. Michler, Quantum Dots for Quantum Information Technologies, Springer (2017).
- [2] L. Schweickert et al., *Appl. Phys. Lett.* **112**, 093106, 1-4 (2018).
- [3] T. Miyazawa et al., *Appl. Phys. Lett.* **109**, 132106, 1-4 (2016).
- [4] P. Mrowiński et al., *Phys. Rev. B* **100**, 115310 (2019).
- [5] Ł. Dusanowski et al., *Opt. Express* **25**, 31122-31129 (2017).

Carrier separation effects in type-II Cd(Se,Te)/ZnTe self-assembled QDs

**P. Baranowski¹, P. Wojnar¹, M. Szymura¹, J. Plachta¹, S. Chusnutdinow¹,
G. Karczewski¹, and T. Wojtowicz²**

¹ Institute of Physics, Polish Academy of Sciences, 02-668 Warsaw, Poland

² International Research Centre MagTop, Institute of Physics, Polish Academy of Sciences,
02-668 Warsaw, Poland

In type II heterostructures it is more favorable for electrons to enter into another semiconductor than for holes. As a result, carrier separation at the interface takes place.

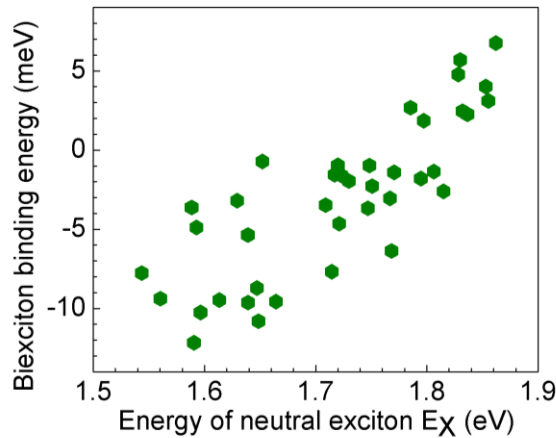


Figure 1 The biexciton (XX)-binding energy (exciton emission energy E_X minus XX emission energy, E_{XX}) plotted versus E_X . Gradual increase of biexciton-binding energy with increasing E_X is an effect of electron-hole spatial separation at type II interface.

emission lines associated to multiexcitonic complexes appear. Interestingly, the spectral distance between single exciton and biexciton lines depends strongly on the Se concentration within the dot. When increasing Se concentration the spectral position of biexcitonic line E_{XX} shifts gradually toward the spectral position of single excitonic line E_X . At a certain Se concentration the biexciton binding energy, defined as $E_X - E_{XX}$, changes its sign and the biexciton line appears at higher energies compared to single excitonic emission. In Figure 1, the biexciton binding energy is plotted vs. the spectral position of the single exciton line for several individual (Cd,Se)Te/ZnTe QDs with various Se concentrations. In the case of low Se concentrations when the emission energy is above 1.8 eV, the biexciton binding energy is positive, whereas it is negative for the dots emitting at energies below 1.7 eV.

The observed effect can also be explained in terms of type I to type II band alignment transition occurring as a result of Se incorporation into CdTe quantum dots. The larger the electron – hole separation at the dot/barrier interface, the stronger the Coulomb repulsion between the two excitons forming the biexcitonic complex [1].

[1] P. Baranowski, M. Szymura, G. Karczewski, A. Rodek, T. Kazimierczuk, P. Kossacki, T. Wojtowicz, J. Kossut, and P. Wojnar, *Appl. Phys. Lett.* **117**, 113101 (2020)

This work has been partially supported by the National Centre of Science (Poland) through grant 2017/26/E/ST3/00253, and by the Foundation for Polish Science through the IRA Programme co-financed by EU within SG OP.

ODMR studies of interfaces of (Cd,Mn)Te/(Cd,Mg)Te QWs

A. Lopion, A. Bogucki, W. Kraśnicki, K. E. Połczyńska, W. Pacuski,
P. Kossacki and A. Golnik*Faculty of Physics, Institute of Experimental Physics, University of Warsaw, ul.
Pasteura 5, 02-093 Warszawa, Poland*

Magnetic ions incorporated in the nanostructures give an extraordinary opportunity to study the local properties of the crystal lattice via the optical properties of the sample. The energy levels of the Mn^{2+} ions are sensitive to the deformation of the lattice and can be studied with the use of the absorption of microwave radiation. Due to the significant exchange interaction between the Mn^{2+} ions and photocarriers in (Cd,Mn)Te an useful local technique is optically detected magnetic resonance (ODMR). ODMR exploits the fact that the optical properties of studied material change when paramagnetic resonance occurs. In our case, we observe the change of the energy shift of excitonic lines in the magnetic field - the change of the giant Zeeman shift under the microwave radiation. The ODMR lets us examine properties of the quantum well (QW) structures locally, in the layer where the magnetic ions are incorporated and can be extremely useful for the study of the formation of the interfaces in the QWs.

Here we present the time-resolved ODMR studies of single (Cd,Mn)Te/(Cd,Mg)Te QWs. A series of QWs was grown by Molecular Beam Epitaxy with the modulation of the magnetic ions content. Restricting the Mn^{2+} ion doping either to the middle of the QD or to the area near the interfaces allows us to probe the strain in the structure locally. Probing different parts of the structure in the ODMR experiment requires the utilization of different excitonic states to ensure high overlap with the magnetic ions. The reflectivity spectra for each studied QW exhibit several distinct features related to excitonic complexes of electrons and holes at higher QW sub-bands. In contrast to the ground state, the maximum amplitude of their wavefunction at a distance from the center of the QW. Indeed, our experimental results confirm that in the samples doped in the interface region the amplitude of the ODMR signal is stronger on the excited states of the QW exciton.

The temporal resolution was achieved by using pulses of microwave excitation and probing the reflectance with AOM modulated supercontinuum laser pulses. The dynamics of magnetization, thus spin-lattice relaxation time, was measured by varying the delay between the microwave pulse and the optical readout of the magnetization state. We observe that the spin-lattice relaxation rate is very similar for magnetic ions localized in the middle of the QW and on the interfaces. Thus, we conclude that the QW is strained homogeneously in the growth. Additionally, we find that the spin-lattice relaxation rate changes non-monotonically with the magnetic field with the minimum at the magnetic field of about 0.5 T.

Manipulation of the electric state of QDs with single magnetic dopants

K. E. Połczyńska, A. Rodek, K. Oreszczuk, Ł. Zinkiewicz, T. Kazimierczuk,
Z. Ogorzałek, P. Kossacki and W. Pacuski

Faculty of Physics, University of Warsaw, Pasteura 5, Warsaw, Poland

Zero-dimensional semiconductor structures such as epitaxial quantum dot (QD) is a model system to probe fundamental interactions in condensed matter. For example, QD can be used to examine the spin of a single magnetic ion [1-5] and its charge fluctuation [4]. Aim of this work is to increase control of the quantum state of the system QD+magnetic dopant. It can be obtained for example by applying an electrical field [5].

In this work, we investigate epitaxial CdSe QDs in ZnSe barriers, doped with a single Fe [3] as a magnetic dopant. We present microluminescence measurements as a function of the electric and magnetic fields. Fixing the voltage provides the selection of the electrical state of a QD and enables the measurement of magnetic properties of chosen state. Such procedure repeated for different voltages provides access to multiple facilities of the quantum system. It becomes extremely useful if investigated QD contains a single dopant, which electric state can be changed deterministically. As we can see in Fig. 1, such a procedure allows a slightly change in the energy of the state of the QD. We can also determine and intentionally change the charge state of the whole quantum dot. When it comes to QDs doped with magnetic ions, there is a chance to change the electrical state of the single dopant.

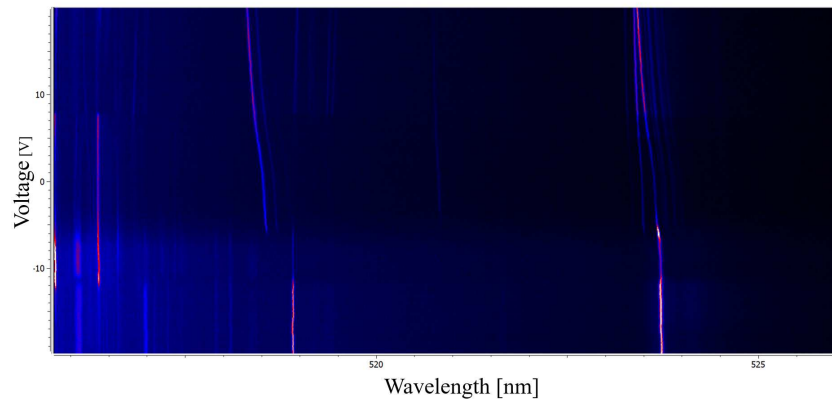


Figure 1: Photoluminescence signal as a function of the applied voltage. While changing the electric state of the QD, their energies and number of lines change.

- [1] L. Besombes et al, *Phys. Rev. Lett.* **93**, 207403 (2004).
- [2] J. Kobak et al, *Nat. Commun.* **5**, 3191 (2014).
- [3] T. Smoleński et al, *Nat. Commun.* **7**, 10484 (2016).
- [4] L. Besombes et al, *Phys. Rev. B* **99**, 035309 (2019).
- [5] Y. Leger et al, *Phys. Rev. Lett.* **97**, 107401 (2006).

Thermal Stability and Single-Photon Emission from GaAs-based Quantum Dots emitting at 1.3 μm

Marek Burakowski¹, Paweł Holewa¹, Anna Musiał¹, Nicole Srocka², David Quandt²,
André Strittmatter^{2,3}, Sven Rodt², Stephan Reitzenstein², and Grzegorz Sęk¹

¹Laboratory for Optical Spectroscopy of Nanostructures, Department of Experimental Physics, Faculty of Fundamental Problems of Technology, Wrocław University of Science and Technology, Wybrzeże Wyspiańskiego 27, 50-370 Wrocław, Poland

²Institute of Solid State Physics, Technische Universität Berlin, Hardenbergstraße 36, 10623 Berlin, Germany

³Present address: Institute of Experimental Physics, Otto-Von-Guericke-Universität Magdeburg, 39106 Magdeburg, Germany

Vast progress during the last two decades has been made in the engineering of semiconductor quantum dots (QDs) as non-classical light sources [1]. Numerous desired quantum photonic applications, such as long-haul secure optical data transmission, require a source of single photons operating at elevated temperatures (not requiring extensive cryogenic cooling systems) and at the telecom bands with minimal losses in fiber transmission.

Hereby, we present investigation of thermal stability of single-photon emission of the metalorganic vapour-phase epitaxy-grown InGaAs/GaAs QDs with strain reducing layer emitting at 1.3 μm deterministically embedded into mesa structures. We demonstrate that their single-photon emission ($g^{(2)}(0)$ from fit lower than 0.01 at 5 K) [2] is preserved up to 50 K with $g^{(2)}(0)$ from fit equal to 0.13 (reduced at higher temperature due to contribution of uncorrelated background emission) and emission from single quantum dots - at least up to 80 K (liquid nitrogen accessible) [3]. We also observed a decrease of antibunching time constant with increasing temperature. It reflects increase of the effective pump rate with temperature related with increase of laser excitation power (to counteract thermal quenching of intensity) and with thermally activated additional carriers. For identification and initial characterization of excitonic complexes, polarization-resolved and excitation-power-dependent microphotoluminescence measurements were performed. Investigated temperature quenching for neutral complexes and negatively charged trion behaves quantitatively different to X^+ (which was chosen for correlation measurements) for which trapped holes in the vicinity of QD are acting as temperature activated reservoir of carries which manifests itself in initial increase of the emission intensity up to 40 K and hence improve thermal stability of our source. Comparison of our findings with reported results of 8-band $k\text{-p}$ calculations for such dots [4] yields that the main mechanism for temperature quenching is the excitation of holes to higher QD states in the valence band with activation energies of approximately 20-30 meV.

Our results indicate and it has already been proven that these structures are adequate for building compact and cryogen-free single-photon source at telecom O-band [4].

- [1] P. Michler, „Quantum Dots for Quantum Information Technologies“, *Springer International Publishing* (2017).
- [2] Ł. Dusanowski et al., „Triggered high-purity telecom-wavelength single-photon generation from p-shell-driven InGaAs/GaAs quantum dot“, *Opt. Express*, **25**, 31122-31129 (2017)
- [3] P. Holewa et al., „Thermal stability of emission from single InGaAs/GaAs quantum dots at the telecom O-band“, *Sci. Rep.*, **10**, 21816 (2020).
- [4] P. Podemski et al., „Interplay between emission wavelength and s-p splitting in MOCVD-grown InGaAs/GaAs quantum dots emitting above 1.3 μm “, *Appl. Phys. Lett.* **116**, 023102 (2020).
- [5] A. Musiał et al., „Plug&Play Fiber-Coupled 73 kHz Single-Photon Source Operating in the Telecom O-Band“, *Adv. Quant. Techn.*, **3**(6), 2000018 (2020).

InAs quantum dots grown on metamorphic buffer layer as single-photon sources at third telecommunication window

Paweł Wyborski¹, Piotr A. Wroński², Anna Musiał¹, Paweł Podemski¹, Fauzia Jabeen^{2,3},
Sven Höfling² and Grzegorz Sęk¹

¹ OSN Laboratory, Department of Experimental Physics,
Faculty of Fundamental Problems of Technology,

Wrocław University of Science and Technology, Wrocław, Poland

² Technische Physik, University of Würzburg and Wilhelm-Conrad-Röntgen-Research Center
for Complex Material Systems, Würzburg, Germany

³ QLM, Quantum Light and Matter group, Faculty of Engineering and Physical Sciences,
University of Southampton, Southampton, United Kingdom

Semiconductor quantum dots (QDs) emitting in the third telecommunication window are promising candidates for non-classical single-photon sources required for long-haul quantum communication, due to their compatibility with the existing silica-fibre-based telecom networks. Widely studied epitaxially-grown InAs/GaAs QDs have proved excellent optical properties based on the very mature growth technologies [1]. Although these QDs are recognized as near-perfect single-photon emitters for quantum information processing purposes, it is challenging to achieve the emission at 1.5 μm in this material system [2]. For these dots the possibility of creating single-photon sources at telecom C-band (~ 1550 nm) using metal-organic vapour-phase epitaxy (MOVPE) with a metamorphic buffer layer was recently demonstrated [3].

Here, we concentrate on InAs QDs grown on a GaAs substrate with a gradient metamorphic buffer layer (MBL) by molecular beam epitaxy (MBE) with sub-monolayer precision. Implementation of the additional layer with graded indium content varying from 6% to 42% offers redshift of emission energy up to the third telecommunication window.

Based on the microphotoluminescence (μPL) measurements with high spatial resolution, we observed sharp emission lines related to the emission from single QDs. The excitation-power-dependent and the polarization-resolved μPL characterization allowed for the identification of a bright μPL line (~ 1538.4 nm) as a charged exciton radiative recombination. We present the results of second-order autocorrelation $g^2(t)$ function measurements in Hanbury Brown and Twiss experiment showing a clear antibunching dip with the as-measured $g^2(t)$ value at the zero delay below 0.21 and the value of 0.05 after correction and deconvolution, confirming the single-photon character of emission. Additional measurements of time-resolved photoluminescence revealed the charged exciton lifetime of 1.95 ns. Based on that, we can estimate value of the fundamental limit of the emission rate for the investigated structures at around 0.5 GHz.

There is acknowledged a support from the Polish National Agency for Academic Exchange.

[1] P. Senellart, G. Solomon and A. White, *Nat. Nanotechnol.* **12**, 11 (2017).

[2] Y. Arakawa and M. J. Holmes, *Appl. Phys. Rev.* **7**, 2 (2020).

[3] S. L. Portalupi, M. Jetter and P. Michler, *Semicond. Sci. Technol.* **34**, 053001 (2019).

Optical emission from ultra-thin CdTe nanowires

J. Plachta¹, P. Wojnar¹, T. Kazimierczuk², P. Kossacki², G. Karczewski¹
T. Wojtowicz³ and J. Kossut¹

¹ Institute of Physics, Polish Academy of Sciences, Aleja Lotników 32/46, PL-02-668 Warsaw, Poland

² Institute of Experimental Physics, Faculty of Physics, University of Warsaw,
ul. Pasteura 5, PL-02-093 Warsaw, Poland

³ International Research Centre MagTop, Aleja Lotników 32/46, PL-02-668 Warsaw, Poland

Cadmium telluride nanowires (NWs) are grown in a system for molecular beam epitaxy by employing the vapor-liquid-solid growth mechanism assisted with gold catalysts. Subsequently, in a process of thermal reevaporation, NWs are thinned down to diameters *even below 10 nm*. In the final step, a (Cd,Mg)Te passivation shell is deposited in order to obtain an efficient optical emission.

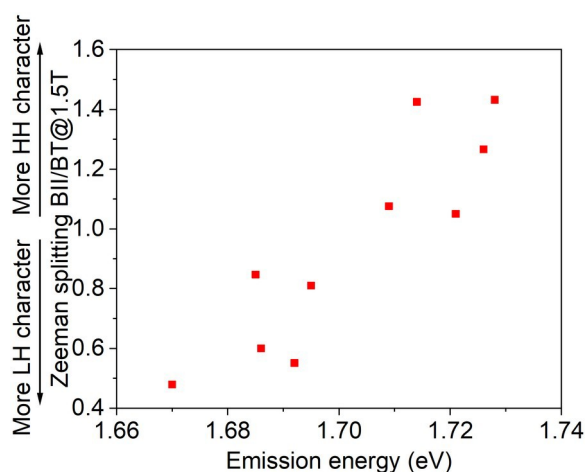


Figure 1. Zeeman splitting ratio of excitonic emission between parallel and perpendicular magnetic fields, measured in 1.5 T. A clear dependence can be observed, with a degeneracy point at around 1.705 eV.

It is found, that the excitonic lines appear in the spectral range from 1.6 eV up to 1.8 eV. Based on our cathodoluminescence (CL) study, we find that the emitting objects can be significantly shorter than the nanowires themselves. Moreover, the emitter region length can be correlated with emission energy, where shorter regions emit in higher energy. Additionally, at relatively high fluencies, a significant blueshift of the emission is observed, which indicates an existence of excited states.

A detailed magneto-optical study performed on several individual nanowires reveals that the valence band landscape depends strongly on the emitter energy and therefore on the size. The insight into these properties is gained by investigating the Zeeman splitting in a magnetic field applied

parallel and perpendicular to the nanowire axis. The nanowires emitting at relatively low energy exhibit a light hole character, whereas the admixture of heavy holes increases with increasing emission energy. This finding indicates competition between strain, promoting light hole excitons, and confinement effects, promoting heavy hole excitons.

Finally, in the structures exhibiting light hole excitonic emission, a distinct emission is found in low excitation power regime. The emission intensity grows superlinearly and is separated from excitonic emission by a few meV, indicating a rare observation of light hole biexciton.

This research was partially supported by the National Centre of Science (Poland) through grant 2017/25/N/ST3/00621, and by the Foundation for Polish Science through the IRA Programme co-financed by EU within SG OP (grant No. MAB/2017/1).

Optical Properties of ZnO Deposited by Atomic Layer Deposition on Sapphire: A Comparison of Thin and Thick Films

A. Adhikari¹, E. Przezdziecka¹, S. Mishra¹, P. Sybilski¹, J. Sajkowski¹, E. Guzewicz¹

¹*Institute of Physics, Polish Academy of Sciences, Al. Lotników 32/46,
02-668 Warsaw, Poland*

Zinc oxide (ZnO) is a wide direct bandgap (3.37eV) semiconductor that has versatile applications in photodetectors, biosensor, optoelectronic devices, etc. ZnO thin films can be deposited by atomic layer deposition (ALD) at a growth temperature of 200°C and below, which is essential for such applications as hybrid organic/inorganic junctions. In the present studies we investigated optical properties of thin (~100 nm) ZnO films and compared them to thick (~1 μm) layers deposited on sapphire substrates by ALD technique at a temperature from 100°C to 300°C. It was found that the thickness of ZnO layer, growth temperature, and post-growth annealing influence both the optical bandgap and Urbach energy. For both thin and thick *as grown* ZnO/Al₂O₃ films, the absorption edge was shifted according to the Burstein–Moss effect [1,2], while in case of annealed films this effect was not visible. The corrected bandgap of ZnO films, calculated excluding the Burstein-Moss effect, strongly depends on the growth temperature rather than the thickness of ZnO film, and it decreased with an increase of growth temperature. Post-growth annealing led to an increase of the energy gap and decrease of Urbach energy. The behavior of the corrected band gap can be understood in terms of oxygen vacancy that occurs in different concentrations in layers grown at different temperature and might be involved in the Zn_i-V_O and/or Zn_i-V_O-H complexes providing shallow donor states.

It was observed that thicker and annealed samples show more intensive and narrower PL bands, which can be assigned to donor and acceptor bound excitons, free electrons to acceptors, and donor-acceptor pairs transitions. Their energy position and relative intensity depend on the applied growth temperature i.e. they are different for O-rich to Zn-rich growth conditions.

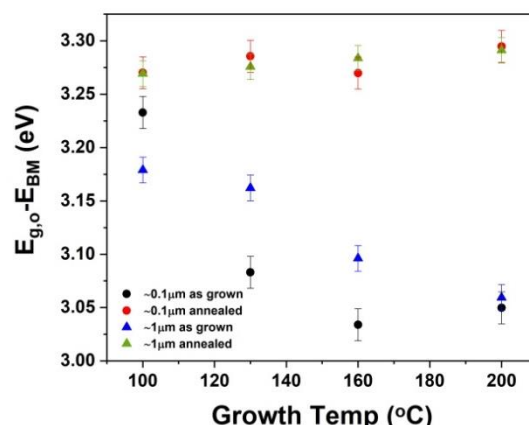


Fig 1. Intrinsic bandgap in thin and thick ZnO layers grown at different temperature

The work was supported by the Polish NCN project DEC-2018/07/B/ST3/03576.

- [1] A. Adhikari, E. Przezdziecka, S. Mishra, P. Sybilski, J. Sajkowski, E. Guzewicz, *Phys. Status Solidi Appl. Mater. Sci.* **2021**, *1*, 2000669.
- [2] E. Przezdziecka, E. Guzewicz, D. Jarosz, D. Snigurenko, A. Sulich, P. Sybilski, R. Jakiela, W. Paszkowicz, *J. Appl. Phys.* **2020**, *127*, 075104.

Structural and excitonic analysis of the ZnO/MgO superlattices on a-polar ZnO substrates grown by MBE

M. Stachowicz¹, A. Wierzbicka¹, J.M. Sjakowski¹, M.A. Pietrzyk¹, P. Dłużewski¹,
E. Dynowska¹, S. Magalhaes², E. Alves², A. Kozanecki¹

¹*Institute of Physics, Polish Academy of Sciences, Al. Lotników 32/46 PL-02-668 Warsaw, Poland*

²*Instituto de Plasmas e Fusão Nuclear, Instituto Superior Técnico, Universidade de Lisboa, 1049-001 Lisboa, Portugal*

Zinc oxide (ZnO) is attracting a tremendous interest for its numerous potential applications in optoelectronics [1], for it is a wide bandgap semiconductor (3.37 eV at room temperature) with a high exciton binding energy of 60 meV, which can increase in ZnMgO/ZnO/ZnMgO quantum wells (QWs) up to 100 meV or more [2]. Due to the high free-exciton binding energy, excitonic emission processes can persist at room temperature. For epitaxial growth of ZnO related films and quasi-ternary alloys, reducing the strains and dislocations is critical. Thereby closely lattice-matched substrates, which are ZnO substrates, are beneficial for two-dimensional growth and enhanced electric, optical and structural properties [3]. Nevertheless of alluded above advantages of growths on single crystal ZnO substrates, obtaining such ZnO epilayers and ZnO/ZnMgO structures without phase separation is still a challenging issue, especially in the case of non-polar orientations, where crystal quality is still poor. Very few works have reported the growth of a-plane ZnMgO layers until now, and the state-of-the-art random alloys are mainly restricted to low thickness and low Mg content (below 30%) [3]. The use of non-polar ZnO substrates simplifies the analysis of the properties of QS, because they are free of internal electric fields and therefore, the observed processes of exciton recombination are not affected by the quantum-confined Stark effect (QCSE) [3].

The aim of this work is a detailed study of non-polar short period MgO/ZnO SLs grown on *a*-ZnO bulk crystalline substrates, and to find out how thicknesses of the MgO layers, in the SLs consisting of 30 pairs of thin (1- 2.5 nm) ZnO quantum wells and (1-3 nm) MgO barrier layers, correlate to the mean content of Mg, whether possible is retaining of WZ structure, and how it affects forming multi-quantum well structures and theirs PL emission. The detailed structural and optical analysis of subjected ZnO/MgO quasi-ternary alloys in form of superlattices allowed to study the influence of different phases of ZnO and MgO on the interface's abruptness. We found that the wurtzite structure is retained in the MgO thin barriers up to 2 nm, but some diffusion of Mg from barriers to ZnO QW's was inevitable as well as the presence of biaxial strains. As a result, a subtle, the size of three monolayers, ZnMgO film is created at the interfaces, which is partly responsible for retaining the wurtzite structure of completely strained MgO layers.

Acknowledgements: The project was supported by the Polish National Science Centre (NCN) based on the decision No: DEC-2018/28/C/ST3/00285.

- [1] M.A. Pietrzyk, M. Stachowicz, et al., Journal of Crystal Growth, 408 (2014) 102-106.
- [2] H. D. Sun, T. Makino, et. al, Jour. Appl. Phys., 91 (2002) 1993.
- [3] L. Beaur, T. Bretagnon, et al., Physical Review B, 84 (2011) 165312.

$s, p - d$ coupling in ZnO doped with 3d transition metal impurities

A. Ciechan, P. Bogusławski

Institute of Physics of Polish Academy of Sciences, al. Lotników 32/46, 02-668 Warsaw, Poland

The $s, p - d$ exchange coupling between free carriers and d -electrons of the transition metal (TM) dopants constitutes the basic feature of diluted magnetic semiconductors. We study the TM dopants ranging from Ti to Cu in ZnO within the density functional theory [1]. The $+U$ terms are employed to improve both the ZnO band structure and the position the TM levels. Detailed features of each ion are analysed, and general trends are indicated.

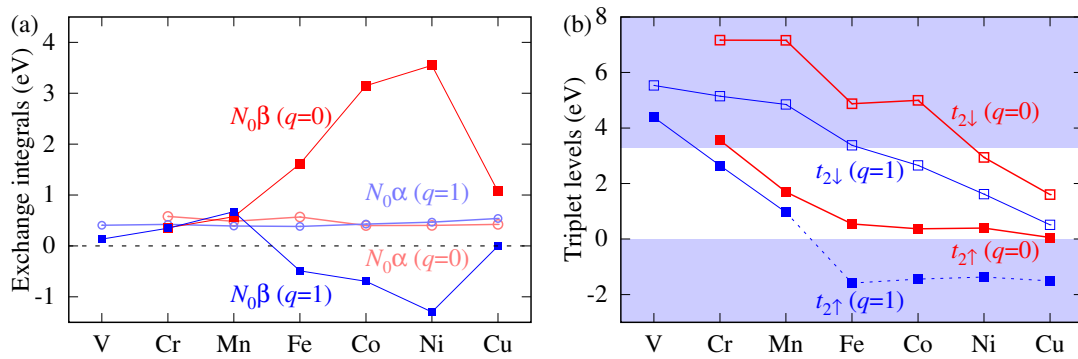


Figure: (a) The exchange constants $N_0\alpha$ and $N_0\beta$, (b) the triplet levels of TM^{2+} (i.e., $q = 0$) and TM^{3+} ($q = 1$) ions in ZnO. In (b), arrows indicate spin of the $t_2(\text{TM})$ triplets, and the zero energy is at the valence band top.

As shown in Figure, the $s - d$ coupling constant $N_0\alpha$ is almost the same for all TM ions, 0.5 eV. In contrast, the $p - d$ constant $N_0\beta$ varies about 10 times when going from V to Cu. In the cases of Fe, Co and Ni, the sign of $N_0\beta$ depends on the charge state of the dopant, since the constant is positive (i.e., ferromagnetic) for 2+ and negative (antiferromagnetic) for 3+ ions. Moreover, $N_0\beta$ for light holes and heavy holes can differ by a factor 2, or even have opposite signs. These unexpected features of $N_0\beta$ were not recognized in previous investigations.

Analysis of wave functions of ZnO:TM reveals the leading mechanisms of both $s - d$ and $p - d$ couplings. Those mechanisms are different for electrons and holes because of the different symmetries of their wave functions. In agreement with the Anderson picture, the main features of the $N_0\beta$ constant are determined by the $p - d$ hybridization between the $d(\text{TM})$ and $p(\text{O})$ orbitals, and thus by the energies of the triplet $t_2(\text{TM})$ levels relative to the valence band maximum, see Figure. In turn, the $N_0\alpha$ originates mainly in the intra-atomic direct exchange between the s and d electrons of the dopant ion. However, the spin polarization of the oxygen neighbours of the TM ion induced by the $p - d$ hybridization leads to the spin polarization of the $s(\text{O})$ orbitals, which enhances the value of $N_0\alpha$. A reasonable agreement with experimental data is obtained.

The authors acknowledge the support from the Projects No. 2016/21/D/ST3/03385, which are financed by Polish National Science Centre (NCN). Calculations were performed on ICM supercomputers of University of Warsaw (Grant No. GB84-37 and G16-11).

[1] A. Ciechan and P. Bogusławski, *Scientific Reports* **11**, 3848 (2021).

Structural properties of thin ZnO films grown by ALD under O-rich and Zn-rich growth conditions and their relationship to electrical parameters

S. Mishra, E. Przezdziecka, W. Wozniak, A. Adhikari, R. Jakiela, W. Paszkowicz,
A. Sulich, M. Ożga, K. Kopalko and E. Guzewicz

Inst. of Physics, Polish Academy of Sciences, Al. Lotnikow 32/46, Warszawa 02-668, Poland

Conductivity control issue in ZnO is major block in the overall practical success of this wide direct bandgap material [1]. Structural and native point defects as well as hydrogen related complexes are prime sources of shallow donor and acceptor states in ZnO and understanding their role is crucial for better conductivity control. Present work details structural properties and their relationship to electrical properties of thin (~ 100 nm) ZnO films grown under O-rich and Zn-rich conditions. The series of ZnO films were deposited by ALD on Si (100) and α -Al₂O₃ substrates at temperature (T_g) of 100 to 300°C. The films were polycrystalline with the average crystallites size (l) of ~ 20 -30 nm which increased after annealing to 80-90 nm. Room temperature (RT) Hall measurements showed that conductivity of the films increased with T_g . Moreover, ZnO/Si films showed lower carrier concentration and higher resistivity than those deposited on α -Al₂O₃. Electron density decreased whereas resistivity increased after post growth annealing (O₂ atm, 800 °C, 3 min) both for thin ZnO/Si and ZnO/Al₂O₃ films as well [Fig.1a]. Calculated Debye length (L_D) was found to be shorter than 1/2 (half of crystallite size) for all the ZnO/ α -Al₂O₃ and as grown ZnO/Si samples, while longer for annealed ZnO/Si deposited at 160°C and below, thus the carrier distribution homogeneity and carrier scattering mode was different for annealed ZnO/Si as compared to ZnO/Al₂O₃. Overall, ZnO/Si films, both *as grown* and annealed, showed lower structural disorder (strain and dislocation density) compared to ZnO/ α -Al₂O₃, indicating Si is much suitable substrate for electronic device fabrications etc. According to SIMS analysis, hydrogen impurity concentration in all *as grown* films is $\sim 10^{21}/\text{cm}^3$ (further lowered by 2 orders of magnitude after annealing [Fig.1c]), clearly higher than corresponding electron density (as grown $\sim 10^{18-19}/\text{cm}^3$), indicating that at least part of hydrogen does not play a role of a donor but significantly affect the electronic density of states and, ultimately, the Urbach energy.

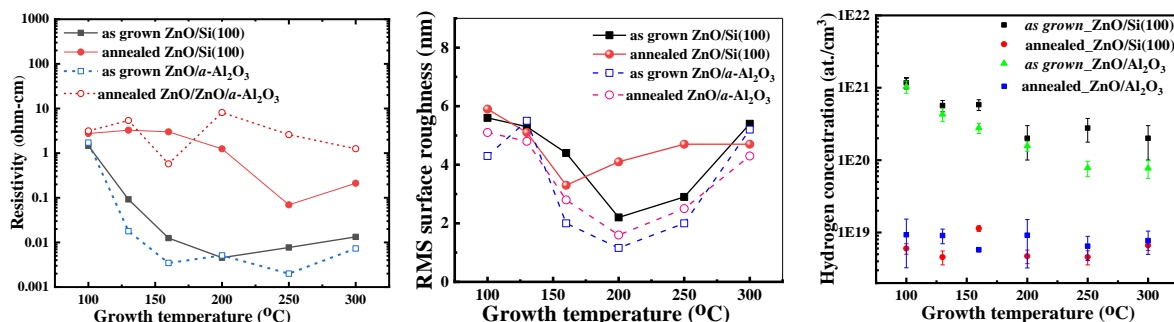


Fig. 1 a) Resistivity b) Roughness c) Hydrogen concentration vs T_g of thin ZnO/Si and ZnO/ α -Al₂O₃ films

Acknowledgements. The work is the result of a research project No. 2018/31/B/ST3/03576 founded by the National Science Centre.

[1] A. Janotti and C. G. van de Walle, *Rep. Prog. Phys.*, **72**(12), 126501, (2009).

[2] E. Przezdziecka, E. Guzewicz, D. Jarosz, D. Snigurenko, Sulich, P. Sybilski, R. Jakiela, W. Paszkowicz, *J. Appl. Phys.* **127**, 075104 (2020).

Investigation of the electromagnetic interaction between the vertically coupled split-ring-based metasurface and antenna

Alexander Chernyadiev¹, Dmytro B. But¹, Cezary Kołaciński^{1,2},
Kęstutis Ikamas³, Alvydas Lisauskas^{1,3}

¹*CENTERA Laboratories, Institute of High Pressure Physics PAS, Warsaw, Poland*

²*Łukasiewicz Research Network - Institute of Microelectronics and Photonics, Warsaw, Poland*

³*Institute of Applied Electrodynamics and Telecommunications, Vilnius University, Vilnius, Lithuania*

Silicon (Si) complementary metal-oxide-semiconductor technology (CMOS) holds plenty of hidden opportunities for the implementation of photonic structures. Metasurfaces realized in such a technology make possible applications like beam steering, programmability of spatial and spectral properties of radiation, and polarization control [1]. We investigate the electromagnetic (EM) coupling between a matrix of split-ring structures and the antenna resonant at 390 GHz, which are integrated into the stack of metal layers of 180 nm Si CMOS process. We examine the coupling strength between these structures and the high frequency impedance of the whole system of coupled resonators (Fig. 1a).

The mechanism of the interaction between the antenna and the metasurface can be explained using electronic circuit equivalents with inductive coupling. Figure 1b presents a fit of impedance obtained using EM simulations and the parallel RLC circuits. Antenna's RLC parameters extracted after the fitting are: 830 Ohm, 64 pH, 2.5 fF, respectively; split-ring's RLC parameters are: 1350 Ohm, 47 pH, 3.5 fF. The RLC equivalent helps us efficiently modify the geometry of the structures to tune their resonances. A splitting of 58% from the resonance frequency might be achieved for optimized coupled structures.

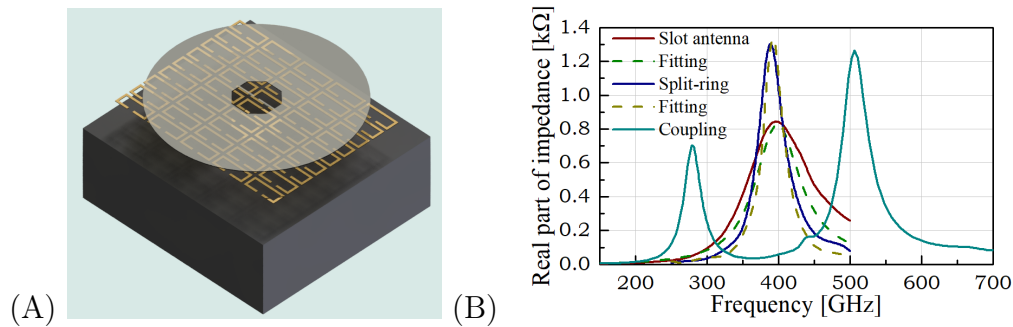


Figure 1: A) A 3-D picture of the EM-coupled resonant planar structures placed on a Si substrate. (B) The frequency dependencies of impedance's real part. Red and blue curves - resonances of the slot antenna and a split-ring; the aquamarine curve - coupled resonators; the dashed curves - fitting by equivalent circuits expression.

References

- [1] P. Wu, R. Pala, G. Shirmanesh Kafaie, W. Cheng, R. Sokhoyan, M. Grajower, M. Alam, D. Lee, H. Atwater, *Nature Communications* **10**, 1 (2019).

Investigation of micro-strain in ZnO/CdO and ZnO/ZnCdO multiple quantum well nanowires grown on Si by PA-MBE

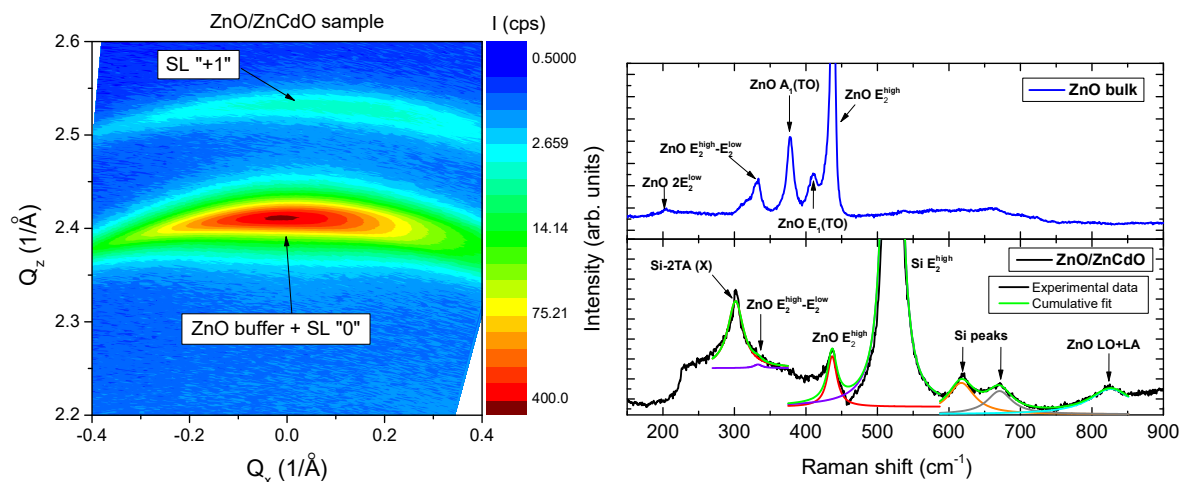
E. Zielony¹, A. Wierzbicka², R. Szymon¹, M.A. Pietrzyk², E. Popko¹

¹ Department of Quantum Technologies, Wrocław University of Science and Technology, Wybrzeże Wyspiańskiego 27, 50-370 Wrocław, Poland

² Institute of Physics Polish Academy of Sciences, Al. Lotników 32/46, PL-02668 Warsaw, Poland

Heterostructures containing ZnCdO alloys have been investigated widely for several years for their potential applications in optoelectronic devices, such as light emitting sources operating from ultraviolet to green/blue wavelengths. Tuning of luminescence from UV to VIS region became possible thanks to alloying of ZnO with CdO that leads to the reduction of the bandgap of obtained compound. It is well known that ZnO crystallizes in a wurtzite structure, in contrast to CdO which yields the cubic rocksalt phase. This makes problems in fabrication of ZnO/CdO or ZnO/ZnCdO heterostructures or quantum wells of satisfying optoelectronic properties. Therefore, much attention is paid to studies of structural and optical properties of produced ZnO/CdO as well as ZnO/ZnCdO thin films.

The present work is dedicated to ZnO/CdO and ZnO/ZnCdO multiple quantum wells (MQWs) nanowires grown by plasma assisted molecular beam epitaxy on Si substrate. The samples were investigated by micro-Raman (μ -Raman) spectroscopy for verification of structural properties as well as the presence of strain. The measurements were supplemented by X-ray diffraction (XRD) studies. For micro-Raman experiments two excitation wavelengths of 514.5 nm and 325 nm were used. The non-resonant Raman spectra show phonon modes originating from the Si substrate as well as ZnO, whereas the resonant Raman measurements exhibit multiphonon modes characteristic only for ZnO. Both non-resonant and resonant Raman spectra of ZnO/ZnCdO and ZnO/CdO MQW heterostructures reveal a red-shift of Raman peaks position with respect to that of bulk ZnO. Moreover, in the case of ZnO/CdO sample a significant broadening of the A_1^{LO} ZnO line with comparison to the one observed for pure ZnO has been observed. Both effects, the red-shift and a broadening of ZnO-related phonon modes indicate a tensile type of strain occurring in analyzed samples. The XRD signals having its source in ZnO buffer and MQWs are also significantly broadened. Such an effect has been assigned to the micro-strain in nanowires as it affects the XRD peak profile [1, 2]. Thus, based on μ -Raman and XRD measurements the value of micro-strain has been estimated for the studied samples and obtained results are consistent. It was concluded that the tensile strain (micro-strain) is a result of the presence of Cd in the ZnCdO alloy of ZnO/ZnCdO MQWs; incorporation of Cd into the ZnO barrier during the growth of ZnO/CdO MQWs; it may be also due to the statistical distribution of the sizes and shapes of nanowires or their coalescence as well [1]. Application of both complementary methods, μ -Raman spectroscopy and XRD, allowed to study the nanowire structures as well as MQWs in the analyzed samples.



[1] E. Zielony, et al., Appl. Surf. Sci. 538 (2021) 148061.

[2] M.A. Pietrzyk, et al., Sensors Actuat. A – Phys. 315 (2020) 112305.

Properties of MgO insulating layers on 6H-SiC and GaN: Photoelectron studies

R. Lewandków¹, M. Grodzicki¹, P. Mazur¹, A. Ciszewski¹

¹ *Institute of Experimental Physics, University of Wrocław, pl. M. Borna 9, Wrocław, Poland*

SiC and GaN have high chemical and thermal resistivity due to their hardness, which allows electronic devices based on these materials to operate in demanding conditions. The elements limiting the operation of GaN/SiC-based devices include leakage current, that lowers the breakdown voltage. This is due to the existence of interfacial states associated with the occurrence of many effects (N defects, O defects).

One of the effective methods of suppressing these effects is the passivation of the surface with oxides with a sufficiently large gap and high dielectric constant. MgO is one of the candidates for the buffer layer and surface passivation, it also has low GaN carrier trap density values, which makes it interesting for device applications.

We present an overview of MgO insulating layers on GaN(0001) and SiC(0001) surfaces. The deposition of MgO layers by electron beam evaporation was characterized in situ by X-ray and ultraviolet photoelectron spectroscopy (XPS, UPS) under ultra-high vacuum conditions.

The XPS results confirmed the formation of the MgO compound at the core levels of Mg 1s and O 1s located at 51.0 eV and 531.6 eV, respectively. The valence and conduction band offsets (VBO, CBO) for the interfaces were determined. The VBOs are equal to 1.4 eV and 1.2 eV for the MgO/SiC and MgO/GaN interfaces. The MgO band gap energies, determined from XPS, are estimated to be 6.7 eV and 6.9 eV for the MgO layers deposited on 6H-SiC and GaN, respectively. CBO is 2.3 eV for both interfaces.

Local electronic structure of thin *p*-type ZnO films doped with nitrogen

Elżbieta Guzewicz¹, Oksana Volnianska¹, Iraida N. Demchenko², Patric Zeller³,
Matteo Amati³, Luka Gregoratti³

¹ *Inst. of Physics, Polish Academy of Sciences, Al. Lotników 32/46, 02-668 Warsaw, Poland*

² *Dept. Chemistry, University of Warsaw, Pasteur str. 1, 02-093 Warsaw, Poland*

³ *Elettra – Sincrotrone Trieste S.C.p.A., Trieste, Italy*

The problem with stable *p*-type doping is the main obstacle in application of ZnO in optoelectronics. Regardless a considerable number of papers reporting *p*-type conductivity of ZnO films, in many cases the obtained results remain controversial.

Our recent cathodoluminescence (CL) study on *p*-type polycrystalline ZnO:N films revealed that the donor-related and the acceptor-related luminescence are clearly separated, i.e. some columns show only acceptor-, while other donor-related CL [1]. This motivated the present scanning photoelectron microscopy (SPEM) study, which was conducted at the ESCA microscopy beamline at the Elettra synchrotron facility in Trieste, Italy. The SPEM enables to probe the electronic structure at submicron scale and thus to obtain the photoemission spectroscopy signal from a single column of growth (Fig. 1a). This unique experiment reveals two types of columns showing different PES spectra in the valence band region. The PES spectra differ in the photoemission intensity in the region 0-2 eV below the valence band maximum (VBM) (Fig. 1b) indicating differences in density of states.

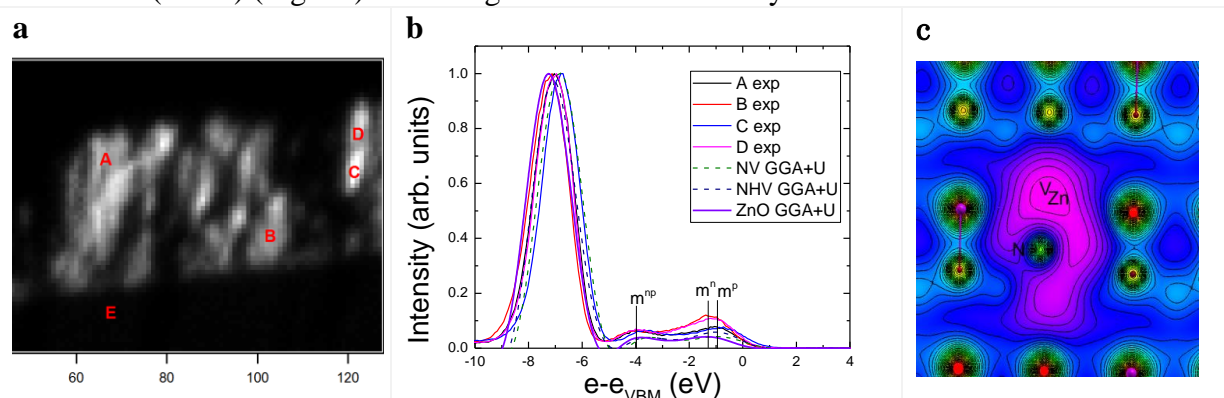


Fig.1. (a) The SPEM image of the cross-section of $\sim 2\mu\text{m}$ thick ZnO:N film, (b) Qualitative comparison of PES spectra (at A,B,C and D points) with calculated density of $d(\text{Zn})$ states (states/eV) (x-axis corresponds to the energy relative to the VBM of pure ZnO), (c) iso-surface of the electron density of ZnO: $V_{\text{Zn}}N_{\text{O}}H_2$ corresponding to 0.005 electron/a.u.³

Density Functional Theory calculations within the generalized gradient approximation using QUANTUM-ESPRESSO code [2] has been performed. The Hubbard-like term +U describing the on-site Coulomb interactions [3] was applied on the $d(\text{Zn})$ and $p(\text{O})$ orbitals. The application of $U(\text{Zn}) = 10$ and $U(\text{O}) = 7$ eV gives the correct electronic structure and a value of the band gap in wurtzite (w) ZnO of 3.3 eV. It has been confirmed that hydrogen forms stable complexes with V_{Zn} and $V_{\text{Zn}}-N_{\text{O}}$ which can be the origin of *p*-conductivity in grains of ZnO:N. Theoretical calculations indicate that such complex formation might be the origin of differences in the valence band density of states in the valence band region.

Acknowledgements. The work is the result of a research project No. 2018/31/B/ST3/03576 founded by the National Science Centre. The authors acknowledge the support from Elettra Sincrotrone Trieste (proposal ID 20180152-Elettra).

[1] E. Guzewicz, E. Przezdziecka, et al., ACS Appl. Mat. Int. **9**, 26143-26150 (2017).

[2] P. Giannozzi *et al.*: J. Phys.: Condens. Matter. **21**, 395502 (2009).

[3] M. Cococcioni and S. de Gironcoli: Phys. Rev. B, **71**, 035105 (2005).

Defects and Magnetism in Heavy Ion Implanted Monocrystalline ZnO

Jacek Gosk¹, Roman Puźniak², Artem Lynnyk²

¹ Faculty of Physics, Warsaw University of Technology, Koszykowa 75, PL-00662 Warsaw, Poland

² Institute of Physics, Polish Academy of Sciences, Aleja Lotnikow 32/46, PL-02668 Warsaw, Poland

After two decades of intensive studies on ZnO base DMSs, still there is no clear agreement about the nature and origin of the magnetic properties of samples prepared by different methods and different groups. In particular, this applies to Co ions implanted ZnO; in the literature base both on experimental and theoretical data consideration, the authors point out on the implantation damages as an origin of magnetic centers in ZnO. On the other hand, there are contradictory opinions shared by the authors of numerous experimental works who did not observed intrinsic ferromagnetic ZnO phase due to different kinds of defects, especially the post implantation ones. In our work [1] it was shown that defect created in irradiated samples with either electrons or protons prove to be magnetically inactive while those implanted by Co ions revealed paramagnetic phase. Thus, in the next step the ZnO were implanted with Co and noble gases Ar and Kr. In order to compare magnetic properties of ZnO an attempt was made to establish implantation conditions introducing damage in those samples, comparable as regards the range and intensity. The structural studies by means of X-ray and preliminary magnetic properties of Co, Ar, and Kr implanted ZnO were reported in our conference paper [2].

In this research, we report on extended and detailed magnetic studies on Co, Ar, and Kr ions implanted ZnO. Complementary structural investigations base on RBS random and aligned spectra were performed by our coworkers [3]. It was shown that in ZnO implanted with magnetic Co and with Ar and Kr noble gases, with energies and doses creating comparable damage, the thin implanted layers do not reached an amorphization level, in the host lattice as regards its range and magnitude.

Magnetization for all samples was studied as a function of magnetic field (H) at constant temperature in the temperature range between 2 and 300 K and as a function of temperature for $H = 1$ and 10 kOe. In Co-implanted ZnO, the paramagnetic and some residual ferromagnetic/superparamagnetic phases (FM/SPM) were revealed, while the Kr- and Ar-implantations do not introduce magnetic centers. The existence of FM/SPM residual phases in Co-implanted layer was confirmed in the measurements of zero field cooled/field cooled magnetization at $H = 10, 50$, and 500 Oe and gave rise to a hysteresis loop appearing in low temperature range from 2 to 15 K.

In conclusion, all investigated Co, Ar, and Kr ions implanted ZnO do not revealed intrinsic/bulk FM. Parametric phase was observed in Co ions implanted ZnO. It could be well explained by weakly interacting Co ions, partly substituting Zn ions and partly at interstitial positions. In addition, some residual supermagnetic/ferromagnetic phases were observed. Assuming the similar nature of defect generated by Co, Ar, and Kr ions it was shown that defects resulting from implantation in the examined energy and intensity range for both magnetic ions as well as nonmagnetic Ar and Kr are not magnetically active.

[1] Z. Werner *et al.*, *NIM B* **358** (2015) 174-178.

[2] J. B. Gosk *et al.*, *Acta Phys. Pol. A* **136** (2019) 628.

[3] Z. Werner *et al.*, *Radiat. Eff. Defects Solids* (2021) DOI:10.1080/10420150.2021.1878521.

Corresponding authors: Jacek.Gosk@pw.edu.pl

Magnetic Ordering and Frustration in GeSnMnTe Multiferroic Crystals

Abdul Khaliq ¹, Monika Arciszewska ¹, Andrzej Avdonin ¹, Beata Brodowska ¹, Vasya E. Slynko ², Evgen I. Slynko ², Lukasz Kilanski ¹

¹ *Institute of Physics, Polish Academy of Sciences, al. Lotnikow 32/46, 02-668 Warsaw, Poland*

² *Institute of Materials Science Problems, Ukrainian Academy of Sciences, Chernovtsy, Ukraine*

Multiferroicity in diluted magnetic semiconductors (DMSs) is paving grounds for a novel class of spintronic materials offering semiconducting, magnetic and ferroelectric properties. Extensive studies on DMSs have previously found low temperature functionalities, electric field control of magnetism, spin injection and tunneling anisotropic magnetoresistance. In comparison of group III-V and II-VI DMSs, IV-VI alloys such as α -GeTe and its derivatives reveal entanglement between ferroelectric and ferromagnetic ordering, giant Rashba spin splitting and ferroic domain wall dynamics. The higher solubility of magnetic impurities in IV-VI crystals and the isoelectronic structure of doped Mn also prove them superior than their counterparts.

In this work, we present Rashba ferroelectric α -GeTe based $\text{Ge}_{1-x-y}\text{Sn}_x\text{Mn}_y\text{Te}$ multiferroics, the impact of Sn on Curie temperature (T_c), carrier concentration and magnetic ordering. The magnetic susceptibility analysis show a sizable drop in the T_c of $\text{Ge}_{1-x-y}\text{Sn}_x\text{Mn}_y\text{Te}$ alloys from 70 K for $x = 0.2$ to about 15 K for $x = 0.8$ as compared to $T_c < 200$ K for GeTe based crystals. Similarly, the carrier concentration values obtained show a typical trend of IV-VI DMSs i.e. 10^{21} cm^{-3} . However, it was observed for the first time in $\text{Ge}_{1-x-y}\text{Sn}_x\text{Mn}_y\text{Te}$ alloy ($y = 0.2 - 0.8$) that the p-type carriers reduced to 10^{19} cm^{-3} which is typically more than 10^{20} cm^{-3} for GeTe crystals. Both the reductions in T_c and p-type carrier concentration are consistent and show that the Ge vacancies were compensated by Sn and Mn. The measured values allow us to tune the magnetic interaction constant J_{pd} . Moreover, the ferroelectric transition temperatures in this work for $\text{Ge}_{1-x-y}\text{Sn}_x\text{Mn}_y\text{Te}$ multiferroics range from around 70 K to 500 K which provide interesting possibilities to observe the domain wall patterns over a range of temperatures.

Non-Abelian Berry phases of electrically driven hole-spin qubits in waveguide QED

Sarath Prem, Marcin Wysokinski, and Mircea Trif

International Research Centre MagTop, Institute of Physics, Polish Academy of Sciences, Aleja Lotników 32/46, PL-02668 Warsaw, Poland

Hole-spins localized in quantum dots or acceptor defects are currently some of the most viable qubit platforms in solid-state systems, as they show long coherence times and possess strong spin-orbit interactions that allow for fast electrical manipulations. However, in most implementations, the presence of a static magnetic field that breaks the time-reversal symmetry is employed, which activates various relaxation channels, such as phonons or charge noise. Building on a recent work by the authors concerning electrically driven hole-spins in *single* mode cavities [1], here we study the interplay between the *continuous* electromagnetic modes in a waveguide QED setup [2] and the non-Abelian Berry phases engendered by the time-dependent electrical fields acting on the holes. Using a Floquet-Born-Markov formalism, we derive an effective density matrix describing the driven hole-spins in the presence of the electromagnetic modes in the waveguide. Then, we calculate various observables associated with the dynamics, such as the dressed spin trajectories, their coherence times, and the photons-mediated entanglement between distant hole-spins [3]. Finally, using an input-output description for the electromagnetic field, we calculate the photonic fluxes exiting the waveguide and show that its transmission depends on the Berry phases stemming from the driven hole spins [3].

- [1] M. M. Wysockiński, M. Płodzień and M. Trif, arXiv preprint arXiv:2012.15804.
- [2] K. Lalumiere, B. C. Sanders, A. F. van Loo, A. Fedorov, A. Wallraff, and A. Blais, Phys. Rev. A **88**, 043806 (2013).
- [3] S. Prem, M. Wysokinski, M. Trif (in preparation).

Electronic Properties and Structural Stability of thin SnTe and PbTe Nanowires

Ghulam Hussain¹, Giuseppe Cuono¹, Alexander Lau¹, Carmine Autieri^{1,2}

¹*International Research Centre MagTop, Institute of Physics, Polish Academy of Sciences, Aleja Lotnikow 32/46, PL-02668 Warsaw, Poland*

²*Consiglio Nazionale delle Ricerche CNR-SPIN, UOS Salerno, I-84084 Fisciano (Salerno), Italy*

The electronic properties and structural stability of thin SnTe and PbTe cubic nanowires (CNs) and pentagonal nanowires (PNWs) are investigated. The PNWs contain a disclination at the center of the nanowires and they are oriented along [001] and [110] directions. From Density Functional Theory, the band structures illustrate a trivial insulating behavior for thin CNs, while bands connecting valence and conduction bands are observed for thin PNWs. We estimated that the topological band structure is expected in SnTe CNs for thicknesses larger than 11 nm. The bands connecting valence and conduction bands in thin PNWs mainly originate from the central atom as we observe from the partial charge density making the disclination responsible for the band crossing and thus metallicity. Moreover, the binding energies are evaluated for CNs and PNWs to study their structural stability, which revealed that the stability increases as the thickness of nanowires increases. The thin SnTe CNs are more stable than the thin SnTe PNWs suggesting that the PNWs recently synthesized could be stabilized by the topological properties.

Electron transport and ARPES study on topological semimetal: TaAs₂

A. S. Wadge¹, G. Grabecki², B. J. Kowalski², C. Autieri¹, K. Dybko^{1,2}, P. Iwanowski^{1,2}, A. Hruban², A. Łusakowski², R. Diduszko², M. Rosmus³, N. Olszowska³, J. Kołodziej³, A. Wiśniewski^{1,2}

¹International Research Centre MagTop, Institute of Physics, Polish Academy of Sciences, Aleja Lotników 32/46, PL-02668 Warsaw, Poland

²Institute of Physics, Polish Academy of Sciences, Aleja Lotników 32/46, PL-02668 Warsaw, Poland

³National Synchrotron Radiation Centre SOLARIS, Jagiellonian University, Czerwone Maki 98, PL-30392 Kraków, Poland

Extremely large magnetoresistance (MR) in topological semimetals has gained an attention in the field of magneto-electronic devices. Recently, it was found that dipnictides RX₂ (e.g. R=Ta, X=As) are one of the best candidates [1]. The single crystals of TaAs₂ were prepared by chemical vapor transport method and X-ray analysis has shown that they have monoclinic structure. We have investigated transport properties of TaAs₂ in presence of magnetic field up to 9 T and in the temperature range from 1.5 K to 300 K. It was found that TaAs₂ shows non-saturating MR up to 14000% at 1.5 K and also exhibits pronounced Shubnikov de Haas oscillations (SdH). They are composed of more than 3 frequencies indicating the presence of several electron pockets and hole pockets [2] and were analyzed by Fourier transform. The sample cut along ($\bar{2}$ 0 1) plane (inset to fig. 1a) showed that the Fermi surface is elliptical in shape (Fig.1a). This result has been confirmed by angle resolved photoemission spectroscopy (ARPES) studies whose results showed the elliptical drumhead surface states on freshly cleaved ($\bar{2}$ 0 1) surface (fig.1b). We also performed first principle theoretical calculations that support our experimental observations.

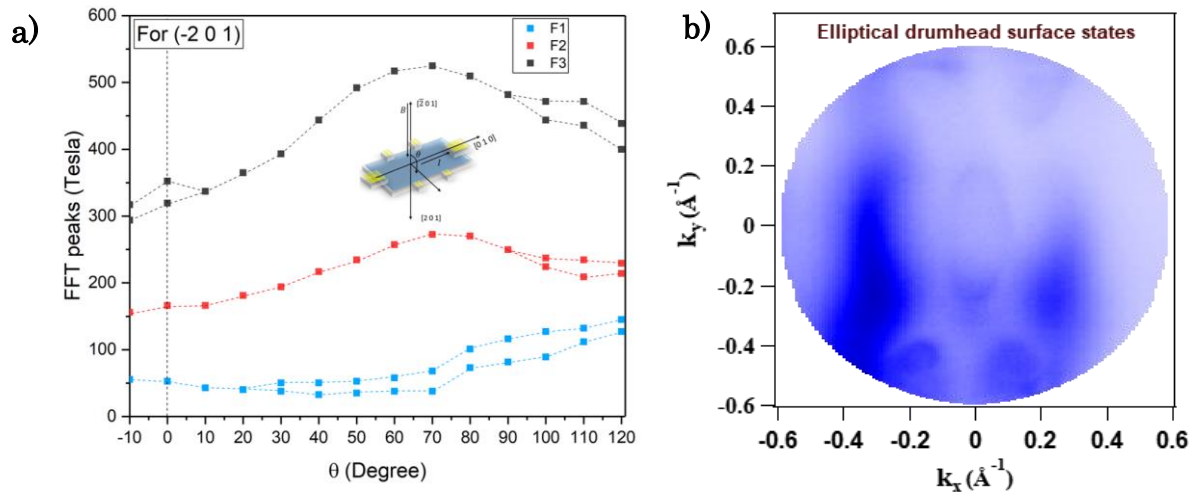


Figure 1 a) Angle dependence of FFT peaks obtained from SdH oscillations. b) Experimental ARPES image showing elliptical drumhead surface states.

[1] T. A. Butcher, et al., Phys. Rev. B **99**, 245112, (2019).

[2] I. Vurgaftman et al., J. Appl. Phys. **84**, 4966, (1998).

Plasma reflectivity of $\text{Pb}_{1-x}\text{Sn}_x\text{Te}/\text{CdTe}/\text{GaAs}$ epitaxial layer in the band inversion region

W. Wołkanowicz¹, M. Szot^{1,2}, J. Polaczyński², K. Karpińska¹, L. Kowalczyk¹,
P. Dziawa¹, B. Taliashvili¹, M. Zięba¹, R. Minikayev¹, E. Łusakowska¹, A. Reszka¹,
K. Dybko^{1,2}, A.M. Witowski³, T. Wojtowicz², T. Story^{1,2}

¹ Institute of Physics, Polish Academy of Sciences, PL-02668 Warsaw, Poland

² International Research Centre MagTop, Institute of Physics, Polish Academy of Sciences, aleja Lotników 32/46, PL-02668 Warsaw, Poland

³ Faculty of Physics, University of Warsaw, PL- 02093 Warsaw, Poland

$\text{Pb}_{1-x}\text{Sn}_x\text{Te}$ is a IV-VI narrow-gap substitutional semiconductor alloy exhibiting, upon changing Sn content, temperature or pressure, the inversion of the parity of conduction and valence bands that results in topological crystalline insulator (TCI) state. The inversion of bands and appearance of topological surface states was originally experimentally observed by surface sensitive techniques such as angle-resolved photoemission (ARPES) and scanning tunneling spectroscopy (STS). It was followed by challenging magnetotransport and magneto-optical experiments, usually dominated by bulk electronic properties. In this work, we study the band inversion effect in a micron-thick $\text{Pb}_{1-x}\text{Sn}_x\text{Te}$ epitaxial layer using reflectivity measurements in the spectral window between phonon excitations in far infrared and interband transitions in mid-infrared, with dominant optical dispersion due to plasma excitations of carriers.

$\text{Pb}_{1-x}\text{Sn}_x\text{Te}$ ($x = 0.5$) layer was grown by molecular beam epitaxy on GaAs (001) substrate with 4 micron thick CdTe buffer. The rock-salt crystal structure and lattice parameter, layer thickness, and chemical composition were examined by X-ray diffraction and scanning electron microscopy, as well as by energy dispersive fluorescence (SEM/EDX) techniques. We carried out optical reflectivity measurements in the infrared spectral range 80 – 350 meV and temperature range $T = 10 - 300$ K, thus covering the crossover temperature $T_0 = 120$ K, corresponding to a zero gap state separating topologically trivial ($T > T_0$) and nontrivial TCI state ($T < T_0$). This spectral range also covers the plasma edge energy 100 - 200 meV expected for $\text{Pb}_{1-x}\text{Sn}_x\text{Te}$ layers with hole concentration of $p = 10^{19} - 10^{20} \text{ cm}^{-3}$.

The observed spectral dependence of the reflectivity of $\text{Pb}_{0.5}\text{Sn}_{0.5}\text{Te}$ layer is, in the entire temperature range studied, dominated by bulk plasma reflectivity effect modulated by thin layer interference effects. One observes almost 100% reflectivity at 80 meV followed by shallow plasma minimum and about 50% reflectivity above plasma frequency (due to exceptionally high, $n = 6$, refractive index of $\text{Pb}_{1-x}\text{Sn}_x\text{Te}$). The experimentally observed changes of the spectra induced by varying the temperature across the inversion point revealed a small but systematic increase of reflectivity in the plasma edge region for $T > 100$ K. We discuss this effect as well as determined electronic (effective mass) and optical (refractive index) parameters in terms of band structure model of $\text{Pb}_{1-x}\text{Sn}_x\text{Te}$ with temperature driven inversion of bands.

This research was partially supported by the Foundation for Polish Science through the IRA Programme co-financed by EU within SG OP as well as by NCN Grant: UMO 2017/27/B/ST3/02470.

Robust Weyl and nodal line semimetal phases in 3D superlattice of Hg-based chalcogenides: ab initio studies

Rajibul Islam¹, Barun Ghosh⁵, Giuseppe Cuono¹, Amit Agarwal², Bahadur Singh⁴, Arun Bansil⁵, Carmine Autieri^{1,3}, and Tomasz Dietl^{1,6}

¹*International Research Centre MagTop, Institute of Physics, Polish Academy of Sciences, Aleja Lotnikow 32/46, PL-02668 Warsaw, Poland*

²*Department of Physics, Indian Institute of Technology, Kanpur 208016, India*

³*Consiglio Nazionale delle Ricerche CNR-SPIN, UOS Salerno, I-84084 Fisciano (Salerno), Italy*

⁴*Department of Condensed Matter Physics and Materials Science, Tata Institute of Fundamental Research, Colaba, Mumbai 400005, India*

⁵*Department of Physics, Northeastern University, Boston, Massachusetts 02115, USA*

⁶*WPI-Advanced Institute for Materials Research, Tohoku University, Sendai 980-8577, Japan*

The research on topological materials emerges as one of the most active fields in the condensed matter physics. We have investigated how the topological phases evolve in zincblende 3D superlattices using relativistic density functional theory (DFT) calculations. We study one superlattice (SL) composed by two topological materials (i.e. HgTe/HgSe) and one topological/trivial SL (i.e. HgTe/CdTe). The crystal structure does not have inversion symmetry but it presents a Kramers-type degeneracy along Γ -Z, while it presents Rashba-like spin-orbit splitting along the other k-space directions. The C_2 symmetry-protected ideal Weyl semimetal phase has been found in HgTe/HgSe 3D SL as shown in Fig.1. The electronic properties of the CdTe/HgTe SL show a nodal line semimetal phase. Finally, we have investigated the effect of strain demonstrating a rich phase diagram of the topological properties.

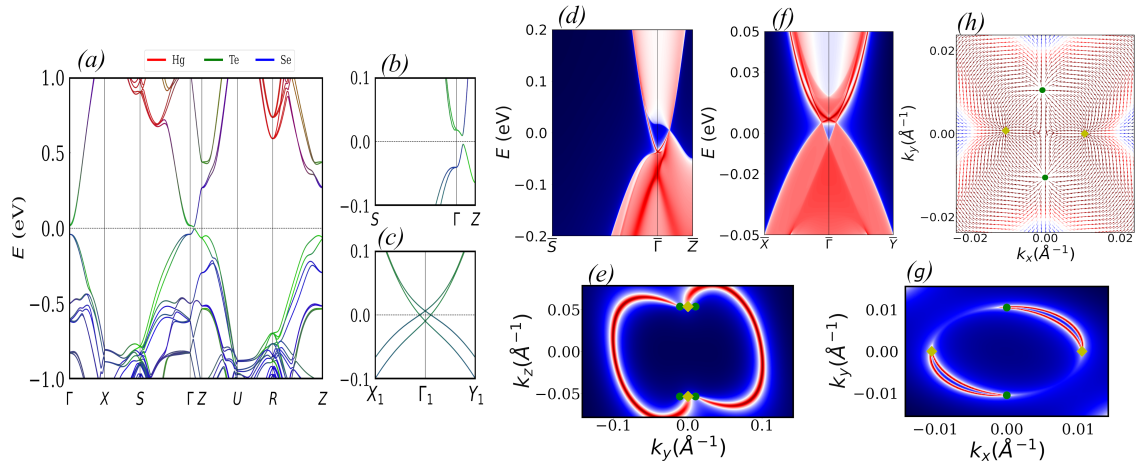


Figure 1: DFT band structure of HgTe/HgSe superlattice with SOC a) full Brillouin along high symmetry line, b) the enlarged view along the S-Γ-Z direction. c) Band structure in the plane of the Weyl points along the path $X_1=(k_x,0,k_z^*)\rightarrow\Gamma_1=(0,0,k_z^*)\rightarrow Y_1=(0,k_y,k_z^*)$ where $k_z^*=0.0536$. The projected surface bands onto the d) (100) f) (001) surface. Fermi arcs and their connection e) for the (100) surface g) and for the (001) surface. h) Berry curvature in the k_z plane containing the four Weyl points. The two Weyl points at $(\pm k_x^*, 0, \pm k_z^*)$ have chirality -1 (yellow marker) while the two Weyl points at $(0, \pm k_y^*, \pm k_z^*)$ have +1 chirality (green marker).

Properties of fractal lattices with higher Chern number

Weronika Pasek¹, Michał Kupczyński¹

¹ *Department of Theoretical Physics, Faculty of Fundamental Problems of Technology,
Wrocław University of Science and Technology, Wrocław, Poland*

The main purpose of our work is to determine the properties of lattice models with a Chern number $|c| > 1$ in fractal geometry. The Chern number is the topological invariant which quantizes the Hall conductivity in the integer quantum Hall effect (IQHE) and is equal to the number of pairs of topologically protected edge states. Edge states with non-trivial Chern number can also appear without magnetic field in Chern insulators [1]. Fractals are mathematical objects of which Hausdorff dimension is different from the topological dimension. They are characterized by the property of self-similarity and recursive definition. Special interest in solid-state physics in fractal geometries results from the latest successful experimental implementations [2-4]. The topological properties of such systems have been recently studied for the Hofstadter model with Chern number $|c| = 1$ [5].

We will analyze two models of fractal lattices Sierpinski gasket and Sierpiński carpet. In our work, we will focus on a few models with a higher Chern number. The first of them is a modified Hofstadter model with added longer-range hoppings [6]. Second is the Lieb lattice, which is a Chern insulator. We have pointed out the edge states and computed the real-space Chern number.

- [1] F. D. M. Haldane, *Phys. Rev. Lett.*, **61**, 2015 (1988).
- [2] T. L. Chen, D. J. Dikken, J. C. Prangsma, F. Segerink, and J. L. Herek, *New J. Phys.*, **16**, 093024 (2014)
- [3] J. Shang, Y. Wang, M. Chen, J. Dai, X. Zhou, J. Kuttner, G. Hilt, X. Shao, J. M. Gottfried, and K. Wu, *Nat. Chem.*, **7**, 7, 389 (2015)
- [4] S. N. Kempkes, M. R. Slot, S. E. Freeney, S. J. M. Zevenhuizen, D. Vanmaekelbergh, I. Swart, and C. Morais Smith, *Nat. Chem.*, **15**, 127–131(2019)
- [5] M. Brzezińska, A. M. Cook, T. Neupert *Phys. Rev. B*, **98**, 205116 (2018)
- [6] D. Wang, Z. Liu, J. Cao, H. Fan, *Phys. Rev. Lett.*, **111**, 186804 (2013)

Tunable Planar Hall Effect in (Ga,Mn)(Bi,As) Epitaxial Layers

T. Andrearczyk¹, J. Sadowski^{1,2}, J. Wróbel¹, T. Figielski¹ and T. Wosiński¹

¹ Institute of Physics, Polish Academy of Sciences, 02-668 Warszawa, Poland

² Dept. Physics and Electrical Engineering, Linnaeus University, SE-391 82 Kalmar, Sweden

Incorporation of a small amount of heavy Bi atoms into epitaxial layers of the prototype dilute ferromagnetic semiconductor (Ga,Mn)As results in a strong enhancement of the spin-orbit interaction in the valence band. This, in turn, causes a significant increase in the magnitude of magnetotransport effects in the quaternary (Ga,Mn)(Bi,As) compound, as evidenced by our recent experiments [1, 2].

In the present study we have investigated the so-called planar Hall effect (PHE) in 50 nm thick (Ga,Mn)(Bi,As) layers, with 6% Mn and 1% Bi contents, grown on semi-insulating (001)-oriented GaAs substrate, under biaxial compressive misfit strain, by the low-temperature MBE technique. PHE consists in developing, as a result of the spin-orbit interaction, a spontaneous transverse voltage in ferromagnetic layers with in-plane magnetization in response to longitudinal current flow [3]. It has been studied on micro-Hall-bars of 20 μm width and 50 μm distance between the voltage contacts, tailored by means of electron-beam lithography and chemical etching. Both the longitudinal magnetoresistivity and PHE resistivity, measured as a function of in-plane magnetic field at liquid helium temperatures, displayed, for the Bi-contained layers, considerably larger magnitudes with respect to those for reference (Ga,Mn)As layers (cf. Fig. 1).

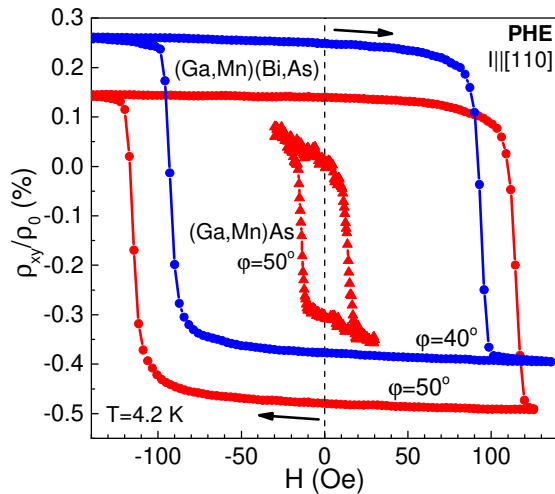


Fig. 1. Normalized PHE resistivity for Hall-bars of the (Ga,Mn)(Bi,As) and (Ga,Mn)As layers measured while sweeping an in-plane magnetic field applied at an angle φ with respect to the bar axis. The curves are vertically offset for clarity.

two hard axes along magnetically non-equivalent in-plane $\langle 110 \rangle$ directions, with the $[-110]$ axis being magnetically easier than the perpendicular $[110]$ one. The tunable two-state behavior of the PHE resistivity at zero magnetic field provides its usefulness for applications in nonvolatile memory devices.

While sweeping the magnetic field up and down the PHE resistivity varies non-monotonously displaying the appearance of a single or double hysteresis loops, depending on the sweeping range of magnetic field and the field orientation. The complex PHE behavior results from reorientation of single ferromagnetic domains in the Hall-bars between the four in-plane $\langle 100 \rangle$ directions, corresponding to equivalent easy axes of magnetization in the layers. Moreover, using an appropriate orientation of the applied in-plane magnetic field with respect to the Hall-bar axis we can realize two distinctly different coercive fields, as shown in Fig. 1. They result from the domain magnetization switching by the angle of 90° , either clockwise or counterclockwise, overcoming one of

- [1] K. Levchenko, T. Andrearczyk, J.Z. Domagała, J. Sadowski, L. Kowalczyk, M. Szot, R. Kuna, T. Figielski, T. Wosiński, *J. Supercond. Nov. Magn.* **30**, 825 (2017).
- [2] T. Andrearczyk, K. Levchenko, J. Sadowski, *et al.*, *Materials* **13**, 5507 (2020).
- [3] T.R. McGuire, R.I. Potter, *IEEE Trans. Magn.* **11**, 1018 (1975).

Electrical and Structural Properties of CZTS-Based Structures for Thin Film Photovoltaic Cells

Igor Perlikowski¹, Eunika Zielony¹, Teoman Özdal² and Hamide Kavak²

¹ Department of Quantum Technologies, Wrocław University of Science and Technology,
Wybrzeże Wyspiańskiego 27, 50-370, Wrocław, Poland

² Department of Physics, Çukurova University, 01330, Adana, Turkey

In order to prevent and limit effects of antropogenic climate change, methods of reducing greenhouse gas emissions have been recently searched for. It appears that electricity and heat production is responsible for nearly one third of emissions of such gases, more than any other industry sector [1]. Thus, development of low-carbon and carbon-free energy sources, including photovoltaic solar cells, seems to be vital. At present, PV cells based on crystalline silicon wafers dominate the global PV market with over 90% of total annual production. Their further potential advancement seems to be limited, though. During the last few years, both average wafer thickness of fabricated c-Si PV cells and silicon usage (expressed in grams per watt-peak) has not significantly changed. There are mainly thin film solar cells based on CIGS, CdTe or amorphous silicon, that represent the remaining 10% of the market [2]. Such devices require less material usage during manufacturing process and are less prone to temperature changes [3]. However, their efficiencies are lower in comparison to traditional c-Si wafer-based PV cells [2].

When it comes to the future of thin film solar cells, CZTS ($\text{Cu}_2\text{ZnSnS}_4$) kesterite thin films are one of the most promising materials. Undeniable assets of CZTS are that it is a nontoxic substance and it contains only easily accessible elements. Nevertheless, there are some obstacles related to the fabrication of CZTS layers with homogenous crystal structure without unwanted secondary phases [4].

In this work, experimental solar cells consisting of sol-gel spin coated CZTS/CdS/ZnO/AZO structures deposited on soda-lime glass covered with Mo were investigated. Essential electrical parameters were obtained with the use of current-voltage characteristics of the samples. Current transport mechanisms in the junctions were analysed as well. Measured Raman scattering spectra revealed an actual composition of the examined structure. Observed Raman bands were related to CZTS and CdS. Moreover, thanks to performing a laser ablation, a formation of an undesirable MoS_2 interlayer between Mo and CZTS films was proved, which implied that Mo is not an appropriate back contact material for CZTS-based solar cells. Additionally, atomic force microscopy was used to obtain and analyse data connected with surface structure of the samples.

[1] IPCC, 2014: *Climate Change 2014: Synthesis Report. Contribution of Working Groups I, II and III to the Fifth Assessment Report of the Intergovernmental Panel on Climate Change* [Core Writing Team, R.K. Pachauri and L.A. Meyer (eds.)]. IPCC, Geneva, Switzerland, 151 pp.

[2] Fraunhofer Institute for Solar Energy Systems, PSE Projects GmbH, *Photovoltaics Report*, Freiburg, 2020.

[3] T. D. Lee, and A. U. Ebong, *Renew. Sust. Energ. Rev.* **70**, 1286-1297 (2017).

[4] T. Özdal, and H. Kavak, *Ceram. Int.* **44** 18928-18934 (2018).

Utilizing Ferroelectric Materials to Tune the Performance of Organic Differential Photodetectors

Arpana Singh¹, Md. Kashif Shamim², Seema Sharma², and Louisa Reissig¹

¹ *Institute of Experimental Physics, Freie University Berlin, Arnimallee 14, Berlin, Germany*

² *Materials Research Laboratory, Anugrah Narayan College, Boring Road, Patna, India*

In our day to day life we are surrounded by a number of electronic appliances. Recent environmental concerns have imposed constraints on the choice of material for the fabrication of such devices. In many applications, lead-free ferroelectric (FE) materials, such as (Na, K) NbO₃ (NKN), have become prominent targets due to their excellent dielectric properties caused by the permanent dipole moment across the material, which can be tuned and controlled by an applied electric field. Our present study dwells on the incorporation of such FE materials as a tunable insulating layer (IL) in our recently developed differential photodetectors. [1] The architecture used is based on a standard MSM photodiode with an inserted thick IL between the metal electrode (M) and the organic photoactive semiconductor layer (S). This converts the DC photocurrent response to steady light illumination, to a transient signal of opposite polarity when switching between light ON / OFF states, thus reacting predominantly to changes in light intensity and not to the light intensity itself. [1] Hu et al [2] demonstrated that the performance of such photodetectors can be tuned and enhanced using conventional FE materials. Encouraged by his results, we study the effect of a range of novel environmental-friendly lead-free NKN and doped NKN FE materials on the performance of MI_{FE}SM photodetectors. MI_{FE}SM devices (Fig.1a) were fabricated by first depositing thin FE films on Pt/Si substrates using a novel pulsed laser technique. Their structural and electronic properties were investigated, confirming appreciable values of remnant polarization with low leakage current, [3] which is prerequisite for the device operation. On top of these FE films a photoactive semiconductor (P3HT/PCBM) layer was deposited using spin-coating, followed by the deposition of a transparent Au metal electrode, which allows sufficient illumination of the S layer. Photocurrent experiments were performed showing a stable characteristic frequency response (Fig.1b) with signal polarity agreeing with the polarity of the pre-polarization of the films before active layer deposition. Initial measurements confirm that the strength of the photocurrent response could be tuned by poling the devices (Fig.1c), demonstrating the potential of such novel materials on tuning the response in differential photodetectors.

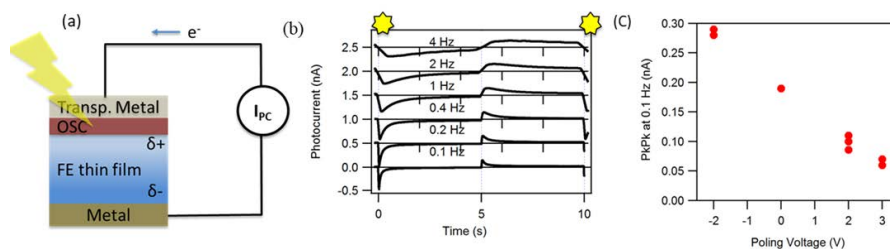


Fig.1. a) Principle of the MI_{FE}SM device architecture b) **Frequency**-dependent photocurrent response c) Peak-to-peak photocurrent at 0.1 Hz after applied voltage for 20 min.

[1] L.Reissig, S. Dalgleish, and K. Awaga, *AIP Advances*, **6**, 1 (2016).

[2] L.Hu, S.Dalgleish, M.M.Matsushita, H. Yoshikawa and K.Awaga, *Nature Communications*, **5**, 1 (2014).

[3] M.K Shamim, S. Sharma, and R.J. Choudhary, *J. Appl. Phys*, **126**, 13 (2019).

Quantum constrictions and inner Corbino contacts in $\text{Cd}_{1-x}\text{Mn}_x\text{Te}$ microdevices

R. Rudniewski^{1,2}, W. Zaleszczyk^{1,2}, Z. Adamus², D. Śniezek²,
P. Ungier¹, T. Wojciechowski^{1,2}, J. Wróbel², T. Wojtowicz¹

¹International Research Centre MagTop, Institute of Physics, Polish Academy of Sciences,
PL-02668 Warsaw, Poland

²Institute of Physics, Polish Academy of Sciences, PL-02668 Warsaw, Poland

We focused on the studies of low dimensional electron transport at low temperatures, in the millikelvin temperature range. We present results of the studies of electrostatically defined conducting channels fabricated from modulation doped CdTe quantum well (QW) structures and structures with addition of Mn impurities into the QW region. The later structures are interesting because of the large and tunable g-factor of two dimensional electrons (2DEG) [1] and possibility of creation of the quantum Hall ferromagnetic state. To determine the amount of magnetic impurities in the QW we performed comparison of the experimental data with simulations of the SdH oscillations obtained with the use of the theory developed in Ref. [2,3]. Studied devices were prepared with the use of multilevel electron beam lithography and contained deposited inner ohmic contacts made of HgTe. It is known, that such interior contacts are connected to the edge currents through Corbino geometry and therefore their coupling is the strongest for the innermost channel (i.e., farthest from the edges) [4,5]. Moreover, quantized resistance plateaus are not observed for Corbino samples; instead, the conductance drops to zero for integer filling factors [6] (see Fig. 1). On the other hand, quantum constrictions can effectively separate inner edge states between opposite sample sides.

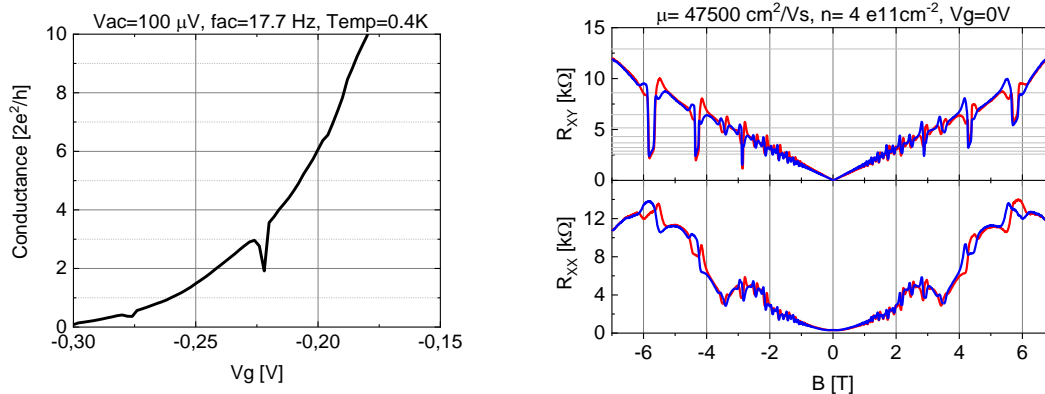


Fig. 1. Closing of the conducting channel by electrostatic potential of split-gate (left) and electron transport measurements with hysteresis like features (right).

The research was partially supported by the Foundation for Polish Science through the IRA Programme co-financed by EU within SG OP (grant No. MAB/2017/1).

- [1] T. Wojtowicz, *et al.*, J.Cryst.Growth, **378**, 214-215 (2000)
- [2] J. Jaroszyński *et al.*, Phys. Rev. Lett., **89**, 266802 (2002)
- [3] J. Kunc *et al.*, Phys. Rev. B, **92**, 085304 (2015)
- [4] J. Faist, *et al.*, Phys. Rev. B, **43**, 9332 (1991)
- [5] R. J. Haug, Semicond. Sci. Technol., **8**, 131-153 (1993)
- [6] S. Kobayakawa, *et al.* J. Phys. Soc. Jpn., **82**, 053702 (2013)

Comparison of Ir-Si-O and Ru-Si-O as Schottky barrier electrodes to amorphous In-Ga-Zn-O

Aleksandra Wójcicka, Krzysztof Piskorski, Marek Wzorek, Andrzej Taube, and
Michał A. Borysiewicz

Łukasiewicz Research Network – Institute of Microelectronics and Photonics, Warsaw, Poland

Amorphous In-Ga-Zn-O is a transparent semiconducting material that has seen a rapid commercial adaptation in thin film transistors controlling the pixels in the majority of currently available displays. This was due to its excellent stability, controllability and large-scale uniformity, the latter related to its amorphous structure. Due to it, the material is also seen as promising for implementation in flexible electronics, where the amorphous structure is beneficial due to less stress generating during bending of the material. A significant hindrance has been the necessity of high temperature processing of the common Pd oxide and Ag oxide based Schottky barriers to In-Ga-Zn-O. Recently, we shown that the ternary conducting oxide Ru-Si-O exhibits a large work function and can be successfully used as Schottky barriers in diode and thin film transistor structures with no thermal processing needed [1,2]. Additionally, the material is X-ray diffraction-amorphous, having the microstructure of nanosized Ru grains embedded in an SiO₂ matrix, beneficial for the flexible electronics area. Based on the predictions of similar properties of the ternary Ir-Si-O system [3], we decided to study its work function and applicability in barriers to In-Ga-Zn-O, to widen the family of materials available for low thermal budget electronic devices.

In this report we demonstrate X-ray amorphous, conductive Ir-Si-O films deposited by means of reactive magnetron sputtering of an Ir-Si target in an argon/oxygen mixture with a changing oxygen content. The deposited films show electrical resistivity increasing with the increase of oxygen content in the sputtering atmosphere. The lowest resistivity, $3 \cdot 10^{-4} \Omega \cdot \text{cm}$, was obtained for pure Ar and the highest, $6 \cdot 10^{-1} \Omega \cdot \text{cm}$, for 7% O₂. Along with the resistivity, the transparency of the films is also increased. The oxygen content in the films saturates at 58 atomic percent with the Ir to Si ratios changing, as devised by EDX measurements. The determined work functions of the films follow the trend of resistivity and are in the range 4.97 to 5.08 as determined by means of photocurrent measurements on MOS structures. TEM investigations reveal a microstructure of Ir grains inside an oxide matrix, similar to the case of Ru-Si-O. To gain more understanding on the behavior of the material, we discuss the results for Ir-Si-O with regard to those obtained for the similar Ru-Si-O, with a focus on the significantly differing deposition conditions for the two. Finally, we fabricated Ru-Si-O and Ir-Si-O diode structures to In-Ga-Zn-O thin films with carrier concentration equal to $3 \cdot 10^{17} \text{ cm}^{-3}$.

This research was financed partially by the statutory funds of the Łukasiewicz Research Network – Institute of Microelectronics and Photonics and partially by the Medical Research Agency, Poland, Project number 2020/ABM/COVID19/0012.

References:

- [1] J. Kaczmariski, M. Borysiewicz, K. Piskorski, M. Wzorek, M. Kozubal, E. Kamińska, IOP Semiconductor Science and Technology 33 (2018) 015010
- [2] J. Kaczmariski, J. Grochowski, E. Kamińska, A. Taube, M.A. Borysiewicz, K.D. Pągowska, W. Jung, A. Piotrowska, IEEE Electron Device Lett. 36 (2015) 469-471
- [3] U. Gottlieb, O. Laborde, P.H. Giauque, M.-A. Nicolet, R. Madar, Microelectronic Engineering 60 (2002) 107-111

Light modes in microcavity with anisotropic and gyrotropic medium

Przemysław Oliwa¹, Witold Bardyszewski²,
Barbara Piętka¹, and Jacek Szczytko¹

¹*Institute of Experimental Physics, Faculty of Physics, University of Warsaw, Pasteura 5, Warsaw, Poland*

²*Institute of Theoretical Physics, Faculty of Physics, University of Warsaw, Pasteura 5, Warsaw, Poland*

Recently, it was demonstrated, that using a tunable optical cavity filled with a birefringent liquid crystal (LC) it is possible to simulate a photonic analog of spin-orbit interaction leading in particular to the so-called Rashba-Dresselhaus coupling between two cavity modes [1]. The description of such structure is highly complicated and typically requires advanced numerical techniques such as e.g. Berreman [2] and Schubert [3] method to ensure perfect correlation with experimental data. On the other hand we may use a simplified approach, assuming, that the cavity consist of two perfect mirrors, so that the electric field does not leak out of the cavity. In this method we get analytical solutions, but the result are qualitative in nature and much less reliable than numerical simulations.

In this work we demonstrate a new, more realistic approach which can be used to describe the optical properties of LC microcavities with higher precision. In our model, we replace Bragg mirrors with very thin dielectric layers with thickness L going to zero and the refractive index n going to infinity in such a way that the product n^2L is constant and proportional to the effective discontinuity of the derivative of the electric field at such a layer. Using our model we can obtain analytical expression for electric field both inside and outside the cavity. In particular we are able to reproduce with great precision the dispersion of modes which was previously obtained using a more involved numerical technique of Berreman, as illustrated in figure 1. The analytical computational technique proposed by us greatly facilitates the analysis of light polarization textures obtained in experiments using LC cavities such as, for example, optical persistent spin helix.

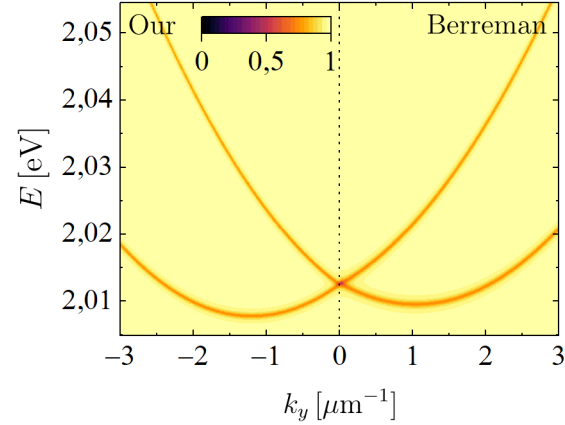


Figure 1: Comparison of momentum-resolved reflectance spectra for our model (left side) and Berreman model (right side), respectively, for Rashba-Dresselhaus coupling in a liquid crystal microcavity.

[1] K. Rechcińska, M. Król, R. Mazur, P. Morawiak, R. Mirek, K. Łempicka, W. Bardyszewski, M. Matuszewski, P. Kula, W. Piecek. P. G. Lagoudakis, B. Piętka and J. Szczytko *Science* **366**, 727-730 (2019).

[2] Berreman, D. W. *J. Opt. Soc. Am.* **62**, 502-510 (1972).

[3] Schubert, M. *Phys. Rev. B* **53**, 4265-4274

Optical properties of dye-doped monocrystalline free-standing blue phase liquid crystal

Marcin Muszyński¹, Eva Otón², Mateusz Król¹, Mateusz Kędziora¹,
Przemysław Morawiak², Rafał Mazur², Przemysław Kula², Wiktor Piecek²,
Barbara Piętka¹, Jacek Szczytko¹

¹ *Institute of Experimental Physics, Faculty of Physics, University of Warsaw,
ul. Pasteura 5, 02-093 Warsaw, Poland*

² *Faculty of New Technologies and Chemistry, Military University of Technology,
ul. Gen. S. Kaliskiego 2, 00-908, Warsaw, Poland*

Blue phase liquid crystals (BPLCs) are highly ordered soft materials that appear in cholesteric liquid crystals in narrow temperature ranges between the chiral nematic phase and isotropic phase. In the BPLC phase, molecules spontaneously form a double twist cylinder structure which self-assembles into a three-dimensional cubic network of ordered topological defects. This periodicity leads to the appearance of a photonic bandgap, and thus, BPLCs are considered photonic crystals. Converging monochromatic light rays passing through the BPLC produce diffraction patterns, called Kossel patterns, which can give information about the lattice orientation of the BP cubic structure, its phase (BPI or BPII) and the order parameter in the BP crystal. Due to the fact that the lattice constant is comparable to the visible light range, this diffraction can be studied by optical methods.

Obtaining monocrystalline BP crystals in large volumes still remains a challenge because current BP crystals are usually polycrystalline (platelets), with limited sized single crystals. In our previous research [1] large 3D Blue Phase macrocrystals were obtained by modifying the precursor mixture. Changing the concentration of the chiral dopant allowed for the control of the lattice orientation and the lattice constant, thus the selective reflection of light.

In this work we prepared analogue BPLC precursors but comprised only by a monomeric mesogenic mixture and chiral dopants with high chirality, to obtain full-polymer monocrystalline BPLC films. By peeling-off the BPLCs films, we obtained free-standing layers that retained their optical properties. The samples were doped with several types of dyes that emit light from inside the crystal. The three-dimensional momentum-resolved tomography of the emission was performed to observe Kossel patterns and the lattice constant and the crystal orientation were determined.

Dye-doped monocrystalline free-standing blue phase is a new way of building hybrid photonic structures that can be easily integrated with 2D materials, e.g. single layers of transition metal dichalcogenides, hBN or 2D perovskites.

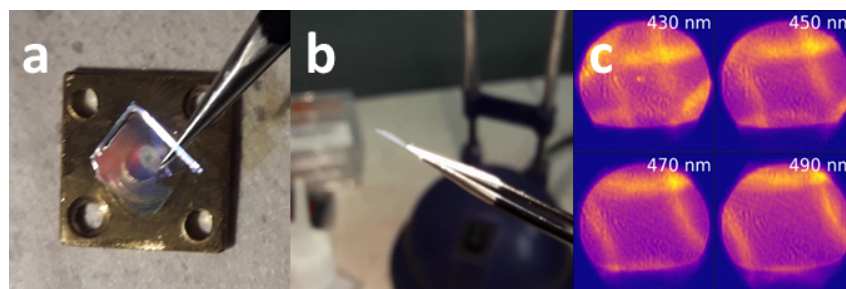


Figure: Blue phase liquid crystal characterisation. (a,b) Photographs of the free-standing sample. (c) Kossel patterns obtained by momentum-resolved tomography.

[1] E. Otón, et al., *Scientific Reports* **10**, 10148 (2020).

The optical tomography of cavity modes in a tunable liquid crystal cavity

**Sara Piotrowska¹, Mateusz Król¹, Katarzyna Rechcińska¹, Przemysław Oliwa¹,
Rafał Mazur², Przemysław Morawiak², Przemysław Kula³, Wiktor Piecek², Barbara
Piętka¹, Jacek Szczytko¹**

¹ *Institute of Experimental Physics, Faculty of Physics, University of Warsaw, Ludwika
Pasteura 5, Warsaw, Poland*

² *Institute of Applied Physics, Military University of Technology, gen. Sylwestra Kalickiego 2,
Warsaw, Poland*

³ *Institute of Chemistry, Military University of Technology, gen. Sylwestra Kalickiego 2,
Warsaw, Poland*

By enclosing a nematic liquid crystalline (LC) birefringent medium inside a microcavity (MC), in which a LC anisotropy can be controlled with an external electric field, we are able to spectrally tune and couple subsequent cavity modes [1]. Recently, we have demonstrated a Rashba-Dresselhaus-like spin orbit coupling (SOC) in such structure, when modes of a different parity were brought into a resonance [2].

In this work, we investigate a polarisation-resolved dispersion of spin-orbit coupled modes in a microcavity, that operates in weak coupling regime, with an organic dye (pyromethene 580) incorporated within a LC layer. We are allowed to trace cavity modes by detecting photons emitted from the nonresonantly excited sample. We performed an angle-resolved tomography to fully map the dispersion relation of the cavity modes for all directions of an in-plane wave vector of the cavity photons. Polarisation-resolved energy-momentum tomographies for all major regimes in LC MC were included in the research: resonance of the modes with opposite parity, when they are coupled by Rashba-Dresselhaus spin-orbit coupling term (Fig. 1) and resonance of the modes of the same parity.

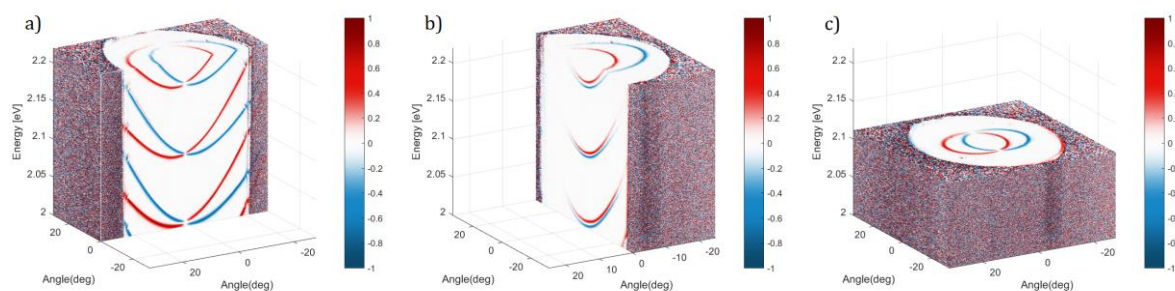


Fig. 1. Dispersion relation tomography, measured in reflectance, illustrating the regime of the resonance of the modes with different parities (voltage applied to the sample).

[1] K. Lekenta et al., Tunable optical spin Hall effect in a liquid crystal microcavity. *Light Sci. Appl.* **7**, 74 (2018).

[2] K. Rechcińska et al., Engineering spin-orbit synthetic Hamiltonians in liquid-crystal optical cavities. *Science* **366**, 727 (2019)

Direct measurement of the anisotropic elementary excitations in an exciton-polariton condensate in a synthetic gauge field

D. Biegańska^{1,2}, M. Pieczarka^{1,2}, E. Estrecho¹, M. Steger³, D. W. Snoke³, K. West⁴, L. N. Pfeiffer⁴, M. Syperek², A. G. Truscott⁵, E. A. Ostrovskaya¹

¹ ARC Centre of Excellence in Future Low-Energy Electronics Technologies and Nonlinear Physics Centre, Research School of Physics, The Australian National University, Canberra, Australia

² Department of Experimental Physics, Faculty of Fundamental Problems of Technology, Wrocław University of Science and Technology, Wrocław, Poland

³ Department of Physics and Astronomy, University of Pittsburgh, Pittsburgh, USA

³ Department of Electrical Engineering, Princeton University, Princeton, USA

³ Laser Physics Centre, Research School of Physics, The Australian National University, Canberra, Australia

In Bose-Einstein condensates of weakly interacting bosons, including exciton polaritons, dispersive branches of collective elementary excitations are present, populated via interparticle interactions. As particles are excited from the ground state condensate into higher energies and higher momenta, their dispersions can serve as a sensitive probe of the strength of these interactions. Due to the presence of TE-TM splitting of the optical modes in the optical microcavity, the polariton condensate excitation spectrum exhibit two branches, similarly to the low-density polariton states. However, the collective Bogoliubov excitation dispersions are predicted to be strongly anisotropic due to the difference in the interaction strengths for polaritons in singlet and triplet spin configurations [1]. This difference breaks the cylindrical symmetry and affects the dispersions, causing clear anisotropy in directions parallel and perpendicular to the condensate polarization vector axis. Furthermore, when the additional cavity anisotropy (birefringence) is present, the collective excitation eigenstates arise as the interplay between the synthetic magnetic gauge field of the microcavity and the interaction anisotropy [2].

In this work, we study experimentally the elementary excitations of an optically trapped high-density exciton-polariton condensate [3]. By measuring polarization- and angle-resolved photoluminescence, we directly observe the anisotropy of the branches and investigate their pseudospin textures in the momentum space, which corresponds to the effective magnetic field distribution. The measurement allows us to extract the inter- and intra-spin polariton interaction constants. This experiment is a direct realization of a non-Abelian gauge field in an interacting quantum liquid, with the presence of diabolical points and the associated spin structure characteristic of a monopole-like magnetic field. It signifies the possibility of using polariton systems in the high-density (non-linear) regime in future studies of synthetic gauge fields and topological physics.

[1] I. A. Shelykh, Y. G. Rubo, G. Malpuech, D. D. Solnyshkov, A. Kavokin, *Physical Review Letters*, **97**, 066402 (2006).

[2] H. Terças, H. Flayac, D. D. Solnyshkov, G. Malpuech, *Physical Review Letters*, **112**, 066402 (2014).

[3] D. Biegańska, M. Pieczarka, E. Estrecho, M. Steger, D. W. Snoke, K. West, L. N. Pfeiffer, M. Syperek, A. G. Truscott, E. A. Ostrovskaya, arXiv:2011.13290 (2020).

Positive Impact of Camphorsulfonic Acid on Perovskite Solar Cell Performance

A. Bohdan¹, A. Wincukiewicz¹, M. Tokarczyk¹, K. Korona¹, E. Kwiatkowska²,
M. Skompska², M. Kaminska¹,

¹ Faculty of Physics, University of Warsaw, Pasteura 5, 02-093 Warsaw, Poland

² Faculty of Chemistry, University of Warsaw, Pasteura 1, 02-093 Warsaw, Poland

Controlling the structural quality of the perovskite film is one of the major problems in the rapidly developing field of third-generation solar cell research. While the current performance of perovskite solar cells (PSC) in laboratories has already achieved the performance of traditional silicon cells (practically the same efficiency), process repeatability and material degradation remain still an issue. The small size of the grains, presence of pinholes, and consequently reduced carrier mobility and increased undesirable diffusion along the grain boundaries, can negatively affect efficiency and lifetime of the PSC.

In this study, the influence of camphorsulfonic acid (CSA) on the parameters of the perovskite material (methylamine lead iodide, MAPi), as well as solar cells with ITO/TiO₂/m-TiO₂/MAPi/Spiro-OMeTAD/Au configuration was investigated for the first time. The concentration of CSA added to the perovskite solution ranged from 0 to 5 mg/ml.

Scanning Electron Microscopy images of the surface morphology revealed an increase in the perovskite grain diameter from 320 nm to 490 with an increase of CSA concentration. At an excess of CSA (> 3 mg / ml), colorless acid precipitates appeared in the perovskite layer, which reduced the active surface of the corresponding solar cells.

X-ray diffraction (XRD) performed on freshly prepared samples showed only perovskite-related reflections, which proves that CSA acidification does not cause immediate degradation of the material. However, as the concentration of CSA increased, an increase in grain disorder was observed. In addition, by tracking the XRD peaks associated with perovskite and lead iodide (product of perovskite decomposition), it was found that unprotected CSA-containing perovskite layers degraded faster compared to pure perovskite layers. This observation happily contrasted with the behavior of the PCS, which by measuring I-V characteristics as a function of time, showed a longer lifetime of CSA perovskite cells. After 1200h, the cell without CSA lost 50% of its initial efficiency, while the cells with 1-3 mg/ml of CSA lost only 20%. We explain this controversy by the difference in the configuration of the perovskite layer – in the first case we deal with unprotected perovskite layer as such, but in the second case with the perovskite layer in the solar cell structure with two-sided coverings: a hole transport layer (Spiro-OMeTAD) or an electron transport layer (TiO₂).

In addition to the stability improvement, there was also an improvement in PCS efficiency from 6.88% for CSA-free cells to 7.18% and 7.35%, for CSA concentrations of 1 and 2 mg/ml, respectively. However, for a higher content of CSA (> 3 mg / ml), the efficiency decreased, most probably due to the mentioned CSA precipitates (a strong decrease in the short-circuit current was observed for such cells). Two main factors contributed to the increase in efficiency. The first was an increase in open-circuit voltage by up to 10%, most likely due to a change in the energy structure of the cell, in particular a positive effect of CSA on the Spiro-OMeTAD HOMO level. The second was the decrease in series resistance, probably due to the better mobility in the CSA-treated perovskite layers.

In conclusion, we showed that the addition of CSA to the perovskite solution positively influences the properties of the perovskite cells, increasing the perovskite grain size, cell efficiency and slowing down the aging process.

Bose-Einstein condensation of exciton-polaritons triggered by magnetic field in coupled planar microcavities

Krzysztof Sawicki¹, Maciej Ściesiek¹, Wojciech Pacuski¹,
and Jan Suffczyński¹

¹*Institute of Experimental Physics, Faculty of Physics, University of Warsaw,
Pasteura St. 5, 02-093 Warsaw, Poland*

A typical feature of pure photonic systems is a weak susceptibility to a magnetic field, making it challenging to control them with an applied external field. In our approach, the exciton-polaritons, hybrid states resulting from the strong interaction between excitons and photons in a microcavity, is used to create the nonlinear response. Thanks to the magnetic dopants, it is possible to efficiently manipulate states' energy through the excitonic component of polaritons, which would be hard to achieve with weakly interacting photons.

In the presented work, we use a multi-level polariton system based on II-VI materials, which shows a relatively strong response to an external magnetic field. This study implements vertically coupled double planar microcavities [1,2], each embedding quantum wells, to observe nonlinear polariton phenomena under non-resonant and quasi-resonant excitation. One of the sets of quantum wells in the investigated system is doped by manganese ions, allowing effective control of the polariton levels using the Giant Zeeman shift. Therefore it is possible to study the impact of magnetic field on Bose-Einstein condensation of polaritons and dual-wavelength polariton lasing in a multi-level polariton system. Apart from the typical polariton condensation that occurs after exceeding the threshold power, we observe also polariton condensation triggered by the magnetic field.

Moreover, we provide a theoretical description of condensation and multistability in optically driven polariton condensate under non-resonant and quasi-resonant excitation. Multistability is the phenomenon resulting from the system's internal memory in which two or more stable states exist for given conditions. In contrast to the polariton bistabilities previously observed as a function of the excitation power in resonantly optically or electrically driven microcavities, in our case, the effect occurs at magnetic field dependence. We develop a Gross-Pitaevskii-based model with a magnetic field that qualitatively explains the occurrence of the hysteresis in the scan with the magnetic field. The calculations suggest that the multistability arises due to exciton-photon detuning-dependent polariton-polariton interactions and can be revealed in magnetophotoluminescence experiments.

Our work expands the studies of coupled polariton systems and opens up new opportunities in the field of polariton lasers and polariton logic devices controlled by external fields.

- [1] K. Sawicki, T. J. Sturges, M. Ściesiek, T. Kazimierczuk, K. Sobczak, A. Golnik, W. Pacuski, J. Suffczyński, *Nanophotonics*, 10(9), 2421-2429 (2021).
- [2] M. Ściesiek, K. Sawicki, W. Pacuski, K. Sobczak, T. Kazimierczuk, A. Golnik, J. Suffczyński, *Communications Materials* 1, 78 (2020).

Point Defect Related Phenomena in Semiconductors with Low Symmetry: Examples of β -Ga₂O₃, Nitride Alloys, and Nitride Devices

Filip Tuomisto

Department of Physics, University of Helsinki, P. O. Box 43, FI-00014 Helsinki, Finland

Positron annihilation spectroscopy is a powerful set of methods for the detection, identification and quantification of vacancy-type defects in semiconductors [1]. In the past decades, it has been used to reveal the relationship between (opto-)electronic properties and specific defects in a wide variety of elemental and compound semiconductors. In typical binary compound semiconductors, the selective sensitivity of the technique is rather strongly limited to cation vacancies that possess significant open volume and suitable charge (negative of neutral).

I will present recent advances in combining state-of-the-art positron annihilation experiments and ab initio computational approaches. The latter can be used to model both the positron lifetime and the electron-positron momentum distribution – quantities that can be directly compared with experimental results. We have applied these methods to study semiconductor systems with less symmetry than “regular” compounds: β -Ga₂O₃ single crystals and thin films [2-4], highly alloyed InGaN and AlGaN [5,6], and both N- and Ga-polar GaN/AlGaN/GaN HEMT structures [7].

We find that both positron annihilation signals exhibit colossal anisotropy, associated with the low symmetry of the β -Ga₂O₃ crystal structure that leads to unusual kind of one-dimensional confinement of positrons in the lattice. We show that the positron annihilation signals are dominated by so-called split Ga vacancies where an unusually strong relaxation of the surrounding atoms takes place. In the InGaN and AlGaN alloys, we show that the formation of various kinds of point defects and their complexes is strongly dependent on the details of the local environment in the random alloy. This is found both for in-grown and for irradiation-induced defects. In HEMTs, we show that N-polar GaN/AlGaN/GaN heterostructures exhibit significant N deficiency at the bottom AlGaN/GaN interface, and that these N vacancies can hamper the device performance through trapping of holes in unoptimized HEMT device structures. We are able to detect and monitor N vacancies thanks to the built-in electric field driven pre-confinement of positrons to the bottom interface of the structure.

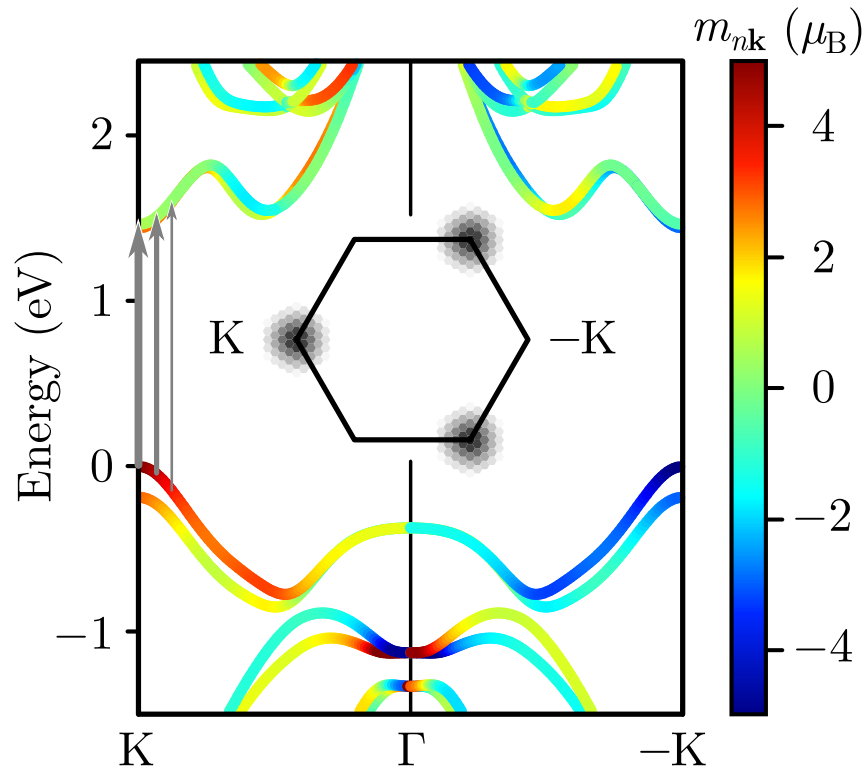
- [1] F. Tuomisto and I. Makkonen, Rev. Mod. Phys. **85**, 1583 (2013).
- [2] A. Karjalainen *et al.*, Phys. Rev. B **102**, 195207 (2020).
- [3] A. Karjalainen *et al.*, Appl. Phys. Lett. **118**, 072104 (2021).
- [4] A. Karjalainen *et al.*, J. Appl. Phys. **129**, 165702 (2021).
- [5] V. Prozheeva *et al.*, Appl. Phys. Lett. **110**, 132104 (2017).
- [6] I. Prozheev *et al.*, Appl. Phys. Lett. **117**, 142103 (2020).
- [7] V. Prozheeva *et al.*, Phys. Rev. Applied **13**, 044034 (2020).

Monolayer Transition Metal Dichalcogenides in Magnetic Fields

Thorsten Deilmann

Institute of Solid State Theory, University of Münster, Germany

The effect of a magnetic field on the optical absorption in semiconductors has been measured experimentally and modeled theoretically for various systems in previous decades. We present a new first-principles approach [1] to systematically determine the response of excitons to magnetic fields, i.e. exciton g factors. By utilizing the GW -Bethe-Salpeter equation methodology we show that g factors extracted from the Zeeman shift of electronic bands are strongly renormalized by many-body effects which we trace back to the extent of the excitons in reciprocal space. We apply our approach to monolayers of transition metal dichalcogenides (MoS_2 , MoSe_2 , MoTe_2 , WS_2 , and WSe_2) with strongly bound excitons for which g factors are weakened by about 30%.



If these monolayers are placed on a ferromagnetic substrate their g factors change. For the prototypical bilayer of WSe_2 on top of a ferromagnetic layer of CrI_3 we find substantially different coupling of both WSe_2 K-valleys to the sublayer. Besides an energetic splitting of a few meV, the corresponding excitons have significantly different interlayer character.

[1] *Phys. Rev. Lett.* **124**, 226402 (2020).

Excitons and Polaritons in van der Waals Hetero-bilayers

Hui Deng

University of Michigan, 450 Church St. Ann Arbor, MI, USA

Van der Waals semiconductors provide a platform for creating two-dimensional crystals layer-by-layer and engineering excitonic states therein with exceptional properties. As moiré lattice form in a heterobilayer, carriers can tunnel between closely-aligned bands in the two neighboring monolayers, leading to hybrid states that combine a large oscillator strength similar to intra-layer excitons and tunability of inter-layer ones. Such hybrid states are manifestations of the formation of moiré lattices. When coupled to cavities, the quantum confined nature of excitons in each moiré cell manifests as strong polariton nonlinearity, providing a potentially highly tunable system for ultra-low-power optoelectronics and quantum polaritonics.

- [1] L. Zhang, Z. Zhang, F. Wu, D. Wang, R. Gogna, S. Hou, K. Watanabe, T. Taniguchi, K. Kulkarni, T. Kuo, S. R. Forrest, and H. Deng, *Nature Communications* **11**, 1 (2020).
- [2] L. Zhang, F. Wu, S. Hou, Z. Zhang, Y.-H. Chou, K. Watanabe, T. Taniguchi, S. R. Forrest, and H. Deng, *Nature* **591**, 7848 (2021).

Tuesday

Tuesday

CdO/MgO cubic superlattices grown by MBE on sapphire

E. Przeździecka¹, A. Wierzbicka¹, P. Dłużewski¹, A. Lysak¹, P. Sybilski¹, I. Sankowska²,
P. Strak³, K. Morawiec¹, R. Jakiela¹, M. Pietrzyk¹, A. Kozanecki¹

¹Institute of Physics, Polish Academy of Sciences, al. Lotników 32/46, Warsaw, Poland

²Łukasiewicz Research Network - Institute of Electron Technology, Al. Lotników 32/46,
Warsaw, Poland

³Institute of High Pressures Physics, UNIPRESS, 01-142, Warsaw, Poland

New highly perspective cubic CdO/MgO short period superlattices (quasi-alloys) were grown on sapphire substrates by plasma assisted MBE. Their crystal quality was characterized using High Resolution X-ray Diffraction and Transmission Electron Microscopy (TEM) techniques and the thicknesses and growth rates of MgO and CdO individual layers were extracted. Small angle X-ray diffraction peaks corresponding to the period of the superlattices ranging from 0.6 to 5 nm were clearly observed. Energy gaps of the obtained cubic structures was moved by control of the sublattices thickness in the wide spectral range $\sim(2.5-6$ eV). Obtained experimental data of band gap energies were compared with theoretical values determined from first principles calculations. Surface roughness parameters for SLs were analysed by small angle X-ray diffraction and AFM and their values obtained by both techniques are comparable. Structural parameters determined by computer simulation of reflectivity data have been used to calculate the rate of deposition for CdO and MgO layers and to quantify observations regarding layer density and surface roughness.

Good-quality MgO/CdO heterostructures, with controlled MgO and CdO thickness, have been first time successfully obtained and characterized what can open the door for their future applications. High transmittance, and band gap engineering in the wide spectral range in these SLs can have significant commercial relevance.

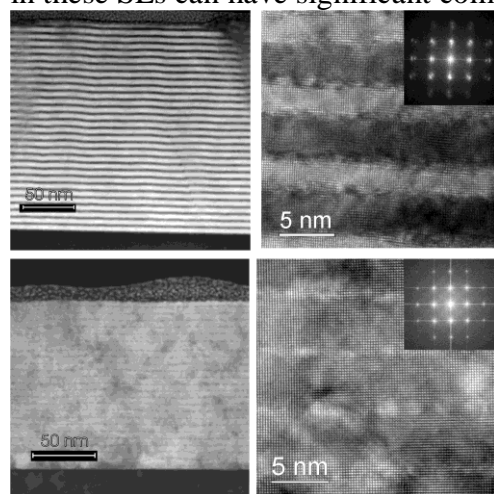


Fig.1. STEM/HAADF (left column) and HRTEM (right column) cross-sectional images two samples taken with the electron beam along the $\langle 001 \rangle$ zone axis.

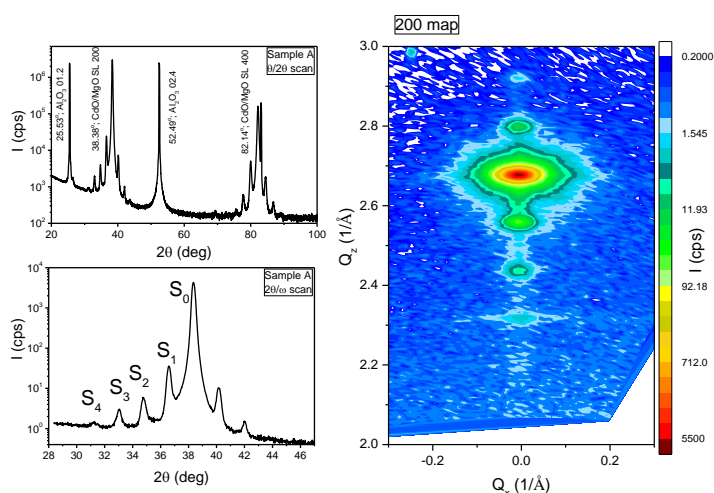


Fig.2. XRD patterns of the CdO/MgO superlattices. Reciprocal space maps from the CdO/MgO SL around the 200 Bragg peak.

Short-Period CdO/MgO Superlattices as Cubic CdMgO Quasi-Alloys E.P, A.W, P.D et al. *Cryst. Growth Des.* 2020, 20, 8, 5466–5472

The Band-Gap Studies of Short-Period CdO/MgO Superlattices E.P, P.S, A.W et al. *Nanoscale Research Letters* 16,; 59 (2021)

Low charge-noise nitrogen-vacancy centers in diamond created using laser writing with a solid-immersion lens

V. Yurgens¹, J. A. Zuber¹, S. Flågan¹, M. de Luca¹, B. Shields¹, I. Zardo¹, P. Maletinsky¹, R. J. Warburton¹ and T. Jakubczyk^{1,2}

¹ Department of Physics, University of Basel, CH-4056 Basel, Switzerland

² Faculty of Physics, University of Warsaw, Pasteura 5 02-093 Warsaw, Poland

The negatively charged nitrogen-vacancy (NV) center in diamond is among the most promising solid-state systems implementations of a quantum bit. However, integration of the NV center into any efficient photonic environment requires microstructuring the diamond at below-micrometer scale. Preserving the low NV zero-phonon line inhomogeneous broadening during this process is a major challenge with standard NV creation methods. This issue severely limits practical applications of NV centers.

Initial studies on pulsed-laser assisted creation of NVs yielded promising results by creating NVs with low inhomogeneous broadening at desired spatial locations in diamond [1]. Crucially, the lattice damage resulting from implantation of energetic ions was avoided. However, the method relied on a narrow window of parameters for successful writing. We widen this window by using a solid immersion lens (SIL), which facilitates laser writing over a broad range of pulse energies and allows for vacancy formation close to a diamond surface without inducing surface graphitization. We operate in the previously unexplored regime where lattice vacancies are created following tunneling breakdown rather than multiphoton ionization [2]. We present NV arrays that have been created between 1 and 40 μm from a diamond surface, all presenting optical linewidth distributions with means as low as 61.0 ± 22.8 MHz [2], including spectral diffusion induced by off-resonant repump for charge stabilization. This emphasizes the exceptionally low charge-noise environment of laser-written NVs. Such high-quality NV centers are excellent candidates for practical applications employing two-photon quantum interference with separate NV centers.

Finally, we propose a model for disentangling power broadening from inhomogeneous broadening in the NV zero-phonon line optical linewidth [2].

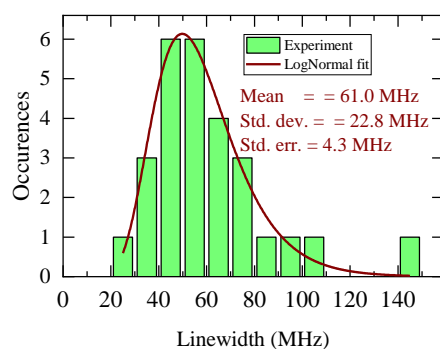


Figure 1. Zero-phonon line linewidth statistics with Lognormal fit revealing the low charge noise and high homogeneity of the fabricated NV centers.

[1] Y.-C. Chen, P. S. Salter, S. Knauer, ... and J. M. Smith, *Nat. Photonics* 11, 77 (2017).

[2] V. Yurgens, J.A Zuber, S. Flågan, M. De Luca, B.J. Shields, I. Zardo, P. Maletinsky, R.J. Warburton, and T. Jakubczyk, *ACS Photonics* (in press) 2021

Revealing exciton masses and dielectric properties of monolayer semiconductors with high magnetic fields

M. Goryca^{1,2}, J. Li², A.V. Stier², T. Taniguchi³, K. Watanabe³, E. Courtade⁴,
S. Shree⁴, C. Robert⁴, B. Urbaszek⁴, X. Marie⁴, and S. A. Crooker²

¹ *Institute of Experimental Physics, Faculty of Physics, University of Warsaw, Poland*

² *National High Magnetic Field Laboratory, Los Alamos, USA*

³ *National Institute for Materials Science, Tsukuba, Ibaraki, Japan*

⁴ *Universite de Toulouse, INSA-CNRS-UPS, LPCNO, Toulouse, France*

In semiconductor physics, many of the essential material parameters relevant for optoelectronics can be experimentally revealed via optical spectroscopy in sufficiently large magnetic fields. For the new class of monolayer transition-metal dichalcogenide (TMD) semiconductors, this field scale can be substantial – many tens of teslas or more – due to the relatively heavy carrier masses and the very large electron-hole (exciton) binding energies. For that reason many fundamental parameters of TMDs were – up to recently – still assumed from density functional theory calculations [1-3] and have not been experimentally measured.

Here we report circularly-polarized absorption spectroscopy of the monolayer semiconductors MoS₂, MoSe₂, MoTe₂, WS₂, and WSe₂ in very high magnetic fields up to 91 T. By encapsulating exfoliated monolayers in hexagonal boron nitride (hBN), we achieve very high optical quality structures that allow to follow the diamagnetic shifts and valley Zeeman splittings of not only the 1s ground state of the neutral exciton, but also its excited 2s, 3s, ..., ns Rydberg states (see Fig. 1). The energies and

diamagnetic shifts provide a direct determination of the effective (reduced) exciton masses and the dielectric properties of these monolayer semiconductors [4-5]. Unexpectedly, the measured exciton masses are significantly heavier than predicted for Mo-based monolayers. Moreover, we also measure other important material properties, including exciton binding energies, exciton radii, and free-particle bandgaps. These results provide essential and quantitative parameters for the rational design of optoelectronic van der Waals heterostructures incorporating 2D semiconductor monolayers.

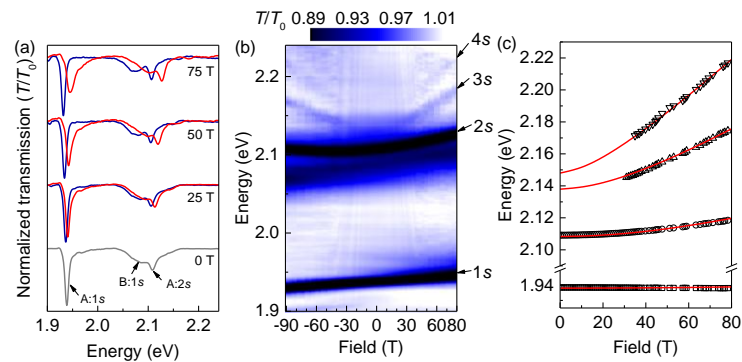


Figure 1. (a) Transmission spectra through monolayer MoS₂ encapsulated in hBN, in both circular polarizations. (b) Intensity map showing all spectra from -91 T to +80 T. The excited Rydberg states of the neutral exciton are visible. (c) The energies of each ns exciton state. Solid curves show model calculations.

- [1] A. Kormányos *et al.*, 2D Materials **2**, 049501 (2015).
- [2] T. C. Berkelbach *et al.*, Phys. Rev. B **88**, 045318 (2013).
- [3] D. Wickramaratne *et al.*, J. Chem. Phys. **140**, 124710 (2014).
- [4] A. V. Stier *et al.*, Phys. Rev. Lett. **120**, 057405 (2018).
- [5] M. Goryca *et al.*, Nat. Commun. **10**, 4172 (2019).

Magnetospectroscopy of Kane Electrons in HgCdTe Alloys

M. Szola^{1,5}, D. Yavorskiy^{1,2}, Y. Ivonyak¹, M. Haras^{1,3}, J. Przybytek¹, I. Yahniuk¹,
D. B. But¹, N. N. Mikhailov⁴, S. Dvoretzky⁴, G. Cywiński¹, J. Łusakowski²,
F. Teppe^{1,5}, S. S. Krishtopenko¹ and W. Knap^{1,5}

¹ CENTERA Laboratories, Institute of High Pressure Physics, PAS, Sokołowska 29/37,
01-142 Warsaw, Poland

² Faculty of Physics, University of Warsaw, Pasteura 5, 02-093 Warsaw, Poland

³ Warsaw University of Technology, Centre for Advanced Materials and Technologies
CEZAMAT, ul. Poleczki 19, 02-822, Warsaw, Poland

⁴ Rzhzanov Institute of Semiconductor Physics SB RAS, 630090, Novosibirsk, Russia

⁵ Laboratoire Charles Coulomb, UMR, CNRS 5221, 34095 Montpellier, France

The main inspiration of current work were the results previously obtained by the part of the co-authors in Mercury Cadmium Telluride (MCT) samples by temperature-dependent THz magnetospectroscopy [1]. The latter revealed the evolution of the energy band-gap with temperature vanishing at a certain temperature. It was shown that although the fermions in MCT alloys are represented by the admixture between the Dirac and spin-1 particles [2], they indeed support the pseudo-relativistic description involving the particle rest-mass and Fermi velocity. In this work, we focus on the band-gap evolution of $\text{Hg}_{1-x}\text{Cd}_x\text{Te}$ epitaxial alloys with cadmium content (x) probed by THz magnetospectroscopy. We studied three MCT samples with different cadmium content $x = 0.15, 0.16$ and 0.17 .

The THz magnetospectroscopy was performed at 2 K by means of thinned Allan-Bradley carbon resistor as a bolometer. As a source of THz radiation, the far-infrared molecular laser and Virginia diodes (VDI) source were used. Experimental resonant energies were analyzed within the pseudo-relativistic description [1] assuming $E_g = 2mc^2$, where m is the fermion rest mass and c is the Fermi velocity. The fitting analysis reveals a good agreement between experimental results and pseudo-relativistic description with Fermi velocity $c = 1.0 \cdot 10^6$ m/s independent of Cd content x .

We have investigated THz magnetospectroscopy of pseudo-relativistic fermions in $\text{Hg}_{1-x}\text{Cd}_x\text{Te}$ alloys. The measured transmission spectra have featured resonant absorption lines corresponding to the optical transition between Landau levels of pseudo-relativistic fermions. Analysis of experimental data within the pseudo-relativistic description [1] allowed us to determine the rest mass m and Fermi velocity c of pseudo-relativistic fermions. The band-gaps $E_g = 2mc^2$ are in a good agreement with the previously measured dependence on Cd content. The values of c are shown to be independent of Cd content.

This research was partially supported by the Foundation for Polish Science through a TEAM/2016-3/25 and by CENTERA Laboratories in the frame the International Research Agendas program for the Foundation for Polish Sciences co-financed by the European Union under the European Regional Development Fund (No. MAB/2018/9). It was also supported by the Terahertz Occitanie Platform, by CNRS through IRP "TeraMIR", by the French Agence Nationale pour la Recherche (Dirac3D project).

[1] F. Teppe et al. Nature Comm. **7**, 12576 (2016).

[2] S.S. Krishtopenko et al. J. Phys.: Condens. Matter **32**, 165501 (2020).

Mn-driven Weyl semimetal phase of $\text{Pb}_{1-x-y}\text{Sn}_x\text{Mn}_y\text{Te}$

A. Łusakowski¹, P. Bogusławski¹, and T. Story^{1,2}

¹*Institute of Physics, PAS, Al. Lotników 32/46, PL-02668, Warszawa, Poland*

²*International Research Centre MagTop, Institute of Physics, PAS, Al. Lotników 32/46, PL-02668, Warszawa, Poland*

Problem

In $\text{Pb}_{1-x}\text{Sn}_x\text{Te}$ the transition between topologically trivial and nontrivial phases may be achieved by changing the tin content x or the lattice parameter. This transition was analysed theoretically in [1], where we discovered a composition window $0.3 < x < 0.5$ between the trivial and the topological crystalline insulator phase characterized by the zero energy gap, where $\text{Pb}_{1-x}\text{Sn}_x\text{Te}$ is in the Weyl semimetal phase. Incorporation of magnetic ions into such crystals, apart from chemical composition and local crystal symmetry changes, leads in general to breaking the time reversal symmetry. In the present work we theoretically study the influence of the Mn ions on both the band structure and the topological properties of $\text{Pb}_{1-x-y}\text{Sn}_x\text{Mn}_y\text{Te}$ [2].

Methods

We consider periodic crystals built from $2 \times 2 \times 2$ supercells of $\text{Pb}_{1-x-y}\text{Sn}_x\text{Mn}_y\text{Te}$ containing 64 atoms. The spatial distributions of cations in the supercells are given by the Special Quasirandom Structures. From the density functional theory calculations we obtain parameters for the tight binding approximation. These parameters are then used for calculations of the band structure and topological indices, based on Chern number concept, which indicate triviality or nontriviality of the systems. The Weyl nodes, which appear in the considered systems at certain conditions, are characterized by their topological charges calculated as integrals of the Berry's curvature over small cubes surrounding the nodes.

Results

The presence of Mn in $\text{Pb}_{1-x}\text{Sn}_x\text{Te}$ affects its topological phase diagram. The composition window of the Weyl semimetal phase and the number of Weyl nodes in the reciprocal space depend on chemical composition and on magnetization. The predicted strong impact of the spin polarization of the Mn sublattice on the energy bands opens an interesting possibility of inducing a transition from the trivial to the Weyl phase by magnetic field or, at sufficiently low temperatures and high Mn contents, by spontaneous magnetization. The effect is expected to occur for $x > 0.35$. The topological characterization of $\text{Pb}_{1-x-y}\text{Sn}_x\text{Mn}_y\text{Te}$ based on Chern number concept agrees very well with the calculated energy band gaps. The small separation of the nodes in the reciprocal space is of the order of 0.01 \AA^{-1} , thus unavailable to the present ARPES experiments, and requiring new experimental tests.

Acknowledgements:

Work supported partially by NCN Grants UMO-2016/23/B/ST3/03725, UMO-2017/27/B/ST3/02470 (AL) and by Foundation for Polish Science through IRA Program cofinanced by EU within SG OP (TS).

[1] A. Łusakowski, P. Bogusławski, and T. Story, *Phys. Rev. B* **98**, 125203 (2018).

[2] A. Łusakowski, P. Bogusławski, and T. Story, *Phys. Rev. B* **103**, 045202 (2021).

Time-delayed nonlinear phenomena in exciton-polariton condensate

M. Furman¹, R. Mirek¹, A. Opala², K. Tyszka¹, M. Król¹, P. Stawicki¹,
B. Seredyński¹, W. Pacuski¹, J. Suffczyński¹, M. Matuszewski², J. Szczytko¹
and B. Piętka¹

¹ *Institute of Experimental Physics, Faculty of Physics, University of Warsaw,
ul. Pasteura 5, 02-093 Warsaw, Poland*

² *Institute of Physics, Polish Academy of Sciences,
Aleja Lotników 32/46, 02-668 Warsaw, Poland*

Nonlinear effects play an important role in exciton-polariton systems and can be used for neuromorphic calculations [1]. So far, nonlinearities of polariton condensates have been studied in the space of various parameters as intensity of emitted light in a function of excitation power [2] or relative spatial position of the two interacting condensates [3]. Here we propose and design experiment, where nonlinear effects are studied in the domain of time.

The nonlinear interactions strongly depend on the particle density in the excitonic reservoir fed by the condensate. In our experiment, two laser pulses are focused on the same position on the sample and delayed in time, giving us an insight into relation between two condensates connected through long-lived excitonic reservoir (Figure). The delay can be tuned in a wide range up to 500 ps. By time resolved measurements using streak camera we determine the lifetime of the condensate, the lifetime of excitonic reservoir and the decay time of effective interactions between condensates separated in time in our system. We have shown that the magnitude of the nonlinearity parameter determined by us can be affected by the excitation power and the delay time between the condensates. Additionally, we have shown that the time-dependent nonlinear effects can be used to create logic operations based on signal encoding in time.

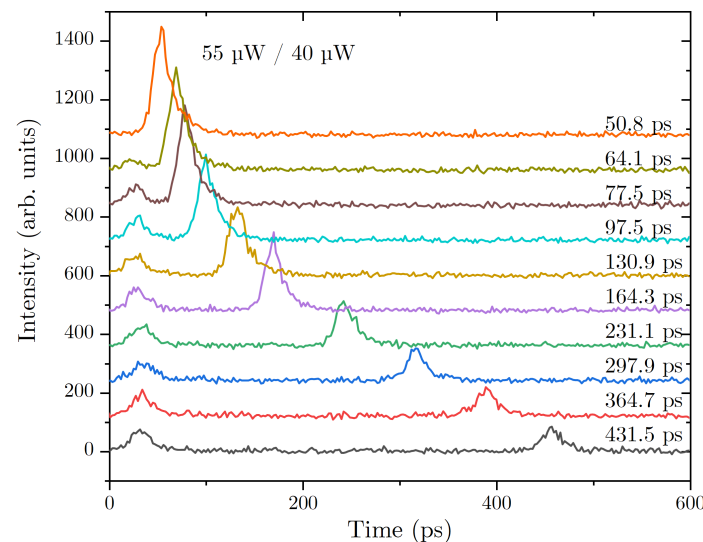


Figure: Time-resolved photoluminescence of two exciton-polariton condensates excited with two laser pulses separated in time (provided above each curve).

- [1] R. Mirek et al., *Nano Letters* **21**, 3715-3720 (2021).
- [2] J. Kasprzak et al., *Nature* **443**, 409 (2006).
- [3] K. G. Lagoudakis et al., *Physical Review Letters* **105** (12), 120403, (2010).

Neuromorphic binarized polariton networks

R. Mirek¹, A. Opala², P. Comaron², M. Furman¹, M. Król¹, K. Tyszk¹,
B. Seredyński¹, D. Ballarini³, D. Sanvitto^{3,4}, T. C. H. Liew⁵, W. Pacuski¹,
J. Suffczyński¹, J. Szczytko¹, M. Matuszewski² and B. Piętk¹

¹*Institute of Experimental Physics, University of Warsaw, Warsaw, Poland*

²*Institute of Physics, Polish Academy of Sciences, Warsaw, Poland*

³*CNR NANOTEC—Institute of Nanotechnology, Lecce, Italy*

⁴*INFN, Sezione di Lecce, Lecce, Italy*

⁵*School of Physical and Mathematical Sciences, Nanyang Technological University, Singapore*

Today's world is generating continuously growing amount of information. We realize a new way to process data quickly and efficiently. We perform neuromorphic computation using exciton-polaritons - quasiparticles having strong nonlinearities and small effective mass allowing for high-speed operations. We use nonlinear interactions in exciton-polariton condensate to create artificial neural network which can surpass electronic neuromorphic systems in terms of energy efficiency and processing speed.

First neuromorphic networks based on exciton-polaritons were proposed theoretically and realized experimentally implementing reservoir computing [1,2]. Our approach is based on creating a binarized network made of nonlinear XOR logic gates [3]. We study nonlinear emission from CdTe-based microcavity with six quantum wells. Nonlinearities observed in real-space imaging allow us to construct all-optical XOR logic gate and perform optoelectronic machine learning. We demonstrate the optoelectronic realization of polariton binary network classifying handwritten digits from MNIST dataset with 96% accuracy. We show that an all-optical XOR logic gate performs ultrafast (below 200 ps) logic operation with high energy efficiency (16 pJ per synaptic operation). Our results introduce a system that improves performance and energy efficiency.

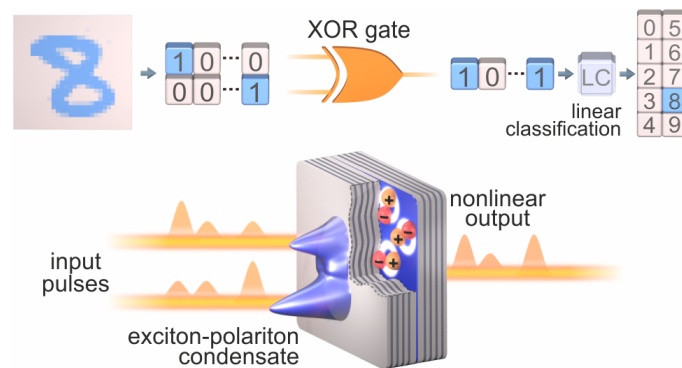


Figure: Scheme of a neuromorphic binarized network used for a handwritten digits recognition. Binarized input signal is nonlinearly transformed using a XOR logic gate and linear classification is performed. Input signal is encoded as a series of picosecond pulses forming exciton-polariton condensate providing nonlinear response.

- [1] A. Opala et al., Physical Review Applied **11**, 064029 (2019).
- [2] D. Ballarini, et al., Nano Letters **20**, 3506-3512 (2020).
- [3] R. Mirek, et al., Nano Letters **21**, 3715-3720 (2021).

Condensation and ballistic propagation of exciton polaritons in AlGaAs microcavity at high temperatures

D. Biegańska¹, M. Pieczarka¹, H. Suchomel², C. Schneider^{2,3}, S. Klemmt²,
S. Höfling^{2,4} and M. Syperek¹

¹*Department of Experimental Physics, Faculty of Fundamental Problems of Technology,
Wrocław University of Science and Technology, Wyb. Wyspiańskiego 27,
50-370 Wrocław, Poland*

²*Technische Physik, Physikalisches Institut and Wilhelm Conrad Röntgen-Research Center for
Complex Material Systems, Universität Würzburg, Am Hubland, 97074 Würzburg, Germany*

³*Institut of Physics, Carl von Ossietzky University of Oldenburg, Ammerländer Heerstrasse
114-118, 26126 Oldenburg, Germany*

⁴*SUPA, School of Physics and Astronomy, University of St. Andrews, St. Andrews KY16 9SS,
United Kingdom*

Exciton polaritons - mixed light-matter quasiparticles emerging from the strong coupling between excitons and photons in a semiconductor optical microcavity - are interacting bosons, which can form a macroscopically coherent state, e.g. a Bose-Einstein Condensate (BEC). The coherent emission of such a condensed state is referred to as polariton lasing, even though no population inversion is involved. With effective masses orders of magnitude lower than that of the free electron, the critical densities (temperatures) required to observe BEC of polaritons are much lower (higher) than that of atoms, making exciton polaritons a perfect platform to achieve condensation at elevated temperatures and even room temperature (RT). RT polariton condensation was currently achieved in various materials, from large bandgap semiconductors to novel materials, such as organic semiconductors, perovskites, and TMDCs. However, in the GaAs-based monolithic microcavities, where the quantum well (QW) excitons binding energy is relatively low, excitons dissociate above cryogenic temperatures. It prevents the formation of the condensate at high temperatures. Here, we employ a strategy to increase the exciton binding energy through band engineering of the Al_{0.2}Ga_{0.8}As/AlAs QWs, exploiting the effect of Γ -X valley mixing [1]. It preserves strong exciton-photon coupling up to 300 K, making it suitable for achieving RT BEC. It would make it a highly advantageous system, with well-established technology, best quality growth and colossal application potential.

In this work, we study the high temperature lasing of polaritons and their ballistic propagation. We employ several excitation schemes, including the pump spot structuring and optical trapping, in order to diminish the influence of incoherent excitonic reservoir on coherent properties of the condensate at high temperatures. We investigate various regimes of polariton lasing, with a careful address of the photon versus the polariton lasing. Most importantly, we observe a propagating polariton condensate, flowing out of the pumping spot at high temperatures (200 K), which is a current record value in this material system.

[1] H. Suchomel, S. Kreutzer, M. Jörg, S. Brodbeck, M. Pieczarka, S. Betzold, C. P. Dietrich, G. Sęk, C. Schneider, and S. Höfling, *Optics Express*, **20**, 24816 (2017).

Low-Frequency Noise in Carbon Nanotube Networks

A. Rehman^{1,*}, A. Krajewska¹, B. Stonio^{1,2}, S. Smirnov³, D. But^{1,2}, M. Filipiak^{1,2}, K. Pavlov², J. Smulko⁴, G. Cywinski^{1,2}, D. Lioubtchenko^{1,3}, W. Knap^{1,2,5}, S. Rumyantsev¹

¹ CENTERA Laboratories, Institute of High Pressure Physics PAS, Sokółowska 29/37, 01-142 Warsaw, Poland

² CEZAMAT, Warsaw University of Technology, Poleczki 19, 02-822 Warsaw, Poland

³ KTH Royal Institute of Technology, Malvinas Väg 10, SE-100 44 Stockholm, Sweden

⁴ Gdańsk University of Technology, G. Narutowicza 11/12, 80-233, Gdańsk, Poland

⁵ Laboratoire Charles Coulomb, University of Montpellier and CNRS UMR 5221, 34950 Montpellier, France

The low-frequency noise measurements play a significant role to explore the hidden characteristics of the materials for their various potential applications in low power and flexible electronics, biological and gas sensing, high frequency and terahertz active and passive elements. For instance, vapors of different chemicals induced Lorentzian components in noise spectra of graphene with distinctive features [1]. Later, this kind of study was further extended to other materials [2]. It can also be used to probe the properties of materials, which cannot be seen in the DC characterization. For example, the low-frequency noise measurements were previously used to examine the possible presence of hidden phase transitions and sliding of charge-density-waves in 1T-TaS₂ devices [3, 4], mechanism of negative photoconductivity and the effect of environment on carbon nanotube network devices [5, 6]. Here, we studied the low-frequency noise characteristics of randomly oriented networks of carbon nanotube-based devices as a function of back-gate voltages in field effect transistors, UV irradiation, and temperature. We also extend our study to different quality of nanotube samples and found that devices, exhibiting low Raman G/D peak ratio have higher noise (Fig.1). This implies that the low-frequency noise measurements can be used to probe the structural quality of nanotube networks. The measurements of noise and resistance under UV illumination and at elevated temperatures reveal at least two important components of resistance that contribute to the total resistance of nanotube networks rather than the generally accepted model of tube-to-tube junction resistance dominance. The electrical and noise measurements of different densities of nanotube networks revealed that though the sheet resistance decreased as the density of nanotubes increased, the low-frequency noise amplitude varied between samples and is not correlated with the change in the resistance. Our study reveals that the low-frequency noise is very sensitive to the structural quality of the sample and can be used as an effective tool to probe the significant characteristics of carbon nanotube-based electronic devices.

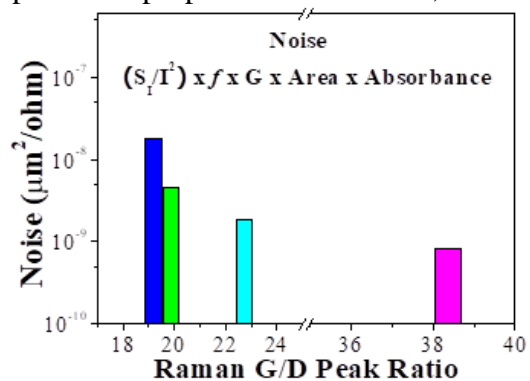


Fig. 1. Area, conductance and absorbance normalized noise of carbon nanotubes devices as function of Raman G/D peak ratio. Device with higher G/D peak ratio exhibits low noise.

- [1]. S. Rumyantsev, G. Liu, M.S. Shur, et al., *Nano Letters* **5**, 2294-2298 (2012).
- [2]. R. Samnakay, C. Jiang, S.L. Rumyantsev, et al., *Applied Physics Letters* **106**, 023115 (2012).
- [3]. G. Liu, S. Rumyantsev, M.A. Bloodgood, et al., *Nano Letters* **6**, 3630-3636 (2018).
- [4]. A. Mohammadzadeh, A. Rehman, F. Kargar, et al., *Applied Physics Letters* (2021).
- [5]. A. Rehman, S. Smirnov, A. Krajewska, et al., *Materials Research Bulletin* **134**, 111093 (2021).
- [6]. A. Rehman, A. Krajewska, B. Stonio, et al., *Applied Physics Letters* (2021).

Carrier density in monolayer MoS₂ govern by hBN encapsulation - unraveling the fine structure of the negative trion

M. Grzeszczyk¹, K. Olkowska-Pucko¹, K. Watanabe², T. Taniguchi³, P. Kossacki¹,
A. Babiński¹ and M. R. Molas¹

¹Institute of Experimental Physics, Faculty of Physics, University of Warsaw, Warsaw, Poland

²Research Center for Functional Materials, NIMS, Tsukuba Japan

³International Center for Materials Nanoarchitectonics, NIMS, Tsukuba, Japan

Two-dimensional layered materials, like semiconducting transition metal dichalcogenides (S-TMDs), are highly sensitive to the environment. This opens up an opportunity to externally control their properties by changing their surroundings. As the thickness of S-TMDs approaches the atomic limit, substrate-induced effects predominate their optical and electronic behavior. [1,2]

In this work, we present a systematic characterization of the optical response of the MoS₂ monolayers (MLs) encapsulated in hexagonal BN (hBN) flakes with varying thickness of the bottom hBN layer ranging from 4 nm to 134 nm. Photoluminescence (PL), photoluminescence excitation, and reflectance contrast experimental techniques are employed. We show that the intensity ratio of the emission due to neutral and charged excitons in MoS₂ ML strongly depends on the bottom hBN flake thickness. This effect indicates a key influence of the bottom hBN layer, particularly, in the limit of few nm, allowing a significant control of the carrier density in the MoS₂ MLs. The high quality of our structures, confirmed by small linewidths of the neutral exciton, which are on the level of a few meV, allows us to unveil the fine structure of negative trions in MoS₂ MLs, as can be appreciated in Fig. 1(a). We assigned the observed T₁, T₂, and T₃ lines to three configurations of a negative trion, *i.e.* an intravalley singlet, an intervalley singlet, and an intervalley triplet, respectively (see Fig. 1(b)). As the appearance of the T₁ and T₂ line is straightforward [3], the observation of the T₃ line in the PL spectrum is surprising. We relate the presence of T₃ line in the spectrum to the small spin-orbit splitting in the conduction band of MoS₂ ML and the photodoping processes.

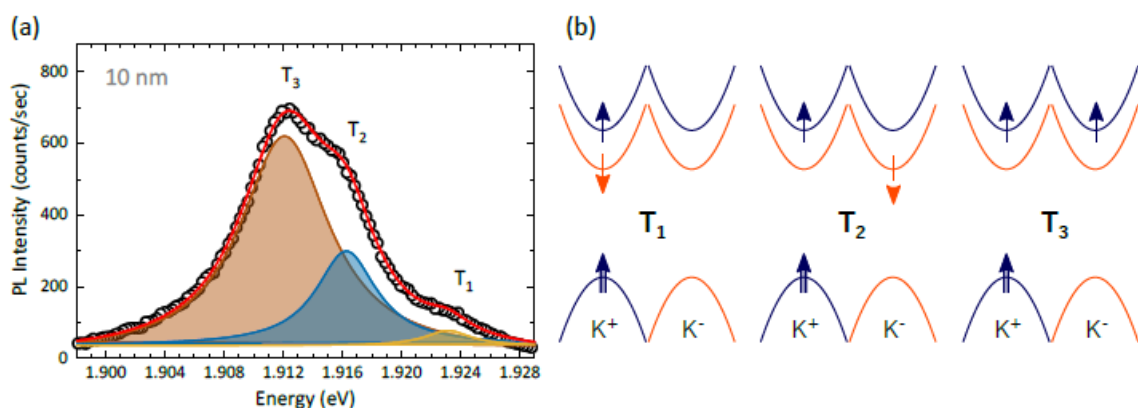


Fig. 1 (a) Photoluminescence spectrum of negative trions measured on the MoS₂ monolayer with 10 nm bottom hBN. The coloured Lorentzians display fits to the corresponding T₁, T₂, and T₃ lines. (b) Schematic illustration of possible spin configurations for optically-active (bright) negative trion formed in the K⁺ point in the monolayer MoS₂.

[1] M. R. Molas, et al., *Physical Review Letters* **123**, 096803 (2019).

[2] M. Grzeszczyk, et al., *Scientific Reports* **10**, 4981 (2020).

[3] J. G. Roch, et al., *Nature Nanotechnology* **14**, 432 (2019).

Characterization of Epitaxial Boron Nitride Layers With Fourier-transform Infrared Spectroscopy

Jakub Iwański, Piotr Tatarczak, Mateusz Tokarczyk, Johannes Binder,
Aleksandra K. Dąbrowska, Grzegorz Kowalski, Roman Stępniewski,
and Andrzej Wyszomolek

Faculty of Physics, University of Warsaw, Pasteura 5, 02-093 Warsaw, Poland

The interest of many scientists around the world is focused on two-dimensional materials. It is believed that heterostructures based on such materials will allow us to make a technological step towards their application in photovoltaics, ultrafast transistors and ultrasensitive photodetectors [1]. In many of these kind of devices hexagonal boron nitride (hBN) plays a crucial role, as hBN is an atomically flat insulator with a wide bandgap (~ 6 eV) that is very resistant to external conditions. Moreover, hBN itself is a prospective material for applications like neutron detectors or single photon sources.

However, all of these potential applications require large areas of hBN. One promising solution to this problem is based on metalorganic vapor-phase epitaxy (MOVPE). Although large scale growth has already been achieved, the quality of the epitaxial hBN layers is still inferior to flakes exfoliated from bulk crystals and needs to be improved.

In this work, we study high quality MOVPE grown hBN [2] by Fourier-transform infrared spectroscopy. Using the Dynamic Dielectric Function (DDF) approach we are able to simulate whole hBN spectrum as presented in Fig. 1. From the simulation we could extract the hBN layer thickness in the range from a atomic monolayer to few μm . The obtained results are in full agreement with X-ray methods. Moreover, by extracting position and damping parameter of E_{1u} phonon line, which corresponds to full width at half maximum (FWHM) of the peak, we gain information about the material quality which includes structural order, strain and defects. Measurements in a wide range of temperatures (80-625 K) allow conclusions about thermal properties of epitaxial layers. A comparison of thermal dependencies for as-grown and delaminated layers [3] (Fig. 1 inset) suggests a strong influence of the interaction between hBN and the substrate on the energy of the E_{1u} mode, providing precious information about the layer-substrate interaction.

The obtained results will be discussed in the context of hBN in van der Waals heterostructures. Information about thermal properties and interactions between the single layers is a must for future successful engineering of these kind of structures.

Acknowledgement: This work has been partially supported by the National Science Centre under grant no. 2019/33/B/ST5/02766.

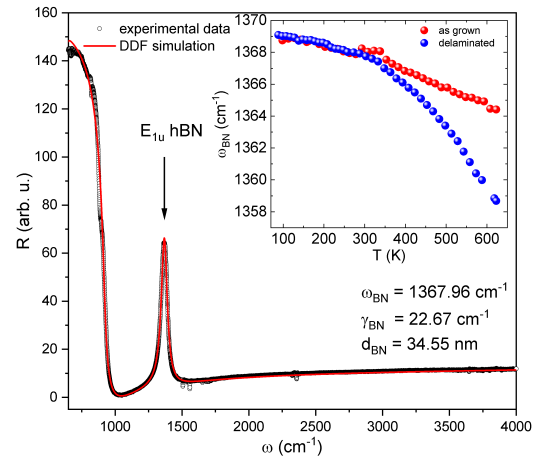


Figure 1: FTIR reflectance spectrum of a hBN layer on sapphire (black circles) together with simulated curve (red line). Inset: Peak position as a function of temperature for as grown (red spheres) and delaminated (blue spheres) layers.

- [1] H. Wang et al., *Nanoscale* **6**, 21 (2014).
- [2] A. Dąbrowska et al., *2D Mater.* **8**, 015017 (2021)
- [3] J. Iwański et al., *Acta Phys. Pol. A* **139**, 4 (2021)

Structural search and stability prediction of new M_xB_{1-x} phases based on *ab initio* calculations and Machine Learning Methods.

M. Sokołowski¹, M. Marchwiany², A. M. Jastrzębska³ and M. Birowska¹

¹University of Warsaw, Faculty of Physics, Pasteura 5, 02-093 Warsaw, Poland

²Interdisciplinary Centre for Mathematical and Computational Modelling (ICM), University of Warsaw, Pawińskiego 5a, 02-106 Warsaw, Poland

³Warsaw University of Technology, Faculty of Materials Science and Engineering, 02-507 Warsaw, Wołoska 141, Poland;

Since the first exfoliation of graphene, the world of two-dimensional (2D) materials has flourished and several thousand stable 2D materials have been predicted theoretically [1]. Just recently a new types of materials consisting of transition metals and boron atoms, called MBenes has entered two this world [2]. Atomically thin materials are extremely promising for electronic and optical applications. Progress in this area would be accelerated by enlarging the broad portfolio of 2D materials by considering the atomically thin alloys.

The subject of research is the search for new two-dimensional metal-boron systems based on the *ab initio* calculations and using machine learning methods. For the structural search, we have developed a software which is designed to facilitate findings of all non-equivalent position of dopants, substituted at the position of the host compound assuming particular lattice. The search protocol starts from generating the alloy structure using trigonal, hexagonal an rectangular lattices. Then, we apply the Density Functional Theory within the GGA+U approach to build a theoretical database, consisting few thousands of structures. Finally, on the top of DFT calculations, the Machine Learning model is constructed to predict the stability of novel M_xB_{1-x} systems.

The study was accomplished thanks to the funds allotted by the National Science Centre, Poland within the framework of the research project 'OPUS 18' no. UMO-2019/35/B/ST5/02538. Access to computing facilities of PL-Grid Polish Infrastructure for Supporting Computational Science in the European Research Space, and of the Interdisciplinary Center of Modeling (ICM), University of Warsaw are gratefully acknowledged.

[1] N. Mounet *et al.* *Nature Nanotechnology* **13**, 246-252 (2018).

[2] M. Khazaei *et al* *Nanoscale* **11**, 11305-11314 (2019).

Synthetic correlated electron system with twisted bilayer graphene quantum dots

A. Wania Rodrigues^{1,2}, Y. Saleem¹, M. Bieniek^{1,2}, P. Hawrylak¹

¹*Department of Physics, University of Ottawa, Canada*

²*Katedra Fizyki Teoretycznej, Politechnika Wrocławska, Polska*

Synthetic correlated electron systems offer the possibility to design topological quantum matter with properties vastly different from its constituents, with superconductivity, ferromagnetism and incompressible liquids of the fractional quantum Hall effect as good examples. Electronic correlations and entanglement associated with it, originate from electron-electron (e-e) interactions in a flat band (i.e. degenerate electronic shells). Recently, two systems, allowing design of the degenerate electronic shells, were proposed: triangular graphene quantum dots with zigzag edges (TGQD)[1-3] and magic angle twisted bilayer graphene (MATBG) [4]. In TGQD one electron energy level collapses at the Dirac point and a degenerate electronic shell arises. At half-filling the shell is spin polarized, but the polarisation is a non-trivial function of the shell filling due to the e-e interactions as in the lowest Landau level. In twisted bilayer graphene (TBG), a structure created by misaligning two graphene sheets stacked on each other, moiré patterns, flat bands and a synthetic Hubbard-like model appear. Depending on the filling of the flat bands, insulating and superconducting states were experimentally observed [5-6].

In this work, we combine the two approaches to build a synthetic correlated electron system by combining two triangular graphene quantum dots with zigzag edges into a bilayer TGQD [3]. The two degenerate electronic shells of each quantum dot combine to a single shell. The properties of the shell can be manipulated with a vertical electric field. We further twist the two triangles with respect to each other and combine the zero-energy shell of each triangle with flat bands originating from the formation of the moiré patterns of the bilayer. We use an ab initio fitted tight-binding model with tunnelling matrix elements covering up to the 6th nearest neighbours [7] and study the formation of the moiré patterns and creation of the flat bands in graphene quantum dots consisting of up to one million atoms as a function of misaligned angles. The effect of twist angle and quantum dot size on the magnetism of the two triangles at half filling will be determined using mean-field and exact diagonalization techniques.

- [1] A. D. Guclu, P. Potasz, O. Voznyy, M. Korkusinski & P. Hawrylak *Phys. Rev. Lett.* **103**, 246805 (2009)
- [2] A. D. Güçlü, P. Potasz, M. Korkusinski & P. Hawrylak, "Graphene Quantum Dots", Springer-Verlag (2014)
- [3] A. D. Guclu, P. Potasz & P. Hawrylak *Phys. Rev. B* **84**, 035425 (2011)
- [4] E. Bistritzer and Allan H. MacDonald, *PNAS* **108**, 12233 (2011)
- [5] Y. Cao, V. Fatemi, A. Demir, S. Fang, S. L. Tomarken, J. Y. Luo, J. D. Sanchez-Yamagishi, K. Watanabe, T. Taniguchi, E. Kaxiras, R. C. Ashoori & P. Jarillo-Herrero, *Nature* **556**, 80 (2018)
- [6] Y. Cao, V. Fatemi, S. Fang, K. Watanabe, T. Taniguchi, E. Kaxiras & P. Jarillo-Herrero, *Nature* **556**, 43 (2018)
- [7] 7. Kerelsky, A., McGilly, L.J., Kennes, D.M., Xian, L., Yankowitz, M., Chen, S., Watanabe, K., Taniguchi, T., Hone, J., Dean, C., Rubio, A., & Pasupathy, A. N., *Nature* **572**, 95–100 (2019)

Effective electron g-factors in electrically gated MoSe₂

K. Oreszczuk¹, A. Rodek¹, M. Goryca¹, T. Kazimierczuk¹, J. Howarth²,
T. Taniguchi³, K. Watanabe³, M. Potemski^{1,4}, and P. Kossacki¹

¹University of Warsaw, Pasteura St. 5, 02-093 Warsaw, Poland

²University of Manchester, Manchester M13 9PL, United Kingdom

³National Institute for Materials Science, Tsukuba, 305-0047, Ibaraki, Japan

⁴LNCMI, 25, avenue des Martyrs, 38042 Grenoble, France

Collective properties of the 2D electron gas (2DEG) have been studied extensively for different systems. Several theoretical models were developed, however, in many systems still struggle to quantitatively predict properties of the 2DEG at low and moderate density. Monolayer transition metal dichalcogenides are an example of a structure with near-ideal two-dimensional quantization, where the magnetooptical measurements reveal significant collective effects [1, 2].

We present an experimental approach to study 2DEG polarizability in electrically gated MoSe₂ monolayer. The oscillator strength of a charged exciton (attractive polaron) reflectivity peak in 2DEG regime is probed at liquid helium temperatures. Analysis of the dependence of the circular polarization degree of the resonance on the magnetic field reveals the effective electron g-factor.

We observe strong enhancement of the optical polarizability at low concentrations (below 10^{12} cm^{-2}). The electron g-factor ranges from around 1.5 at moderate and high concentrations to more than 3 at low concentrations, compared to about 2 obtained directly from analysis of the Zeeman shift of the optical transitions in the neutral regime [3]. Our direct magnetooptical measurement sheds more light on the issue of the collective properties in the regime of low concentrations. Moreover, at high concentrations, the value of the effective g-factor should approach the single particle g-factor value [4], paving the way to an alternative approach revealing the single electron properties of monolayer MoSe₂.

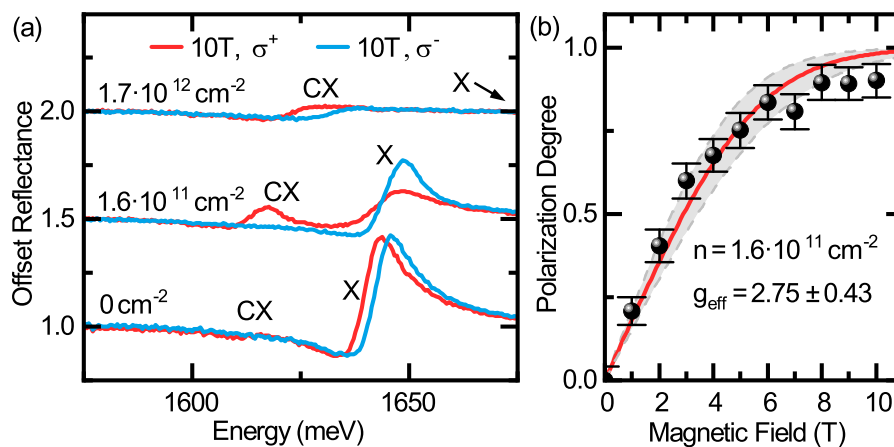


Figure 1: (a) Reflectance spectrum of the MoSe₂ monolayer at zero, low and high 2DEG concentration regimes. (b) Magnetic field dependence of the polarization degree of the CX peak at low concentration. Red line: fit resulting in electron g-factor value of 2.75.

- [1] J. Li et. al. *Phys. Rev. Lett.* **125**, 147602 (2020)
- [2] S. Larentis et. al. *Phys. Rev. B.* **97**, 201407(R) (2018)
- [3] M. Koperski et al., *2D Mater.* **6**, 015001 (2019)
- [4] C. Attacalite et al., *Phys. Rev. Lett.* **88**, 256601 (2002)

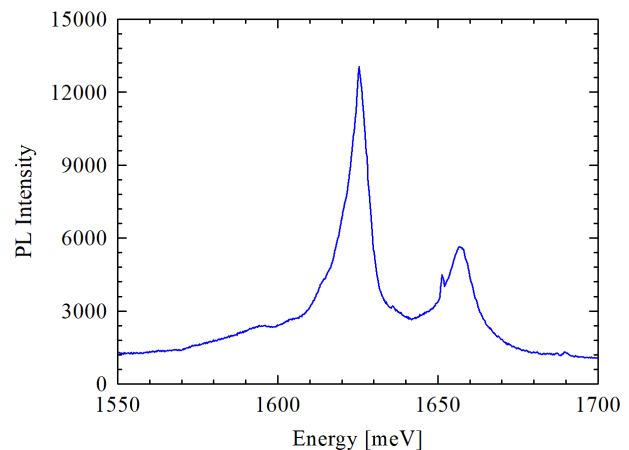
ZnSe as an epitaxial protection of MBE grown MoSe₂/hBN

Blanka Tronowicz¹, Julia Kucharek¹ and Wojciech Pacuski¹

¹ *Institute of Experimental Physics, Faculty of Physics, University of Warsaw, Pasteura St.5, 02-093 Warsaw, Poland*

Exfoliated transition metal dichalcogenides exhibit the best optical properties when they are mechanically sandwiched (encapsulated) between hBN flakes. Recent discovery that MBE growth of good optical quality TMDs require also hBN substrate [1] induced a question of how to protect surface of epi-grown TMDs? The most natural solution would be growth of hBN but this is very difficult due to very high growth temperature of hBN ($T > 1200^\circ\text{C}$). Instead, other wide gap semiconductors should be considered as cap materials. In this work we propose that ZnSe is a strong candidate, because it is transparent in visible spectral range and growth temperature of ZnSe is low enough (order of 300°C) to not affect TMD layer.

To verify our hypothesis, we have grown in MBE monolayer of MoSe₂ on the exfoliated hBN flakes and then covered the structure by a 50 nm thick layer of ZnSe. Although photoluminescence of such structure seems to be typically weaker comparing to not covered one, but locally it can be quite spectacular. Fig. 1 shows the spectrum collected from the ZnSe/MoSe₂/hBN structure at 9 K. There are visible well resolved excitonic lines related to neutral exciton (X) at 1660 meV and charged exciton (CX) at 1620 meV. Importantly, linewidths are comparable to best results reported for MoSe₂. Therefore optimized ZnSe coverage may be an efficient way of protecting the epi-grown TMDs.



[1] W. Pacuski, M. Grzeszczyk, K. Nogajewski, A. Bogucki, K. Oreszczuk, J. Kucharek, K.E. Połczyńska, B. Seredyński, A. Rodek, R. Bożek, T. Taniguchi, K. Watanabe, S. Kret, J. Sadowski, T. Kazimierczuk, M. Potemski, P. Kossacki, Nano Letters 20, 3058 (2020).

Narrow Excitonic Lines Of Monolayer Transition Metal Dichalcogenides Deposited Directly On AlGa_N Substrate

Łukasz Zinkiewicz¹, Magdalena Grzeszczyk¹, Julia Sławińska², Aleksander Rodek¹, Kenji Watanabe³, Takashi Taniguchi⁴, Marek Potemski^{1,5}, Czesław Skierbiszewski², and Piotr Kossacki¹

¹ *Institute of Experimental Physics, Faculty of Physics, University of Warsaw, Poland.*

² *Institute of High Pressure Physics, Polish Academy of Sciences, Warsaw, Poland.*

³ *Research Center for Functional Materials, NIMS, Tsukuba, Japan.*

⁴ *International Center for Materials Nanoarchitectonics, NIMS, Tsukuba, Japan*

⁵ *LNCMI, CNRS-UGA-UPS-INS-EMFL, Grenoble, France*

Monolayers of transition metal dichalcogenides (TMDs), such as MoSe₂, MoS₂, WSe₂ and WS₂ are well-known for their distinctive optical properties: strong light-matter interaction and the valley selective optical selection rules. Unfortunately, optical transition linewidths of TMDs deposited on the most popular silicon/silicon dioxide substrates are in the range of a few tens of meV (for sulphur based compounds) and 10 meV (for diselenides) at a low temperature [1,2]. This is caused by significant inhomogeneous contribution to the linewidth, related mainly to the surface roughness.

One common solution to this problem was presented by Cadiz et al. [3] and is based on encapsulation of TMDs monolayers into hexagonal boron nitride (hBN) flakes. The hBN provides exceptionally flat surface and suppresses the influence from environment and thus leads to the narrowing of the observed photoluminescence linewidths well below 10 meV.

Here we present another approach – deposition of TMDs monolayers directly on atomically-flat GaN/AlGa_N substrates by the dry-transfer method. The nitride semiconductor market, ranking the second right after the silicon, delivers a novel generation of optoelectronic devices, such as displays, energy-saving lighting or biosensors [4]. Integration of TMDs with group III nitrides based substrates would be an important step towards exploiting the unique optical and electrical properties of both types of the materials and may result in emerging of a new class of optoelectronic devices. We show that excitonic linewidths of monolayers of TMDs deposited on AlGa_N are reduced to values comparable to hBN encapsulated samples.

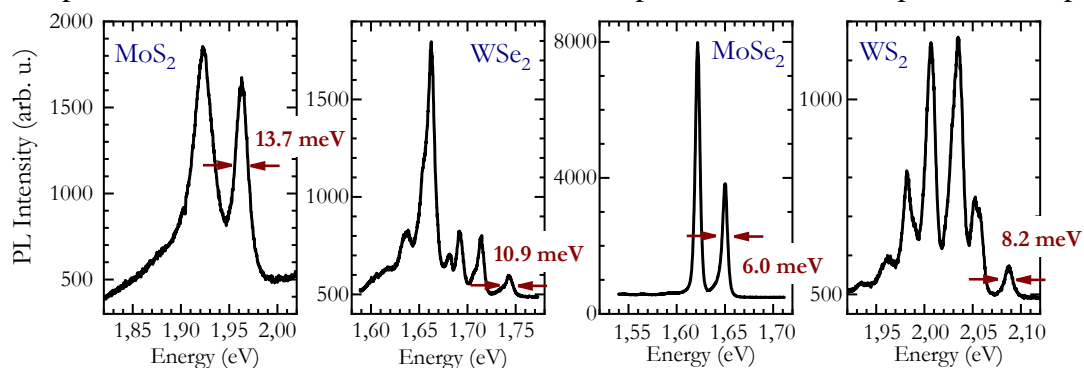


Figure 1: Photoluminescence spectra acquired at 10K of monolayers of common TMDs deposited on AlGa_N substrate demonstrate narrow excitonic lines. The monolayers are capped with a thin layer of hBN. The horizontal scale spans 200 meV on each plot for easier comparison of the spectra.

[1] H. Zeng, et al., *Nat. Nanotechnol.* **7**, 490 (2012).

[2] J. Ross, et al., *Nat. Commun.* **4**, 1474 (2013).

[3] F. Cadiz, et al., *Phys. Rev. X* **7**, 021026 (2017).

[4] S. Lee, et al., *Nano Energy* **1**, 145-151 (2012).

Effect of intrinsic and Rashba spin-orbit coupling on DOS in twisted bilayer graphene

J. Jastrzębski¹, A. Wania Rodrigues¹, K. Sadecka¹, J. Pawłowski¹, M. Bieniek^{1,2},

¹ *Department of Theoretical Physics, Wrocław University of Science and Technology, Poland*

² *Department of Physics, University of Ottawa, Canada*

Studies on graphene and other two-dimensional crystals remain one of the leading topics in condensed matter physics and materials science. Among the many intriguing phenomena realized via interface interactions in this materials, spin-orbit interaction (SOI) in graphene is particularly attractive for application to spintronics and topological physics [1]. Transition metal dichalcogenides (TMDs) are graphene-like 2D materials [2] characterized by much larger SOI than reported in graphene [3]. Recent theoretical and experimental studies revealed that graphene proximitized by TMDs can acquire enhanced SOI through interfacial coupling, which can strongly modify electronic properties of twisted bilayer graphene [4,5].

In the following work TBG/TMDs heterostructure will be studied theoretically from the point of view of their electronics and topological properties. Effects of spin-orbit interaction induced in TBG by TMDs will be analyzed based on sp^3d^5 [6] tight-binding model. Next, combined roles of electric field and induced SOC on density of states in this system will be considered. The effect of magnetic field will also be analyzed.

- [1] C. L. Kane and E. J. Mele, *Phys. Rev. Lett.* **95**, 226801 (2005)
- [3] D. Xiao, G. B. Liu, W. Feng, X. Xu, and W. Yao, *Phys. Rev. Lett.* **108**, 196802 (2012).
- [2] M. Bieniek, P. Hawrylak, *et al. Phys. Rev. B* **97**, 085153 (2018)
- [4] J. X. Lin, Y. H. Zhan E. Morissette, J. I. A. Li *et al. arXiv*, 2102.06566, (2021)
- [5] H. S. Arora, , R. Polski, Y. Zhang, *et al. Nature* **583**, 379–384 (2020).
- [6] M. Gmitra, J. Fabian, *Phys. Rev. Lett.* **119**, 146401 (2017)

Stability and Electronic Structure of Functionalized 2D Molybdenum Nitrides – MXenes

Jan Kołodziejczyk and Jacek A. Majewski

Faculty of Physics, University of Warsaw, ul. Pasteura 5, Warsaw, Poland

MXenes are relatively new family of low dimensional materials, which has been gaining more and more popularity in recent years. MXenes are mainly carbides and nitrides of early transition metals and they combine the properties of both components. Bare MXenes typically exhibit metallic behaviour and, therefore, are known to be good electric conductors. Interestingly, this property changes with functionalization of their surfaces. It occurs that functionalizing groups can change metallic MXenes into semiconducting ones, and not only open the band gap but also influence other properties, just opening the path towards many potential applications, *e.g.*, in electronics, optoelectronics, and thermoelectricity.

In this communication, we present probably the first reported studies of geometry, stability, and electronic structure of bare and functionalized molybdenum nitrides Mo₂N (MXenes). The studies are based on first-principles calculations in the framework of density functional theory (DFT) employing pseudo-potentials and plane-wave basis as implemented in the *QUANTUM ESPRESSO* package. Here, we discuss the results for the bare, and functionalized with oxygen and fluorine Mo₂N layers. All three systems are predicted to be stable at room temperature. The bare Mo₂N is metallic with good electric conductivity. Functionalization of Mo₂N with F leads to opening of the band gap by 0.09 eV and emergence of *n*-type semiconductor, whereas the Mo₂N functionalization with O creates *p*-type semiconductor with energy gap of 0.49 eV.

Further, we consider the influence of the functionalization of Mo₂N with Cl and OH groups on the effectiveness of energy band gap tuning. We have started also the calculations of physical quantities that determine the thermoelectric properties of these materials.

Acknowledgement: This research has been supported by the NCN grant OPUS-16 (UMO-2018/31/B/ST3/03758).

The origin of red light emission in GaN:B alloys.

Ewelina B. Rozbiegała^{1,2}, Karolina Pięta¹, Sebastian Złotnik³, Jarosław Gaca¹,
Krzysztof P. Korona⁴, and Jacek M. Baranowski¹

¹ Łukasiewicz - Institute of Microelectronics and Photonics, al. Lotników 32/46, 02-668
Warsaw, Poland

² Warsaw University of Technology, Faculty of Materials Science and Engineering, Wołoska
141, 02-507 Warsaw, Poland

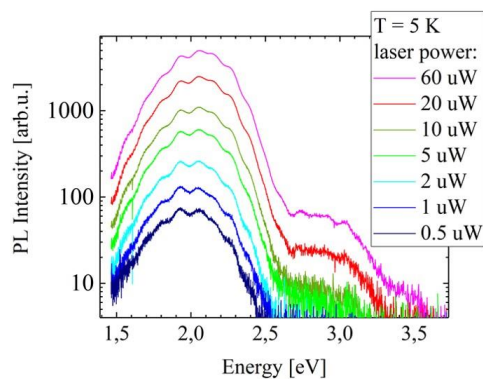
³ Military University of Technology, Institute of Applied Physics, gen. Sylwestra Kaliskiego 2
Warsaw, Poland

⁴ University of Warsaw, Faculty of Physics, Ludwika Pasteura 5 Warsaw, Poland

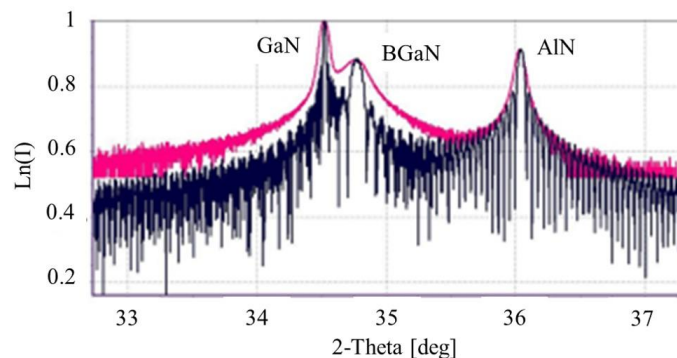
Advances in fabrication technologies for nitrides based on Al-Ga-In-N alloys have led to commercially available high efficiency light emitting devices for green and blue regions. However, the nitride based solid state light sources covering the full of visible spectrum have not been realized up to now. Therefore, the red light emission from nitrides is still of interest.

The aim of this work is to present and explain the origin of red light emission from boron doped GaN. The epitaxial growth of GaN:B alloys and investigation of their structural and emission properties are presented. The GaN:B epi-layers were grown by MOCVD using sapphire substrates and AlN buffer layer. The gas source precursors trimethylgallium (TMG), triethylborane (TEB), and ammonia have been used and hydrogen as a carrier gas. The X-ray diffraction revealed that solubility of boron is limited to 2-3%, and characterizes strong distortions around B atoms. The luminescence measurements have shown that the red luminescence is present for wide range of boron concentration in undoped GaN:B and Si doped GaN:B epi-layers as well. The red luminescence peak around 2.1 eV very weakly depends on temperature between 5K and 300K, and has lifetime of the order of few μ s, what indicates that deep levels are involved.

The mechanism of red luminescence in GaN:B is explained by model proposing trapping of electrons by B s-state. Atomic potentials for the B s-state are 1.9eV deeper than the Ga s-state, which form the conduction band of GaN. Our tight-binding calculations shows that B atoms incorporated into Ga sites create a strong local distortions around B atoms with the B s-state below the Ga s-state. Thus, the band off-sets between bottom of conduction bands of GaN and B local s-state will be able to confine electrons. Strain region around B atom may lead to the formation of quantum dot providing space quantization for electron. Recombination between trapped electron in such quantum dot with a hole from the valence band of GaN attracted by Coulombic interaction will be of an excitonic character and will lead to the red emission.



a) PL power dependence;



b) X-Ray Diffraction; red-experiment, black simulation

Physical structure for observation of inverse Faraday effect enhanced by twisted plasmon modes.

Piotr A. Drózd¹, Valentin Kachorovskii^{1,2,3}, Paweł Prystawko¹, Mateusz Słowikowski^{1,4}, Maciej Filipiak^{1,4}, Dmitri Yavorski^{1,5}, Maria Szola^{1,5} and Wojciech Knap¹

¹*CENTERA Laboratories, Institute of High Pressure Physics PAS, Warsaw, Poland*

²*Ioffe Institute, St. Petersburg, Russia*

³*Rensselaer Polytechnic Institute, Troy, New York, USA*

⁴*CEZAMAT, Warsaw University of Technology, Warsaw, Poland*

⁵*Faculty of Physics, University of Warsaw, Warsaw, Poland*

The Inverse Faraday Effect (IFE) — the appearance of stationary magnetic moments magnetization caused by circularly polarized light — has been mostly studied in magnetic materials. Recently, the IFE was predicted in the periodic lattice of metallic disks or spheres placed the vicinity of two dimensional electron liquid and subjected to the external circularly polarized radiation [1]. The radiation causes the DC current loops in the electron liquids, thus leading to appearance of static magnetic moments. Physically, the interaction between metal disks and two dimensional electron liquid, the "twisted" plasmonic modes are excited which lead (due to rectification) to appearance of DC circulating current. In this work, we present the basic idea of IFE enhanced by twisted plasmons. The mechanism of the effect is described and the theoretical predictions are presented. The GaN/AlGaIn is proposed as a basic system for the experimental realization of the IFE. In order to observe IFE experimentally, the GaN/AlGaIn HEMT like structure was prepared with 2 dimensional electron gas as a channel. On top of the structure, the periodic lattice of metal disks were fabricated with use of electron beam lithography. In addition, the frequency of twisted plasmonic modes can be slightly tuned with use of conducting back - gate layer that is present in epitaxial structure. We present the theoretical predictions and the technological realization of the structure as well as its basic characterization. The frequency of the twisted plasmonic modes is expected to be in range of 0.6 - 1.2 THz thus leading to potential applications in terahertz physics and technology.

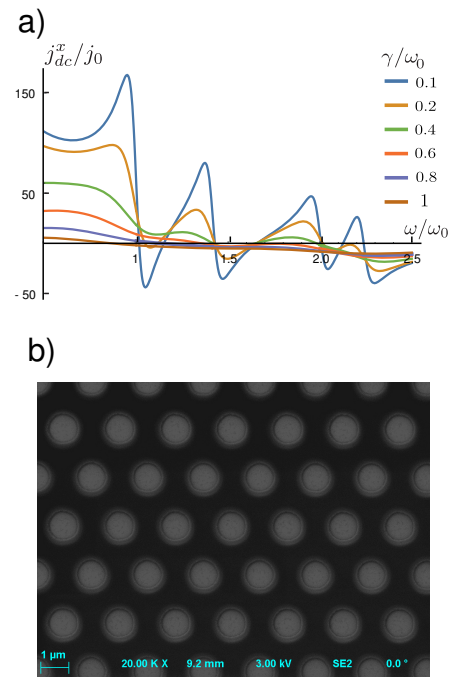


Figure 1: a) Plasmonic resonances in optically-induced circulating dc current for different values of the quality factor (here $\gamma = 1/\tau$ where τ is the momentum relaxation time)[1]. b) Periodic lattice of metal disks on the presented structure.

[1] S. O. Potashin, V. Y. Kachorovskii, and M. S. Shur, Phys. Rev. B **102**, 085402 (2020).

Revealing 3D nanoscale inhomogeneities of Si and Ge dopants incorporation into GaN by electrochemical etching

**N. Fiuczek¹, M. Sawicka¹, P. Wolny¹, H. Turski¹, A. Feduniewicz-Żmuda¹,
K. Nowakowski-Szkudlarek¹, M. Siekacz¹ and C. Skierbiszewski¹**

¹ *Institute of High Pressure Physics PAS, Sokołowska 29/37, Warsaw, Poland*

N-type doping of GaN is well-controlled up to very high concentrations both in plasma-assisted molecular beam epitaxy (PAMBE) - with Si concentration up to $2 \times 10^{20} \text{ cm}^{-3}$ - and in metal-organic phase epitaxy (MOVPE) - with Si concentration up to $6 \times 10^{19} \text{ cm}^{-3}$. [1] However, not much is known about the lateral distribution of Si atoms in GaN. Typical methods of doping quantification are usually limited to one or two dimensions. In this work we propose to use electrochemical etching (ECE) to access the information about uniformity of Si and Ge incorporation to GaN on a nanometer scale in all three dimensions (3D). ECE technique, due to its sensitivity to local doping level, is used to fabricate porous structures in n-doped materials, in particular in GaN:Si. [2]

In this work, GaN:Si layers were grown by PAMBE controlling the morphology. When the surface of the sample is atomically-flat during epitaxy, the Si adatoms incorporate uniformly. On the other hand, in case of a step-bunched surface the Si atom incorporation is non-uniform. By the analysis of the pore arrays observed after ECE (see Fig.1) we conclude that the local Si incorporation in the area of step-bunch is about three times higher than in the neighboring atomic terraces area. Differences in etching of the step-bunched samples results from the fact that a step-bunch moves slower than the average step on a flat terrace.

Furthermore, we study incorporation of Ge into $\text{In}_{0.03}\text{Ga}_{0.97}\text{N}$ in an extremely high doping regime $> 6 \times 10^{20} \text{ cm}^{-3}$ that is unavailable to Si. We find a fingerprint of a uniform Ge incorporation because a uniform pore distribution is observed after ECE.

In summary, we discuss the applicability of ECE to access the 3D information about the dopant incorporation and use this technique to conclude on how the growth conditions and surface morphology influence on the dopant distribution.

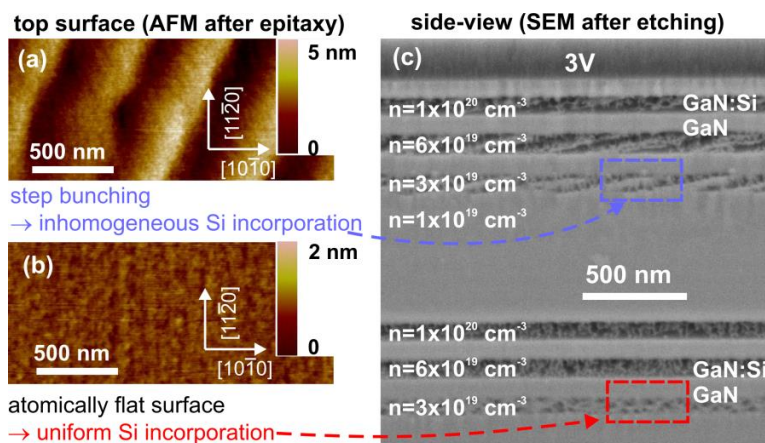


Figure 1 Surface morphology images (a) when the surface of the sample is step-bunched and Si incorporation is inhomogeneous, and (b) when the surface is atomically-flat and Si incorporation is homogenous. (c) The corresponding SEM cross-section images taken after ECE under 3 V reveal pore arrays for these two cases, where the average dopant concentration is identical.

This work was supported partially by National Science Center Poland within grant no. 2019/35/D/ST5/02950 and under POIR.04.04.00-00-4463/17-00 project of the Foundation for Polish Science co-financed by the European Union under the European Regional Development Fund.

[1] S. Fritze et al., Applied Physics Letters 100, 122104 (2012)

[2] M. Sawicka et al., Nanoscale 12, 6137 (2020)

Biaxial Relaxation Coefficient in Group-III Nitride Quantum Wells and Thin Films

Slawomir P. Lepkowski and Abdur-Rehman Anwar

*Institute of High Pressure Physics - Unipress, Polish Academy of Sciences, ul. Sokołowska
29/37, 01-142 Warszawa, Poland*

A common feature of nanostructures built from group-III nitride semiconductors is the presence of strains which originate from large differences in lattice parameters and thermal expansion coefficients between nitride materials. Strain changes the electronic band structure of semiconductor structures altering their fundamental physical properties such as the energy gap and the energy of the optical transitions. In thin films and quantum wells grown on *c*-plane substrates, an internal biaxial stress in the plane perpendicular to the *c* axis generates the biaxial strain, which is described by the in-plane and out-of-plane strain components. Both these strain components are related to each other via a single parameter, called the biaxial relaxation coefficient. So far, this coefficient was studied experimentally and theoretically assuming that it is a strain-independent quantity, equal to $2C_{13}/C_{33}$, according to the linear theory of elasticity.

In this work, we study the biaxial relaxation coefficient in group-III nitride quantum wells and thin films using the third-order elasticity theory. *We demonstrate that this coefficient depends significantly on strain.* This effect is confirmed by our recent *ab-initio* calculations performed in the framework of the hybrid-density functional theory [1].

We apply the second- and third-order elastic constants for wurtzite AlN, GaN, and InN, which have been obtained using the hybrid-density functional theory calculations with the exact deformation-gradient tensors [1,2]. First, we investigate the biaxial relaxation coefficient in AlN thin films grown on AlGaIn substrate. We find that the biaxial relaxation coefficient of AlN increases significantly from 0.574 to 0.613 with decreasing Al content in substrate. This effect originates from tensile strain in AlN films. Then, we consider GaN quantum wells grown on AlGaIn substrates. In this case, the biaxial relaxation coefficient of GaN slightly increases from 0.471 to 0.474 with increasing Al content in AlGaIn substrate. This effect arises from compressive strain in GaN wells. Next, we study GaN films on InGaIn virtual substrates, i.e., on fully relaxed InGaIn buffer layers. We find that due to tensile strain, the biaxial relaxation coefficient in GaN film decreases from 0.471 to 0.422 with increasing In content in InGaIn virtual substrate. Then, we consider InN quantum wells grown on InGaIn virtual substrates. We find that due to compressive strain, the biaxial relaxation coefficient in InN well increases significantly from 0.695 to 0.771 with increasing the In content in InGaIn.

Finally, we study the biaxial relaxation coefficient in quantum wells and thin films made of ternary nitride alloys, i.e., InGaIn and AlGaIn. In this case, we take into account the nonlinear composition dependence of the second-order elastic constants, while for the third-order elastic constants, the linear (Vegard-like) dependence on composition is assumed [3]. We predict that the magnitude of strain has significant contribution to the biaxial relaxation coefficient, particularly in In-rich InGaIn/GaN quantum wells, InGaIn films on InN substrates, and Al-rich AlGaIn films on GaN substrates.

[1] S. P. Lepkowski and A. R. Anwar, submitted to J. Phys.: Condens. Matter

[2] S. P. Lepkowski, Phys. Rev. B **102**, 134116 (2020).

[3] S. P. Lepkowski, J. Appl. Phys. **117**, 105703 (2015).

Comparative study of magnetic properties of Mn^{3+} magnetic clusters in GaN using classical and quantum mechanical approach.

Y.K. Edathumkandy, K. Das and D. Sztenkiel

Institute of Physics, Polish Academy of Sciences, Warszawa, Poland

Currently, simulations of many-body quantum systems are known to be computationally too demanding to be solved on classical computers. The main problem is that the computation time (number of elementary operations) and memory necessary for performing the calculations usually grow exponentially with the number of particles N . Efficient approach to simulate many-body quantum systems is the use of classical approximation. For example, ferromagnetic hysteresis loops [1,2], spin waves, domain wall motion and precessional or thermally assisted magnetization switching processes have been investigated using this approach. However, it is known that, at low temperatures the allowed spin fluctuations in this approach are overestimated what corresponds to enhanced thermal fluctuations [2]. It is important then to somehow assess the validity of this classical approximation. Therefore in this work [3], we compare the results of numerical calculations of magnetic clusters (singlet, pairs, triplets and quartets coupled by ferromagnetic superexchange interaction) in (Ga,Mn)N, where the Mn spins are treated classically with those where they are treated quantum-mechanically (crystal field model) [4,5]. In the first case, we solve the Landau-Lifshitz-Gilber (LLG) equation, that describe the precessional dynamics of spins represented by classical vectors. On the other hand, in the crystal field model, the Mn^{3+} state (d^4 configuration, with $S=2$, $L=2$) is characterized by the set of orbital and spin quantum numbers $|m_S, m_L\rangle$. The relevant energy level structure of singlet, pair, triplet and quartet of Mn ions are found by the numerical diagonalization of full 25×25 , $25^2 \times 25^2$, $25^3 \times 25^3$ and $25^4 \times 25^4$ Hamiltonian matrix respectively [5]. Particular attention is paid to use numerical parameters that ensure the same single ion magnetic anisotropy in classical and quantum approximation. Finally, a detailed comparative study of magnetization $M(H, T)$ as a function of magnetic field H , temperature T , number of ions in given cluster and the strength of superexchange interaction J , obtained from both approaches, will be presented.

[1] R. F. L. Evans *et al.*, *Phys.Rev. B* **91**, 144425 (2015).

[2] R. F. L. Evans *et al.*, *J. Phys.: Condens. Matter* **26**, 103202 (2014).

[3] Y.K. Edathumkandy *et al.*, in preparation

[4] J. Gosk, *et al.*, *Phys.Rev. B* **71**, 094432 (2005).

[5] D. Sztenkiel *et al.*, *New J. Phys.* **22**, 123016 (2020)

The work is supported by the National Science Centre, Poland, through projects OPUS 2018/31/B/ST3/03438 and by the Interdisciplinary Centre for Mathematical and Computational Modelling at the University of Warsaw through the access to the computing facilities.

Reduction of Al incorporation into AlGaIn layers grown by molecular beam epitaxy in Ga-droplet regime

D. Majchrzak^{1,2}, M. Grodzicki^{1,3}, P. P. Michałowski⁴, K. Moszak^{1,2}, W. Olszewski^{1,3}
and D. Hommel^{1,3}

¹ Łukasiewicz Research Network – PORT Polish Center for Technology Development,
Stabłowicka 147, 54-066 Wrocław, Poland

² Institute of Low Temperature and Structure Research PAS, Okólna 2, 50-422 Wrocław,
Poland

³ Institute of Experimental Physics, University of Wrocław, Maksa Born'a 9, 50-204 Wrocław,
Poland

⁴ Łukasiewicz Research Network – Institute of Microelectronics and Photonics, Lotników
32/46, 02-668 Warsaw, Poland

Much of the interest have been paid to AlGaIn material, which is used in blue/deep UV optoelectronic and high-power devices [1,2]. The growth kinetics of AlGaIn alloys by either molecular beam epitaxy (MBE) or metalorganic vapor phase epitaxy (MOVPE) have been investigated by many groups [3–7]. However, the incorporation probability of Al in AlGaIn by changing the Al/Ga flux ratio and keeping the Al flux constant has not been systematically studied. Furthermore, no significant changes in Al incorporation probability were observed by these groups so far.

All samples in our study were grown by plasma-assisted MBE on MOCVD AlGaIn/AlN/sapphire templates at temperature of 710°C or 760°C. The surface quality of the layers and Al concentration was investigated in situ by using reflection high-energy electron diffraction (RHEED), atomic force microscopy (AFM) and X-ray photoelectron spectroscopy (XPS). In our study, growth kinetics of AlGaIn structures grown by plasma-assisted MBE is investigated. Our findings reveal that increasing of Ga flux influences Al incorporation probability, only when stepping into the Ga-droplet growth regime. This leads to decrease of Al concentration in whole AlGaIn layers (confirmed by secondary ion mass spectrometry) and improves their surface quality. We show that the degree of Al concentration reduction depends on the Al/N ratio. For Al fluxes higher than active nitrogen flux the Al droplets are observed on the surface and the Al incorporation is almost constant. Moreover, for the Al/N ratios higher than unity the surface of the layers become poorer with visible large crystallites, which may have negative impact on the uniformity and performance of the device fabricated with such layers.

Acknowledgments: This work was performed under Grant No. TEAM TECH/2016-3/16 from the Foundation for Polish Science and Grant PRELUDIUM 19 No. 2020/37/N/ST3/02248 from the National Science Centre (NCN) Poland.

- [1] M. Kneissl and J. Rass, *III-Nitride Ultraviolet Emitters: Technology and Applications*, Springer, 2015.
- [2] Y. Nagasawa and A. Hirano, *Appl. Sci.* **8**, 1264 (2018).
- [3] E. Iliopoulos and T.D. Moustakas, *Appl. Phys. Lett.* **81**, 295–297 (2002).
- [4] J.R. Jenny, J.E. Van Nostrand and R. Kaspi, *Appl. Phys. Lett.* **72**, 85–87 (1998).
- [5] D.G. Zhao, *et al.*, *Appl. Surf. Sci.* **253**, 2452–2455 (2006).
- [6] S. Takigawa, *et al.*, *Jpn. J. Appl. Phys.* **43**, 952 (2004).
- [7] D.V. Dinh, *et al.*, *Sci. Rep.* **9**, 15802 (2019).

Band and Defect States in Amorphous SiCN

A. Tkachuk¹, A. Sukach², V. Tetyorkin², O. Porada³, A. Kozak³, V. Ivaschenko³

¹*V. Vynnychenko Central Ukrainian State Pedagogical University, Kropyvnytskyi, Ukraine*

²*V. Lashkaryov Institute of Semiconductor Physics, NAS Ukraine, Kyiv, Ukraine*

³*Institute for Problems of Materials Sciences NAS of Ukraine, Kyiv, Ukraine*

Silicon carbon nitride (SiCN) amorphous films are promising materials for different applications in micro- and optoelectronics, since combine semiconductor properties of silicon carbide and dielectric properties of its nitride. As thin passivation and protective layers that can be deposited at low temperatures, they can find application in technology of IR detectors based on narrow-gap A_3B_5 and A_2B_6 semiconductors. The investigated films were deposited on boron-doped silicon substrates and quartz substrates by plasma-enhanced chemical vapor deposition using hexamethyldisilazane as a main precursor and characterized by X-ray diffraction spectroscopy, optical and Fourier transform infrared spectroscopy, atomic force microscopy, photoluminescence.

The charge transport was studied from measurements of direct current as a function of bias voltage and temperature. Due to asymmetry of metal and semiconductor interfaces, the distribution of traps in space may be inhomogeneous, thus affecting the charge transport. In order to clarify this effect, the direct current measurements have been carried out on samples with the film thickness 0.39 ± 0.03 and 0.83 ± 0.03 μm . Indium contacts with a diameter of 2 mm were vacuum evaporated onto the film surface and thermally annealed in an atmosphere of pure hydrogen at a temperature of ~ 500 °C for 10-15 minutes. The back contact to p -Si substrates was deposited by vacuum sputtering of chromium and aluminum.

It is shown that the dominant transport mechanism in the investigated samples is the space-charge limited (SCL) current, caused by unipolar injection of electrons from the In contact [1]. However, the I - V characteristics in samples with different thickness of a -SiCN films exhibit significant difference not only in a magnitude of the measured current, but also in a shape of I - V curves. Namely, in samples with the thinner film the presence of four characteristic I - V dependences was observed, which is typical for the SCL current caused by shallow traps. At the same time, in the case of samples with the thicker film the current-voltage characteristic was confined within the so-called Lampert triangle, two bounding sides of which correspond to Ohm's law at low voltages and Child's trap-free square law at high voltages, respectively. In the transition voltage region the superquadratic I - V dependences were observed. The Lampert triangle unambiguously indicates the presence of deep traps. The observed difference in the current-voltage characteristics in samples with different thickness of a -SiCN films may be attributed to inhomogeneous distribution of traps in space.

Experimental data were interpreted within a model of the local trap band with an exponential distribution of traps. From theoretical analysis of the measured current-voltage characteristics a number of band and trap parameters of a -SiCN films (density of states in the conduction band, concentration and mobility of free electrons, energy and density of trap states) were evaluated.

[1] A.V. Sukach, V.V. Tetyorkin, A.I. Tkachuk et al. *J. Non-Cryst. Sol.*, 523, 119603 (2019).

Terahertz spectroscopy of 2D-plasmons in AlGaIn/GaN heterostructures

P. Sai,¹ K. Stelmaszczyk,¹ M. Sakowicz,¹ M. Filipiak,^{1,2} M. Słowikowski,^{1,2} D.B. But,¹
P. Prystawko,¹ G. Cywiński,¹ S. Romyantsev,¹ W. Knap^{1,3}

¹ CENTERA Laboratories, Institute of High Pressure Physics PAS, ul. Sokołowska 29/37,
01-142 Warsaw, Poland

² CEZAMAT, Warsaw University of Technology, 02-822 Warsaw, Poland

³ Laboratoire Charles Coulomb, University of Montpellier and CNRS UMR 5221, 34950
Montpellier, France

Plasmonics of two-dimensional electron systems has a great application potential in Terahertz (THz) optoelectronics, in particular, for the creation of all-electronic, compact, and gate-tunable THz detectors and emitters. Nitrides based heterostructures are characterized by an excellent performance in this field demonstrating both, plasma wave resonant detection and emission [1,2].

In this work, THz plasmon resonances were studied in GaN-based grating gate structures by Fourier-Transform Infrared Spectroscopy (FTIR) and THz Time Domain Spectroscopy (TDS) at 4.2 K and 300 K, respectively. Metal gratings of different periods (P) were integrated with the two-dimensional electron gas in AlGaIn/GaN in order to couple long-wavelength THz radiation and short-wavelength gated plasmons.

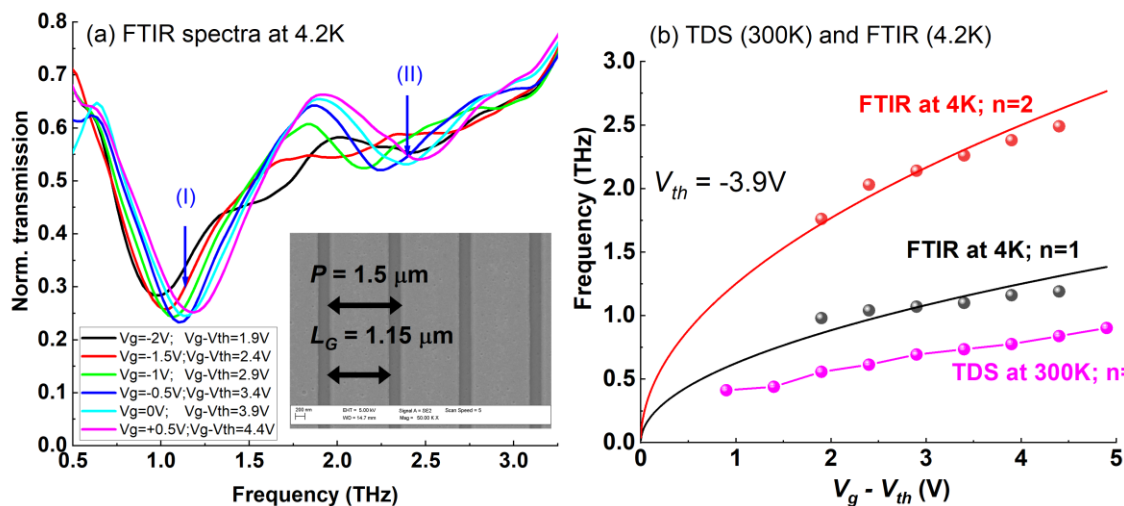


Fig. 1. (a) FTIR transmission spectra of AlGaIn/GaN plasmonic structure measured at 4.2 K and different gate voltages V_g . The arrows indicate the frequencies of the fundamental mode (I) and its second harmonic (II) plasmon resonances at $V_g=0V$. The SEM image of the grating segment used in the measurements is shown in the inset. (b) Frequency of the plasmon resonances measured as a function of the gate voltage swing $V_g - V_{th}$ at the temperatures of 4.2 K and 300 K.

Studied plasmon resonances are shown in Fig.1. The resonant frequencies observed in the measured transmission spectra correspond to gated 2D-plasmons with wave vectors defined by reciprocal lattice vectors of the metal grating coupler. Additionally, tunability of a plasmon frequency by applying the gate voltage was demonstrated at both, 4.2 K and 300 K. These results are very promising for developing tunable and compact plasmonic THz devices operating in a wide range of temperatures.

[1] A. El Fatimy, S. B. Tombet, F. Teppe, et al., *Electronics Letters* **42**, 1342-1344 (2006).

[2] A. El Fatimy, N. Dyakonova, Y. M. Meziani, et al., *J. Appl. Phys.* **107**, 024504 (2010).

Strain and lattice vibration mechanisms in GaN-AlGa_{1-x}N core-shell nanowires on Si substrate

E. Zielony¹, R. Szymon¹, A. Wierzbicka², A. Reszka², W. Perwez², M. Sobanska², Z.R. Zytkeiwicz²

¹ Department of Quantum Technologies, Wrocław University of Science and Technology, Wybrzeże Wyspiańskiego 27, 50-370 Wrocław, Poland

² Institute of Physics Polish Academy of Sciences, Al. Lotników 32/46, PL-02668 Warsaw, Poland

Gallium nitride (GaN) is one of the most suitable candidates for opto- and microelectronic applications, including short wavelength and high frequency devices. In particular, GaN grown in a form of nanowires (NWs) has aroused large scientific interest. Due to the large surface-to-volume ratio fundamental limitations of heteroepitaxy of highly lattice-mismatched structures could be overcome leading to new possibilities in fabrication of nano-sized devices.

In this work we use Raman scattering and X-ray diffraction (XRD) techniques to elaborate a comprehensive analysis of strain and lattice vibration mechanisms in self-assembled GaN-Al_xGa_{1-x}N core-shell NWs grown by plasma-assisted molecular beam epitaxy on Si (111) substrate. The samples consisted of GaN NW parts overgrown by Al_xGa_{1-x}N segments with the nominal Al content $x = 0.1, 0.25, 0.5, 0.75$ and 1 . Scanning electron microscopy (SEM) was used to measure dimensions of the NWs and their distribution on the substrate. In the transmission mode a core-shell structure was clearly visible. Raman measurements were performed at room temperature in the backscattering configuration without polarization detection, using 514.5 nm and 325 nm excitation wavelengths. The non-resonant Raman spectra revealed phonon modes originating from the Si substrate as well as from GaN and AlN, whereas the resonant Raman measurements exhibited vibration modes characteristic only for GaN. By analysing frequency position of the GaN-like and AlN-like E_2^{high} vibration modes as well as of GaN-like $A_1(LO)$ mode, we were able to study chemical composition, strain in NWs, as well as lattice vibrations mechanisms. Various lattice vibration mechanisms, such as: temperature effects (laser heating), phonon confinement, micro-strain in NWs and phonon-plasmon interaction, were considered and analysed within this work to explain the observed phonon modes shifts. The biaxial in-plane strain (ϵ_{xx}) in the NWs was calculated based on the estimated E_2^{high} Raman lines shifts with respect to that of bulk GaN and bulk AlN. Resonant Raman measurements allowed us to determine the composition of the NWs with low Al content. XRD studies supplemented Raman measurements by the analysis of micro-strain in GaN-AlGa_{1-x}N core-shell NWs. Based on the XRD reciprocal space maps the values of a - and c -lattice parameters were determined allowing estimation of the in-plane and out-of-plane (ϵ_{zz}) strain values. The results obtained from XRD were in a good agreement with those derived from Raman measurements.

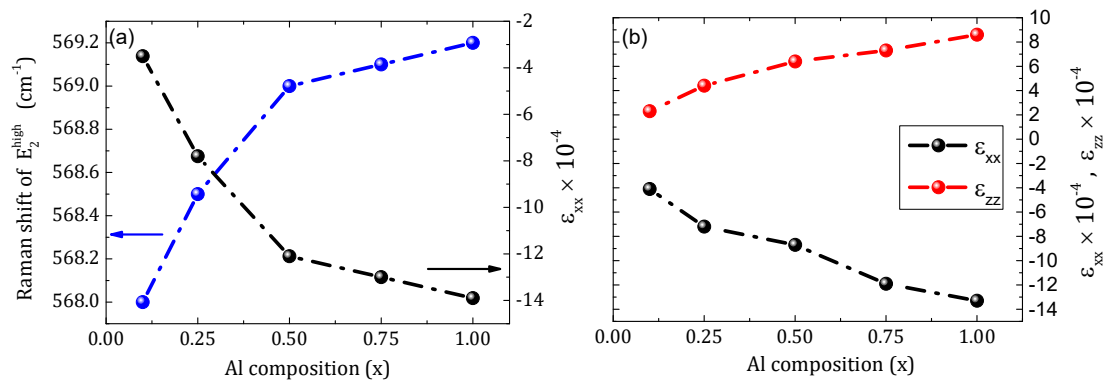


Fig. 1. The values of ϵ_{xx} and ϵ_{zz} strain components determined from (a) Raman and (b) XRD measurements of GaN-Al_xGa_{1-x}N core-shell NWs.

This work was supported by the grant 8211104160 of Department of Quantum Technologies, Wrocław University of Science and Technology and by the National Science Centre grant 2016/23/B/ST7/03745.

Magnetization steps in dilute bulk GaN:Mn

Katarzyna Gas¹, Piotr Wiśniewski², Dariusz Sztenkiel¹, Aneta Grochot¹,
Małgorzata Iwinska³, Tomasz Sochacki³, Hanka Przybylinska¹, Michał Bockowski³,
and Maciej Sawicki¹

¹ *Institute of Physics, Polish Academy of Sciences, Warsaw, Poland.*

² *Institute of Low Temperature and Structure Research, Polish Academy of Sciences,
Wrocław, Poland*

³ *Institute of High Pressure Physics, Polish Academy of Sciences Warsaw, Poland*

The ferromagnetic form of GaN may have an enormous technological relevance due to the already dominating role of the nitride family in light industry, high-frequency, and high-power electronics. In particular, the existence of sizable piezoelectromagnetic coupling has been evidenced recently in homogeneous (single-phase) (Ga,Mn)N [1], an effect that opens the door for realization of external electric field driven, repeatable magnetization reversal. It is, therefore, very important to understand the physics which governs the behavior and magnetic properties of transition metals in nitrides.

In this paper we report on magnetic properties of the Mn impurity in bulk GaN. Our 1'' in diameter single crystals were crystallized by halide vapor phase epitaxy [2] with Mn concentration ranging from 1×10^{18} to $5 \times 10^{19} \text{ cm}^{-3}$. The characterization of magnetic anisotropy in combination with electron paramagnetic resonance revealed predominantly the Mn^{3+} (d^4) configuration. Such a center is characterized by a very strong single ion magnetic anisotropy. The trigonal-symmetry surrounding and Jahn-Teller effect lead to splitting of the five lowest spin quantum levels (characterized by spin quantum numbers $m_S = -2, -1, 0, 1, 2$). Around $H = 0$ the ground state is composed mostly of $m_S = 0$ and with the increase of magnetic field $m_S = -1$ and $m_S = -2$ become sequentially the lowest states, leading to a well-developed staircase-like magnetization curve at sub-Kelvin temperatures. The unique shape and positions of the magnetization steps are accurately described using a single ion crystal field approach, taking into account the tetrahedral cubic field with trigonal distortion, spin-orbit interaction, static tetragonal Jahn-Teller distortion, and magnetic field [3]. The obtained perfect agreement between the experimental $m(H)$ and theory means that for such strong dilutions there is no need to invoke terms corresponding to Mn-Mn interactions (pair or triplets) and that the concentration of magnetically isotropic Mn^{2+} centers is negligibly small in the samples. The latter finding is of great importance for commercialization of industry-relevant, high quality, insulating substrates.

This work has been supported by the National Science Centre, Poland through OPUS (DEC-2018/31/B/ST3/03438) grant and TEAM TECH program of the Foundation for Polish Science co-financed by the European Union under the European Regional Development Fund (No.POIR.04.04.00-00-5CEB/17-00).

[1] D. Sztenkiel *et al.*, Nature Comm. **7**, 13232 (2016).

[2] M. Bockowski *et al.*, Journal of Crystal Growth **499**, 1-7 (2018).

[3] D. Sztenkiel *et al.*, New J. Phys. **22**, 123016 (2020).

Quantum well states in Bi₂Te₃ upon deposition of ultrathin Fe cap layer

Tomasz Sobol^{1,2}, Jacek Szade^{1,2}

¹ August Chelkowski Institute of Physics, 75. Pułku Piechoty 1, 41-500 Chorzów, Poland

² National Synchrotron Radiation Centre SOLARIS, Jagiellonian University, Czerwone Maki 98, 30-392 Kraków, Poland

Topological Insulators (TI) are materials that attracted the large attention of scientists in the last decades. This was determined mainly by their possible applications resulting from their unique properties. The existence of metallic surface states on insulating bulk is the most important feature of this class of materials. These specific electronic states, known as topological surface states (TSS) are characterized by a chiral spin arrangement in which the electron momentum is locked to the spin.

The experimental investigations of TIs physical properties and possible applications require most often their surface modification. It is known that deposition of ferromagnetic metals can break the time-reversal symmetry of TI causing the energy gap opening, although the situation is still controversial. On the other hand, it is known that deposition of various molecules or non-magnetic atoms leads to appearance of quantum well states and preserves TSS [1-3].

In our experiment, we covered the surface of the single crystal of Bi₂Te₃ with very thin Fe films and we investigated the modification of the electronic structure close to Fermi edge with Angle-Resolved Photoelectron Spectroscopy (ARPES) using the synchrotron radiation (UARPEs beamline, SOLARIS, Kraków). Upon deposition of Fe we observed gradual filling of the bulk conduction band and lowering of the Dirac point energy position, similarly to that reported in [1,4], although the position of the Dirac point do not depend of Fe thickness. Formation of the energy gap did not occur, instead, we observed the formation of the M-shape valance subbands (quantum well states) (Figure 1 b, c). These kinds of subbands were also detected for Bi₂Te₃ [1] and Bi₂Se₃ [2,3] as a result of their exposition to air or other molecules. Formation of the quantum well states can be explained by band bending and quantum confinement effects. Further studies are planned to fully explain and understand the observed phenomena in these systems.

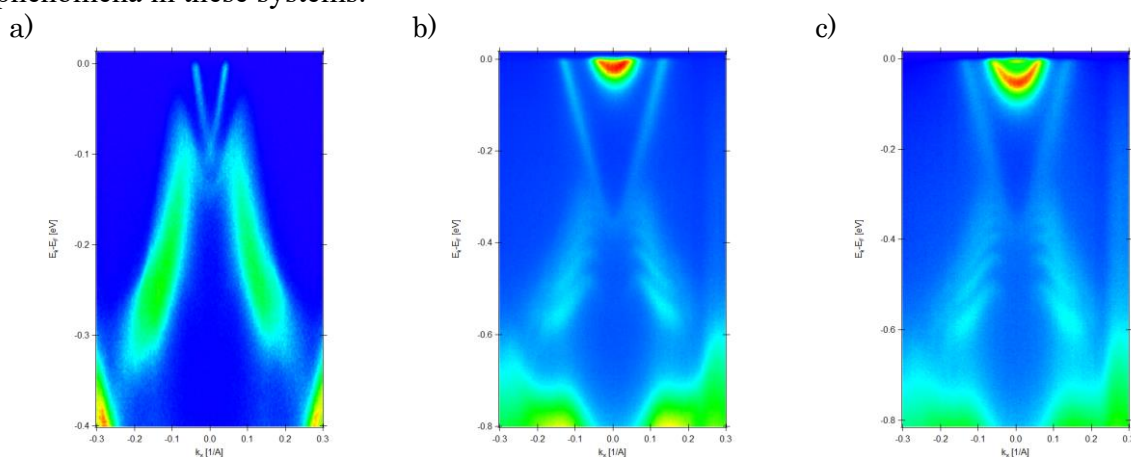


Figure 1 Bi₂Te₃ ARPES measurements with 20 eV photon energy. a) ARPES measurement of clean Bi₂Te₃ single crystal. b) and c) ARPES measurements of Bi₂Te₃ with 0.2 Å (b) and 0.5 Å (c) of Fe deposited on the surface.

[1] Chaoyu Chen, X. et al. 3694–3698 | PNAS | March 6, 2012 | vol. 109 | no. 10 (2012)

[2] Bianchi, M. et al. Nat. Commun. 1:128 doi: 10.1038/ncomms1131 (2010).

[3] Bahramy, M.S. et al. Nat. Commun. 3:1159 doi: 10.1038/ncomms2162 (2012).

[4] L. Andrew Wray, et al. Nature Phys. 7, 32 (2010).

Berry Curvature Dipol in Monolayers of Transition Metal Dichalcogenides.

Maciej Lis¹, Jakub Tworzydło¹

¹ Faculty of Physics, University of Warsaw, ul. L. Pasteura 5, 02-093 Warszawa, Poland

The Berry curvature arises in TMDCs due to a strong coupling between the conduction and valence bands. It can be qualitatively described within a familiar model of massive Dirac fermions. Using the improved and optimized model of WTe₂ [1], which properly accounts for the effects of strong spin-orbit coupling in this material, we perform a detailed quantitative analysis of the Berry curvature. The quantity of our interest is the Berry curvature dipol (BCD), which was detected in a transport measurement of nonlinear Hall effect [2]. We illustrate the appearance of BCD along constant energy contours. We present the results of BCD dependence on Fermi energy and out-of-plane electric field. Our findings can be useful in optimizing experimental transport measurements sensitive to the Berry curvature.

[1] A. Lau, R Ray, D Varjas, and A. Akhmerov, *Phys. Rev. Materials* **3**, 054206 (2019).

[2] Q. Ma, S. Xu, H. Shen, D Macneill, V. Fatemi, T. Chang, A. M. Mier Valdivia, S. Wu, Z. Du, C. Hsu, S. Fang, Q. D. Gibson, K. Watanabe, T. Taniguchi, R. J. Cava, E. Kaxiras, H. Lu, H. Lin, L. Fu, N. Gediky, and P. Jarillo-Herrero, *Nature* **565**, 337–342 (2019)

Signature of Chiral Anomaly and Magnetotransport in (001) Strained "Grey" Tin

Jakub Polaczyński¹, Alexandr Kazakov¹, Rafał Rudniewski¹, Bartłomiej Turowski¹, Zbigniew Adamus², Tomasz Wojciechowski¹, Tomasz Wojtowicz¹ and Valentine V. Volobuev¹

¹ International Research Centre MagTop, Institute of Physics, Polish Academy of Sciences, Aleja Lotników 32/46, PL-02668 Warsaw, Poland

² Institute of Physics, Polish Academy of Sciences, Aleja Lotników 32/46, PL-02668 Warsaw, Poland

The low-temperature allotrope of tin, known as α -Sn or grey tin, is a zero-gap semiconductor with an inverted band structure, similar to that of HgTe. According to theoretical predictions [1, 2], various topological phases can be induced in this material, e.g. by applying external strains, making it one of the few elemental topological materials. In a thin layer, a *tensile* in-plane strain opens the gap at the Γ -point of Brillouin zone, establishing a 3D topological insulator phase. Contrary, under a *compressive* in-plane strain the conduction and valence bands overlap along k_z , forming a 3D Dirac semimetal (DSM) phase [3]. The external magnetic field lifts the degeneracy of Dirac cones and splits them into pairs of Weyl cones of opposite chirality, creating a Weyl semimetal (WSM). Grey tin is therefore a versatile platform for the studies of topological properties of solids, with possible applications e.g. in spintronics [4] and infrared optoelectronics.

We have performed a molecular beam epitaxy (MBE) growth of thin (50 and 150 nm) layers of grey tin on hybrid CdTe/GaAs (001) substrates, which introduce the compressive strain of - 0.1% and ensure the stability of the layers at room temperature. The samples were shaped into Hall-bars (50 $\mu\text{m} \times 400 \mu\text{m}$) using electron-beam lithography and wet etching. During the presentation, we will discuss the results of magnetotransport studies, showing two characteristic features: unusual, negative longitudinal magnetoresistance (NLMR) in the magnetic field parallel to the current and magnetoresistance (MR) oscillations in the Hall geometry. We will analyze NLMR in the context of so-called chiral anomaly. This phenomenon, first predicted for chiral particles, is often regarded as a smoking gun of WSM [2], which is expected in our compressively strained layers of α -Sn. Our experimental magnetoresistance data follow the parabolic dependence on magnetic field, predicted theoretically [5] for chiral-anomaly-related NLMR. Other possible sources of NLMR, such as inhomogeneity-related current jetting effect, will also be discussed. The Berry phase derived from MR oscillations is approximately 0, indicating the trivial character of carriers. It suggests that both topologically trivial and non-trivial fermions coexist in our layers of grey tin, giving further insight into its band structure, which was mainly studied by Angle-Resolved Photoemission Spectroscopy (ARPES) – a surface-sensitive technique.

This research was partially supported by the Foundation for Polish Science through the IRA Programme co-financed by EU within SG OP (Grant No. MAB/2017/1).

- [1] L. Fu and C. L. Kane, *Phys. Rev. B* **76**, 045302 (2007).
- [2] H. Huang and F. Liu, *Phys. Rev. B* **95**, 201101(R) (2017).
- [3] C.-Z. Xu et al., *Phys. Rev. Lett.* **118**, 146402 (2017)
- [4] J.-C. Rojas-Sánchez et al., *Phys. Rev. Lett.* **116**, 096602 (2016)
- [5] D. T. Son and B. Z. Spivak, *Phys. Rev. B* **88**, 104412 (2013)

An interaction-driven transition between the Wigner crystal and the Fractional Chern insulator in topological flat bands

Michał Kupczyński¹, Błażej Jaworowski^{2,3}

¹ *Department of Theoretical Physics, Faculty of Fundamental Problems of Technology, Wrocław University of Science and Technology, Wrocław, Poland*

² *Max-Planck-Institut für Physik komplexer Systeme, D-01187 Dresden, Germany*

³ *Department of Physics and Astronomy, Aarhus University, DK-8000 Aarhus C, Denmark*

We investigate the topological phase transitions between the Wigner crystallization (WC) and the Fractional Chern Insulator (FCI) phase. FCIs are quantum liquid phases related to the partially filled Chern Insulators - insulators with non-trivial band topology exhibiting a non-zero Hall conductance in analogy to Landau level (LL) physics, but in systems preserving translational symmetry [1-4]. Similarly to LL physics, at the low-density limit, strongly correlated liquid phases compete with WCs [5-7]. We have shown that the Wigner crystallisation occurs on nontrivial bands of Chern Insulators for filling fractions when the FCI is absent [8].

In our work, We analyze an interaction-driven transition between crystalline and liquid states, filling factors $\nu = 1/5, 1/7, 1/9$. Using exact diagonalization for finite size systems with periodic boundary conditions, we distinguish different phases, which stability depends on the interaction range, controlled by the screening parameter of the Coulomb interaction. The crystalline phases are identified by a crystallization strength, calculated from the Fourier transforms of pair correlation density, while the Fractional Chern insulator phases are characterized using momentum counting rules, entanglement spectrum, and overlaps with corresponding Fractional Quantum Hall states. The type of phase depends on a particular single particle model and its topological properties. We show that for $\nu = 1/7$ and $\nu = 1/5$ it is possible to tune between the Wigner crystal and Fractional Chern insulator phase in the kagome lattice model with the band carrying the Chern number $C = 1$. In contrast, in the $C = 2$ models, the Wigner crystallization was absent at $\nu = 1/5$, and appeared at $\nu = 1/9$, suggesting that $C = 2$ FCIs are more stable against the formation of crystalline order.

- [1] F. D. M. Haldane Phys. Rev. Lett., 61, 2015 (1988)
- [2] T. Neupert, L. Santos, C. Chamon, and C. Mudry Phys. Rev. Lett., 106, 236804 (2011)
- [3] D. Sheng, Z.-C. Gu, Gu, K. Sun, and L. Sheng Nat. Commun., 2, 289 (2011)
- [4] N. Regnault and B. A. Bernevig Phys. Rev. X, 1, 021014 (2011)
- [5] E. Wigner, Phys. Rev. 46, 1002 (1934)
- [6] K. Maki and X. Zotos Phys. Rev. B 28, 4349 (1983)
- [7] K. Yang, F. D. M. Haldane, and E. H. Rezayi, Phys. Rev. B 64, 081301 (2001) [8] B. Jaworowski, A.D. Güçlü, P. Kaczmarkiewicz, M. Kupczyński, P. Potasz, A. Wójs, New J. Phys. 20, 063023 (2018)
- [9] M. Kupczyński, B. Jaworowski, A. Wójs arXiv:2105.05488

Growth of Gray Tin epilayers on insulating (001)-CdTe/GaAs substrates and its Angular Resolved Photoemission Spectroscopy studies

Bartłomiej Turowski¹, Rafał Rudniewski¹, Marcin Rosmus², Marta Aleszkiewicz³,
Tomasz Wojciechowski¹, Wojciech Zaleszczyk¹, Zahir Muhammad¹,
Natalia Olszowska², Tomasz Wojtowicz¹, Valentine V. Volobuev¹

¹ International Research Centre MagTop, Institute of Physics, Polish Academy of Sciences,
Aleja Lotników 32/46, PL-02668 Warsaw, Poland

² National Synchrotron Radiation Centre SOLARIS, Jagiellonian University,
Czerwone Maki 98, PL- 30392 Kraków, Poland

³ Institute of Physics, Polish Academy of Sciences, Aleja Lotników 32/46,
PL-02668 Warsaw, Poland

Gray tin (α -Sn) is an elemental topological material in which topological insulator - zero-gap semiconductor - Dirac semimetal transitions can be realized by strain engineering [1]. Bulk α -Sn is stable only below 13.2°C. However, α -Sn phase can be stabilized above room temperature in the form of thin epitaxial film [2]. Recent experimental studies of this material have been focused mainly on α -Sn grown on narrow gap semiconducting substrates [3, 4], which makes transport investigations problematic and limits potential application of this material [4].

In this work, 30-200 nm thick films of α -Sn were grown by molecular beam epitaxy on (001)-oriented GaAs substrates with thick CdTe buffers. Structural characterization carried out by means of high-energy electron diffraction, atomic force and scanning electron microscopy as well as X-ray diffraction (XRD) confirms the high quality of the samples

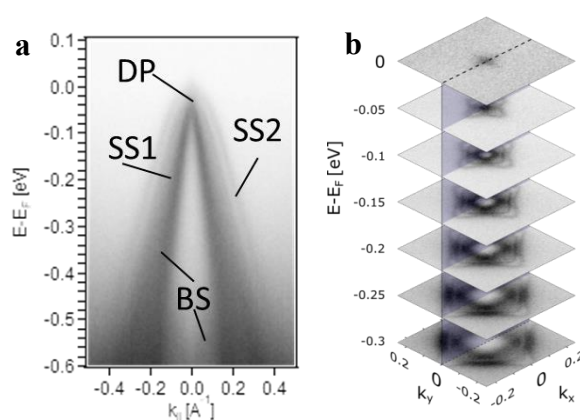


Figure 1. (a) ARPES $E(k_{||})$ spectra showing Dirac point (DP), surface states (SS) and bulk states (BS) in $\bar{\Gamma} - \bar{X}$ direction; (b) constant energy surface map of (001) α -Sn.

obtained. XRD measurements revealed -0.1 % in-plane compressive strains, a prerequisite for the formation of Dirac semimetal (DSM) phase. The gray tin band structure was studied by angle resolved photoemission spectroscopy (Figure 1) as a function of temperature and film thickness. It was shown that the prepared samples poses DSM phase in the thickness range of 30-200 nm and in the temperature range of 10-300 K.

Our results constitute an important basis for further reliable investigation of transport properties and possible application of α -Sn in spin-charge conversion devices [4].

The work is partially supported by the Foundation for Polish Science through the IRA Programme co-financed by EU within SG OP (Grant No. MAB/2017/1). We thank NSRC SOLARIS for beamtime allocation.

- [1] Dongqin Zhang, *et al.*, *Phys. Rev. B* **97**, 195139 (2018).
- [2] R.F.C. Farrow, *et al.*, *J. Cryst. Growth* **54**, 507 (1981).
- [3] Cai-Zhi Xu, *et al.*, *Phys. Rev. Lett.* **118**, 146402 (2017).
- [4] J.-C. Rojas-Sánchez, *et al.*, *Phys. Rev. Lett.* **116**, 096602 (2016).

Magnetic disorder in intrinsic topological magnets $\text{MnBi}_2\text{Te}_4/(\text{Bi}_2\text{Te}_3)_n$

**J. Sitnicka,¹ K. Sobczak,² P. Skupiński,³ A. Reszka,³ I. Fedorchenko,⁴
K. Graszka,³ N. Olszowska,⁵ J. Kołodziej,⁵ M. Tokarczyk,¹ Z. Adamus,³
B. J. Kowalski,³ H. Deng,⁶ K. Park,⁷ M. Konczykowski,⁸ L. Krusin-Elbaum,⁶ A. Wołoś¹**

¹ Faculty of Physics, University of Warsaw, ul. Pasteura 5, 02-093 Warsaw, Poland

² Faculty of Chemistry, University of Warsaw, Żwirki i Wigury 101, 02-089 Warsaw, Poland

³ Institute of Physics Polish Academy of Sciences, al. Lotników 32/46, 02-668 Warsaw, Poland

⁴ Kurnakov Institute of General and Inorganic Chemistry, 119991 Moscow, Russia

⁵ Solaris National Synchrotron Radiation Centre, Jagiellonian University, Czerwone Maki 98,
30-392 Krakow, Poland

⁶ Department of Physics, The City College of New York - CUNY, New York 10031, USA

⁷ Virginia Tech, Blacksburg, Virginia 24061, USA

⁸ Laboratoire des Solides Irradiés, École Polytechnique, CNRS,

The interaction between magnetism and topological states can produce many exotic phenomena, one of them is the quantum anomalous Hall effect (QAHE) [1, 5]. QAHE requires breaking the time reversal symmetry and topologically non-trivial band structure with the Fermi level inside the surface Dirac gap. The recently discovered and successfully prepared intrinsic topological magnet MnBi_2Te_4 [2] and its derivative compounds $\text{MnBi}_2\text{Te}_4/(\text{Bi}_2\text{Te}_3)_n$ [3] have gained particular research interest because magnetic and topological states are well incorporated together in these systems. Taking advantage of the lack of doping and alloying disorders in $\text{MnBi}_2\text{Te}_4/(\text{Bi}_2\text{Te}_3)_n$, as the MnBi_2Te_4 ferromagnetic layer is a natural magnetic extension [4] of the surface of the Bi_2Te_3 topological insulator (TI) quantized transport properties have been observed in these bulk systems in a much higher temperature regime [5] than in usual magnetically doped TI samples [2, 6].

However, so far QAHE has been observed only on selected samples of these compounds [5, 7], which indicates that their magnetic properties are not yet fully known. In particular, the effects of randomly substituted Mn in Bi_2Te_3 and magnetic disorder in MnBi_2Te_4 have not been thoroughly analyzed so far. Therefore we decided to focus on these two effects. We examined the magnetic properties of bulk $\text{MnBi}_2\text{Te}_4/(\text{Bi}_2\text{Te}_3)_n$ with a different number of n ($n > 1$) which we correlated with structural studies. Our ferromagnetic resonance spectroscopy analysis indicates that both of these disorders cannot be neglected as they have a significant effect on the Curie temperature of studied samples. We also investigated the influence of magnetic disorder on the band structure of TSS with the use of angular resolved photoemission spectroscopy measurements correlated with density functional theory calculations.

[1] C.-X. Liu, S.-C. Zhang and X.-L. Qi, *Annu. Rev. Condens. Matter Phys.* **7**, 301 (2016).

[2] M. M. Otrokov, et al., *Nature*. **576**, 416 (2019).

[3] I. I. Klimovskikh, et al., *npj Quantum Mater.* **5**, 54 (2020).

[4] M. M. Otrokov, et al., *2D Mater.* **4**, (2017).

[5] H. Deng, Z. Chen, A. Wołoś, M. Konczykowski, K. Sobczak, J. Sitnicka, I. V. Fedorchenko, J. Borysiuk, T. Heider, Ł. Pluciński, K. Park, A. B. Georgescu, J. Cano, and L. Krusin-Elbaum, *Nat. Phys.* **17**, 36 (2021).

[6] X. Kou, et al., *Nat. Commun.* **6**, 8474 (2015).

[7] Y. Deng, et al., *Science* **367**, 895 (2020).

This work was supported by the National Science Center (Poland), grant 2016/21/B/ST3/02565.

Yu-Shiba-Rusinov Qubit

A. Mishra¹, P. Simon², T. Hyart¹, and M. Trif¹¹*International Research Centre MagTop, Institute of Physics, Polish Academy of Sciences, Aleja Lotnikow 32/46, PL-02668 Warsaw, Poland*²*Université Paris-Saclay, CNRS, Laboratoire de Physiques des Solides, 91405, Orsay, France*

Magnetic impurities in *s*-wave superconductors lead to spin-polarized Yu-Shiba-Rusinov (YSR) in-gap states and a chain of magnetic impurities offers one of the most viable routes for the realization of Majorana bound states. They hold a promise for topological quantum computing, but this ambitious goal looks distant since no quantum coherent degrees of freedom have yet been identified in these systems. To fill this gap we propose an effective two-level system, a YSR qubit, stemming from two nearby impurities. Using a time-dependent Green's function approach, we derive an effective Hamiltonian describing the YSR qubit evolution as a function of distance between the impurity spins, their relative orientations, and their dynamics. We employ numerical and analytical methods to show that the YSR qubit can be controlled and read out utilising the dynamics of the magnetic impurities. Finally, we address the effect of the spin noises on the coherence properties of the YSR qubit, and show a robust behaviour for a wide range of experimentally relevant parameters. Looking forward, the YSR qubit could facilitate the implementation of a universal set of quantum gates in hybrid systems where they are coupled to topological Majorana qubits.

[1] A. Mishra, S. Takei, P. Simon, and M. Trif, *Physical Review B* **103**, L121401 (2021).

UARPES - Beamline in Polish Synchrotron for the measurements of solids band structure

Natalia Olszowska¹, Marcin Rosmus¹, Jacek J. Kołodziej^{1,2}

¹NSRC Solaris, Jagiellonian University, Czerwone Maki 98, Kraków, Poland

²Institut of Physics, Jagiellonian University, Łojasiewicza 11, Kraków, Poland

Ultra AngleResolved Photoemission Spectroscopy (UARPES) beamline allows measurements of the fundamental quantities, i.e. energy and momentum, describing a photoelectron state in the space outside of a solid, and in consequence it allows getting information about the electron states in a solid as dispersion relation $E(k_x, k_y, k_z)$. Band structure engineering of crystals, heterostructures is extensively employed for tailoring of the electronic band structure for quantum-, opto-, spin- magnetoelectric devices.

In the case of UARPES beamline, synchrotron radiation allows using the energy excitation in energy range 8-140 eV (up to 500eV by using higher harmonics from undulator) with photon flux on the sample about 5×10^{11} photons/s. The beamline consists of quasiperiodic Elliptical Polarisation Undulator (EPU) source (Apple II type), collimating mirror, two monochromators in one chamber, two focusing mirrors and exit slit. Quasiperiodic undulator allows to reducing second harmonic and gives the fractional harmonics which are filtered by monochromator. In the consequence multiplication of the bands is not observed in measurements spectrum. They are available in parallel and antiparallel modes and the light polarization is under full control. The important elements are also two monochromators: Plane Grating (PGM) and Normal Incidence (NIM), which can be used with two gratings for each in the one vacuum chamber. The PGM works with 600 l/mm and NIM works with 2000 l/mm gratings. Beamline resolving power is 20 000 over the full energy range and nominal resolution is around 1 meV for low energies. The beam size at sample is around $200\mu\text{m} \times 200\mu\text{m}$.

The heart of end station is hemispherical (radius = 200 mm) spectrometer VG SCIENTA DA-30L with electrostatic deflector to 3D mode (k_x, k_y, E) measurements. Detector has high angular resolution as 0.1° (\mathbf{k} -vector resolution $0.002\text{-}0.01\text{\AA}^{-1}$ for photon energy range 8-140 eV) and energy resolution better than 1.8 meV. Scienta software SES 1.6 cooperates with remote control 5-axis cryogenic manipulator and with monochromator. Energy configurator allows the automatically beamline setting (monochromator, undulator, mirrors) depending on the user's needs (energy, resolution, phase). Using the liquid helium, nitrogen and heater the temperature can be controlled from 6 to 500 K. The analytical chamber is equipped in LEED diffractometer with MCP by OCI to detect surface reconstruction.

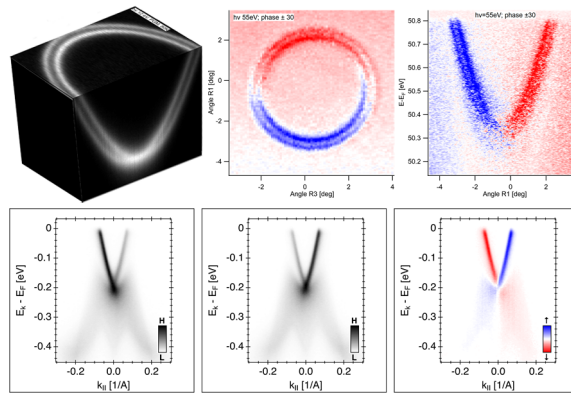


Figure 1: Circular dichroism observed on Au(111) and Bi₂Te₃ samples, as an example of UARPES beamline research capabilities.

A novel method for thermal characterization of superlattice sample

M. Pawlak¹, N. Jukam², A. Ludwig², T. Kruck², N. Spitzer², D. Dziczek¹, A.L. Shafiq³ and A. D. Wieck²

¹*Institute of Physics, Faculty of Physics, Astronomy and Informatics, Nicolaus Copernicus University, Grudziadzka 5, 87-100 Torun, Poland*

²*Chair of Applied Solid-State Physics, Experimental Physics VI, Ruhr-University Bochum, Universitaetsstrasse 150, D-44780 Bochum, Germany.*

³*Department of Physics, Faculty of Science & Health, Koya University, Koya KOY45, Kurdistan Region - F.R. Iraq*

Typically, the thermal parameters of superlattices have been studied using time-resolved thermoreflectance. However, this method assumes thermal diffusivity value, which is the quotient of the thermal conductivity and the product of density and specific heat. The last two parameters are always calculated for superlattice from their values volumetric materials. If we define an equivalent volumetric heat capacity ρc_{eff} as a weighted average of the AlAs and GaAs heat capacities, the equivalent thermal diffusivity is

$$\alpha_{eff} = \frac{k_{measured}}{(\rho c)_{eff}} \quad (\rho c)_{eff} \equiv (l_{GaAs}/l) \rho_{GaAs} c_{GaAs} + (l_{AlAs}/l) \rho_{AlAs} c_{AlAs} \quad (1)$$

where l is the superlattice period thickness. In this work, we present a method by which we can measure all thermal parameters both perpendicular and parallel to the surface. Fig. 1 shows the measurement of the thermal diffusivity compared with the calculated one using eq. 1. at different temperatures.

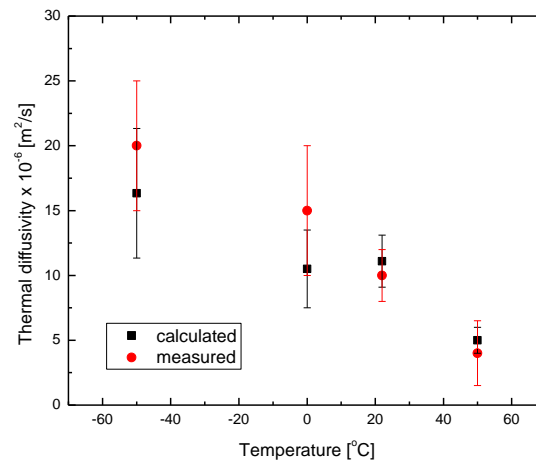


Fig. 1. Relation between measured and calculated values of the thermal diffusivity as a function of temperature.

Acknowledgement: This work was funded by the National Science Centre Poland grant based on Decision no. 2015/19/D/ST3/02388

[1] M. Pawlak, N. Jukam, T. Kruck, D. Dziczek, A. Ludwig, A. D. Wieck, *Measurement* **166** (2020), 108226

[2] M. Pawlak, T. Kruck, N. Spitzer, D. Dziczek, A. Ludwig, A. D. Wieck, under review

Bifunctional Nanocomposites with Plasmonic and Magnetic Properties as Substrates for Surface-enhanced Raman Scattering (SERS) Measurements.

Mateusz Kędziora^{1,2}, Karol Kołataj^{2,3}, Robert Ambroziak², Jan Krajczewski² and Andrzej Kudelski²

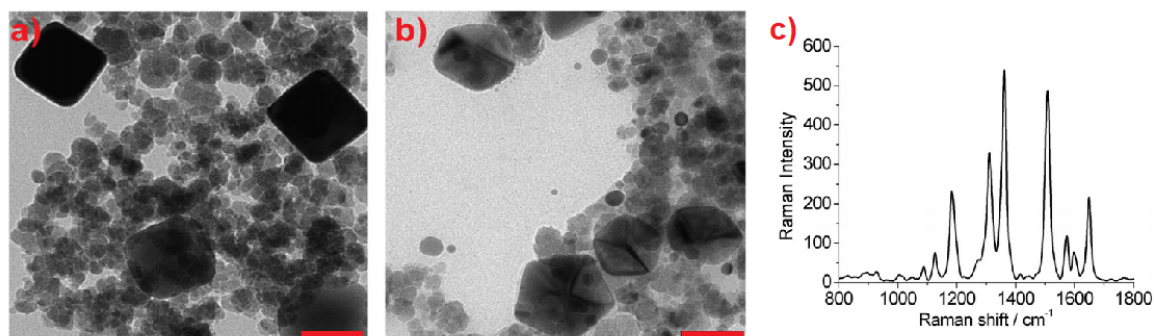
¹*Institute of Experimental Physics, Faculty of Physics, University of Warsaw, Pasteura 5, 02-093 Warsaw, Poland*

²*Faculty of Chemistry, University of Warsaw, ul. Pasteura 1, 02-093 Warsaw, Poland*

³*Faculty of Physics and Center for NanoScience, Ludwig-Maximilians-University, Geschwister-Scholl-Platz 1, 80539 Munich, Germany*

Surface-enhanced Raman scattering occurs when the analyzed substance is very close to the surface of a noble metal (such as Ag, Au or Cu) or semiconductor (e.g. ZnO, CdTe or CuO) nanostructures [1] and the efficiency of the Raman signal increases by up to eight orders of magnitude. Recently many scientific research are devoted to develop substrates for SERS measurements [2], and the most important problem is the inhomogeneous deposition of nanoresonators on analyzed surface.

In this paper we report a method of synthesizing nanoresonators in which the noble metal nanoparticles are prepared before being bound to the magnetic nanostructures, which allows us to manipulate the shape and size of plasmonic nanostructures and hence the properties as SERS substrates. By combining with γ -Fe₂O₃ (maghemite) we obtain the possibility of manipulating nanoparticles on a macroscopic scale which leads to very homogeneous SERS substrates. We also carried out a transmission electron microscopic analysis, X-ray powder diffraction and X-ray photoelectron spectroscopy measurements of the nanocomposites obtained.



a) TEM micrographs of nanocomposites with cubic-Ag and b) decahedral-Ag, scale bars correspond to 50 nm, c) Raman spectra of organic dye (rhodamine 6G) on cubic-Ag and γ -Fe₂O₃ nanocomposites.

[1] B. Yang, S. Jin, S. Guo, Y. Park, L. Chen, B. Zhao and Y. Mee Jung *ACS Omega* **4**, 23 (2019).

[2] J. Krajczewski, M. Kędziora, K. Kołataj and A. Kudelski, *RSC Advances* **9**, 32 (2019).

Temperature induced polymorphic transition in GaTe/GaAs(001) layers grown by molecular beam epitaxy

P.S. Avdienko¹, I.V. Sedova¹, D.A. Kirilenko¹, D.D. Firsov², O.S. Komkov² and S.V. Sorokin¹

¹Ioffe Institute, 26 Politekhnikeskaya, St. Petersburg, 194021, Russian Federation

²St.Petersburg Electrotechnical University "LETI", 5 Prof. Popova, SPb, 197376, Russia

The development of epitaxial growth techniques of two-dimensional group IIIA metal monochalcogenides (GaTe, GaSe, InSe, etc.) is of a great importance due to their potential applications in optoelectronics [1]. However, despite the successful demonstration of prototypes of GaTe-based semiconductor devices, GaTe still remains a much less studied material in comparison with both GaSe and InSe. This paper reports on the study of the structural and optical properties of GaTe layers grown by molecular beam epitaxy (MBE) on GaAs(001) substrates at the $T_S = 450\text{--}550^\circ\text{C}$ temperatures under weak Te-rich conditions (Te/Ga $\sim 10\text{--}18$). The GaTe growth rate was as low as ~ 1.5 nm/min. The layers were characterized by powder X-ray diffraction (XRD), transmission electron microscopy (TEM), and photoluminescence spectroscopy (PL) techniques.

As other III-VI's bulk GaTe crystals consist of vertically ordered ~ 0.8 nm-thick layers bonded together by a weak van der Waals forces. GaTe preferentially crystallizes in the monoclinic α -structure (m-GaTe), which is more thermodynamically stable than the hexagonal close-packed β -structure (h-GaTe). Hexagonal h-GaTe converts into monoclinic one with the increase in sample thickness or environmental temperature [2]. The critical thickness ($h_{h \rightarrow m}$) value of the h- to m-GaTe polymorphic transition in GaTe/GaAs(001) layer grown by MBE at low $T_S = 450^\circ\text{C}$ (Te/Ga ≈ 10) was estimated earlier as ~ 90 nm [3]. Since the growth temperature is a key factor for phase control of GaTe, one should expect the strong dependence of $h_{h \rightarrow m}$ on the growth temperature. Indeed, the powder XRD measurements confirmed the co-existence of m- and h-GaTe in relatively thick layers, and the intensity of the peaks of h-GaTe decreases in layers grown at higher T_S . The critical temperature of phase transition was found to be $\sim 540\text{--}550^\circ\text{C}$, since the GaTe layers grown at $T_S = 550^\circ\text{C}$ consist only of the m-GaTe phase. These findings were also confirmed by selected area electron diffraction measurements (SAED). Cross-section TEM image of the GaTe layer grown at $T_S = 550^\circ\text{C}$ demonstrate the sharp layer/substrate interface; the m-GaTe layer consists of a grains with an average size of 50-100 nm. Although the orientation of the (-210) planes of m-GaTe is close to that of (001) of GaAs, the grains are slightly misoriented relative to the crystal lattice of the substrate at angles $\pm 10^\circ$. No GaTe growth was found at $T_S > 550^\circ\text{C}$ for the Ga and Te fluxes used.

All GaTe layers grown at $T_S > 500^\circ\text{C}$ demonstrate pronounced near band-edge emission at $T = 11\text{K}$. An increase in T_S leads to an increase in the contribution of exciton emission (1.72–1.76 eV) compared to the bands associated with the recombination of the donor-acceptor pairs (DAP) (1.57 eV) and the emission of centers localized at the domain edges (1.45 eV). In addition, the shortest-wavelength peak in the PL spectra also exhibits a blue shift with increasing growth temperature, which confirms the enhancement of the free exciton contribution in near band-edge emission. The study of the polarization dependence of excitonic PL will also be presented in detail. The work was partially supported by the RFBR (project #20-32-90178).

[1] X. Yuan et al., *Nano Research*, **8**(10), 3332 (2015)

[2] E. Borisenko et al., *J. Cryst. Growth*, **535**, 125548 (2020)

[3] C.J. Bae et al., *AIP Advances*, **7**(3), 035113 (2017)

CdTe/PbTe periodic structures as photonic crystals

K. Karpińska^{1,2}, G. Karczewski^{1,3}, A. Witowski², J. Polaczyński^{1,4},

J. Korczak^{1,2}, S. Schreyeck³, S. Chusnutdinow¹, T. Story^{1,4}, M. Szot¹

¹*Institute of Physics, Polish Academy of Sciences, Aleja Lotników 32/46, PL-02668 Warsaw, Poland*

²*Faculty of Physics, University of Warsaw, Pasteura 5, PL-02093 Warsaw, Poland*

³*Universität Würzburg, Am Hubland, D-97074 Würzburg, Germany*

⁴*International Research Centre MagTop, Institute of Physics, Polish Academy of Sciences, PL-02668 Warsaw, Poland*

Dynamic advancement of meta-materials research allows to create unique optical systems with properties unreachable in standard semiconductor structures. Photonic crystals are one of the most intensively studied example of such a material. In analogy to semiconductors, photonic structures exhibit optical band gap with well-controlled energetic width. This effect is the strongest for photonic crystals made of materials that differ significantly in their refractive index values as it is in the case of CdTe ($n_{\text{CdTe}} = 2.75$) and PbTe ($n_{\text{PbTe}} = 5.75$). The possibility of manufacturing of high quality CdTe/PbTe periodic structures containing multilayers or PbTe (CdTe) quantum dots obtained by molecular beam epitaxy (MBE) [1, 2] as well as expected photonic behavior of such a structures will be presented in this paper.

We have conducted simulations of light propagation in CdTe/PbTe periodic heterostructures using an open-source software Meep (MIT Electromagnetic Equation Propagation), which exploits the finite-difference time-domain (FDTD) method [3]. The calculations showed the existence of photonic band gap already for 10-period CdTe/PbTe structures of both types. Next, the multilayer CdTe/PbTe samples were prepared using the MBE method. In order to obtain the photonic crystals consisting of PbTe dots embedded in CdTe matrix some of the layered structures were subject to thermal treatment. The scanning electron microscopy (SEM) and reflectivity measurements of layered samples and matrices of almost symmetrical PbTe dots obtained with these methods were carried out. In the case of quantum dot structures, the SEM showed some derogations from periodicity, influence of which on the photonic effect occurrence in the examined CdTe/PbTe structures was further investigated. These heterogeneities have been included into the simulations and comparison of the obtained results with experimental reflectivity spectra will be discussed.

[1] Karczewski G. et al. Nanotechnology 26, 135601 (2015)

[2] Szot M. et al. Cryst. Growth Des. 11, 4794 (2011)

[3] A.F. Oskooi, et al., Computer Physics Communications, 181, 687-702 (2010)

Growth mechanism of $\text{MnBi}_2\text{Te}_4/(\text{Bi}_2\text{Te}_3)_n$ self-assembling superlattices

P. Skupiński¹, K. Sobczak², K. Graszka¹, A. Reszka¹, A. Avdonin¹, Z. Adamus¹,
M. Arciszewska¹, J. Sitnicka³, A. Wołos³

¹ Institute of Physics, Polish Academy of Sciences, Al. Lotników 32/46, 02-668 Warsaw, Poland

² Faculty of Chemistry, Biological and Chemical Research Centre, University of Warsaw, Żwirki i Wigury 101, 02-089 Warsaw, Poland

³ Faculty of Physics, University of Warsaw, ul. Pasteura 5, 02-093 Warsaw, Poland

MnBi_2Te_4 crystals are known to have a layered crystalline structure built of septuple layers arranged in the sequence of Te-Bi-Te-Mn-Te-Bi-Te monolayers along the crystal c-axis [1, 2, 3]. The adjacent septuple layers are bonded to each other by van der Waals interactions with the van der Waals gap created between the layers. Synthesis of the pure MnBi_2Te_4 phase is a complex task. Even with high concentration of manganese in the bismuth telluride melt, the tendency to separate the MnBi_2Te_4 septuple layers by Bi_2Te_3 quintuple layers is very strong during the crystal growth. So far, the size of single-phase MnBi_2Te_4 crystals does not exceed a few millimeters [1]. The regularity of the multi-phase $\text{MnBi}_2\text{Te}_4/(\text{Bi}_2\text{Te}_3)_n$ crystal structure is an amazing phenomenon due to the long distance ordering of large building blocks. The manganese-rich septuple layers can be separated by a quite regular number (n) of quintuple Bi_2Te_3 layers and such sequence can be repeated for several dozen times. This behavior suggests the existence of a mechanism which controls the deployment of the manganese septuple layers during the growth process.

In our growth model the van der Waals gap inside the crystalline structure determines the appearance of a preferential growth direction along the layers, making the building block-layers perpendicular to the crystallization front (the boundary between solid and liquid). The enthalpy of formation for Bi_2Te_3 is -970 meV and it is much lower than for the transformation of Bi_2Te_3 to MnBi_2Te_4 , equal to -5 meV [4]. Thus the primary solid surface of the crystallization front contains the edges of Bi_2Te_3 quintuple layers separated by the van der Waals gaps. On such surface, the initiation of new edges of the MnBi_2Te_4 septuple layers is impossible unless the surface contains lattice defects which can act as seeds for the edges of MnBi_2Te_4 septuple layers. The edges of MnBi_2Te_4 septuple layers, which initially are randomly placed on the Bi_2Te_3 surface, start a diffusion-driven competition for the manganese atoms, which leads to a reduction in their number and increase the distances between them. This mechanism interferes with the process of the pure MnBi_2Te_4 phase formation and explains the observed regular structures of $\text{MnBi}_2\text{Te}_4/(\text{Bi}_2\text{Te}_3)_n$ crystals.

[1] A. Zeugner et al., Chem. Mater. 31 (2019) 2795.

[2] Z. S. Aliev et al., J. Alloys Compd. 789 (2019) 443.

[3] D. Souchay, et al., J. Mater. Chem. C, 7 (2019) 9939.

[4] M.-H. Du, et al., Adv. Funct. Mater. (2020) 2006516, and supplement.

We would like to acknowledge National Science Center, Poland, grant no 2016/21/B/ST3/02565.

Modeling transmission spectra for a thin conductive layer on a semi-insulating substrate

Daniil Pashnev, Justinas Jorudas, Roman Balagula, Andrzej Urbanowicz, and
Irmantas Kašalynas

Center for Physical Sciences and Technology, Vilnius, 10257 Lithuania

Nowadays thin conducting layers such as graphene and two-dimensional (2D) electron gas (2DEG) are widely utilized for the development of high-frequency electronics and THz photonics [1], [2]. Time-domain spectroscopy (TDS) systems apply as contactless characterizing and quality control method of such structures in the THz range. Experimental THz transmission spectra are used to find complex-valued sheet conductance by using Fresnel equations [3]. Applying Drude model allows define dc-sheet conductance and scattering time values which, in turn, can be easily converted into the 2D concentration and mobility of carriers. In recent work [4], the authors solved Maxwell's equations for delta-thin conductive layer on semi-insulating substrate and found analytical equations for modulus of the transmission coefficient. The interesting feature of the model is that the thickness of the dielectric substrate can be taken into account. Therefore, Fabry-Perot oscillations in THz transmission spectrum can be modeled directly what may increase the accuracy of extracted parameters. Moreover, analytical model-based approach can be more powerful and flexible than the matrix calculations.

In this work we investigated applicability of the analytical model to describe the high-frequency characteristics of conductive 2DEG channel on semi-insulating substrate acquired with THz TDS system. Theoretical transfer matrix method [5] and Hall experiments in Van der Pauw geometry [6] were also applied for results validation. The samples under test were fabricated of a commercial AlGaIn/GaN high electron mobility transistor structures on SiC wafer with room temperature 2DEG density and mobility being in the range of $(3.5-11) \cdot 10^{12} \text{ cm}^{-2}$ and $(1500-1800) \text{ cm}^2/(\text{V}\cdot\text{s})$, respectively. Transmission through the samples was measured with THz-TDS (Teravil T-SPEC 800) system in frequency range from 0.1 to 3.5 THz. Samples were mounted in a liquid nitrogen-cooled optical cryostat with temperature control within the range of 80-300 K. Modeling results were found in a good agreement with measured THz transmission spectra, providing values of sheet conductance and scattering time of 2DEG layer in different samples at different temperatures. Estimated electron mobility and density values were also found in good agreement with those measured in Hall experiment. Finally, both analytical and transfer matrix methods gave similar results within accuracy of experimental measurements demonstrating that analytical model-based approach can be further developed for description of more complex structures with several thin conductive layers.

The work was supported by the Research Council of Lithuania under Polish-Lithuanian initiative DAINA through the "TERAGANWIRE" project (grant No. S-LL-19-1).

- [1] J. Sun et al., *Opt. Express*, **28**(4), 4911, (2020).
- [2] R. Ivaškevičiūtė-Povilauskienė et al., *Opt. Mater. Express*, **9**(11), 4438, (2019).
- [3] J. D. Buron et al., *Nano Lett.*, **12**(10), 5074–5081, (2012).
- [4] G. I. Syngayivska and V. V. Korotyeyev, *Ukr. J. Phys.*, **58**(1), 40–55, (2013).
- [5] S. Khorasani and B. Rashidian, *J. Opt. A Pure Appl. Opt.*, **4**(3), 251–256, (2002).
- [6] J. Jorudas et al., *Micromachines*, **11**, 12 (2020).

Optical emission from highly strained CdTe/(Zn,Mg)Te nanowires

**P. Wojnar¹, M. Muszyński¹, P. Baranowski¹, M. Wójcik¹, S. Kret¹
G. Karczewski¹, T. Wojtowicz²**

¹ *Institute of Physics, Polish Academy of Sciences, 02-668 Warsaw, Poland*

² *International Research Centre MagTop, Institute of Physics, Polish Academy of Sciences, 02-668 Warsaw, Poland*

Semiconductor nanowires represent a versatile platform for studying material configurations which cannot be obtained in the planar geometry under normal conditions. In particular, it is possible to create highly lattice mismatched heterostructures without formation of misfit dislocations.

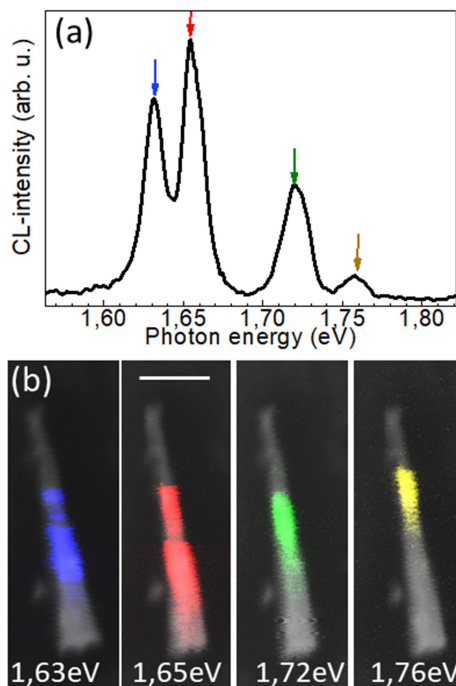


Figure 1. Cathodoluminescence (CL) from a single nanowire. (a) emission spectrum, $U=5\text{keV}$, $I=500\text{pA}$, $T=10\text{K}$ (b) CL-maps at various energies, scale bar 400nm

eV), Figure 1. This shift is caused, most likely, by the compressive strain acting on nanowire cores. We cannot, however, exclude the impact of Zn and Mg diffusion from the shell into the core. Moreover, we demonstrate that each emission line originates from a different part of the nanowire which suggests that there are several exciton localization areas along the nanowire axis, Figure 1. The emission energy from these objects depends, most likely, on particular strain conditions at their positions. In order to verify this statement, we plan to correlate CL maps with structural properties of the crystalline lattice measured by transmission electron microscopy.

This work has been partially supported by the National Centre of Science (Poland) through grant 2017/26/E/ST3/00253, and by the Foundation for Polish Science through the IRA Programme co-financed by EU within SG OP.

In this work, we report the growth of highly lattice mismatched CdTe/(Zn,Mg)Te core/shell nanowires by molecular beam epitaxy by employing the vapor-liquid-solid growth mechanism assisted with gold catalysts. Mg concentration in the shell is about 0.2, which results in the lattice mismatch between the core and the shell semiconductor being as large as 4.9%. A series of nanowires with various shell thicknesses ranging from 2 nm up to 10 nm is grown. The most intensive near band edge luminescence is observed in nanowires with the average shell thickness of 6 nm, whereas no luminescence is observed in samples with the average shell thickness larger than 8 nm and smaller than 4 nm. In the case of large shell thicknesses, misfit dislocations are, most likely, formed which acts detrimentally on the near band edge optical emission intensity. On the other hand, when the shell is not thick enough, the surface states are not passivated leading also to the overall decrease of the emission intensity.

Individual nanowires from the sample with the most intensive optical emission are studied by means of cathodoluminescence (CL). We find that the emission spectrum from a single nanowire consists of several emission lines appearing at energies significantly higher than the CdTe band gap (1.59

THz emission from GaAs/GaAlAs heterostructure

D. Yavorskiy^{1,2}, M. Szola^{2,3}, T. Tarkowski¹, W. Knap², V. Umansky⁴, P. Nowicki⁵,
J. Wróbel⁵ and J. Łusakowski¹¹Faculty of Physics, University of Warsaw, ul. Pasteura 5, 02-093 Warsaw, Poland²Centra Laboratories, Institute of High Pressure Physics, Polish Academy of Sciences, ul. Sokołowska 29/37, 01-142 Warsaw, Poland³Laboratoire Charles Coulomb, UMR, CNRS 5221, 34095 Montpellier, France⁴Weizmann Institute of Science, Rehovot 76100, Israel⁵Institute of Physics, Polish Academy of Sciences, al. Lotników 32/46, 02-668 Warsaw, Poland

Possibility of generation of THz radiation from electrically driven semiconductor devices is one of the most challenging and promising goals of THz science and technology. Even though such devices already exist on the market, like electronic frequency multipliers [1], resonant tunneling diodes [2] or quantum cascade lasers [3], new solutions are still needed.

In the present work we studied a THz emission from rectangular samples based on a high-electron-mobility GaAs/Ga_{0.64}Al_{0.36}As heterostructure with 2DEG. We focused on measurements of emission spectra at different conditions like: supply voltage, temperature and magnetic field. Home-made Fabry-Perrot interferometer with a Golay cell was used to register emission spectra. All measurements were carried out at 4.2 K. We found that:

1. The emission spectrum consist of one broad peak centered at about 400 GHz.
2. The emission spectrum almost does not depend on the applied voltage.
3. The emission occurred in a threshold manner and its appearance coincided precisely with a jump of the current in I-V characteristics.
4. The emission vanished abruptly at a weak magnetic field of about 0.1 T.
5. The emission vanished at the temperature higher than 10 K.

Summarizing, we observed a 400 GHz (1.6 meV) emission from samples based on a high-electron-mobility GaAs/Ga_{0.64}Al_{0.36}As heterostructure. The observed spectrum cannot be attributed to a transition between $1s$ - $2p$ shallow impurity levels neither in the quantum well nor in the barrier because the energy of the emitted photons is equal to 1.6 meV and is about two times too small [4, 5]. Based on the observed dependences of the emission on applied voltage, magnetic field and temperature and on numerical calculations of the band structure of the heterostructure we propose that the mechanism of generation of the radiation could be attributed to impurity states in the quantum well.

This research was partially supported i) by the Polish National Science Centre under grants number UMO-2017/27/N/ST7/01771 and UMO-2019/33/B/ST7/02858 and ii) by the Foundation for Polish Science through the IRA Programme co-financed by EU within SG OP grant number MAB/2018/19.

[1] T. W. Crowe et al. 36th Int. Conf. Infrared, Millim. and THz Waves, Huston, USA, Ed. M. Koch, 2001.

[2] K. Kasagi et al. J. Appl. Phys. 125: 151601, 2019.

[3] I. Melngailis et al. Phys. Rev. Let., 23(19): 1111–1114, 1969.

[4] D. A. Firsov et al. Lithuanian Journal of Physics, 54(1): 46–49, 2014.

[5] S. D. Ganichev et al. Joint 32nd International Conference on Infrared and Millimeter Waves and the 15th International Conference on Terahertz Electronics, pages 623–624, 2007.

THz ratchet effect in HgTe-based interdigitated structures

I. Yahnuk¹, A. Kazakov^{2,3}, N. N. Mikhailov⁴, S. Dvoretsky⁴, M. Otteneder⁵,
J. Ziegler⁵, T. Dietl^{2,3}, D. Weiss⁵, V. Kachorovskii⁶, G. Budkin⁶, V. V. Belkov⁶, L. Golub⁵,
W. Knap¹ and S. Ganichev^{1,6}

¹ CENTERA Laboratories, Institute of High Pressure Physics PAS, 01-142 Warsaw, Poland

² International Research Centre MagTop, PL-02-668, Warsaw, Poland.

⁴ Institute of Physics PAS, PL-02-668, Warsaw, Poland.

⁴ Rzhanov Institute of Semiconductor Physics SB RAS, 630090, Novosibirsk, Russia

⁵ University of Regensburg, Terahertz Center, D-93040 Regensburg, Germany

⁶ Ioffe Institute, 194021 St. Petersburg, Russia

HgTe/CdHgTe quantum wells (QWs) are two-dimensional (2D) materials in which features of the band structure are characterized by QW thickness. In the case of thin- ($d_{\text{QW}} < d_c$) and thick- ($d_{\text{QW}} > d_c$) HgTe QWs, a parabolic band structure with a normal and an inverted band sequence can be realized, respectively [1]. Indeed, at a certain critical thickness ($d_{\text{QW}} = 6.3$ nm), the system is characterized by a Dirac-like band structure. These peculiar properties make HgTe QWs very attractive for investigations of ratchet effects.

Here, we report on the observation of terahertz radiation induced ratchet effects in HgTe/HgCdTe-based quantum well structures with interdigitated structures. For investigations, we used various HgTe QWs with thickness of 8.0, 7.0, and 6.3 nm, corresponding to parabolic dispersion with inverted band structure (8.0 and 7.0 nm) and linear dispersion (6.3 nm).

The lattice contains periodically deposited stripes with different width and spacing and, therefore, exhibits no inversion symmetry. We demonstrate that THz laser radiation ($f = 2.54$ or 0.69 THz) shining on the modulated device results in a directed electric current generated by the ratchet effect. We observe a typical behavior of the ratchet current upon controllable variation of the radiation polarization state. The ratchet current consists of a few linearly independent contributions including the Seebeck thermo-ratchet effect, as well as the "linear" and "circular" ratchet effects, sensitive to the corresponding polarization of the driving electromagnetic force.

The application of different electrostatic potentials to the two different subgratings of the dual-grating-gate structure enables us to change in a controllable way the degree and the sign of the structure asymmetry as well as to analyze the photocurrent behavior upon changing the carrier type and density. Sweeping either U_{G1} or U_{G2} gate voltages we have demonstrated that the helicity driven photocurrent is as well proportional to the degree of the electrostatic potential asymmetry. These data reveal that the photocurrent reflects the degree of asymmetry induced by different top gate potentials and even vanishes for a symmetric profile. Strikingly, despite no magnetic field was applied, at large negative gate voltages (hole conductivity) the current exhibits sign-alternating oscillations as a function of gate voltage.

To summarize, experiments on different types of HgTe-based superlattices provide a self-consistent picture demonstrating that the photocurrents (i) are generated due to the presence of the asymmetric superlattices, (ii) are characterized by specific polarization dependencies, (iii) change the direction upon reversing the in-plane asymmetry of the electrostatic potential as well as changing the carrier type, and (iv) for high negative gate voltages are characterized by a complex sign-alternating gate voltage dependence.

[1]. M. König et al., Science **318**, 5851 (2007)

Band Structure Engineering in 3D Topological Insulators

L. Plucinski

PGI-6, FZ Juelich, Germany

We will discuss our combined experimental and theoretical results on band structure engineering in 3D topological insulator (3D TI) bilayers and superlattices. These results show how new topologies emerge in complex structures, as compared to the routine Fermi level control by alloying, and provide a starting point in a search for novel topological phases. In topological pn-junction we have demonstrated Fermi level control by the relative thicknesses of the layers [1], while in superlattices that combine Bi₂Te₃ quintuple layers and Bi-bilayers we have predicted dual topological properties, and experimentally demonstrated the existence of non-trivial topological crystalline insulator (TCI) crossings away from the surface Brillouin zone center [2].

Further, we will present the termination-dependent band structure and related spin texture in the intrinsic magnetic topological insulator BiMnTe family [3], and discuss recent progress in setting up a high-resolution spin-polarized laser-ARPES system at PGI-6 in Juelich, Germany, an effort directed towards direct imaging of the Dirac gap in magnetic TIs.

[1] M. Eschbach et al., *Realization of a vertical topological p-n junction in epitaxial Sb₂Te₃/Bi₂Te₃*

heterostructures, Nature Comm. **6**, 8816 (2015)

[2] M. Eschbach et al., *BiTeI is a dual topological insulator*, Nature Comm. **8**, 14976 (2017)

[3] R. C. Vidal et al., *Orbital Complexity in Intrinsic Magnetic Topological Insulators MnBi₄Te₇ and MnBi₆Te₁₀*, Phys. Rev. Lett. **126**, 176403 (2021)

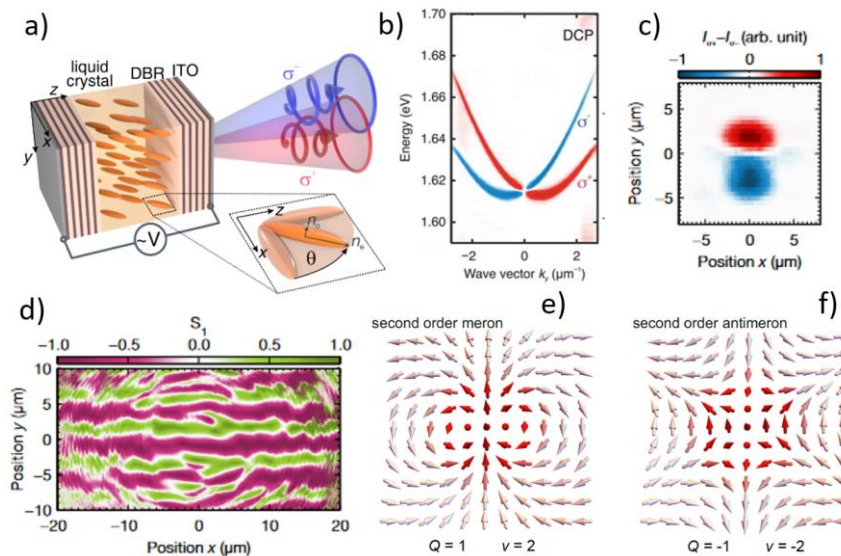
Synthetic Hamiltonians in optical cavities: "solid-state physics" of "massive photons with spin"

Jacek Szczytko

Institute of Experimental Physics, Faculty of Physics, University of Warsaw, Poland

Spin-orbit optical interactions in photonic systems exploit the analogy between the quantum mechanical description of electronic spin-orbit system and synthetic Hamiltonians derived for propagation of electromagnetic waves in dedicated spatial structures. Topological photonics carries a key promise for the development of integrated optical circuits – otherwise photons being uncharged cannot have their flow oriented by an electric field. We have invented a method to control electrically spin-orbit coupling (SOC) of light using specially designed photonic structures - birefringent microcavities (Fig).

In solid-state systems with broken inversion symmetry, SOC leads to the so-called Dresselhaus and Bychkov-Rashba SOC Hamiltonians, which are of particular interest in the context of spintronics, topological insulators, and superconductors. However, SOC in solid-state matter cannot be easily controlled and modified. Clever engineering of diverse gauge fields in optics could provide control over physical parameters of quantum system. Using a liquid crystal-filled photonic cavity, our team managed to emulate an optical spin Hall effect for parameters range far beyond those previously considered experimentally and theoretically [1]. We discovered Rashba-Dresselhaus spin-orbit coupling in a photonic system and showed control of an artificial Zeeman splitting [2]. We have demonstrated how to structure light such that its polarization behaves like a collective of spins in a ferromagnet forming half-skyrmion (also known as merons) [3]. Recently we observed optical analogue of persistent spin helix, reciprocal Young's and Stern-Gerlach experiments [4]. Our results illustrate an effective approach of engineering artificial gauge fields and synthetic Hamiltonians with photons for the simulation of nontrivial condensed matter and quantum phenomena.



Figure

a) scheme of liquid crystal microcavity;
b) polarization-resolved reflectivity showing Rashba-Dresselhaus spin-orbit coupling of light [2];
c) optical analogue of Stern-Gerlach experiment [4];
d) optical persistent spin helix (experiment) [4];
e) polarization texture of second order meron and
f) second order anti-meron [3] (model).

- [1] K. Lekenta, et al., *Tunable optical spin Hall effect in a liquid crystal microcavity*, Light Sci. Appl. 7, 74 (2018).
- [2] K. Recheńska, et al. *Photonic Engineering of Spin-Orbit Synthetic Hamiltonians in Liquid Crystal*, Science 366, 727 (2019)
- [3] M. Król et al. *Observation of second-order meron polarization textures in optical microcavities*, Optica Vol. 8, 255 (2021)
- [4] M. Król et al. *Old experiments in new light: Young's double-slit and Stern-Gerlach experiments in liquid crystal microcavities* <https://arxiv.org/abs/2104.09674> (2021)

Fabrication, Characterization and Property Tuning of Phosphorene, Chromium Trihalides and Related 2D Materials

Jacek B. Jasinski ¹

¹ Center for Renewable Energy Research, University of Louisville, Louisville, KY 40292, USA

Since the discovery of graphene in 2004, two-dimensional (2D) materials have attracted significant attention as they provide new opportunities for unique fundamental studies and enable novel high-performance device structures for a variety of applications. While graphene, along with hexagonal boron nitride (h-BN) and transition metal dichalcogenides (TMDs) have been among some of the most studied, there are many others, less explored 2D materials, many of which possess additional interesting characteristics and exhibit unique properties. In our research, we focus on two of such groups, both originating from van der Waals (vdW) systems. The first one is phosphorene and related group V materials that exhibit a highly anisotropic crystal structure and strong in-plane anisotropy of many of their properties, including mechanical and optical responses or electron and heat transport. The second group is chromium trihalides, which being vdW magnetic materials can provide an opportunity of studying low-dimensional magnetism. We synthesize these materials in their bulk form using a short transport growth method while 2D flakes are obtained by the subsequent layer exfoliation.

For phosphorene and group V materials, our focus is on understanding the post-synthesis processing and how external stimuli, such as electrochemical intercalation, high pressure, or strain can affect the structure and properties of these materials. Of particular interest is to understand how structural phase transitions, especially the transition between the orthorhombic honeycomb puckered α (A17) phase and the rhombohedral buckled β (A7) phase can be altered by intercalation and high pressure. Understanding the interplay between composition, intercalation level, and pressure can provide means for controlled reversible switching between the α and β phases and thus, enable the dynamic tuning of physical properties of these materials. In addition, our studies on phosphorene-based materials are also focused on other aspects, including surface functionalization, as well as sensing and thermoelectric properties.

In the case of chromium trihalides, our efforts concentrate on the fabrication, characterization, and measurements of magnetic properties. In particular, the electron paramagnetic resonance (EPR) is used to measure the magnetic behavior as a function of temperature and to monitor the changes in the magnetic ordering within these materials.

Coexistence of Surface and Bulk Ferromagnetism in a Topological Insulator

Kajetan M. Fijalkowski, Matthias Hartl, Martin Winnerlein, Pankaj Mandal,
Nan Liu, Steffen Schreyeck, Karl Brunner, Charles Gould,
and Laurens W. Molenkamp

*Faculty for Physics and Astronomy (EP3), Universität Würzburg, Am Hubland,
D-97074, Würzburg, Germany*

Institute for Topological Insulators (ITI), Am Hubland, D-97074, Würzburg, Germany

The anomalous Hall effect (AHE)[1], despite being over one hundred years old, remains of significant modern research interest as its investigation in novel magnetic materials continues to reveal rich physics. One recent example of this is the quantum anomalous Hall effect (QAHE)[2], which offers potential for the academic study of axion electrodynamics[3] as well as for practical applications in quantum metrology[4]. Moreover, combination of the QAHE with conventional s-wave superconductors could one day bring to life a still elusive chiral Majorana fermion quasi-particle[5], a potential building block of topological quantum computing.

The QAHE is a consequence of the interplay between topology and magnetism, yet the mechanism driving magnetism in the prototypical QAHE material systems V (or Cr)-doped $(Bi, Sb)_2Te_3$ remains an open question; one that requires an answer in order to gain a deeper understanding of the fundamental physics underlying the QAHE itself. Our work aims to shed light on this complex magnetic state by means of detailed electrical transport analysis.

Here we present the investigation of the magneto-transport properties of V-doped $(Bi, Sb)_2Te_3$ based topological insulator structures. We find that the AHE response contains two contributions of opposite sign. The components are found to depend differently on carrier density, leading to a sign inversion of the total anomalous Hall effect as a function of applied gate voltage. The two contributions have different magnetization reversal fields which, in combination with a temperature dependent study, points towards the coexistence of two ferromagnetic orders in the system. Moreover, we find that the sign of total anomalous Hall response of the system depends on the thickness and magnetic doping density of the magnetic layer. This thickness dependence suggests that the two ferromagnetic components originate from the surface and bulk of the magnetic topological insulator film[6]. Our work provides a valuable hint towards determining the origin of magnetism in this material system. Moreover, the characteristic shape of the anomalous Hall signal in the case where the two contributions are comparable in amplitude, produce an identical phenomenology to that commonly attributed to skyrmion states[7]. Our findings therefore suggest the necessity to reexamine these earlier claims.

- [1] N. Nagaosa, J. Sinova et al., *Rev. Mod. Phys.* **82**, 1539 (2010)
- [2] C.-Z. Chang, J. Zhang et al., *Science* **340**, 6129 (2013)
- [3] S. Grauer, K. M. Fijalkowski et al., *Phys. Rev. Lett.* **118**, 246801 (2017)
- [4] M. Götz, K. M. Fijalkowski et al., *Appl. Phys. Lett.* **112**, 072102 (2018)
- [5] M. Kayyalha, D. Xiao et al., *Science* **367**, 64-67 (2020)
- [6] K. M. Fijalkowski, M. Hartl et al., *Phys. Rev. X* **10**, 011012 (2020)
- [7] K. Yasuda, R. Wakatsuki et al., *Nat. Phys.* **12**, 555-559 (2016)

Dephasing by Mirror-Symmetry Breaking with Resulting Magnetoresistance across the Topological Transition in $\text{Pb}_{1-x}\text{Sn}_x\text{Se}$

A. Kazakov¹, W. Brzezicki¹, T. Hyart¹, B. Turowski¹, J. Polaczyński¹, Z. Adamus²,
M. Aleszkiewicz², T. Wojciechowski^{1,2}, J. Domagała², A. Varykhalov³, G. Springholz⁴,
T. Wojtowicz¹, V. V. Volobuev¹, T. Dietl^{1,6}

¹International Research Centre MagTop, Institute of Physics, Polish Academy of Sciences,
Aleja Lotnikow 32/46, PL-02668 Warsaw, Poland

²Institute of Physics, Polish Academy of Sciences, Aleja Lotnikow 32/46, PL-02668 Warsaw,
Poland

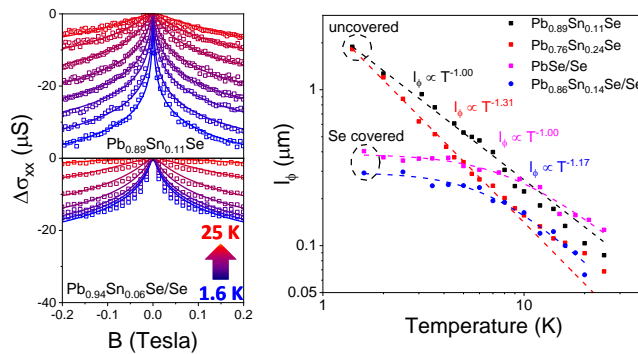
³Helmholtz-Zentrum Berlin für Materialien und Energie, Albert-Einstein Strasse 15, 12489
Berlin, Germany

⁴Institut für Halbleiter- und Festkörperphysik, Johannes Kepler University,
Altenbergerstrasse 69, A-4040 Linz, Austria

⁶WPI Advanced Institute for Materials Research, Tohoku University, 2-1-1 Katahira, Aoba-ku,
Sendai 980-8577, Japan

Weak localization (WL) and weak antilocalization (WAL) belong to the family of one-electron interference phenomena. The WL results from constructive interference of the time-reversed backscattering paths of a diffusing carrier. However, massless Dirac fermions encircling the Fermi surface acquire an additional π Berry phase, which turns WL negative magnetoresistance (MR) to a positive WAL MR. Thus WAL is considered to be an indication of surface states in 3D topological insulators. In this report, by using topological crystalline insulator $\text{Pb}_{1-x}\text{Sn}_x\text{Se}$ as an example, we show that symmetries of the system rather than its topology lead to the quantization of the Berry phase.

First, we consider the case of cubic lead-tin monochalcogenides and show that in such systems the quantization of the Berry phase ϕ of electrons encircling the Fermi surface depends simultaneously on the crystalline mirror and time-reversal symmetries, and appears



Evolution of the WAL MR with increasing the temperature in uncovered (left, upper panel) and Se covered (left, lower panel) epilayers. Experimental points (empty squares) are fitted using one-channel Hikami-Larkin-Nagaoka expression for a strong spin-orbit (solid lines). Right figure shows, that $l_\phi(T)$ in uncovered epilayers do not saturate down to 1.5 K (black and red), while in Se covered epilayers l_ϕ saturates below 5-7 K (blue and magenta).

for both topologically trivial and non-trivial phases. Thus, an intentional breaking of the mirror symmetry, e.g. by an additional amorphous insulator layer, introduces a new length scale that controls the magnitude of WAL MR. Indeed, according to these theoretical predictions we have experimentally observed WAL MR in both topologically trivial and non-trivial compositions x of $\text{Pb}_{1-x}\text{Sn}_x\text{Se}$ thin films grown by MBE. Moreover, the suppression of WAL MR at low temperatures was observed in thin films covered with an additional amorphous Se layer. Saturation of the phase coherence length l_ϕ , observed in Se covered layers, is governed by a new length scale which is determined by the destruction of the quantized value of ϕ .

This work was partially supported by the Foundation for Polish Science through the IRA Programme co-financed by EU within SG OP (Grant No. MAB/2017/1).

Rashba Effect in Topological PbSnSe/PbEuSe Quantum Wells

R. Rechciński¹, M. Galicka¹, M. Simma², V.V. Volobuev^{2,3,4}, O. Caha⁵,
J. Sánchez-Barriga⁶, P.S. Mandal⁶, E. Golias⁶, A. Varykhalov⁶, O. Rader⁶, G. Bauer²,
P. Kacman¹, R. Buczko¹ and G. Springholz²

¹*Institute of Physics, Polish Academy of Sciences, Warsaw, Poland*

²*Institute for Semiconductor Physics, Johannes Kepler University, Linz, Austria*

³*International Research Centre MagTop, Institute of Physics,
Polish Academy of Sciences, Warsaw, Poland*

⁴*National Technical University "KhPI", Kharkiv, Ukraine*

⁵*Masaryk University, Brno, Czech Republic*

⁶*Helmholtz-Zentrum Berlin für Materialien und Energie, Berlin, Germany*

Topological crystalline insulator (TCI) $\text{Pb}_{1-x}\text{Sn}_x\text{Se}$ quantum wells (QWs) on $\text{Pb}_{1-y}\text{Eu}_y\text{Se}$ barriers are studied experimentally and theoretically as a function of QW thickness and the Sn content x , encompassing both the topological nontrivial and trivial phases [1]. The theoretical tight-binding results are compared with experimental angle resolved photoemission (ARPES) investigations of epitaxial heterostructures grown by molecular beam epitaxy.

TCI quantum wells provide a unique opportunity to study carefully the different origins of the Rashba splitting and its dependence on various structural parameters. Due to the inversion symmetry of the IV-VI compounds, the Rashba effect in these QWs emerges from the asymmetry of quantum confinement. This so-called structure inversion asymmetry (SIA) may stem from various roots, such as different barriers on the two sides of the QW, details of the structure of the exposed surface, as well as a charge imbalance at surfaces and interfaces. All these features influence the energy spectrum differently, and can be studied experimentally by tuning the parameters of the heterostructure components, as well as by modifying the surface structure and chemical composition by surface doping. Most importantly the energy spectrum depends critically on the topological phase of the $\text{Pb}_{1-x}\text{Sn}_x\text{Se}$, which can be altered by changing the Sn content

Here it is shown both theoretically and experimentally that in these quantum wells the Rashba effect can take the form of either spin splitting of typical QW subbands, or hybridization between the topological surface and interface states. An effective theoretical low-energy description of the system will be presented, which allows to quantify the relative contributions of the various sources of SIA to the observed energy spectra.

[1] Rechciński, R. et al., *Adv. Funct. Mater.* 2008885 (2021).

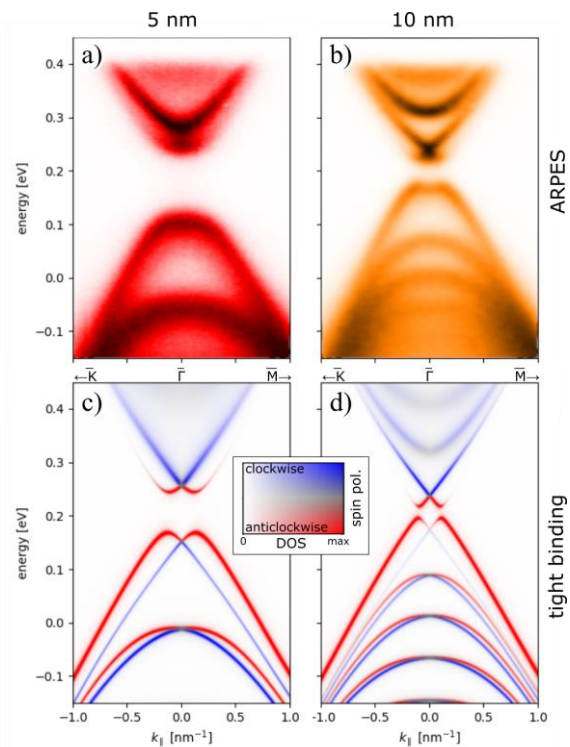


Figure: ARPES spectra (a,b) and calculated spin-resolved surface spectral functions (c,d) of asymmetric $\text{Pb}_{0.9}\text{Eu}_{0.1}\text{Se}/\text{Pb}_{0.6}\text{Sn}_{0.4}\text{Se}$ QWs.

Optical persistent spin helix phenomenon in liquid crystal microcavities

K. Rechcińska¹, M. Król¹, P. Oliwa¹, R. Mazur², P. Morawiak²,
P. Kula⁵, W. Piecek², P. G. Lagoudakis^{6,7}, W. Bardyszewski³, M. Matuszewski⁴,
B. Piętko¹, and J. Szczytko¹

¹*Institute of Experimental Physics, Faculty of Physics, University of Warsaw, Poland.*

²*Institute of Applied Physics, Military University of Technology, Warsaw, Poland.*

³*Institute of Theoretical Physics, Faculty of Physics, University of Warsaw, Poland.*

⁴*Institute of Physics, Polish Academy of Sciences, al. Lotników 32/46,
PL-02-668 Warsaw, Poland.*

⁵*Institute of Chemistry, Military University of Technology, Warsaw, Poland.*

⁶*Skolkovo Institute of Science and Technology, Skolkovo 143025, Russian Federation.*

⁷*Department of Physics and Astronomy, University of Southampton, Southampton, UK.*

Recently, a lot of work has been devoted to research on synthetic Hamiltonians and effective gauge fields. In particular it has been shown that in a liquid crystal microcavity it is possible to simulate the Rashba-Dresselhaus spin-orbit coupling [1] previously known from semiconductor physics. SU(2) symmetry of this Hamiltonian leads to an interesting phenomenon of persistent spin helix [2], which is robust against disorder. In this state electrons can retain spin coherence over long distances, which is a desirable effect for spintronic devices.

In this paper we report on the direct observation of an analogous phenomenon in an optical cavity filled with liquid crystal [3]. We optically determined the formation of a persistent spin helix polarization texture of cavity photons. Our system allows for full determination of the pseudospin, which is preserved in polarisation of photons transmitted through the microcavity. We observe periodic in space precession of spin for photons moving in plane of the cavity.

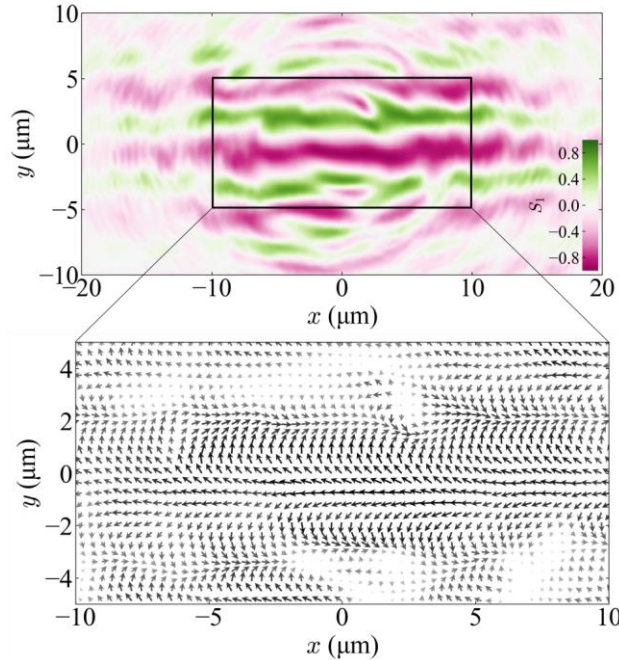


Fig. 1 Experimental spatial dependence of polarization of light transmitted through the microcavity expressed in terms of S_1 Stokes parameter (top panel). Measured Stokes vectors projected onto linear polarization plane (bottom panel).

[1] K. Rechcińska *et al.*, *Science* **366**, 727 (2019),

[2] B.A. Bernevig *et al.*, *Phys. Rev. Lett.* **97**, 236601 (2006),

[3] M. Król, K. Rechcińska *et al.*, *arXiv:2104.09674* (2021).

Acknowledgements This work was supported by the Ministry of Higher Education, Poland under project "Diamantowy Grant" 0005/DIA/2016/45; the Polish National Science Centre grants: 2016/23/B/ST3/03926 and 2018/31/N/ST3/03046; and by the Ministry of National Defense Republic of Poland Program – Research Grant MUT Project 13-995.

Light-matter interaction in birefringent microcavity with two-dimensional hybrid perovskite at room temperature

K. Łempicka¹, M. Król¹, A. Wincukiewicz¹, P. Morawiak², R. Mazur², W. Piecek²,
P. Kula³, T. Stefaniuk⁴, M. Kamińska¹, L. De Marco⁵, D. Ballarini⁵, D. Sanvitto⁵,
M. Matuszewski⁶, J. Szczytko¹, B. Piętka¹

¹*Institute of Experimental Physics, Faculty of Physics, University of Warsaw, Warsaw, Poland*

²*Institute of Applied Physics, Military University of Technology, Warsaw, Poland*

³*Institute of Chemistry, Military University of Technology, Warsaw, Poland*

⁴*Institute of Geophysics, Faculty of Physics, University of Warsaw, Warsaw, Poland*

⁵*CNR Nanotec, Institute of Nanotechnology, Lecce, Italy*

⁶*Institute of Physics, Polish Academy of Sciences, Warsaw, Poland*

Two-dimensional (2D) organic-inorganic perovskites exhibit desirable optoelectronic properties, such as high exciton binding energy at room temperature and can be easily tuned in energy by changing the organic or inorganic ions or thickness of the layer. It makes them an ideal system for the investigation of strong light-matter coupling phenomena and they open a new path towards polaritonic devices working at room temperature. In this work we present a novel architecture of a photonic structure with a 2D-perovskite incorporated in a cavity with highly birefringent medium, with the optical anisotropy controlled by external electric field. The strong light-matter coupling condition in our structure is achieved at room temperature which makes our system valuable for photonic applications that require tunable light emitters with non-linear interactions. Our structure, schematically shown in Fig. 1 a, consists of the perovskite layer ($[\text{C}_6\text{H}_5(\text{CH}_2)_2\text{NH}_3]_2\text{PbI}_4$) deposited using spin-coating technique on a top DBR and the photonic cavity is filled with a nematic liquid crystal (LC). The main advantage of using the LC layer is the possibility to control the effective refractive index of the liquid crystal [1] over extremely wide range by external electric field and engineer the coupling of subsequent cavity modes of different parity the excitonic resonance in the perovskite (Fig. 1 b). The emission from such a hybrid structure demonstrates strongly coupled exciton-polariton modes with clear anti-crossing revealed on linearly polarized cavity modes (Fig. 1 c, d). Our platform allows us to observe many photonic phenomena related to spin-orbit effects in exciton-polaritons, in particular, the Rashba-Dresselhaus regime in strongly coupled light-matter system.

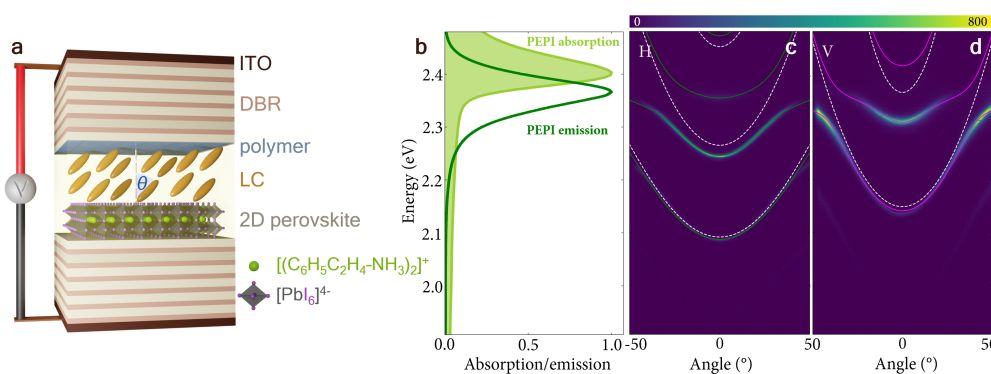


Figure 1. (a) Scheme of a microcavity containing a thin layer of 2D-perovskite and LC. (b) Normalized absorption (light green line) and emission (dark green line) spectra of a 2D-perovskite with major absorption at 2.4 eV. (c-d) Angle-resolved photoluminescence spectra of microcavity showing a strong-coupling regime detected in horizontal (H) and vertical (V) polarization. The Rabi energy, Ω , obtained through fitting of coupled oscillator model (solid lines) for H polarized mode close to the exciton energy is 94.4 meV and for V polarized mode is 108.7 meV.

[1] K. Rechcińska et al. *Science*, **366**, 6466, pp. 727-730 (2019).

Topological phase transition in an all-optical exciton-polariton Su-Schrieffer-Heeger lattice

M. Pieczarka^{1,2}, E. Estrecho¹, S. Ghosh³, M. Wurdack¹, M. Steger⁴, D. W. Snoke⁴,
K. West⁵, L. N. Pfeiffer⁵, T. C. H. Liew³, A. G. Truscott⁶, and E. A. Ostrovskaya¹

¹ ARC Centre of Excellence in Future Low-Energy Electronics Technologies and
Nonlinear Physics Centre, Research School of Physics, The Australian National University,
Canberra, ACT 2601, Australia

² Department of Experimental Physics, Faculty of Fundamental Problems of Technology,
Wrocław University of Science and Technology, Wyb. Wyspiańskiego 27, 50-370 Wrocław,
Poland

³ Division of Physics and Applied Physics, School of Physical and Mathematical Sciences,
Nanyang Technological University, Singapore 637371, Singapore

⁴ Department of Physics and Astronomy, University of Pittsburgh, Pittsburgh, PA 15260, USA

⁵ Department of Electrical Engineering, Princeton University, Princeton, NJ 08544, USA

⁶ Laser Physics Centre, Research School of Physics,
The Australian National University, Canberra, ACT 2601, Australia

Topological insulators are a class of electronic materials exhibiting robust edge states immune to perturbations and disorder at the boundaries of materials of different topological nature. This concept has been successfully adapted in photonics, where topologically nontrivial waveguides and topological lasers were developed. This idea has also been implemented in exciton polaritons, allowing for the realisation of topological physics in this nonlinear and non-Hermitian system. However, exploring the nontrivial properties in a given photonic system, including exciton polaritons, is limited to a fabricated sample, without the flexibility to reconfigure the structure in-situ.

Here, we demonstrate an all-optical realisation of the orbital Su-Schrieffer-Heeger (SSH) model in a microcavity exciton-polariton system, whereby a cavity photon is hybridised with an exciton in a GaAs quantum well [1]. We induce a zigzag potential for exciton polaritons all-optically by shaping the nonresonant laser excitation using a digital micromirror device (DMD). The potential is generated due to the photo-excited hot electron-hole pairs repulsively interacting with polaritons. We measure the eigenspectrum and topological edge states of a polariton lattice directly in a nonlinear regime of bosonic condensation. Furthermore, taking advantage of the tunability of the optically induced lattice, we modify the intersite tunnelling by changing the distance between the lattice sites and realise a topological phase transition to a trivial state. Our results open the way to study topological phase transitions on-demand in fully reconfigurable hybrid photonic systems that do not require sophisticated sample engineering.

[1] M. Pieczarka et al., arXiv:2102.01262 (2021)

Highly anisotropic optical response of GeS

**N. Zawadzka¹, Ł. Kipczak¹, T. Woźniak², M. Grzeszczyk¹, A. Babiński¹
and M. R. Molas¹**

¹ *Institute of Experimental Physics, Faculty of Physics, University of Warsaw, Warsaw, Poland*

² *Department of Semiconductor Materials Engineering, Wrocław University of Science and Technology, Wrocław, Poland*

Two-dimensional layered van der Waals (vdW) semiconductors, such as transition metal dichalcogenides (*e.g.* MoS₂, WSe₂), have emerged as a fascinating class of materials for exploring novel excitonic phenomena. Inspired by these exciting achievements, a new group of emerging vdW semiconductors, *i.e.* group-IV monochalcogenides MX (where M = Ge, Sn or Pb and X = S, Se or Te), has attracted an increasing attention due to their anisotropic optical properties originating from low-symmetry orthorhombic crystal structure analogous to black phosphorous.

In this work we investigate the optical response of bulk germanium sulphide (GeS) using the polarization-resolved photoluminescence (PL), reflectance contrast (RC), and Raman scattering (RS) performed in a wide temperature range (5-300 K).

We found that the low-temperature ($T=5$ K) PL spectrum of the studied GeS is characterized by four emission lines, denoted as X, L₁, L₂, and L₃. In contrast, the corresponding RC spectrum consists of a single resonance, which energy coincide with the X line. Moreover, polarization-resolved measurements revealed that all the emission lines

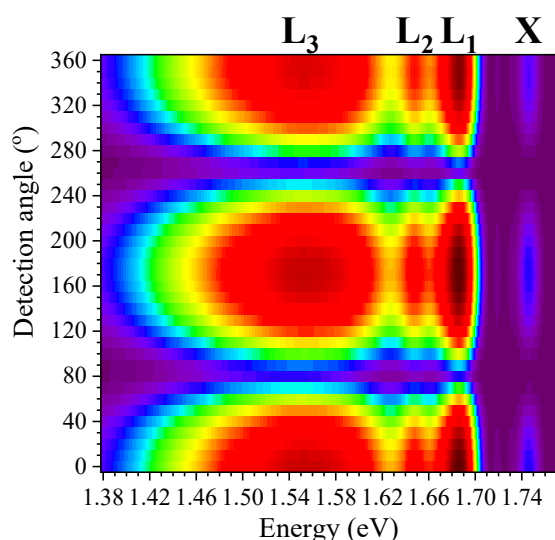


Figure: False-color map of the PL spectra as a function of the detection linear polarization angle.

are linearly polarized along the same direction, see the Figure. In accordance with Ref. [1], we ascribe the X line to a direct transition of a free exciton polarized along the armchair crystallographic direction at the Γ point of the Brillouin zone. In order to verify the origin of the L₁, L₂, and L₃ lines, the PL spectra were measured from $T=5$ K up to room temperature. Upon increasing the temperature, the L₁, L₂, and L₃ emission lines progressively disappear from the spectra. Only the X peak is observed at about 120 K and contributes to the PL spectra up to room temperature. We associate the L emission lines to with recombination processes assisted by disorder, defects/impurities or phonons. Particularly, this kind of emissions can be pronounced in bulk GeS in which the energetically-lowest transition is indirect [1].

Note that the shape of the measured PL spectrum of bulk GeS at $T=5$ K is typical for materials with long-lived ground states. It is similar for example for the low-temperature PL spectrum of WS₂ monolayer, which suggests the attribution of the low-energy lines to the localized excitons [2] or phonon replicas of dark excitons [3].

[1] A. Tołłoczko, *et al.*, *Materials Advances* **1**, 1886 (2020).

[2] M. R. Molas, *et al.*, *Nanoscale* **9**, 13128 (2017).

[3] M. Zinkiewicz, *et al.*, *Nano Letters* **21**, 2519 (2021).

Influence of the local field effect on nonlinear spectroscopy signals from 2D semiconductors

T. Hahn^{a,b}, A. Rodek^c, J. Kasprzak^{c,d}, T. Kazimierczuk^c, K. Nogajewski^c, K. Polczyńska^c,
K. Watanabe^e, T. Taniguchi^e, M. Potemski^{c,f}, P. Kossacki^c,
T. Kuhn^a, P. Machnikowski^b and D. Wigger^b

^a*Institut für Festkörpertheorie, Universität Münster, Münster, Germany*

^b*Department of Theoretical Physics, Wrocław University of Science and Technology, Poland*

^c*Institute of Experimental Physics, Faculty of Physics, University of Warsaw, Poland*

^d*Université Grenoble Alpes, CNRS, Grenoble INP, Institut Néel, Grenoble, France*

^e*National Institute for Materials Science, Tsukuba, Ibaraki, Japan*

^f*Laboratoire National des Champs Magnétiques Intenses, Grenoble, France*

Among two-dimensional materials monolayers (ML) of transition metal dichalcogenides (TMDCs) have emerged as an outstanding subject in solid state physics. Their light absorption and emission properties are governed by tightly bound excitons due to strong Coulomb interaction. Moreover the spin texture of valence and conduction bands impose optical selection rules offering the possibility of valley-selective excitations. In this context nonlinear spectroscopy constitutes an excellent method to investigate the exciton properties of TMDCs.

We model the different excitonic states in terms of few-level systems. The exciton-exciton interaction is incorporated by the local field effect (LF) and excitation induced dephasing (EID); the former increases the transition energies and the latter the dephasing proportionally to the exciton occupation. Utilizing these easily accessible models, one can even find analytical solutions for the state dynamics after ultrafast optical excitations. In a combined theoretical and experimental work we study the impact of LF and EID on signals obtained by two different techniques of nonlinear spectroscopy:

(i) We present a study on pump-probe spectroscopy on a MoSe₂-ML encapsulated in hBN [1]. The delay scan for co-circular excitation (Fig. 1) exhibits spectral dynamics which are well reproduced by the simulation in a two-level system (2LS). After the pump pulse the LF increases the oscillation frequency, visible as a line shift ($\tau > 0$) whereas EID imposes a faster decoherence decreasing the signal amplitude. At negative delays the pump pulse arrives last, which changes the exciton dynamics abruptly leading to spectral oscillations. Regarding cross-circular excitation, modeled by a three-level system gives additional access to the inter-valley scattering.

(ii) In four-wave mixing spectroscopy both exciton coherence and occupation dynamics can be probed. Depending on the applied pulse areas our simulations predict spectral line splittings that should persist on a few ps timescale when probing the occupation dynamics [2]. The found effects can instructively be explained by considering the impact of the relative phase between the applied pulses on the Bloch vector.

[1] A. Rodek, T. Hahn, et al., arXiv:2103.05328 (2021).

[2] T. Hahn, J. Kasprzak, et al., New J. Phys. 23 023036 (2021).

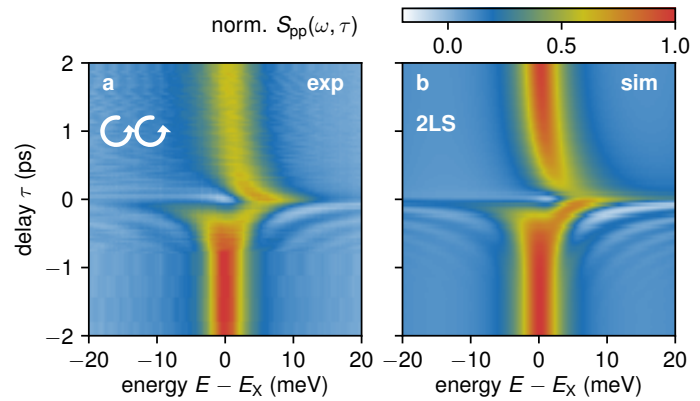


Figure 1: Delay scan of pump-probe spectra for co-circular excitation. (a) Experiment and (b) simulation.

Exciton-exciton interactions in MoSe₂ probed by nonlinear spectroscopy in charge-tunable device

A. Rodek¹, K. Oreszczuk¹, T. Kazimierczuk¹, J. Howarth², T. Taniguchi³,
K. Watanabe³, M. Potemski^{1,4} and P. Kossacki¹

¹*Institute of Experimental Physics, University of Warsaw, Pasteura 5, Warsaw, Poland*

²*National Graphene Institute, University of Manchester, M13 9PL, Manchester UK.*

³*National Institute for Materials Science, Tsukuba, 305-0047, Ibaraki, Japan*

⁴*Laboratoire National des Champs Magnetiques Intenses, CNRS-UJF-UPS-INSA, 25, avenue des Martyrs, 38042 Grenoble, France*

We study the influence of the electronically controlled n-type doping on the exciton-exciton interactions in the regime of high concentrations of photogenerated carriers ($n \approx 10^{12} \text{ cm}^{-2}$). The experiments are performed on an hBN-encapsulated MoSe₂ heterostructure with graphene contacts which enable to tune the free carrier concentration. The exciton complexes are created by resonant excitation with laser pulses. Selection of the light's energy and polarization permits to choose particular charged (CX) or neutral (X) excitons. Non-linear spectroscopy is performed in an ultrafast pump-probe setup with μm spatial resolution. Short laser pulses ($\Delta t \sim 100 \text{ fs}$) make it possible to create large non-equilibrium X and CX densities. Reflection from the sample is analysed spectrally, allowing for the extraction of resonance parameters' dynamics. In a neutral regime the optical spectrum exhibits only neutral exciton feature. For this case in the coincidence we can see a significant blueshift of the resonance originating from the exciton-

exciton interactions and high concentration of photo-generated carriers, which decays in the timescale of a few ps [1]. This picture experiences a drastic change in the negatively-charged regime. In particular, the energy of both X and, now visible, CX transitions redshifts upon the pump excitation with a notable rise time, that strongly depends on the polarization configuration. Another emergent feature is significantly longer decay. While the polarization-dependent effects can be generally attributed to rapid intervalley scattering a qualitative change of resonance behaviour indicates dominating role of exciton-carrier interactions in the ultrafast timescale.

Our findings shed light upon the complex landscape of exciton-exciton and exciton-carrier interactions in the two dimensional transitional metal dichalcogenides and lead to further development of their fundamental understanding.

[1] A. Rodek, T. Hahn, et al., *arXiv*:2103.05328 (2021).

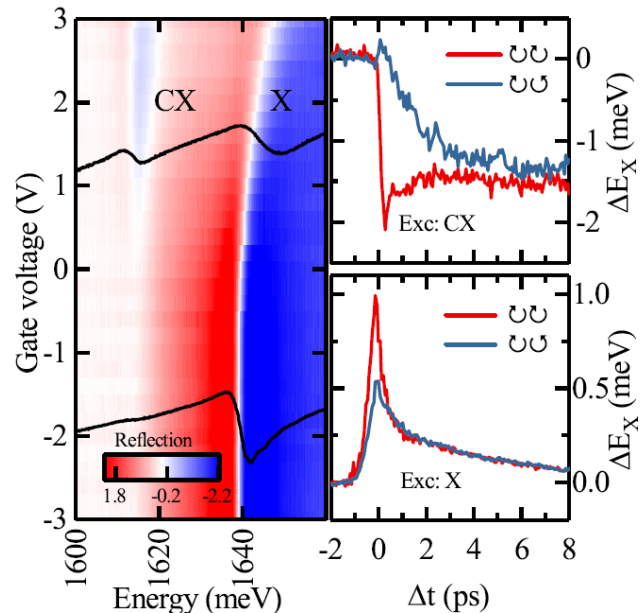


Figure 1. Reflection spectra as a function of gate voltage and X energy dynamics at -2V under X excitation and at +2V under CX excitation.

The Influence of the Buffer Layer on the Properties of Two Stage Epitaxial Boron Nitride Samples

Aleksandra K. Dąbrowska, Mateusz Tokarczyk, Jakub Iwański,
Grzegorz Kowalski, Rafał Bożek, Johannes Binder,
Roman Stępniewski, Andrzej Wysmolek

*Institute of Experimental Physics, Faculty of Physics, University of Warsaw,
ul. Pasteura 5, 02-093 Warsaw, Poland*

Boron nitride (BN) in the sp^2 – hybridized structure is characterized primarily by a wide bandgap (about 6 eV) and resistance to harsh external conditions [1]. The combination of these two properties enables its use in a wide range of applications. The main focus is on deep UV light sources and hBN as one of the building blocks in van der Waals heterostructures, for example as an insulating barrier. In order for the created structures to be as effective as possible, it is necessary to develop a growth method that will result in the formation of a material with good optical and structural properties on the large-scale.

Metal Organic Vapour Phase Epitaxy (MOVPE) of boron nitride is carried out on sapphire substrates with triethylboron (TEB) and ammonia as precursors of boron and nitrogen, respectively. The new growth method – two stage epitaxy - allows to avoid the chaotic nucleation of boron nitride on the substrate, characteristic for Flow-rate Modulation Epitaxy (FME), by introducing a thin (a few nanometers), pre-ordered, Continuous Flow Growth (CFG) buffer layer [2]. This new growth method leads to the formation of boron nitride with an almost ideal lattice constant and to the reduction of the concentration of point-like defects in the structure. Interestingly enough, in-depth studies revealed the correlation between the properties and growth conditions of the CFG stage with structural properties and smoothness of the whole (two stage) sample (Fig. 1). In this communication the influence of the nitridation, temperature, pressure and the growth time on the properties of the two stage samples is discussed.

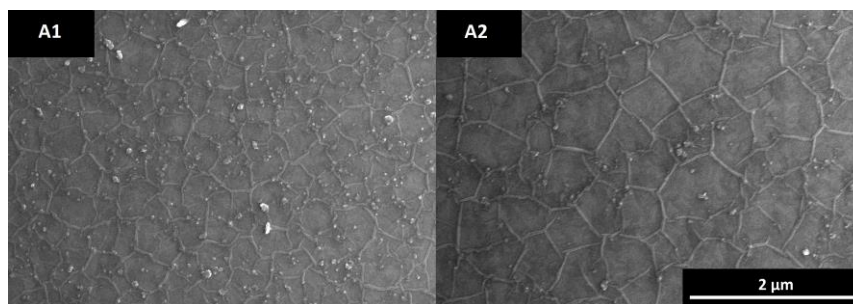


Fig. 1 Scanning Electron Microscopy (SEM) image of the two stage samples grown in the same conditions but annealed and stabilized before the growth in nitrogen (A1) and hydrogen (A2).

Our studies show the direction for further research on the two stage growth aimed in obtaining uniform boron nitride layer with excellent optical and structural properties including control over the smoothness of BN surfaces which is important for building van der Waals heterostructures with other two dimensional materials. The proposed growth method shows great potential for the production of high quality, epitaxial h-BN which is crucial for large-scale optoelectronic applications based on 2D materials.

[1] K.S. Novoselov et al., *Science* 353.6298, aac9439 (2016)

[2] A.K. Dabrowska et al., *2D Mater.*, **8**, 015017 (2021)

Acknowledgement: This work has been partially supported by the National Science Centre under grant no. 2019/33/B/ST5/02766

Filtering Properties of Epitaxial Boron Nitride

Adrianna Wójcik^{1,2}, Aleksandra K. Dąbrowska¹, Sylwia Kozdra², Johannes Binder¹,
Andrzej Wyszomolek¹, Paweł P. Michałowski²

¹ Faculty of Physics, University of Warsaw, Pasteura 5, 02-093 Warsaw, Poland

² Łukasiewicz Research Network – Institute of Microelectronics and Photonics,
al. Lotników 32/46, 02-668 Warsaw, Poland

The water desalination and purification processes based on membrane filtration have significantly developed due to considerable improvements in the technology of nanoporous 2D materials. In particular porous graphene [1] and molybdenum disulfide [2] have been demonstrated as promising candidates for water desalination. Molecular Dynamics simulation has shown that nanoporous boron nitride allows for effective salt rejection with high water permeability [3]. This together with high thermal and chemical stability of boron nitride indicates its strong prospective for filtering applications.

In this work, we demonstrate the potential of porous sp^2 -hybridized boron nitride grown by MOVPE for desalination of water. The investigated sample has complex morphology consisting of differently oriented flakes of various sizes yielding porous layers. The surface of the sample has been subjected to a heavy water-salt solution at various temperatures. The Secondary Ion Mass Spectrometry (SIMS) technique has been used to determine depth profiles of sodium, deuterium and oxygen in the boron nitride structure. The obtained diffusion profiles of the Na show that salt penetrates only to the limited depth. The deuterium and oxygen profiles demonstrate simultaneous permeation of a heavy water through the entire depth of the boron nitride sample.

The presented results show that the porous 3D structure consisting of sp^2 -bonded BN acts like a sieve separating salt from water therefore being a promising material for its desalination.

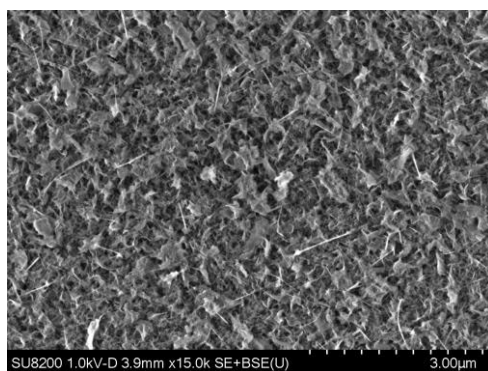


Fig 1. SEM image of the porous sp^2 -bonded boron nitride structure.

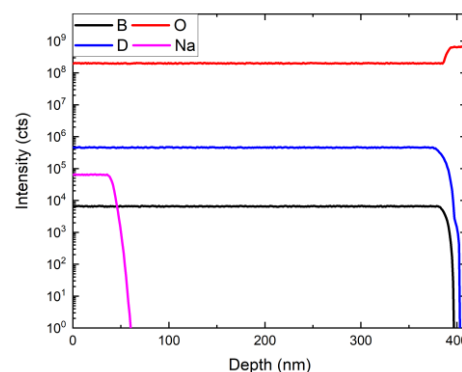


Fig 2. SIMS depth profile measured for the BN sample heated at 45°C temperature.

Acknowledgement: This work has been partially supported by the: National Science Centre under grants no. 2019/33/B/ST5/02766 and 2018/31/D/ST5/00399.

[1] S. Homaeigohar, M. Elbahri, *NPG Asia Mater* **9**, 427 (2017).

[2] H. Li, T.J. Ko, M. Lee, H.S. Chung, S.S. Han, K.H. Oh, A. Sadmani, H. Kang, Y. Jung, *Nano Lett.*, **19**, 5194-520 (2019)

[3] H. Gao, Q. Shi, D. Rao, Y. Zhang, J. Su, Y. Liu, Y. Wang, K. Deng, R. Lu *J. Phys. Chem. C* **40**, 121 (2017)

The optical signature of few-layer ReSe₂

Ł. Kipczak, M. Grzeszczyk, K. Olkowska-Pucko, A. Babiński, and M. R. Molas

Institute of Experimental Physics, Faculty of Physics, University of Warsaw, Warsaw, Poland

Semiconducting transition metal dichalcogenides (S-TMDs) such as MoS₂, MoSe₂, WS₂, WSe₂ and MoTe₂ invariably attract attention due to their unique electronic structures and resulting optical properties. Recently, rhenium-based compounds of the type ReX₂ (X = S or Se) have emerged as intensively investigated members of S-TMDs family, thanks to their weak interlayer coupling and in-plane anisotropy.

In this work optical properties of thin ReSe₂ layers with thicknesses ranging from mono- (1 ML) to nona-layer (9 MLs) are investigated [1]. The photoluminescence (PL) and Raman scattering (RS) were measured at low ($T=5$ K) and room ($T=300$ K) temperature, respectively.

The low-temperature PL spectra of atomically thin ReSe₂ flakes comprise two well-resolved emission lines, which experience a blueshift of about 120 meV when the layer thickness is decreased from 9 MLs to a monolayer limit. The energy of those peaks can be used to determine the layer thickness, but this approach is effectively limited, especially due to the low-temperature conditions of the measurement. The analysis of low-energy interlayer Raman modes allows unambiguous identification of the structure thickness in thin layers of S-TMDs. However, demanding experimental conditions, namely approaching the excitation laser line as close as 5 cm⁻¹, hardly make that method a simple characterization tool of S-TMDs. We show that more convenient way to determine the flake thickness in thin ReSe₂ layers relies on the determination of the energy difference between two phonon A_g modes of intralayer vibrations

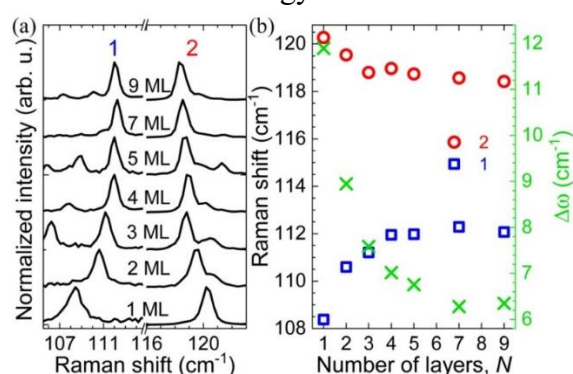


Figure 1: (a) Raman spectra of thin layers ReSe₂ from 1 ML to 9 ML. (b) the layer dependence of Raman shift for modes 1 and 2 accompanied by their energy difference, $\Delta\omega$.

observed between 107 cm⁻¹ and 120 cm⁻¹ (labelled with 1 and 2 in Figure). The peak 1 increases its energy and the energy of the peak 2 decreases with the increasing thickness. The energy difference between the peaks changes from 12 cm⁻¹ to almost 6 cm⁻¹ between 1 ML and 9 MLs. The peak 1 evolution is characteristic for most A_g modes in ReSe₂ and can be explained in terms of interlayer interactions [2]. The opposite evolution of the peak 2, is commonly related to the surface effects [3]. Due to the distinct energy evolution of both peaks, their energy difference ($\Delta\omega$) defines an optical signature of few layer ReSe₂ and provides a simple mean to identify the sample thickness in a few layer limit. Such an approach is usually used for other S-TMDs, e.g. thin layers of MoS₂ [4]. Our results also expose similarities between the investigated ReSe₂ and ReS₂, but the amplitude of the effect observed by us in ReSe₂ is substantially larger than in the one demonstrated in ReS₂ [5]. Moreover, the pronounced Davydov splittings of the peak 1 are observed from 3 ML to 9 ML, which points out the resonance character of the used excitation.

- [1] Ł. Kipczak, *et al.*, J. Appl. Phys. **128**, 044302 (2020).
- [2] G. Froehlicher, *et al.*, Nano Letters **15**, 6481 (2015).
- [3] X. Luo, *et al.*, Phys. Rev. B **88**, 075320 (2013).
- [4] Ch. Lee, *et al.*, ACS Nano **4**, 2695 (2010).
- [5] D. Chenet *et al.*, Nano Letters **15**, 5667 (2015).

The influence of the magnetic ordering on the electronic properties of bilayer NiPS₃/FePS₃ – an *ab initio* study of vdW heterostructure.

K. Kotur¹ and M. Birowska¹

¹University of Warsaw, Faculty of Physics, Pasteura 5, 02-093 Warsaw, Poland

The vertical stacking of the 2D materials into the vdW heterostructures has attracted much attention during last years [1], mostly due to a new phenomena that can be observed in such heterostructures. Just recently the 2D magnetic crystals have been experimentally reported [2], opening the possibility to study the vdW layered magnets, exhibiting different magnetic phases [3,4]. Proximity effects between magnetic layers might serve as sensitive tool to examine details of the magnetic structure.

Here, we present a comprehensive *ab initio* study of the prototypical example of vdW magnetic system NiPS₃/FeS₃. The individual layers are the members of large family of transition metal phosphorus trichalcogenides MPX₃ [5], which are antiferromagnets. The impact of the intralayer and interlayer magnetism on the electronic properties of heterobilayer is examined in the framework of the density functional theory. In particular, the band alignments, band offsets and band gaps are investigated and compared with isolated layers. Our results have demonstrated the moderate influence of intralayer magnetism on the electronic and energetic properties of the system along with negligible impact of interlayer magnetism on these properties. In addition, spatial separation of charges at the band edges are demonstrated, implying the possible existence of the interlayer excitons in NiPS₃/FePS₃ structure.

The study was accomplished thanks to the funds allotted by the National Science Centre, Poland within the framework of the research project 'SONATA12' no. UMO-2016/23/D/ST3/03446. Access to computing facilities of TU Dresden ZIH for the project "TransPheMat", PL-Grid Polish Infrastructure for Supporting Computational Science in the European Research Space, and of the Interdisciplinary Center of Modeling (ICM), University of Warsaw are gratefully acknowledged.

- [1] D. L. Duong et al, *ACS Nano* **11**, p. 11803–11830 (2017).
- [2] B. Huan et al., *Nature* **546**, p. 270-273 (2017).
- [3] D. Zhong et al. *Science Advances* **3**, p. 1-6 (2017).
- [4] M. Birowska, P.E.F. Junior, J. Fabian, J. Kuntzmann, *Phys. Rev. B* **103**, L121108 (2021).
- [5] R. Brec, *Solid State Ionics* **22**, p. 3-30 (1986)

Proximity spin-orbit coupling in graphene/1T-TaS₂ heterostructure and its sensitivity to charge density wave ordering: Density Functional Theory calculations

K. Szałowski¹, M. Gmitra², and D. Kochan³

¹*Department of Solid State Physics, Faculty of Physics and Applied Informatics, University of Łódź, ul. Pomorska 149/153, PL90-236 Łódź, Poland*

²*Institute of Physics, Pavol Jozef Šafárik University in Košice, Park Angelinum 9, 040 01 Košice, Slovakia*

³*Institute for Theoretical Physics, University of Regensburg, 93040 Regensburg, Germany*

Van der Waals heterostructures consisting of graphene and other two-dimensional material offer an unique possibility to design the system with desired properties by exploiting the idea of the proximity effect [1]. One of the highly useful properties which graphene can acquire in this manner is enhanced spin-orbit coupling. It has been demonstrated that heterostructures based on monolayer graphene and monolayer transition metal dichalcogenide constitute particularly interesting platforms for applications in spintronics [2].

The possible presence of additional orderings in transition metal dichalcogenide opens the way towards advanced controlling of the proximity spin-orbit coupling. A particularly intriguing candidate is a system with charge density wave ordering, 1T-TaS₂ [3]. In this transition metal dichalcogenide a sequence of charge density wave states is detected [4] with pronounced David star-like deformation of the crystalline lattice.

In the paper we present the results of first principles calculations of the electronic properties of heterostructure composed of monolayer graphene and monolayer 1T-TaS₂, for different stackings. The cases of normal (metallic) phase and commensurate charge density wave phase in TaS₂ monolayer are compared and contrasted. In both cases a significant *p*-type doping of graphene is predicted, with preserved structure of Dirac cones. Phenomenological effective tight-binding Hamiltonians [5,6] are used to fit the first-principles data in the vicinity of *K*-points and to extract the parameters quantifying the orbital and spin-orbital proximity effects. A particularly interesting finding is the significant dependence of the band structure on the presence or absence of charge density wave ordering.

The work was financially supported by the National Science Centre (Poland) under Grant No. 2015/19/B/ST3/03142, by the Ministry of Education, Science, Research and Sport of the Slovak Republic under Grant No. VEGA 1/0105/20, and by Deutsche Forschungsgemeinschaft (Germany) - Project-ID 314695032—SFB 1277.

- [1] I. Žutić, A. Matos-Abiague, B. Scharf, H. Dery, K. Belashchenko, *Materials Today* **22**, 85 (2019).
- [2] M. Gmitra, J. Fabian, *Phys. Rev. B* **92**, 155403 (2015).
- [3] K. Rossnagel, *J. Phys.: Condens. Matter* **23**, 213001 (2011).
- [4] I. Lutsyk, M. Rogala, P. Dąbrowski, P. Krukowski, P.J. Kowalczyk, A. Busiakiewicz, D.A. Kowalczyk, E. Łacińska, J. Binder, N. Olszowska, M. Kopciuszynski, K. Szałowski, M. Gmitra, R. Stępniewski, M. Jałochowski, J.J. Kołodziej, A. Wysmołek, Z. Klusek, *Phys. Rev. B* **98**, 195425 (2018).
- [5] M. Gmitra, D. Kochan, P. Högl, J. Fabian, *Phys. Rev. B* **93**, 155104 (2016).
- [6] D. Kochan, S. Irmer, J. Fabian, *Phys. Rev. B* **95**, 165415 (2017).

Magneto-optical properties of monolayer MoSe₂ grown by molecular beam epitaxy on hexagonal boron nitride

K. Oreszczuk¹, W. Pacuski¹, A. Rodek¹, T. Kazimierczuk¹, K. Nogajewski¹,
T. Taniguchi², K. Watanabe², M. Potemski^{1,3}, and P. Kossacki¹

¹University of Warsaw, Pasteura St. 5, 02-093 Warsaw, Poland

²National Institute for Materials Science, Tsukuba, 305-0047, Ibaraki, Japan

³LNCMI, 25, avenue des Martyrs, 38042 Grenoble, France

Monolayers of transition metal dichalcogenides (TMDs) draw a lot of attention as semiconducting materials with robust optical properties, strong Coulomb interaction and an optically accessible valley degree of freedom. Extraordinary properties of TMDs make them promising candidates for photonics and optoelectronics. Fundamental research on such systems usually required using exfoliated samples, as they provided the best optical properties, in particular narrow linewidths of excitonic transitions. Exfoliation process, however, suffers from limited scalability and large inhomogeneity, hindering the perspectives of potential commercial applications.

Techniques such as Molecular Beam Epitaxy (MBE), which are free of this disadvantages, usually yielded only structures characterized by considerable spectral broadening, hindering most of the interesting optical effects. Only recently, first narrow-line and high optical quality MBE-grown MoSe₂ monolayers were reported on [1]. The extraordinary optical properties were achieved with growth process including using atomically flat hexagonal boron nitride substrate.

In this work, we present the extensive study on the magneto-optical properties of the MBE-grown MoSe₂ monolayers. We compare the Zeeman shifts of neutral (X) and charged (CX) excitonic peaks with the results reported for exfoliated samples. We also employ two different time-resolved techniques to study the carrier relaxation and recombination processes in our samples. The streak camera spectroscopy reveals the short lifetimes of excitonic complexes, yielding the values of about 1.5 ps for CX and below 1 ps for X. To study the carrier dynamics in the regime of fast relaxation rates more precisely, we employ the Excitation Correlation Spectroscopy (ECS) technique [2]. We analyse the characteristic times of ECS signal decay at different temperatures. Our studies pave the way to understanding the carrier localization effects and influence of non-radiative recombination channels in MBE-grown MoSe₂.

[1] W. Pacuski et. al., *Nano Lett.* 20, 5, 30583066 (2020)

[2] D. von der Linde et. al., *J. Lumin.* 2425, Part 2, 675 (1981)

Photoconductivity of hexagonal boron nitride grown by MOVPE

J. Rogoża¹, J. Binder¹, A. K. Dąbrowska¹, R. Stępniewski¹, A. Wysmolek¹

¹*Faculty of Physics, University of Warsaw, Pasteura 5, 02 – 093 Warsaw, Poland*

Boron nitride (BN) is a very promising candidate for optoelectronic applications in the deep ultraviolet spectral range due to its exceptional physical properties, such as high chemical stability, thermal conductivity and wide bandgap energy. A large cross section for neutron capture renders BN an outstanding candidate for neutron detectors, while the possibility of effective p-type doping opens up new possibilities of application as a transparent contact in UV emitting devices based on nitrides.

In this communication studies of photoconductivity of epitaxially grown h-BN by Metal Organic Vapour Epitaxy (MOVPE) are presented. In order to verify the role of defects on the conductivity of the epitaxial material, samples were annealed in nitrogen atmosphere at 1000 °C for 10 minutes. A gold-palladium alloy was used to obtain photodetector structures by a maskless lithography system in a lift-off process (fig. 1).

Room temperature photocurrent spectra of our epitaxial layers are dominated by processes related to the photoionization of deep centers. A laser-driven light source was used to excite photocurrent in the range 170-1000 nm. Broad photocurrent peaks, that may be associated with doping or defects centers, were detected for both samples in the visible and near UV region. Signals related to excitonic transitions in the DUV range are also observed. This gives us opportunity to further discuss the nature of the band gap in hexagonal boron nitride. The obtained results constitute an important first step towards the use of hexagonal boron nitride in DUV optoelectronics.

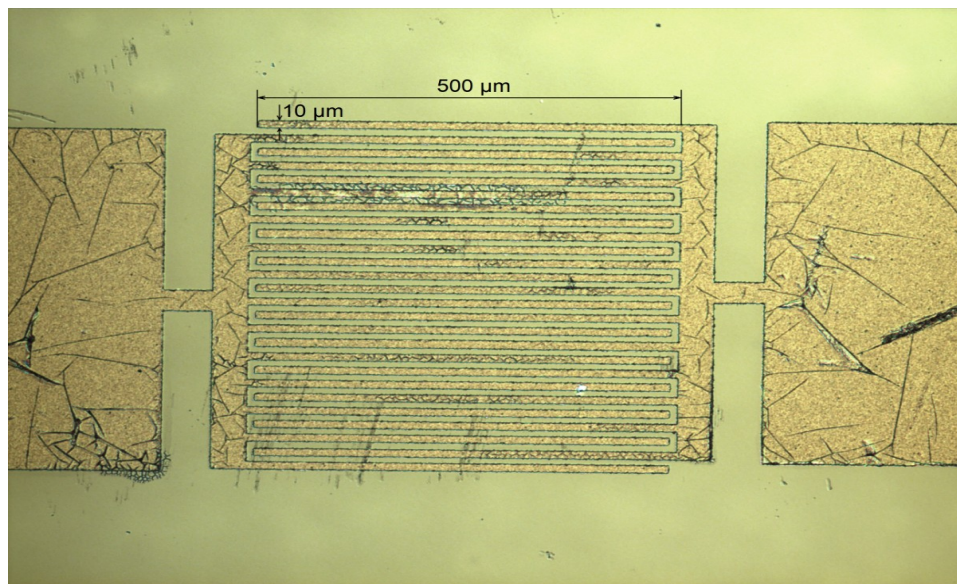


Fig 1. a) Optical image of the investigated sample showing the photodetector structure. The visible lines on the metalization are related to h-BN wrinkles arising during the lithography process.

Acknowledgments:

This work was partially supported by the National Science Centre grant no 2019/33/B/ST5/02766.

Toward Magnetic – Semiconductor Van der Waals Heterostructures Grown by Molecular Beam Epitaxy

Julia Kucharek, Rafał Bożek, Mateusz Goryca and Wojciech Pacuski

*Institute of Experimental Physics, Faculty of Physics, University of Warsaw, Pasteura 5,
PL02-093 Warszawa, Poland*

One of the greatest challenges and needs of our time is the efficient processing and storage of information, preferably in the same structure. This motivates activities to extend the understanding of interactions between the spins of magnetic ions and the spins of free carriers in various semiconductors including 2D materials. It is also important to establish effective control of electronic properties, such as current or accumulated charge, by spin orientation or application of magnetic field. Here, we propose a hybrid magnetic-semiconductor vdW heterostructure as a way to combine spin and semiconductor properties in one device to study mutual interaction of these two kinds of materials.

The first aim of this work is to elaborate growth of such vdW heterostructures by Molecular Beam Epitaxy (MBE). All our samples are based on molybdenum diselenide (MoSe_2) grown on exfoliated hexagonal boron nitride (hBN) flakes. hBN flakes are exfoliated and deposited on Si with polycrystalline SiO_2 (Si/SiO_2) buffer. On top of MoSe_2 we have grown 3 different potentially layered and magnetic materials: manganese selenide (MnSe), rhenium selenide (ReSe_x) and vanadium selenide (VSe_x).

All of heterostructures were investigated with Atomic Force Microscope (AFM). Dimensionality and coverage of the MoSe_2 were the most important factors for the evaluation of heterostructures by AFM. In the next step we have checked the influence of added magnetic layers on MoSe_2 photoluminescence (PL) spectra. After that, we have selected VSe_x on MoSe_2 sample for magnetic field measurements since VSe_x tends to grow flatly on MoSe_2 (in contrary to other two materials). Moreover, MoSe_2 PL is not quenched when MoSe_2 is covered with VSe_x , instead only a small shift of excitonic line (5 nm) is observed. We have used magnetic field sweeps (0-10 T in 10 K) to verify whether VSe_x reveals any spin-dependent impact on MoSe_2 PL, but so far within experimental accuracy g-factors of $\text{VSe}_x/\text{MoSe}_2$ and MoSe_2 are similar. Therefore observation of interlayer interactions requires further optimisation of sample design.

Intrinsic and extrinsic spin-orbit coupling in monolayer nitrogene.

Paulina Jureczko*, Marcin Kurpas¹

¹*Institute of Physics, University of Silesia in Katowice, ul. 75 Pułku Piechoty 1, 41-500 Chorzów*

**paulina.jureczko@us.edu.pl*

Monolayer nitrogene was recently predicted to be stable two-dimensional material even far above the room temperature [1]. It is an indirect gap nonmagnetic insulator, with the gap of 4 eV [1]. Nitrogene crystallizes in a centrosymmetric buckled honeycomb lattice, similar to other graphene analogues, such as, silicene, blue phosphorene or arsenene [2,3]. Although the electronic, mechanical and thermal properties of nitrogene have been studied by several authors [1,4–6], the spin-orbital effects have not been studied in detail yet. Here, we perform a systematic theoretical study of the spin-orbit coupling in this material. Specifically, we employ first-principles methods to obtain the basic orbital and spin-orbital properties of nitrogene, also in the presence of an external transverse electric field. We calculate the spin-mixing parameter b^2 and spin-orbit fields Ω to extract essential information about the intrinsic and extrinsic spin-orbit coupling in the band structure. We find, that the values of b^2 are very small, on the order of 10^{-6} , similar to those of graphene [7]. The values of $\hbar\Omega$ are below $1 \mu\text{eV}$ for $E=1 \text{ V/nm}$. Our results show, that even if nitrogene is a heavier element than carbon, the effective spin-orbit coupling in the bands close to the band gap is weaker for nitrogene than for graphene, due to the specific topology of the band structure.

- [1] V. O. Özçelik, O. U. Aktürk, E. Durgun, and S. Ciraci *Phys. Rev. B*, vol. 92, p. 125420, 2015.
- [2] F. Ersan, D. Kecik, V. O. Özçelik, Y. Kadioglu, O. Aktürk, E. Durgun, E. Aktürk, and S. Ciraci *Applied Physics Reviews*, vol. 6, no. 2, p. 021308, 2019.
- [3] F. Ersan, E. Aktürk, and S. Ciraci *Phys. Rev. B*, vol. 94, p. 245417, 2016.
- [4] B. Peng, D. Zhang, H. Zhang, H. Shao, G. Ni, Y. Zhu, and H. Zhu *Nanoscale*, vol. 9, pp. 7397–7407, 2017.
- [5] J. Lee, W. Wang, and D.-X. Yao *Scientific Reports*, vol. 6, 2016.
- [6] J. Lee, W.-C. Tian, W. Wang, and D.-X. Yao *Scientific reports*, vol. 5, p. 11512, 2015.
- [7] M. Kurpas, P. E. Faria Junior, M. Gmitra, and J. Fabian *Phys. Rev. B*, vol. 100, p. 125422, 2019.

Electronic coupling in hybrid monolayer transition metal dichalcogenide/2D perovskite heterostructures

M. Karpińska^{1,2}, M. Liang³, R. Kempt⁴, K. Finzel⁴, M. Kamminga³,
N. Zhang¹, M. Dyksik^{1,5}, D. K. Maude¹, J. Jasiński⁵, J. Ziegler⁶,
A. Surrente⁵, M. Baranowski^{1,5}, J. Ye³, A. Chernikov⁶, A. Kuc⁷,
L. Kłopotowski², and P. Plochocka¹

¹*Laboratoire National des Champs Magnétiques Intenses, UPR 3228,
CNRS-UGA-UPS-INSA, Grenoble and Toulouse, France*

²*Institute of Physics, Polish Academy of Sciences, 02-668 Warsaw, Poland*

³*Zernike Institute for Advanced Materials, University of Groningen,
9747 AG Groningen, The Netherlands*

⁴*Technische Universität Dresden, 01062 Dresden, Germany*

⁵*Department of Experimental Physics, Faculty of Fundamental Problems of Technology,
Wrocław University of Science and Technology, 50-370 Wrocław, Poland*

⁶*Department of Physics, University of Regensburg, 93053 Regensburg, Germany*

⁷*Helmholtz-Zentrum Dresden-Rossendorf, 01328 Dresden, Germany*

Layered van der Waals stacks are currently the focus of great interest due to their unprecedented flexibility, originating essentially from the almost total relaxation of lattice matching requirements. Additionally, as opposed to the single layers, the heterostructures exhibit novel and exotic properties, such as energy [1] or charge transfer [2]. As an extra advantage, these phenomena can be further tuned in a desirable way by selecting the specific materials or applying external fields. We present the results of experimental and theoretical studies of novel hybrid transition metal dichalcogenide (TMD)/2D perovskite stacks, which provide us with an insight into understanding of the mechanism of the electronic coupling between these two different families of materials.

DFT calculations of a WS₂/(PEA)₂PbI₄ heterostructure ensemble reveal a novel band alignment, where direct electron transfer is blocked by the organic spacer of the 2D perovskite [3]. In contrast, the valence band forms a cascade from WS₂ through the spacer to the inorganic layer of PbI₄ octahedra, allowing hole transfer. These predictions are supported by low temperature optical spectroscopy studies, which provide compelling evidence for both charge transfer and non-radiative transfer of the excitation (energy transfer) between the layers. We also present evidence for a long lived inter-layer exciton (IX) formed in another system composed of a MoSe₂ monolayer and (PEA)₂PbI₄ 2D perovskite. The appearance of IX was confirmed by both theory and experiment. Our results show that TMD/2D perovskite heterostructures provide a flexible and convenient way to engineer the band alignment, providing promising possibilities for the future applications in novel optoelectronic devices.

[1] L. Wu et al., *ACS Nano* **13**, 2, 2341–2348 (2019).

[2] F. Ceballos et al., *Nano Lett.* **17**, 3, 1623–1628 (2017).

[2] M. Karpińska et al., *ACS Appl Mater Interfaces* (2021).

Plasma-assisted MBE growth of CdMgO Random alloys on Al₂O₃ substrate

A. Adhikari¹, A. Lysak¹, A. Wierzbicka¹, P. Sybilski¹, B. Witkowski¹, E. Przezdziecka¹

¹*Institute of Physics, Polish Academy of Sciences, Al. Lotników 32/46,
02-668 Warsaw, Poland*

Unlike other II-VI semiconductors, CdO-based transparent oxide has great potential application for the fabrication of many photovoltaic applications. However, a low optical bandgap (2.3 eV at RT) restricts its use in case of optoelectronic application purposes. It is possible to tune the bandgap by means of alloying with MgO (7.8 eV at RT) which can be used for light emission over UV to the visible regime. Recently it was demonstrated that the direct bandgap of {CdO/MgO} superlattices (SLs) grown on *c*- and *r*- sapphire substrate by plasma-assisted molecular beam epitaxy (PA-MBE) technique, can be tuned from 2.6 eV to 6 eV by varying the thickness of CdO and MgO monolayers in the SLs structures[1].

In this work, we investigated Cd_xMg_{1-x}O alloy deposited on *m*- and *c*-oriented sapphire substrate using the PA-MBE technique, with varying concentrations of Mg dopant from 0 to 96%. The influence of Cd-rich to Mg-rich conditions was studied in detail. From the composition analysis, done by the Energy-dispersive X-ray spectroscopy (EDX) method, the concentrations of Mg and Cd in the alloys were determined. A structural and morphological study of CdMgO random alloys was carried out using X-ray diffraction (XRD) and Atomic Force Microscope (AFM) techniques. XRD analysis of 220 and 111 diffraction peak of CdMgO on *m*- and *c*-plane sapphire respectively confirmed the presence of cubic rocksalt structure. Calculated lattice parameters decreases with an increase in Mg²⁺ dopant in CdMgO alloys. The optical properties of thin films were investigated by UV-Vis spectroscopy at room temperature. From the absorption curve, the optical bandgaps are determined and it was found that the bandgap of films changes from 2.6eV to 5.6eV with varying Mg concentration from 0 to 96%. The lattice parameters are fitted with Cd concentration using modified Vegard's law and the bowing constant found to be -0.0826 and -0.1003 nm for CdMgO alloys on *m*- and *c*-plane sapphire substrate respectively. The negative bowing suggests repulsive interaction between O-2p and Cd-3d states. Our present work sheds light on Cd-rich to Mg-rich CdMgO random alloys and opens up new prospects for the design of novel optoelectronic devices.

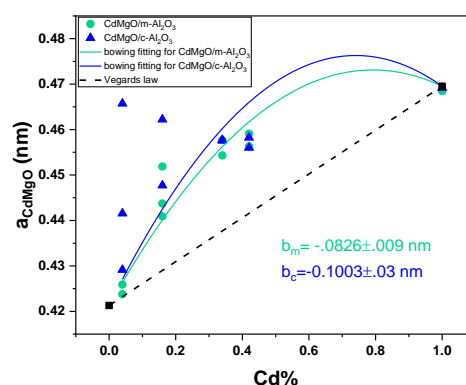


Fig1. Lattice parameter of the CdMgO alloy vs Cd atomic concentration

- [1] E. Przezdziecka, P. Strąg, A. Wierzbicka, A. Adhikari, A. Lysak, P. Sybilski, J.M. Sajkowski, *Nanoscale Res. Lett.* **2021**, 16, 59.

RBS based structural investigation of ZnO/ZnCdO structures grown on Al₂O₃ a- and r- oriented substrates by MBE

M. Stachowicz¹, E. Przezdziecka¹, J.M. Sajkowski¹, M.A. Pietrzyk¹, A. Pieniazek¹,
S. Magalhaes², D. Faye², E. Alves², A. Kozanecki¹

¹ Institute of Physics, Polish Academy of Science, al. Lotnikow 32/46, PL-02668 Warsaw, Poland

² Centro Tecnológico Nuclear, Instituto Superior Técnico, Universidade de Lisboa, P-2686953 Sacavém, Portugal

The wide band gap II- IV semiconductors have become of increasing technological importance, in particular for the development of light emitting sources such as diodes and lasers, operating in the visible to ultraviolet region. Such devices are based on heterojunctions and quantum well layers and so, because to the large concentration gradients present, inter-diffusion of the matrix components during growth and thermal processing is of inevitable concern, which may lead to substantial changes in the composition of the interface and doped layer or well profiles. This leads to band gap configuration modifications and consequently changes the devices parameters. Therefore quantitative knowledge of the inter-diffusion is essence.

In this work we present the results of Rutherford Back Scattering (RBS) study of the temperature induced inter-diffusion in ZnO/ZnCdO structures. In our experiments, we have grown three series of structures which differ one from another in details of growth procedures, layer arrangement and Cd content in range from 1.5 to 8%. In the experimentation conducted on subjected structures also other techniques were employed, such as Atomic Force Microscopy (AFM), Photoluminescence (PL) and Scanning Electron Microscopy (SEM).

Comparison of results for as grown and annealed structures suggest that disturbed lattice structure, due to presence of Cd, was partly recovered after thermal treatment. Chosen annealing temperature and time was enough to induce low range inter-diffusion of Cd ions into neighboring ZnO layers, which was well visible in the RBS depth profiles and confirmed with NDF simulations.

Summarizing, we may conclude that the growth temperature was a major influence on the effectiveness of Cd incorporation into ZnO matrix. Very important success here is an observation of inter-diffusion and quantifying its extent in the structures with low Cd content using RBS technique.

Acknowledgements: The project was supported by the Polish National Science Centre (NCN) based on the decision No: DEC-2018/28/C/ST3/00285

Influence of As Doping on the Properties of MBE Grown Nonpolar ZnO Thin Films

A. Lysak¹, E. Przeździecka¹, K. M. Paradowska², A. Wierzbicka¹, P. Sybilski¹,
J. Sajkowski¹, R. Jakiela¹, E. Placzek-Popko², A. Kozanecki¹

¹Institute of Physics, Polish Academy of Sciences, al. Lotników 32/46, Warsaw, Poland

²Department of Quantum Technologies, Faculty of Fundamental Problems of Technology, Wrocław University of Science and Technology, Wybrzeże Wyspiańskiego 27, Wrocław, Poland

Zinc oxide is characterized by its direct wide-bandgap (3.37 eV) and high exciton binding energy (60 meV) and has significant potential for applications in optoelectronic devices. However, applications are restricted by the possibility of doping of ZnO to *p*-type. In this work As-doped nonpolar *a*-ZnO thin films grown by molecular beam epitaxy (MBE) on *r*-plane Al₂O₃ are investigated. Different concentrations of As doping ($1.5 \cdot 10^{18}$ - $3 \cdot 10^{19}$ at./cm³) were achieved by changing the temperature of the As-effusion cell from 190 °C to 220 °C.

We studied optical and electrical properties of *a*-ZnO thin films with different concentration of As. We applied several experimental techniques such as Hall effect measured at room temperature, temperature dependent photoluminescence (PL), transmittance, SIMS, angle dependent micro-Raman spectroscopy and X-ray diffraction. All as-grown samples showed *n*-type conductivity that increased with As concentration (determined by SIMS). It was found that the concentration of As atoms increases much faster with the increase of As effusion cell temperature than the concentration of electrons (Fig. 1). It was found that PL spectra strongly depend on the concentration of As-dopant (Fig. 2). At low temperatures, the intensity of the D⁰X lines decreases with increasing As doping thus suggesting that isolated As atoms are not responsible for *n*-type conductivity. Free exciton lines (FX) and free-electron to acceptor transitions (FA) dominate at room temperature.

Transmittance measurements were used to estimate the optical bandgap energy (E_g) and it was shown that E_g of As-doped films varies from 3.312 to 3.336 eV, depending on the As concentration. It was found that the increase in Urbach energy was associated with an increase in disorder in the ZnO layers due to a rise in As content. Based on all the results, we think that the number of acceptors increases due to the increase of As concentration (Fig. 2), but also disorder in samples increases so probably also a number of donor related defects, thus confirming amphoteric character of As impurity.

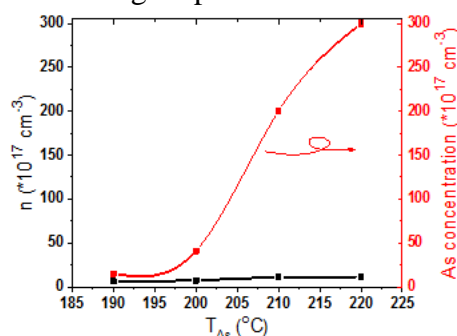


Fig. 1. Concentration of electrons and As atoms vs temperature of As cell.

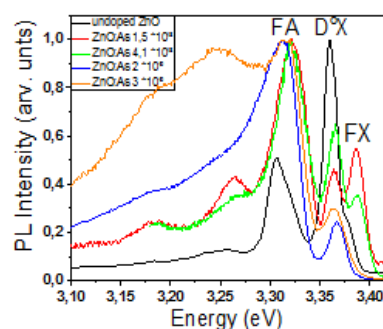


Fig. 2. PL spectra depend on the As concentration in ZnO.

This work was supported by the Polish National Science Center under Grant No. 2019/35/B/ST8/01937

[1] Przeździecka, E., et al. "Influence of As doping on the properties of nonpolar ZnO." *Thin Solid Films* 720 (2021): 138520.

CuO thin films obtained by hydrothermal method – growth technology, properties and applications

Monika Ozga, Bartłomiej Witkowski, Piotr Sybilski, Marek Godlewski

Institute of Physics Polish Academy of Sciences, al. Lotnikow 32/46, 02-668 Warsaw, Poland

Copper (II) oxide is a p – type semiconductor with a direct and narrow band gap in the range of 1.2 - 2.1 eV, which fits very well to the spectrum of solar radiation. CuO is as well characterized by high absorption. These properties make this oxide a very good material for photovoltaic applications. CuO is considered as a cheaper and less toxic alternative to other materials commonly used in thin film solar cells such as CdTe and CIGS. Most importantly, thin CuO films appear to be able to eliminate the silicon from photovoltaic structures. What is more, high absorption allows a reduction in the amount of material used compared to c-Si based photovoltaic cells.

Thin films of CuO are obtained by a modified hydrothermal method. The technology is simple, fast and environmentally safe. It does not require the use of complicated equipment or toxic precursors. It is characterized by a high growth rate (from 38 s up to 6 minutes) and a low process temperature (below 100°C). The reaction mixture consists only of deionized water and copper acetate. If the pH of the solution needs to be changed, sodium hydroxide is used as the regulator. Appropriate manipulation of the mixture and process parameters allow to control the thickness of the obtained layers in a wide range.

The modified hydrothermal technology will be presented along with the growth mechanism of CuO thin films, current results of research on electrical properties and potential application of discussed films in photovoltaic structures.

ACKNOWLEDGEMENTS

This work was partially supported by the National Centre for Research and Development TECHMATSTRATEG1/347431/14/NCBR/2018

Multifactorial investigations of the deposition process - material property relationships of ZnO:Al thin films deposited by magnetron sputtering in DC, pulsed DC and RF modes using different targets.

Aleksandra Wójcicka¹, Ildikó Cora², János Lábár², Zsolt Fogarassy², Adél Rácz²
Tatyana Kravchuk³, and Michał A. Borysiewicz¹

¹ *Lukasiewicz Research Network – Inst. of Microelectronics and Photonics, Warsaw, Poland*

² *Inst. for Techn. Physics and Mater. Science, Centre for Energy Research, Budapest, Hungary*

³ *Technion - Israel Institute of Technology, Haifa, Israel*

Transparent conductive oxides (TCOs) are a group of materials characterized by low resistivity, wide band gap and high optical transmission. They are extensively used as transparent electrodes in touch screens and displays and are developed as transparent contacts in LEDs and laser diodes. Sputter-deposited indium-tin oxide (ITO) is the TCO of choice for commercial applications. However, due to the scarcity and cost of indium, there is a strong effort to replace ITO with other ubiquitous materials, notably Al-doped zinc oxide (AZO).

The properties of the deposited films strongly depend on parameters of the deposition process, the source material (target) and the substrate. While most reports focus on only one of these aspects in a limited way, not enabling a full understanding, we decided to perform detailed investigations of all of these. Therefore, 100 nm-thick AZO films were deposited in 6N-pure Ar using different sputter modes, variable target power, and gas pressure onto various substrates, chosen depending on the properties that we explore: silicon, quartz and sapphire. For selected process parameters, we used two AZO targets differing by color (white or graphite) and density. The electrical, optical, and structural properties of the deposited films were examined by means of four-point probe, spectral transmission and ellipsometry and X-ray diffraction, respectively. High-resolution transmission electron microscopy images enabled to find microstructural differences in the films with very different electrical and structural characteristics. The surface chemistry of selected films was studied using X-ray photoemission spectroscopy and the uniformity of Al doping was investigated by means of secondary ion mass spectrometry. Furthermore, we studied the chemical composition and surface morphology of the sputtering targets used and the films deposited by means of scanning electron microscopy and energy-dispersive X-ray spectrometry.

The experimental results show that the crystalline structure improves with a decrease of the pressure. At the pressure of $0.5 \cdot 10^{-2}$ mbar we observe the highest intensity and the narrowest FWHM of (00.2) ZnO diffraction line for all powers and modes. This correlates with the lowest resistivities for the low pressure, e.g. $1.5 \cdot 10^{-3} \Omega \cdot \text{cm}$, which is almost an order of magnitude lower than for the high pressures. Not the lowest (100 W) nor the highest (250 W) powers applied do not determine the lowest resistivity, while the power of 200W was found to yield the highest quality films in a number of properties. We show that there are competing mechanisms of film growth behind such behavior. The optical transmittance drops with the increase in pressure, while the energy gap remains to be at 3.56 eV. We did not find significant differences in sputtering for different targets, as with the different power modes. One exception was a change of resistivity by a factor of 40% with changes in the pulsed DC frequency.

This work was supported by the National Centre for Research and Development, Poland, project 'OxyGaN' - M-ERA.NET2/2019/6/2020, by the Hungarian NRD Fund, grant number 2019-2.1.7-ERA-NET-2020-00002 and by the Israel Ministry of Science and Technology in the frames of the M-era.net Programme.

Luminescence Properties of ZnO:Eu³⁺ Thin Film Grown by Plasma Assisted Molecular Beam Epitaxy on a-Al₂O₃

Juby Alphonsa Mathew, Anastasiia Lysak, Jacek M. Sajkowski, Rafał Jakiela,
Yaroslav Zhydachevskyy, Marcin Stachowicz, Ewa Przeździecka, Adrian Kozanecki

Institute of Physics Polish Academy of Sciences, Aleja Lotników 32/46, 02-668 Warsaw, Poland

Zinc oxide has been considered as a promising candidate in UV optoelectronic applications for decades. Nowadays, there has been a great interest in obtaining visible luminescence of rare earth (RE) ions in ZnO since energy transfer from the ZnO host to REs ions is expected to be efficient. Trivalent Europium (Eu³⁺) has been in prime focus due to its intrinsic pure red emission via intra 4f electronic transitions.

We here report for the first time on the effective in-situ doping of Eu³⁺ ions into ZnO epitaxial layers during growth on a-plane sapphire substrate using plasma assisted Molecular Beam Epitaxy (MBE) technique by precise control of the growth parameters. The morphology of the as-grown ZnO:Eu³⁺ film was investigated using Atomic Force Microscopy (AFM) and Scanning Electron Microscopy (SEM) techniques. Secondary Ion Mass Spectrometry (SIMS) was used to probe the elemental composition and the results obtained indicated the effective incorporation of Eu³⁺ into the ZnO host crystal. We show that the layers can be uniformly doped up to the level of $2 \times 10^{20} \text{ cm}^{-3}$. Optical properties of ZnO:Eu³⁺ layer were investigated via photoluminescence (PL), photoluminescence excitation (PLE) and cathodoluminescence (CL) measurements. Luminescence characterization revealed both allowed and forbidden transitions from ⁵D₀ excited state of Eu³⁺ to the ⁷F_{J=0,1,2,3} ground states at excitation over the band gap. Multiple peaks observed in the forbidden electric dipole transition range ⁵D₀ → ⁷F_{J=0, 2} pointed out the presence of more than one optically active Eu³⁺ centers in the film. Cathodoluminescence measurements confirmed this observation. In conclusion to our work, it is evident that MBE technology is a reliable and repeatable technology for realization of red emitting sources based on ZnO:Eu.

Keywords: ZnO: Eu³⁺, PA- Molecular Beam Epitaxy, Luminescence Properties, Compositional Analysis: SIMS

Acknowledgement: This work is supported by Polish National Science Centre (NCN) under the project UMO-2019/35/B/ST8/01937

Low-temperature Cathodoluminescence of Nitrogen-doped ZnO Films Deposited at Low-temperature by Atomic Layer Deposition

Mahwish Sarwar, Bartłomiej S. Witkowski, Elżbieta Guziwicz

Institute of Physics, Polish Academy of Sciences, Al. Lotnikow 32/46, 02-668 Warsaw, Poland

In optoelectronics, the hurdle for wide application of ZnO is lack of stable *p*-type ZnO. Many research groups have reported *p*-type conductivity of ZnO by doping nitrogen as an acceptor but the results are not repeatable. According to recent reports, for the effective *p*-type doping with nitrogen, the ZnO oxygen-rich growth conditions play a vital role. Such conditions result in low formation energy of zinc vacancy defect [1], so the $V_{Zn}H$ and $V_{Zn}NOH$ complexes, that provide shallow acceptor states, can be effectively created. According to our previous findings [2, 3], within the Atomic Layer Deposition (ALD) technique, acceptor conductivity of ZnO:N can be obtained at low growth temperature that ensures oxygen-rich conditions.

In this research work, ZnO:N films were deposited at 100°C by ALD on silicon substrates and post-growth annealed at 800°C. To view the acceptor doping and its activation after annealing, low-temperature Cathodoluminescence (CL) spectra with cross-sectional SEM images were recorded at 5.34 K. CL spectra reveals donor-related emission at 3.35 eV (369.7 nm) and acceptor related emission at 3.31 eV (374.21 nm) [3]. The CL maps were analyzed in order to find out the ALD growth and post growth annealing conditions to achieve more intensive acceptor luminescence. The increased intensity of acceptor-related emissions was recorded after prolonged annealing in oxygen atmosphere, but orientation of the crystallites plays a role as well.

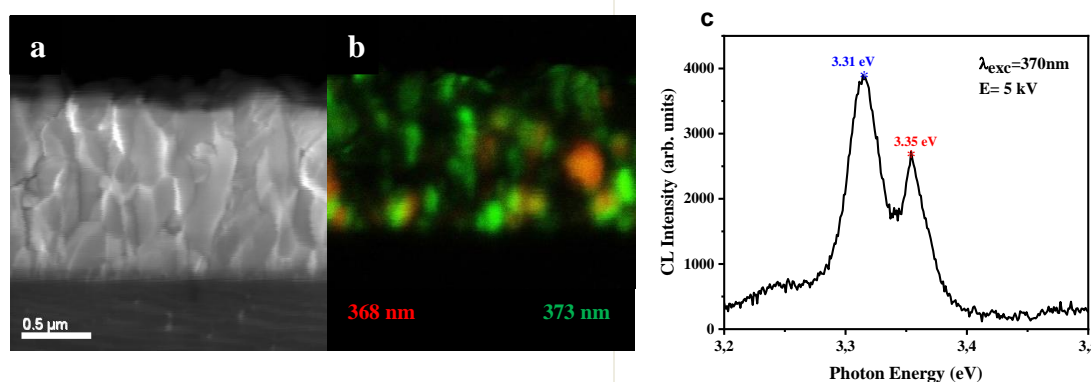


Figure. (a) Cross sectional view of annealed ZnO:N, (b) Low temperature CL maps representing emissions at different energies. (c) CL spectra of ZnO:N film.

Acknowledgement. The work was supported by the Polish research project 2018/31/B/ST3/03576 founded by the National Science Centre.

- [1] A. Janotti & C.G. Van de Walle, *Rep. Prog. Phys.* 72, 126501 (2009)
- [2] E. Guziwicz, E. Przedziecka, D. Snigurenko, D. Jarosz, B. S. Witkowski, P. Dłuzewski, and W. Paszkowicz, *ACS Appl. Mater. Interfaces*, (2017)
- [3] E. Przedziecka, E. Guziwicz, B. S. Witkowski, *Journal of Luminescence* (2018)

Schottky contacts to ALD-ZnO: transport mechanisms and effects of the H₂O₂ functionalization

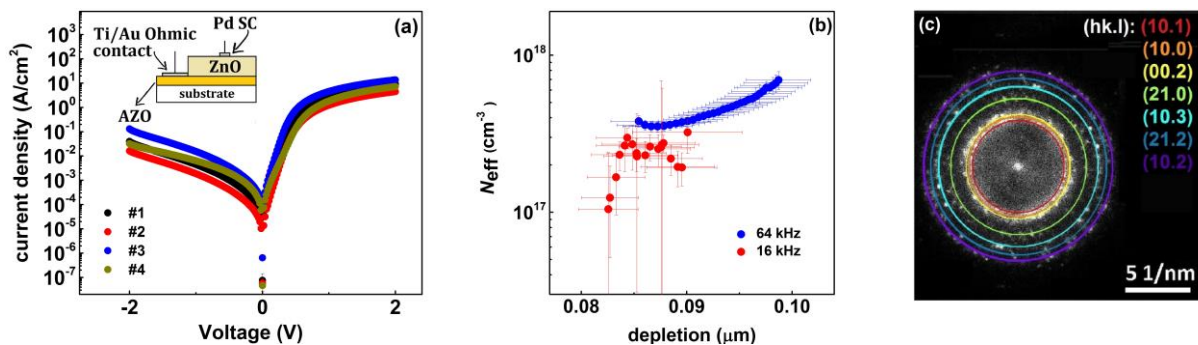
R. Schifano¹, T. A. Krajewski¹, P. Dłużewski¹, W. Zajkowska¹,
B. Kurowska¹, G. Łuka², K. Kopalko¹, E. Guzewicz¹, P. S. Smertenko³

¹Institute of Physics, PAS, Al. Lotników 32/46, 02-668 Warsaw, Poland

²Central Office of Measures, Elektoralna 2, 00-139 Warsaw, Poland

³Dept. of Optoelectronics, Institute of Semiconductor Physics, NAS of Ukraine,
Prospekt Nauki 45, 03028 Kyiv, Ukraine

ZnO, especially when deposited with low cost techniques, like Atomic Layer Deposition (ALD), is among the most promising semiconducting candidates for modern electronic/optoelectronic applications with the realization of Schottky diodes (SCs) being driven both by application as well as by material characterization purposes. Vertical structures based on Pd SCs were realized to ZnO/AZO bilayers grown by ALD using H₂O₂ functionalization [1], method previously successfully used in the case of single crystal ZnO [2]. Considering that the ALD grown ZnO films present high carrier concentrations ($<10^{18}$ cm⁻³) a preliminary annealing study on the separated ZnO and AZO layers was performed and, on this basis, the ZnO/AZO bilayers were annealed at 450 °C for 30 min to reduce the carrier concentration due possibly to a H effusion. Then, they were functionalized with a H₂O₂ dip prior to Pd deposition with the full device structure displayed in the inset of Fig.1(a). The obtained SCs exhibited a rectification ratio of $\sim 10^2$ at -2V/+2V as shown in Fig.1(a) with a detailed analysis based on the differential approach pointing to field enhanced emission from defective channels as the main leaking mechanisms. Furthermore, Capacitance vs Voltage measurements were performed and evidenced presence of a ~ 85 nm thick surface layer with reduced effective donor concentration as shown in Fig.1(b). Transmission Electron Microscopy supports this finding considering that evidence for a ~ 50 -300 nm thick oxygen rich surface layer has been found and oxygen excess defects (V_{Zn} and O_i) are acceptor like [3]. Finally, the same analysis revealed that this layer consists of ZnO crystallites with grain size ~ 10 nm embedded into an amorphous matrix as shown in Fig.1(c) as additional effect of the H₂O₂ functionalization.



This work has been performed within the Polish National Science Centre (NCN) project UMO- 2016/22/E/ST3/00553.

[1] R. Schifano et al., *Appl. Surf. Sci.* **552**, 149067 (2021).

[2] A. Janotti et al., *Phys. Rev. B* **76**, 165202 (2007).

[3] R. Schifano et al., *Appl. Phys. Lett.* **91**, 193507 (2007).

Voltage and Frequency Dependent Electrical Characteristics and Interface State Density of Ni/ZnO Schottky Diodes

Sadia Muniza Faraz^{1,*}, Zarreen Tajwar¹, Qamar ul Wahab², Volodymyr Khranovskyy², Alexander Ulyashin³, Rositsa Yakimova²

¹Department of Electronic Engineering, NED University of Engineering and Technology,
Karachi - 75270, Pakistan

²Department of Physics, Chemistry and Biology, Linköping University, 58183 Linköping, Sweden

³SINTEF Industry Forskingsveien 1, 0314 Oslo, Norway

*smuniza@neduet.edu.pk

Abstract:

Frequency and voltage dependent electrical characteristics are reported for Ni/ZnO Schottky diodes. Schottky diodes are realized from Nano-structured ZnO thin-films grown by DC-magnetron sputtering. Their electrical characterizations are performed by current-voltage (I-V), capacitance-voltage (C-V) and conductance-voltage (G-V) measurements and barrier height (ϕ_B), ideality factor (n) and doping concentration (N_D) are extracted. The diodes exhibited a typical non-linear rectifying behavior with a barrier height of 0.68 eV and ideality factor greater than unity. Charge transport mechanism and possible reasons responsible for non-idealities are investigated. The density of interface states (N_{SS}) below the conduction band are extracted from the current-voltage and capacitance-voltage measured values. The interface state density (N_{SS}) extracted as a function of $E_C - E_{SS}$ is found to be in the range $1.74 \times 10^{12} - 1.87 \times 10^{11}$ eV⁻¹ cm⁻² from $E_C - 0.51$ to $E_C - 0.64$ eV below the conduction band edge. The insight and understanding of their behavior will be helpful in the realization of more efficient devices.

Experimental studies of electron transmission through conventional superconductor/type-I Weyl semimetal junctions

G. Grabecki,¹ P. Iwanowski,^{1,2} A. Dąbrowski,¹ A. Hruban,¹ K. Dybko,^{1,2},
A. Łusakowski,¹ T. Wojtowicz,² T. Wojciechowski,^{1,2} R. Jakiela¹, and A. Wiśniewski^{1,2}

¹*Institute of Physics, Polish Academy of Sciences, Aleja Lotnikow 32/46, PL-02668 Warsaw, Poland*

²*International Research Centre MagTop, Institute of Physics, Polish Academy of Sciences, Aleja Lotnikow 32/46, PL-02668 Warsaw, Poland*

Recently, introducing superconductivity in topological materials raised a wide research interest owing to the possibility of non-zero momentum Cooper pairing, which would open possibility of formation of zero-energy modes that are equivalent to Majorana fermions [1, 2]. One of the proposals is introducing nonzero superconducting order parameter into topological materials by inducing superconductivity through the proximity effect. However, to realize this concept, high electron transmission through superconductor (S)/Weyl semimetal (WSM) junction is necessary, which is often reduced by various interface defects [3]. We have measured differential conductance across the junctions between type-I Weyl semimetal, niobium phosphide (NbP) and conventional superconductors: lead (Pb), niobium (Nb) and indium (In). Single crystals of NbP, grown by chemical vapor transport method, were carefully characterized by XRD, EDX, SEM, and ARPES techniques and by electron transport measurements [4]. (001) surface of NbP crystals were covered by 100-300 nm thick metallic layers of Pb, Nb and In. DC current-voltage characteristics and AC differential conductance across S/WSM interface as a function of the DC bias were measured. Upon cooling of the devices during which the metals become superconducting, all the junctions show conductance increase around the zero bias voltage, indicating contribution of the Andreev reflection process. In the case of Pb and Nb however, the absolute conductance values are very small indicating that the effective junction area is much smaller than that expected from the contact geometry. In contrast, in the case of In the conductance near the zero bias is very high and just reaches the values expected from the contact geometrical area. We have shown that this is possible because of In diffusion into NbP, where the metal atoms penetrate the interface barrier and thus may form very transparent S/WSM interface inside. Our observation directly demonstrates the possibility of inducing superconductivity in a type-I Weyl semimetal [4].

The research was partially supported by the Foundation for Polish Science through the IRA Programme co-financed by EU within SG OP (Grant No. MAB/2017/1)

[1]. See e.g. B. A. Bernervig and T. Hughes, *Topological Insulators and Topological Superconductors*, (Princeton University Press, Princeton, New Jersey, 2013).

[2]. See e.g. J. Alicea, Rep. Prog. Phys. **75**, 076501 (2012).

[3]. M. D. Bachmann, N. Nair, F. Flicker, R. Ilan, T. Meng, N. J. Ghimire, E. D. Bauer, F. Ronning, J. G. Analytis, and P. J. W. Moll, Sci. Adv. **3**: e1602983 (2017).

[4]. G. Grabecki, A. Dąbrowski, P. Iwanowski, A. Hruban, B. J. Kowalski, N. Olszowska, J. Kołodziej, M. Chojnacki, K. Dybko, A. Łusakowski, T. Wojtowicz, T. Wojciechowski, R. Jakiela, and A. Wiśniewski, Phys. Rev. B **101**, 085113 (2020).

One-dimensional Dirac modes of a pentagonal topological crystalline insulator nanowires

Saeed Samadi, Rafał Rechciński and Ryszard Buczko

*Institute of Physics, Polish Academy of Sciences, Aleja Lotników 32/46, 02-668
Warsaw, Poland*

We study topological properties of SnTe and (Pb,Sn)Se nanowires (NWs) grown in [011] crystallographic direction with pentagonal cross-section. We use tight binding calculations and compare the results with the properties of square NWs grown along [001].

In IV-VI topological crystalline insulators bulk crystals the band inversion appears in four nonequivalent L points in the three-dimensional Brillouin zone (BZ) [1]. In the case of square NWs grown along [001] direction, all L points are projected to one \bar{L} point of one-dimensional BZ. Therefore, we obtain many solutions in the vicinity of \bar{L} in the energy region of the bulk gap. However, it turns out that only some of these states have Dirac-like spectrum corresponding to NW hinges. They can be interpreted as manifestations of a higher order topological phase which is locally protected by $\{110\}$ crystal symmetries [2].

The NW with pentagonal symmetry is composed from five trigonal segments of uniform rock-salt lattice which host five $\{100\}$ facets and radially diverging twin boundaries which can be either cationic or anionic, as illustrated in Fig. 1(a). These NWs are periodic along [011] direction, featuring two valleys in two different projections of L points situated in $\bar{\Gamma}$ and \bar{Z} points in one-dimensional BZ. We perform band structure calculations with various thicknesses. Due to topological properties of the twin boundary, only in cationic case there exist topological states at the core with their counterpart on the surface. The localization of the core state is shown in Fig. 1(b) and (c).

In both cases we investigate the protection of topological states against symmetry breaking and hybridization with surface states. For small radius we consider hinges hybridizing with each other. Only in pentagonal wire there exist one mode at the hinges and one at the core which are protected against hybridization and crystal symmetry breaking.

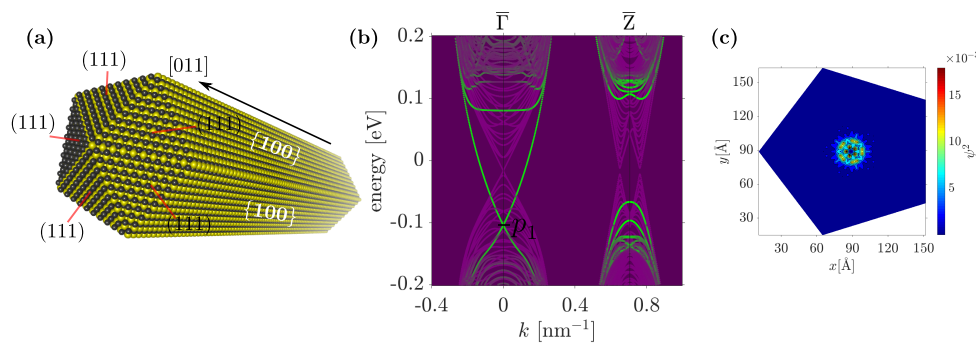


Figure 1: (a) The structure model of pentagonal NW. (b) Band structure of 14 nm thickness of SnTe NWs with cationic twin planes. (c) Squared moduli of wave functions at Dirac point denoted by p_1 .

This work was supported by the Polish National Science Centre under project No. 2016/23/B/ST3/03725. Tight-binding calculations were carried out at the Academic Computer Centre in Gdańsk.

[1] T. H. Hsieh et al., *Nat. Commun.* **3**, 982 (2012)

[2] F. Schindler et al., *Sci. Adv.* **4**, eaat0346 (2018)

Topological effects in SnTe-class multilayers and nanowires

W. Brzezicki^{1,2}, Nguyen Minh Nguyen¹, Timo Hyart¹

¹ *International Research Centre MagTop, Institute of Physics, Polish Academy of Sciences,
Aleja Lotnikow 32/46, PL-02668 Warsaw, Poland*

² *Institute of Theoretical Physics, Jagiellonian University, ulica S. Łojasiewicza 11, PL-30348
Kraków, Poland*

We investigate the topological properties of the low-energy states appearing at atomic steps [1,2] and magneto-transport across the topological transition in the multilayer Sn(Pb)Te(Se) compounds [3] as well as the (001) nanowires. We show that magnetic domain walls crossing atomic surface steps can support topological low-energy bound states that lead to similar tunneling conductance as Majorana zero-modes [2]. In this respect such steps behave similarly to the SnTe nanowires where we have also found topological end states at non-zero Zeeman magnetic field, even in the absence of superconductivity. In both cases topology is related with the non-trivial subspace degree of freedom, characteristic for the binary compounds, which can lead to in-gap end-states in one dimension [4]. For even SnTe multilayers we study quantization of the Berry phase along Fermi cross sections due to time-reversal and mirror symmetries to explain magnetoresistance in Pb(Sn)Se. We show by microscopic calculation of the Cooperon propagator that the Hikami-Larkin-Nagaoka formula can be generalized to account for mirror symmetry breaking to explain the emergent length scale present in samples covered by amorphous Se [3].

[1] W. Brzezicki, M. Wysokinski, and T. Hyart, Phys. Rev. B 100, 121107(R) (2019).

[2] G.P. Mazur, K. Dybko, A. Szczerbakow, J. Z. Domagala, A. Kazakov, M. Zgierski, E. Lusakowska, S. Kret, J. Korczak, T. Story, M. Sawicki, and T. Dietl, Phys. Rev. B 100, 041408(R) (2019).

[3] A. Kazakov, W. Brzezicki, T. Hyart, B. Turowski, J. Polaczyński, Z. Adamus, M. Aleszkiewicz, T. Wojciechowski, J.Z. Domagala, O. Caha, A. Varykhalov, G. Springholz, T. Wojtowicz, V.V. Volobuev, and T. Dietl, arXiv:2002.07622.

[4] W. Brzezicki and T. Hyart, Phys. Rev. B 101, 235113 (2020).

I acknowledge support by Narodowe Centrum Nauki (NCN, National Science Centre, Poland) Sonata Bis 9 Project No. 2019/34/E/ST3/00404.

Soft Point Contact Spectroscopy Studies of PbTe/SnTe Multi-Layered System

P. Sidorczak¹, W. Wołkanowicz², R. Minikayev², S. Kret², Z. Ogorzałek¹,
T. Wojtowicz³, D. Wasik¹, M. Gryglas-Borysiewicz¹, K. Dybko^{2,3}

¹*Faculty of Physics, University of Warsaw Pasteura 5, Warsaw, Poland*

²*Institute of Physics, Polish Academy of Sciences,
Aleja Lotnikow 32/46, Warsaw, Poland*

³*International Research Centre MagTop, Institute of Physics,
Polish Academy of Sciences, Aleja Lotnikow 32/46, Warsaw, Poland*

Topological superconductivity represented by still elusive p-wave superconductors holds great promise for quantum computation and information storage. According to theoretical predictions [1] and first experiments [2], interface of narrow-band gap semiconductors with periodic misfit dislocations is a potential candidate for such superconducting mechanism.

The investigated here multilayer PbTe/SnTe sample was grown using molecular beam epitaxy on 4 μm thick CdTe buffer on GaAs wafer. The high quality of the structure was confirmed by X-Ray diffractometry. Transmission Electron Microscopy confirmed presence of periodic network of misfit dislocation at PbTe/SnTe interfaces. Electron transport was investigated using four probe technique and soft point contact spectroscopy, at temperatures from 60 K to 1.4 K in magnetic field up to 2 T. At low temperatures substantial resistance drop was observed. Figure 1 shows measured differential conductance spectrum. The observed shapes were sensitive to temperature and magnetic field changes, disappearing at fields higher than 2 T. According to the literature [3], such spectrum indicates possibility of p-wave superconductivity. This aspect will be discussed together with estimation of supposedly found superconducting gap as a function of temperature and magnetic field.

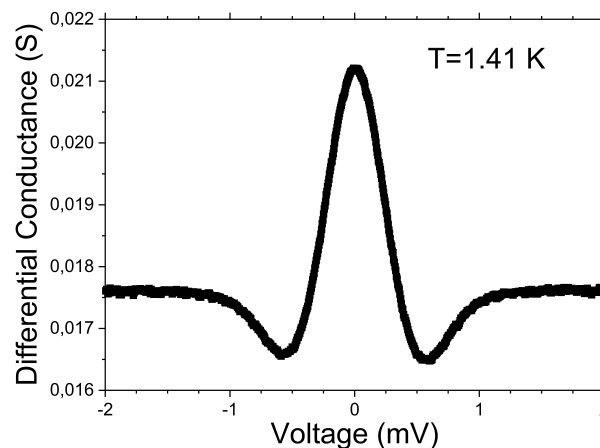


Figure 1: Differential Conductance Spectrum measured at $T = 1.41\text{ K}$ and $B = 0\text{ T}$.

The research was partially supported by the Foundation for Polish Science through the IRA Programme co-financed by EU within SG OP and the National Science Centre (Poland) through OPUS (UMO-2017/27/B/ST3/02470) project.

- [1] Evelyn Tang, Liang Fu, *Nat. Phys.*, **10** 964, (2014)
- [2] N.Ya. Fogel et al. *Phys. Rev. Lett* **86** 3, (2001).
- [3] He Wang, Lei Ma, Jian Wang *Science Bulletin* **63** 17, (2018).

Magnetotransport properties of MBE-grown NiTe₂ - a new candidate for Dirac fermion studies.

Z. Ogorzałek¹, B. Serebnyński¹, S. Kret², W. Zajkowska², R. Bożek¹, M. Tokarczyk¹, M. Baj¹, W. Pacuski¹, J. Sadowski^{1,2,3} and M. Gryglas-Borysiewicz¹

¹ Faculty of Physics, University of Warsaw, Pasteura 5, Warsaw, Poland,

² Institute of Physics, Polish Academy of Sciences, al. Lotników 32/46, Warsaw, Poland,

³ Department of Physics and Electrical Engineering, Linnaeus University, Kalmar, Sweden

The recent discovery of topological semimetals (TSMs) with linear Dirac cone-shaped band dispersion, opened a new path of research in the condensed matter physics. In some special TSMs, called type-II Dirac TSMs, the Dirac cone is strongly tilted as a result of broken Lorentz symmetry. As a consequence many peculiar physical phenomena, such as angle-dependant chiral anomaly, [1] exotic superconductivity [2] and large, non-saturating magnetoresistance [3] appear. Here we focus on the NiTe₂ which has recently been shown to be type-II Dirac TSM with Dirac node about 80 meV above Fermi level (E_F) which is much closer to E_F than in other previously reported type-II Dirac TSMs such as PtTe₂ and PdTe₂. [4] To obtain high crystalline materials, many techniques had been used [4,5,6] but molecular beam epitaxy (MBE) seems the most promising one as it enables a good control of the growth processes via in-situ monitoring with reflection high energy electron diffraction characterization system which is essential for the growth of the large-scale, homogeneous samples.

Here, we present a study on the magnetotransport properties of the first MBE-grown layers of NiTe₂ [7] grown on 2-inch semi-insulating GaAs (111)B. The NiTe₂ layers were grown at three different temperatures to optimize the sample quality. The Hall effect measurements, performed in a cryostat with magnetic field up to 12 T and in temperature range from 300 K to 1.4 K and helium gas atmosphere, revealed that the samples are metallic with n-type carrier concentrations. Although the resistivity values are in a good agreement with the values for the layers grown by other techniques, [4,5,6] the residual resistivities stay much higher. The possible explanation will be proposed. A transmission electron microscopy studies proved epitaxial relation between layer and substrate ($[-1-120]$ NiTe₂ \parallel $[-110]$ GaAs) and high quality of the films but at high growth temperature the length of the unperturbed layer decreases to 50 nm. By analyzing the magnetoresistance and conductivity tensor, we have found that the proposed control of the growth conditions permits to improve the quality of the layers and to vary the Hall concentration by two orders of magnitude, paving the way to control the position of the E_F which is crucial for Dirac fermion studies.

[1] Lv Y. Y. et al., *Phys. Rev. Lett.* **118**, 096603 (2017)

[2] Alidoust, M. et al., *Phys. Rev. B: Condens. Matter Mater. Phys.* **95**, 155124 (2017)

[3] Xiong Ali, M. et al. *Nature* **514** 205–208 (2014).

[4] Chunqiang Xu et al., *Chem. Mater.* **30**, 4823–4830 (2018)

[5] Qianqian Liu et al., *Phys. Rev. B* **99**, 155119 (2019)

[6] Wenkai Zheng et al., *Phys. Rev. B* **102**, 125103 (2020)

[7] Serebnyński B. et al, (2021), *in preparation*

Electronic structure of $\text{Sn}_{1-x}\text{Mn}_x\text{Te}$ thin films studied by ARPES

M. Zięba¹, B. Turowski², V.V. Volobuev², B.J. Kowalski¹, N. Olszowska³, M. Rosmus³,
J. Kołodziej³, A. Kazakov², T. Wojciechowski^{1,2}, M. Aleszkiewicz¹, K. Gas¹, M. Sawicki¹,
A. Łusakowski¹, T. Wojtowicz², T. Story^{1,2}

¹*Institute of Physics, Polish Academy of Sciences, al. Lotników 32/46, 02-668 Warsaw, Poland*

²*International Research Centre MagTop, Institute of Physics, Polish Academy of Sciences, al. Lotników 32/46, 02-668 Warsaw, Poland*

³*Solaris National Synchrotron Radiation Centre, ul. Czerwone Maki 98, 30-392 Kraków, Poland*

$\text{Sn}_{1-x}\text{Mn}_x\text{Te}$ is a IV-VI semimagnetic (diluted magnetic) semiconductor with the direct electron band gap located near L-points in the Brillouin zone (BZ). The inverted ordering of the L_6 band of light holes and the L_{6+} conduction band, observed in SnTe and expected in $\text{Sn}_{1-x}\text{Mn}_x\text{Te}$, results in the transition to topological crystalline insulator state. In the electronic structure of this material the second valence band of heavy holes, located along Σ high symmetry line and characterized by large density of states, is crucial for carrier-induced ferromagnetic properties and excellent thermoelectric parameters of $\text{Sn}_{1-x}\text{Mn}_x\text{Te}$. The aim of this study is to use angle-resolved photoemission spectroscopy (ARPES) technique to directly study the electron energy dispersion in the valence band and test the proposed models of temperature and composition evolution of electronic band structure of $\text{Sn}_{1-x}\text{Mn}_x\text{Te}$.

To facilitate the atomically clean surface needed for successful ARPES experiments we used MBE system to epitaxially grow on (111) BaF_2 substrates one micron thick monocrystalline layers of $\text{Sn}_{1-x}\text{Mn}_x\text{Te}$ with nominal Mn content $x = 0, 0.015$, and 0.05 . Using an UHV suitcase we transferred the layers from our MBE growth chamber to Solaris synchrotron facility. The layers were examined by XRD, SEM/EDX, AFM, Hall effect, conductivity, and magnetization measurements confirming p-type conduction and ferromagnetic transition at $T_C \approx 8$ K (for layer with $x = 0.05$).

We carried out ARPES measurements of the (111) surface of $\text{Sn}_{1-x}\text{Mn}_x\text{Te}$ exploring theoretically indicated regions of the bulk and surface BZ. In photon energy dependent (18-130 eV) ARPES spectra taken along the $\bar{M}-\bar{\Gamma}-\bar{M}$ direction we observed projections of Dirac cones at $\bar{\Gamma}$ and \bar{M} points of the surface BZ with different Fermi velocities. Characteristic pockets observed in the bulk Γ -K direction can be tentatively assigned to Σ band. The comparison of Fermi surface maps for varying Mn content showed important evolution of the electronic structure but without qualitative change of the bands ordering. No important changes of the band structure were observed in the low temperature region studied ($T = 8$ -270 K). The experimentally observed electron dispersion is analyzed with the help of DFT calculations of electronic structure of $\text{Sn}_{30}\text{Mn}_2\text{Te}_{32}$ rock-salt slabs.

This research was partially supported by the Foundation for Polish Science through the IRA Programme co-financed by EU within SG OP (grant No. MAB/2017/1) and by the National Science Centre, Poland Grant: UMO 2017/27/B/ST3/02470.

Corner states, hinge states and Majorana modes in SnTe nanowires

Nguyen Minh Nguyen¹, Wojciech Brzezicki¹, and Timo Hyart^{1,2}

¹*International Research Centre MagTop, Institute of Physics, Polish Academy of Sciences, Aleja Lotnikow 32/46, PL-02668 Warsaw, Poland*

²*Department of Applied Physics, Aalto University, 00076 Aalto, Espoo, Finland*

SnTe materials are one of the most flexible material platforms for exploring the interplay of topology and different types of symmetry breaking. We study symmetry-protected topological states in SnTe nanowires in the presence of various combinations of Zeeman field, s -wave superconductivity and inversion-symmetry-breaking field. We uncover the origin of robust corner states and hinge states in the normal state. In the presence of superconductivity, we find inversion-symmetry-protected gapless bulk Majorana modes, which give rise to quantized thermal conductance in ballistic wires. By introducing an inversion-symmetry-breaking field, the bulk Majorana modes become gapped and topologically protected localized Majorana zero modes appear at the ends of the wire.

.

Temperature effect on the location of the resonant $\text{Cr}^{2+/3+}$ level in PbTe:Cr

A. Królicka¹, K. Gas¹, M. Sawicki¹, J. Korczak^{1,2}, R. Minikayev¹, A. Reszka¹,
A. Kwiatkowski³, M. Gryglas-Borysiewicz³, T. Story^{1,2}, K. Dybko^{1,2}

¹*Institute of Physics, Polish Academy of Sciences, Aleja Lotnikow 32/46, PL-02668 Warsaw, Poland.*

²*International Research Centre MagTop, Institute of Physics, Polish Academy of Sciences, Aleja Lotnikow 32/46, PL-02668 Warsaw, Poland.*

³*Faculty of Physics, University of Warsaw, Pasteura 5, Warsaw, Poland.*

Chromium is a resonant donor impurity in PbTe with a $\text{Cr}^{2+/3+}$ mixed valence energy state, located about 100 meV above the conduction band minimum (at $T=4$ K) [1]. It also pins the Fermi level position when the electron concentration reaches $1.2\text{-}1.4 \times 10^{19} \text{ cm}^{-3}$. This behavior results from the process of self-ionization of Cr^{2+} ions, generating conduction electrons ($\text{Cr}^{2+} \rightarrow \text{Cr}^{3+} + e$). The problem of resonant states has been studied, e.g. in HgSe:Fe [2], PbTe:In [3], PbTe:Tl [3, 4], PbTe:Cr [5], PbTe:Cr,I [6]. These effects combined with fixing the Fermi level in the region of enhanced density of states (DOS) may result in increasing the Seebeck coefficient, and hence the thermoelectric figure of merit. In order to obtain such enhancement, significant parameters of the band structure, e.g. the width of the resonant level, change of its energetic position with temperature, and its starting location at low temperatures need to be established. Despite such general studies exist [7], a more detailed band structure analysis, related to the shape and location of the $\text{Cr}^{2+/3+}$ state, is crucial for obtaining an enhancement of the Seebeck coefficient in the controlled manner.

To this end, the temperature dependences of the carrier concentration of PbTe:Cr with various Cr contents are studied in the wide temperature range (4-300 K). The results are analyzed, using the model, where the corresponding neutrality equation is solved with the density of states of Cr represented by the Gauss and Lorentz functions, centered in the conduction band. The aim of the procedure was to obtain the same set of parameters for all measured samples. Magnetic measurements confirmed the coexistence of Cr^{3+} as well as Cr^{2+} ions. The certain amount of nanocrystalline Cr_2Te_3 and Cr_5Te_8 inclusions has been also identified [8]. The latter has been confirmed by EDX and XRD.

This study has been supported by the National Science Centre for Development (Poland) through grant TERMOD No TECHMATSTRATEG2/408569/5/NCBR/2019 and by the National Science Centre (Poland) through OPUS (UMO - 2017/27/B/ST3/02470) project and by the Foundation of Polish Science through the IRA Programme co-financed by EU within SG OP.

- [1] T. Story et al., *Acta Physica Polonica A* **87**, 229-232 (1995),
- [2] A. Lenard et al., *Journal of Low Temperature Physics* **80**, 15-29 (1990),
- [3] V.I Kaidanov et al., *Fizika i Tekhnika Poluprovodnikov* **26**, 201-222 (1992),
- [4] J.P. Heremans et al., *Science* **321**, 554-557 (2008),
- [5] B. Paul et al., *Journal of Applied Physics* **109**, 103710 (2011),
- [6] B. Paul et al., *Applied Physics Letters* **98**, 262101 (2011),
- [7] V.D. Vulchev et al., *Physica Status Solidi* **99**, 53-56 (1987),
- [8] K. Gas et al., *Journal of Magnetism and Magnetic Materials*, accepted (2021), arXiv:2101.05705.

Growth and optical properties of type II ZnTe/ZnSe core/shell nanowire quantum dots

P. Baranowski¹, P. Wojnar¹, M. Szymura¹, R. Georgiev¹, S. Chusnutdinow¹,
G. Karczewski¹, and T. Wojtowicz²

¹ Institute of Physics, Polish Academy of Sciences, 02-668 Warsaw, Poland

² International Research Centre MagTop, Institute of Physics, Polish Academy of Sciences, 02-668 Warsaw, Poland

A recent observation of excitonic Aharonov-Bohm effect in core/shell nanowires has opened an exciting opportunity to study coherently rotating states in these structures [1], which could be, subsequently, applied in the field of quantum information storage. An important task for the observation of these states is the separation of electron-hole wavefunctions within a nanowire. In ref [1], it has been achieved on GaAs crystal phase quantum dots, which are characterized by a type II band alignment.

In this work, an alternative approach for fabrication of quantum dots with type II band alignment inside a nanowire built of II-VI semiconductors is presented. A scheme of the investigated structure is shown in Figure 1. The nanowire heterostructures are grown by molecular beam epitaxy by applying the vapor-liquid-solid growth mechanism assisted with gold catalysts. In the first step, ZnTe short axial insertion inside (Zn,Mg)Te nanowire is fabricated by turning off Mg-flux for a few seconds during the (Zn,Mg)Te nanowire growth. Since ZnTe has a smaller bandgap than (Zn,Mg)Te, a sufficiently short insertion can be considered as a quantum dot inside a nanowire. Subsequently, a few monolayers thick ZnSe shell is deposited around the entire nanowire. ZnTe/ZnSe heterostructure is well-known for the type II character, where electrons tend to localize in ZnSe and holes in ZnTe region. In the last step, the nanowires are coated in a (Zn,Mg)Te passivation shell with the thickness of about 20 nm in order to reduce the impact of surface states on the optical emission.

Optimization procedure of the above mentioned structure has been performed. In particular, the several parameters, such as: the length of ZnTe axial insertion, the thickness of the ZnSe shell and Mg concentration inside (Zn,Mg)Te are adjusted. Our goal has been to observe an optical emission from ZnTe/ZnSe nanowire quantum dot. In the case of a ZnTe/ZnMgTe reference structure without ZnSe shell, one observes clearly two distinct optical emission lines coming either from the nanowire (Zn,Mg)Te cores or from the ZnTe quantum dot. The addition of only one monolayer thick ZnSe shell significantly changes the optical emission spectrum. The emission energy of the quantum dot emission shifts significantly from 2.38 eV to 2.00 eV. Simultaneously, its intensity drops by about two orders of magnitude and the decays times increase by the factor of about 10. These observations are consistent with the type I to type II band alignment transition resulting from the presence of ZnSe shell. In μ -photoluminescence the broad emission at 2.00 eV splits into several relatively lines coming from individual nanowire quantum dots. This association is confirmed by the appearance of multiexcitonic emission lines when increasing the excitation power.

[1] Corfdir P, *et al.* *Adv. Mater.* **31** 1805645 (2019)

This work has been partially supported by the National Centre of Science (Poland) through grant 2017/26/E/ST3/00253, and by the Foundation for Polish Science through the IRA Programme co-financed by EU within SGO

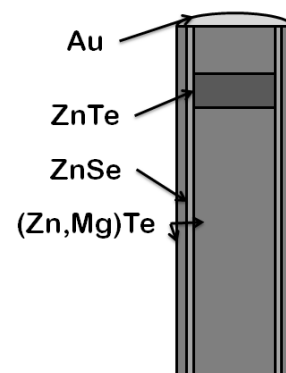


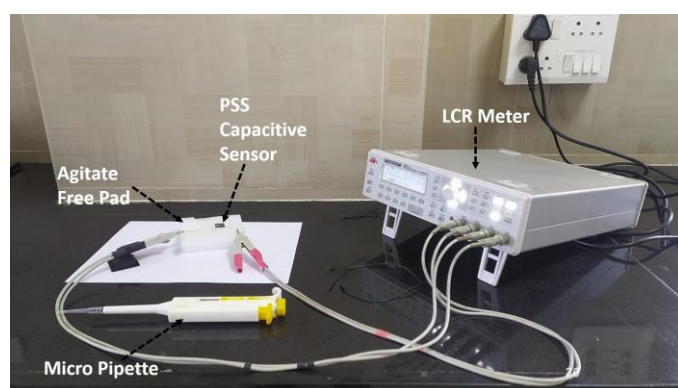
Figure 1. Scheme of the investigated nanowire heterostructure.

Macro Porous Structure Silicon Capacitive Sensor for Aqueous Methyl Alcohol

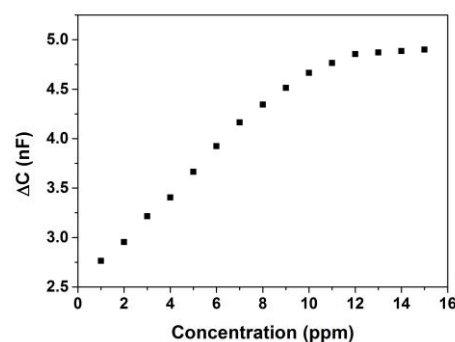
S. M. Gheewala¹, P. N. Patel¹ and R. Dhavse¹

¹ Electronics Engineering Department, Sardar Vallabhbhai National Institute of Technology, Surat-395007, India.

A very low-cost capacitive sensor device based on macro Porous Structure Silicon has been used to detect and quantifying the presence of aqueous methyl alcohol solution. The Porous Structure Silicon was fabricated by a Laser etching process using commercial Pulse Fiber Laser. A device has a large number of pores to sensing the aqueous methyl alcohol solution is filtered into the pore. The experimental result shows the possible changes in the dielectric constant of the Porous Structure Silicon capacitive device.



(a)



(b)

Fig. (a) Experimental Setup, (b) Capacitance measured for Different concentration of Methyl Alcohol.

- [1]S. M. Gheewala, P. Chinthakunta, P. N. Patel, and R. Dhavse, J. of Solid State Technology 64 (2), 4725-4739 (2021).
- [2]S. M. Gheewala, CCIS springer 1214, 68-79 (2020).
- [3]E. Kayahan, Acta Physica. polonica A 127 (4), 1397-1399 (2015).
- [4]E. Kayahan, Z. B. Bahsi, A.y. Oral, and M. Sezer, Acta Physica. polonica A 127 (4), 1400-1402 (2015).
- [5]O. Yilmaz, E. Kayahan, F. Goren, and F. Dumludag, Acta Physica. polonica A 125 (2), 288-289 (2013).
- [6]M. E. Azim-Araghi, S. Ashrafabadi, and F. Kanjuri, Acta Physica. polonica A 122 (1), 170-173 (2012).
- [7]P. N. Patel, V. Mishra, A. K. Panchal, and N. H. Maniya, Sensors & Transducers Journal, 139 (4), 79-86, (2012).
- [8]P. N. Patel, V. Mishra, and A. K. Panchal, Digest J.Nanomaterials and Biostructures, 7(3), 973 – 982, (2012).

MBE Growth of HgTe-based Structures on (001)-CdTe/GaAs Hybrid Substrates and their Transport Studies

Zhifeng Yu¹, Jakub Grendysa², Rafał Rudniewski¹, Jakub Polaczyński¹, Valentine V. Volobuev¹, Aleksandr Kazakov¹, Dawid Jarosz², Wojciech Zaleszczyk¹, Tomasz Wojciechowski¹, Marta Aleszkiewicz³, Tomasz Wojtowicz¹, and Michał Marchewka²

¹ International Research Centre MagTop, Institute of Physics, Polish Academy of Sciences, Aleja Lotników 32/46, PL-02668 Warsaw, Poland

² Center for Microelectronics and Nanotechnology Research, University of Rzeszów, Pionia 1, 35-310 Rzeszów, Poland

³ Institute of Physics, Polish Academy of Sciences, Aleja Lotników 32/46, PL-02668 Warsaw, Poland

In addition to wide applications in the field of infrared detectors, HgTe-based structures have aroused great interest in the last decade since the experimental realization of the quantum spin Hall (QSH) effect [1]. In the family of topological insulators, HgTe is well-known for its high mobility [2] and band structure that is tunable from trivial to non-trivial regime by adjusting the thickness [1] or applying strain [2]. At the same time, the growth of HgTe by molecular beam epitaxy (MBE) is very demanding because of the very narrow temperature window that gives high quality structures.

In the present work, the un-doped quantum wells and thick, 3D-like layers of HgTe were grown by MBE on insulating (001)-CdTe/GaAs hybrid substrates. X-Ray diffraction (XRD), scanning electron microscopy (SEM) and atomic force microscopy (AFM) indicated high quality of the substrates that were produced for this purpose. The growth of HgTe was performed in another MBE system, which required hybrid substrate etching and “refreshing” before the actual growth of HgTe-based structures. The growth was monitored by reflection high-energy electron diffraction (RHEED), and the reconstruction change in [100] azimuth occurring with the temperature variation was used to determine the proper growth temperature. According to the results from XRD, SEM and Nomarski optical microscopy, the crystalline quality, interface and surface morphology of the grown structures are reasonable. Preliminary magneto-transport studies have been performed at 4.2 K and in magnetic fields up to 8 T, as shown in Fig. 1. Pronounced Shubnikov-De Haas (SdH) oscillations were observed, which

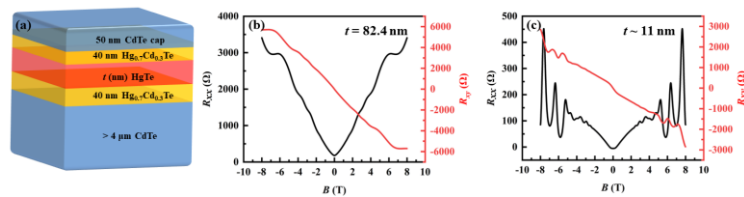


Fig. 1. (a) Scheme of HgTe-based structure. Magneto-transport behavior of (b) 3D HgTe layer and (c) HgTe quantum well with thickness of ~11 nm.

start from ~2.5 T. Hall plateaus were also observed in the 80-nm thick HgTe layer indicating the contribution from two-dimensional conducting channel.

Our preliminary results provide us with a solid basis for further investigation of magnetic doping of HgTe-based structures.

The work is partially supported by the Foundation for Polish Science through the IRA Programme co-financed by EU within SG OP (Grant No. MAB/2017/1).

[1] M. König, *et al.*, *Science*. **318**, 5851 (2007).

[2] C. Brüne, *et al.*, *Phys. Rev. Lett.* **106**, 12 (2011).

Charged exciton dissociation energy in (Cd,Mn)Te quantum wells with variable disorder and carrier density

A. Lopion, A. Bogucki, K. E. Połczyńska, W. Pacuski, T. Kazimierczuk,
P. Kossacki and A. Golnik

*Faculty of Physics, Institute of Experimental Physics, University of Warsaw, ul.
Pasteura 5, 02-093 Warszawa, Poland*

The (Cd,Mn)Te/(Cd,Mg)Te quantum wells are typically p-type even without intentional doping. The hole gas originates from the background doping of the (Cd,Mg)Te barrier material and/or from the surface states [1]. On top of that, both invoked mechanisms lead to formation of the Coulomb fluctuations, which affects the confined quantum well states. This Coulomb disorder can be reshaped using above-barrier illumination, which we exploit in the present work.

We report on magneto-photoluminescence of (Cd,Mn)Te/(Cd,Mg)Te quantum wells excited by photons with varied energy. By controlling the laser illumination we modify both the carrier density [2] and Coulomb disorder. Three different regimes are analyzed: low hole density with low disorder, low hole density with significant disorder, and high hole density regime. The use of diluted magnetic semiconductor as a quantum well material allows us to induce spin singlet-triplet transition of charged exciton by magnetic field [3]. This transition is used as a tool to determine charged exciton dissociation energy. Surprisingly, we find that the positively charged exciton dissociation energy defined as an energy necessary to unbind additional hole by flipping its spin is constant for broad range of parameters such as carrier density and Coulomb fluctuations despite large impact of those parameters on the observed distance between X and X⁺ lines in the PL spectra.

- [1] W. Maślana, et al., *Appl. Phys. Lett.* **82**, 1875 (2003).
- [2] P. Kossacki, et al., *Phys. Rev. B* **60**, 16018 (1999).
- [3] P. Kossacki, et al., *Phys. Rev. B* **70**, 195337 (2004).

Raman magnetospectroscopy of CrPS₄Tomasz Fał¹, Adam K. Budniak², Yaron Amouyal²,
Efrat Lifshitz², Jan Suffczyński¹¹*Faculty of Physics, University of Warsaw, Pasteura 5, Warsaw, 02-093, Poland*²*Technion - Israel Institute of Technology, Haifa, 3200003, Israel*

Two-dimensional (2D) lamellar materials such as graphene or transition metal chalcogenides play currently a role of benchmark materials for various electrical and electro-optical applications. However, they lack magnetism. In contrast, ternary transition metal phosphorus chalcogenides emerged recently as ultimate 2D magnets, and offered a plethora of new physical phenomena. CrPS₄ is a prominent representative of a magnetic lamellar material, highly attractive for optoelectronic and spintronic applications. It is a van der Waals semiconductor, which in its bulk form undergoes a transition at 38 K between anti-ferromagnetic and paramagnetic phase. [2] Despite an increasing number of studies on CrPS₄, its magneto-optical properties have not been established so far.

We present a Raman spectroscopy study of bulk CrPS₄ samples synthesized by vapor transport method [1]. The measurements are performed at a temperature from 5 K to 250 K and in the magnetic field of up to 6 T applied in Faraday or Voigt configuration, with polarization resolved excitation and detection.

A Raman spectrum of bulk CrPS₄ excited at 514.5 nm is shown in Fig. 1a. Two subsets of lines representing two groups of vibrational modes are distinguished. The directions of their linear polarizations are perpendicular to each other (denoted as H and V), even under circularly polarized excitation. We observe that the intensity of certain Raman lines depends on the magnetic field and temperature in a non-trivial relationship. Fig. 1b depicts the degree of change of intensity in the magnetic field of the exemplary line at 215.26 cm⁻¹, which is found to follow the magnetic susceptibility curve of CrPS₄. [3] Qualitatively the same conduct, with the maximum of the dependence at the critical temperature of 38 K is found for several lines also at Voigt configuration.

In a view of our results the Raman magnetospectroscopy provides an efficient mean for studies magnetic phase transitions in layered antiferromagnetic semiconductors.

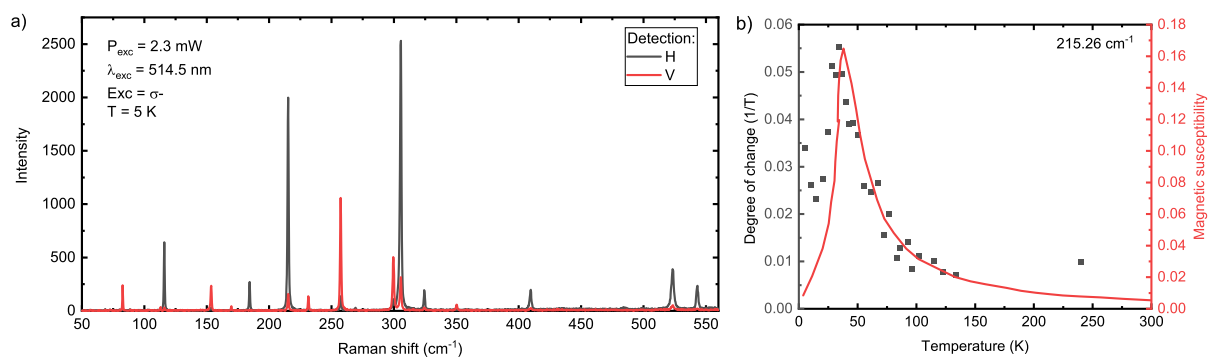


Figure 1: a) Polarized Raman spectrum of bulk CrPS₄ at B = 0 T. Spectral width of the narrowest line is 0.6 cm⁻¹. b) Degree of change of intensity of the line at 215.26 cm⁻¹ with the magnetic field was found to follow the magnetic susceptibility curve.

[1] A. K. Budniak et al. *Small*, 16(1):1905924, 2020.

[2] R. Diehl et al. *Acta Crystallographica Section B*, 33(5):1399–1404, 1977.

[3] Q. L. Pei et al. *Journal of Applied Physics*, 119(4):043902, 2016.

Pressure driven phase transitions in bulk HfS₂

M. Grzeszczyk¹, J. Gawraczyński², T. Woźniak³, J. Ibáñez-Insa⁴
M. R. Molas¹, A. Babiński¹

¹*Faculty of Physics, University of Warsaw, Warsaw, Poland*

²*Centre of New Technologies, University of Warsaw, Warsaw, Poland*

³*Department of Semiconductor Materials Engineering, Wrocław University of Science and Technology, Wrocław, Poland*

⁴*Geosciences Barcelona (GEO3BCN), CSIC, 08028 Barcelona, Spain*

About 60 transition metal dichalcogenides (TMDs) are currently recognized, but among them, Mo- and W-based compounds have attracted the most attention, while other TMDs are only just being explored. Group IVB, Hf- and Zr- based TMDs are theoretically predicted to have higher mobility and higher sheet current density. The literature however lacks a systematic study of their fundamental properties. Our study aims to provide more knowledge on structural properties of bulk HfS₂. We employ Raman scattering spectroscopy to follow the structure as a function of hydrostatic pressure.

There are four Raman modes observed around 140, 270, 330, and 340 cm⁻¹ in the scattering spectrum of bulk HfS₂ at ambient pressure. Three highest-energy phonons can be assigned to E_g, A_{2u}(LO), and A_{1g} modes, respectively. The lowest energy feature can be attributed to the second-order feature, observed due to symmetry breaking of the selection rules through disorder or the participation of strongly localized electronic states.[1] Selected Raman scattering spectra recorded at series of pressures up to 27 GPa are shown in Figure. Following the evolution of the Raman spectra, we can identify two phase transitions. The transition above 9 GPa is characterized i.e. by the appearance of new low-energy modes emerge. Simultaneously the features previously assigned as A_{2u}(LO) and A_{1g}, exhibit intensity ratio inversion. At the pressure above 18 GPa yet another phase transition takes place. All previously seen peaks disappear from the spectrum, while other, very broad structures appear. During decompression, the modes redshift with decreasing pressure, however overall the spectra remain unchanged. We conclude that the material enters an amorphous phase above 18 GPa, and that transformation is irreversible. The origin and characteristics of each phase transition will be further discussed.

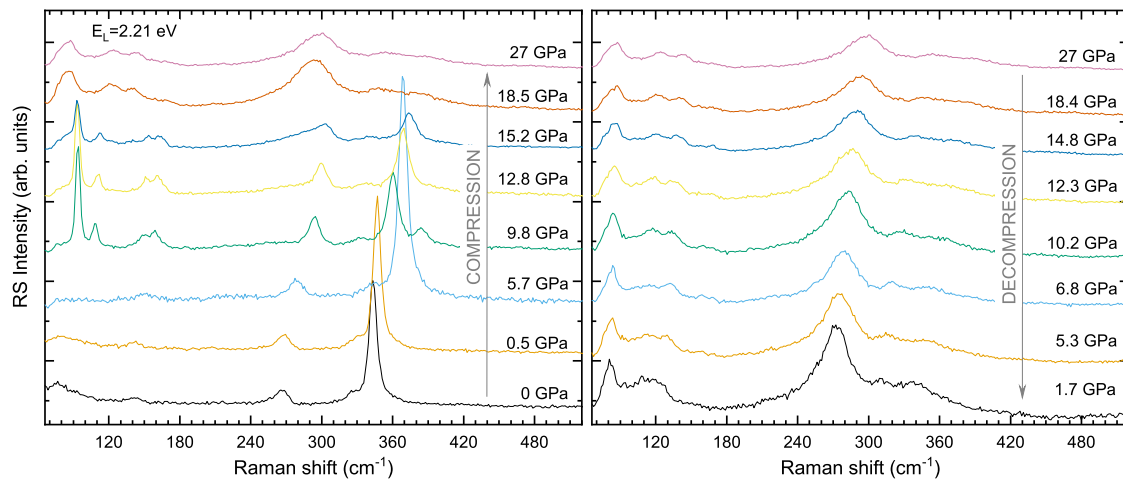


Figure 1: Raman scattering spectra of bulk HfS₂ as a function of hydrostatic pressure up to 27 GPa, collected during compression/decompression.

[1] J. Ibáñez et al., *Scientific Reports* **8**, 12757 (2018)

Open circuit voltage spectra influenced by extended and local defects

B.A. Orlowski¹, K. Gwozdz², K. Goscinski¹, S. Chusnutdinow¹, M. Galicka¹, E. Guzewicz¹, B.J. Kowalski¹

¹*Institute of Physics, Polish Academy of Sciences, Al. Lotnikow 32/46, Warsaw, Poland*

²*Wroclaw University of Science and Technology, Wybrzeże Wyspińskiego 27, 50-370 Wroclaw, Poland*

The paper concerns the influence of extended and local defects states on open circuit voltage (V_{oc}) spectra of semiconductors photo junctions. The measured illumination intensity spectra are compared with analogical spectra described by the proposed theoretical model [1].

The photo junction can consist of two semiconductors with different p and n type of conductivity and different crystalline and electronic band structures. The amount of electrons and holes photo-generated on each side of a junction is exactly the same, which results in a remarkably higher relative increase of minority carrier densities than for majority carrier densities on each side of a junction. It leads to the dominations of shifts of quasi Fermi level energy values of electrons and holes as compared to the common thermal equilibrium Fermi level, up for minority electrons (p -type side) and down for minority holes (n -type side). In this case, the difference of the electrons quasi Fermi level shifts on the both sides of a junction corresponds to the electric potential contribution of electrons to the V_{oc} value. Analogical contribution to the V_{oc} gives the difference of the holes quasi Fermi level shifts difference present on the sides of a junction. The total sum of the quasi Fermi level energy shifts on the both sides of a photo junction for the electrons and for the holes contributes to the open circuit voltage V_{oc} . The extended and local defects can damp the value of dominating minority quasi Fermi level shifts in the spectra and it lowers the change of the measured V_{oc} value in comparison to the predicted by the model for the case without the defects. Similarity and differences of the spectra measured and predicted illustrate the role of defects.

In the experiment, the number of laser photons bunches illuminating the sample was changed by the shutter opening time and the V_{oc} value was measured correspondingly. As a result, the intensity of illumination spectra of the V_{oc} was obtained. Thank to this, the effect of the V_{oc} value damping steps was observed for particular illumination intensity regions. In comparison to the predicted spectra, the related experimental spectra are disturbed by experimental conditions, sample treatment and steps caused by defects located at the V_{oc} distance relatively to the thermal equilibrium Fermi level.

The damping defects were studied in the region of 120 meV from the thermal equilibrium Fermi level for the Si p/n homojunction and the ZnTe/CdTe photo junction [1]. The spectra indicate correlation with the local defects for the Si p/n junction [2] and with the extended defects [2, 3] for the ZnTe/CdTe.

1. B.A. Orlowski, K. Gwozdz, M. Galicka, S. Chusnutdinow, E. Placzek-Popko, M.A. Pietrzyk, E. Guzewicz, B.J. Kowalski, *Acta Phys. Pol. A*, **134**, 590-595 (2018)
2. E. Zielony, K. Olender, E. Placzek-Popko, T. Wosiński, A. Racino, Z. Gumienny, G. Karczewski, S. Chusnutdinow, *J. Appl. Phys.* **115**, 244501 (2014)
3. K. Wichrowska, T. Wosinski, Z. Tkaczyk, V. Kolkowsky, G. Karczewski, *J. Appl. Phys.* **123**, 161522 (2018)

Influence of dimensionality on electrical properties of TiO₂ thin films

K. Kulinowski¹, M. Radecka², and B. J. Spisak¹

¹*Faculty of Physics and Applied Computer Science,*

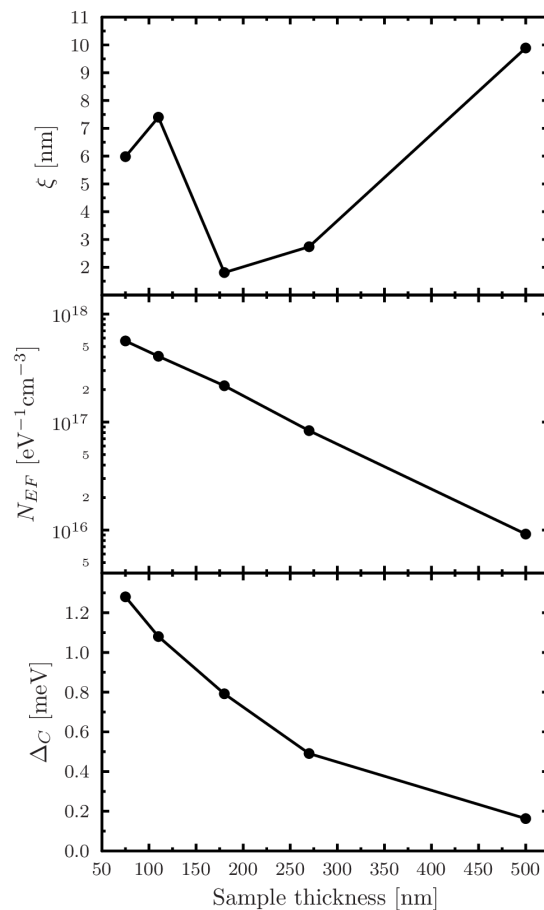
²*Faculty of Materials Science and Ceramics,*

AGH University of Science and Technology, Al. A. Mickiewicza 30, 30-059 Kraków, Poland

Titanium dioxide belongs to wide band gap transition-metal oxides, with the band gap changing between 3.0 eV and 3.2 eV for the rutile and anatase, respectively [1]. The conduction band of TiO₂ is predominantly composed from Ti 3d states which leads to profound consequences for the electron effective mass and related mobility of the carriers are concerned.

In this work, we have studied TiO₂ thin films deposited by UHV sputtering with the ultimate aim of determining a crossover from Efros-Shklovskii variable range hopping (ES VRH) to Mott VRH and influence of dimensionality of VRH on electrical properties [2, 3]. For this purpose, resistance measurements as the function of temperature were carried out. Furthermore, the resistance of the samples was determined as an inverse of a slope of I-V characteristics for temperatures ranging from 20 K to 300 K.

For studied 2D and 3D samples, the VRH regimes were considered. A crossover was evaluated between samples with a thickness of 110 nm and 270 nm. For each film a crossover from ES VRH to Mott VRH (2D and 3D) was calculated at a temperature changing between 85 K and 105 K. With these analyses, various electrical parameters of TiO₂ thin films such a localization length ξ or density of states on Fermi level N_{EF} and Coulomb gap energy Δ_C was determined.



Localization length ξ , density of states on Fermi level N_{EF} and Coulomb gap energy Δ_C vs. sample thickness.

K.K. is supported by the EU Project POWR.03.02.00-00-I004/16. M.R., and B.S. are supported by Polish Minister of Science and Higher Education within the framework of subvention for science in 2021.

[1] R. G. Breckenridge and W. R. Hosler, Phys. Rev. **91**, 793 (1953)

[2] A. Yildiz, S. Lisesivdin, M. Kasap, and D. Mardare, J. Non-Cryst. Solids, **354**, 45 (2008).

[3] A. Yildiz, N. Serin, T. Serin, and M. Kasap, Jpn. J. Appl. Phys., **48**, 11 (2009).

Two examples of Mn-based antiferromagnetic semiconductors

Karel Výborný

*Institute of Physics, Academy of Sciences of the Czech Rep.,
Cukrovanická 10, Praha 6, CZ-16253*

Research into solid state physics draws a substantial part of its motivation from the prospect of new electronic concepts and development of corresponding devices. A good example of this are novel memory elements. In this talk, I will discuss the "material basis" for such research forming a part of the field called nowadays antiferromagnetic (AFM) spintronics [1]. Two semiconducting materials containing manganese – a popular choice for element endowed with magnetic moment – will be in my focus: MnTe which has been studied extensively since 1970's and NaMnAs which is only little explored as of now. Both experimental characteristics [2] and theoretical approaches [3] pertaining to those two systems will be discussed. Particular attention will be given to the anisotropic magnetoresistance (AMR). This is an effect present not only in ferromagnets but also in AFMs and it can be used to "read out" the magnetic state of an AFM, the last step in the work cycle of a memory element. Phenomenology of the AMR will be discussed and avenues towards its microscopic understanding in MnTe [4] as well as other AFM materials [5] outlined.

- [1] V. Baltz et al., *Rev. Mod. Phys.* **90**, 015005 (2018).
- [2] D. Kriegner et al. (2016), doi: 10.1038/ncomms11623
- [3] K. Výborný et al., *Phys. Rev. B* **80**, 165204 (2009).
- [4] D. Kriegner et al., *Phys. Rev. B* **96**, 214418 (2017).
- [5] D. Wagenknecht et al., *J. Magn. Magn. Mat.* **513**, 167078 (2020).

Efficiency of blue LEDs: impact of Point defects and GaN growth temperature

Camille Haller¹, Thomas Weatherley¹, Yao Chen¹, Jean-François Carlin¹, Raphaël Butté¹, and Nicolas Grandjean¹

¹ *Institute of Physics, Ecole Polytechnique fédérale de Lausanne, CH-1015 Lausanne, Switzerland*

The blue light emitting diode (LED) gave birth to the solid-state lighting revolution in the late 90s. This is related to their extraordinary performance [1], which, in combination with high-efficiency phosphors, leads to white LEDs with peak luminous efficacy exceeding 300 lm/W.

The active region of blue LEDs consists in InGaN/GaN quantum wells (QWs), which possess extremely high internal quantum efficiency (IQE) despite huge dislocation density. This has been ascribed to carrier localization in potential fluctuations induced by InGaN random alloy disorder. However, high efficiency LEDs commonly feature an InGaN layer, which is underneath the InGaN/GaN QW active region (Figure 1). This underlayer (UL) is known to dramatically increase the efficiency of blue LEDs. Several explanations have been proposed such as screening of threading dislocations due to V-pit formation, decrease of the internal electric field in the InGaN/GaN QWs due to band bending, or improved carrier injection. Another hypothesis is that defects are present at the GaN surface and lead to non-radiative recombination centers once incorporated in InGaN/GaN QWs. Thus, the role of the InGaN UL is to capture those defects resulting in a "clean" GaN surface before the growth of the InGaN/GaN QW active region [2]. In this talk, we will present a comprehensive study of the effect of InGaN UL on the internal quantum efficiency of InGaN/GaN QWs [3]. We will confirm that the role of this layer is to incorporate defects present at the GaN surface. Points defects are then imaged by cathodoluminescence, with an evidence of two types of defects [4]. We will also stress the role of the GaN buffer layer growth temperature [5]. An origin of those defects will be proposed in view of secondary ion mass spectrometry analysis.

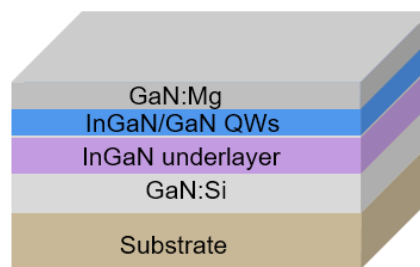


Figure 1: schematic of a commercial blue LED epitaxial structure

- [1] S. Nakamura, M. Senoh, and T. Mukai, *Jpn. J. Appl. Phys.* **32**, L8 (1993)
- [2] C. Haller, J.-F. Carlin, G. Jacopin, D. Martin, R. Butté, and N. Grandjean, *Appl. Phys. Lett.* **111**, 262101 (2017)
- [3] C. Haller, J.-F. Carlin, G. Jacopin, W. Liu, D. Martin, R. Butté, and N. Grandjean, *Appl. Phys. Lett.* **113**, 111106 (2018)
- [4] T. Weatherley *et al.*, *Nano Lett.* 2021, **21**, 5217 (2021)
- [5] Y. Yao *et al.*, *Appl. Phys. Lett.* **118**, 111102 (2021)

Instantaneous decay rate analysis of time resolved photoluminescence: application to nitride layers and heterostructures

Agata Kaminska

¹*Institute of Physics, Polish Academy of Sciences, Al. Lotników 32/46, 01-142 Warsaw, Poland*

²*Cardinal Stefan Wyszyński University, College of Science, Department of Mathematics and Natural Sciences, Dewajtis 5, 01-815 Warsaw, Poland*

³*Institute of High Pressure Physics, Polish Academy of Sciences, Sokołowska 29/37, 01-142 Warsaw, Poland*

The new method of data treatment is proposed for the determination of the carrier recombination processes in optically excited matter measured by time-resolved photoluminescence (TRPL). The analysis includes basic recombination modes, which most generally can be divided into monomolecular (e.g. radiative Wannier-Mott exciton recombination or nonradiative Shockley-Read-Hall), bi-molecular (e.g. band-to-band recombination), and tri-molecular (Auger recombination) or higher-order processes of optical relaxation.

The method is based on the introduction of instantaneous PL decay rate τ_{PL} plotted as a function of the PL intensity or of the time. Such an approach provides deep insight into the time evolution of the recombination of the optically excited systems and can be applied to the time evolution of a variety of optically active structures. The demonstration of its strength is given by the application to III-nitride based systems, including highly doped and semi-insulating thick nitride layers, and polar and non-polar multi-quantum wells (MQWs). It is shown that the application of this method allows determining the dominant recombination process and the values of the ABC parameters which describe the time evolution of the optically generated population of excited carriers [1-3]. At low temperatures (5 K), the mono- and bi-molecular processes determine the carrier relaxation, and the tri-molecular Auger recombination contribution is negligible. At room temperature, the data indicate an important contribution of Auger processes. It is also shown that asymptotic (low excitation), one-exponential recombination rate has a different character depending on the presence of the electric fields across the structure.

[1] R.N. Hall, *Phys. Rev.* **83**, 228 (1951).

[2] W. Shockley, W. T. Read, *Phys. Rev.* **87**, 835 (1952).

[3] P. Strak, K. Koroński, K. Sobczak, J. Borysiuk, K. P. Korona, K. Sakowski, A. Suchocki, E. Monroy, S. Krukowski, and A. Kaminska, *J. Alloy. Compd.* **823**, 153791-1-18 (2020).

Nanoscale Optoelectronics of Layered Crystals, Heterostructures and van der Waals Nanowires

Eli Sutter¹, Peter Sutter²

¹*Department of Mechanical and Materials Engineering*

²*Department of Electrical and Computer Engineering*

University of Nebraska-Lincoln, Lincoln, NE 68588, USA

Two-dimensional (2D) layered materials such as graphene, hexagonal boron nitride, and a family of transition metal dichalcogenide have attracted significant interest due to novel properties that arise in the atomically thin materials regime. Much less explored are layered van der Waals crystals and heterostructures that, assembled from 2D building blocks, lie between the monolayer and bulk limits. In the bottom-up synthesis of such van der Waals materials, phenomena such as spontaneous phase separation, transformations between different crystal polymorphs, hybrid dimensionality, and introduction of defects provide unprecedented opportunities for controlling morphology, interface formation, and novel degrees of freedom such as interlayer twist. But going beyond a single layer also poses extraordinary challenges, both due to the diversity and complexity of the possible few-layer structures and the difficulty of probing functionality, such as optoelectronics, at the relevant length scales.

Here I will show that the combination of imaging, nanobeam electron diffraction and cathodoluminescence (CL) spectroscopy performed in scanning transmissions electron microscopy provides advanced materials characterization and optoelectronic measurements at the ultimate resolution limit. I will discuss nanometer-scale measurements of light-matter interactions in 2D semiconductors with focus on group IVA (Ge,Sn) chalcogenides. Such nano-optical experiments allow us to characterize light emission with spatial resolution far below the diffraction limit, e.g., to measure luminescence from confined geometries, e.g., nanowires, nanoflakes, interfaces built into heterostructures of layered crystals, progressively changing optoelectronic properties in chiral twisted van der Waals nanowires or probe photonic waveguide modes in van der Waals materials.

Magnetic Constitution of Thermoelectric PbTe:Cr

Katarzyna Gas¹, Aleksandra Królicka¹, Sławomir Kret¹, Krzysztof Dybko^{1,2},
Tomasz Story^{1,2} and Maciej Sawicki¹

¹ *Institute of Physics, Polish Academy of Sciences, Aleja Lotników 32/46, PL-02668
Warsaw, Poland.*

² *International Research Centre MagTop, Institute of Physics, Polish Academy of
Sciences, Aleja Lotników 32/46, PL-02668 Warsaw, Poland*

The efficiency of the ever-so-much important thermoelectric energy conversion is described by the material thermoelectric figure of merit (zT). One of the most promising ways of zT improvement leads via band gap engineering towards the enlargement of the density of states at the Fermi level, e.g. via the band convergence [1], or a co-doping to induce a resonant level in the electric transport relevant band [2]. Cr in PbTe is a particularly interesting example since Cr atoms form a mixed valence $\text{Cr}^{2+/3+}$ donor centers resonant with the PbTe conduction band [3].

In this paper we report on detailed temperature and magnetic field dependence of magnetization of IV-VI semiconductor PbTe doped with mixed valence transition metal $\text{Cr}^{2+/3+}$. The material is studied by a SQUID magnetometer in order to quantitatively determine the contribution of single substitutional $\text{Cr}^{2+/3+}$ as well as of various Cr-Te magnetic nanocrystals, including their identification. The applied experimental procedure reveals the presence of about 10^{19} cm^{-3} paramagnetic Cr ions, of which 2/3 are the Cr^{3+} ions formed via self-ionization of Cr^{2+} resonant donors. These are known to improve the zT of this semiconductor. The magnetic finding agrees with previous Hall effect studies thus providing a new experimental support for the proposed electronic structure model of PbTe:Cr system with resonant $\text{Cr}^{2+/3+}$ state located (at low temperatures) about 100 meV above the bottom of the conduction band. Below room temperature a ferromagnetic-like signal points to the presence of Cr-rich nanocrystalline precipitates. Two most likely candidates, namely: Cr_2Te_3 and Cr_5Te_8 are identified upon dedicated temperature cycling of the sample at the remnant state. As an ensemble, the nanocrystals exhibit (blocked) superparamagnetic properties. Also HR-TEM confirmed the presence of numerous single nanometer size precipitates of Cr-Te compounds. The magnetic susceptibility of both n- and p-type PbTe in the temperature range $100 < T < 400 \text{ K}$ has been established. These magnitudes are essential to properly account for the high temperature magnetic susceptibility of PbTe:Cr [4].

This study has been supported by the National Science Centre (Poland) through project OPUS (UMO - 2017/27/B/ST3/02470) and by the National Science Centre for Development (Poland) through grant TERMOD No TECHMATSTRATEG2/408569/5/NCBR/2019 and by the Foundation of Polish Science through the IRA Programme co-financed by EU within SG OP.

[1] Y. Pei *et al.*, *Nature* **473**, 66 (2011).

[2] J. P. Heremans *et al.*, *Science* **321**, 554 (2008).

[3] T. Story *et al.*, *Acta Phys. Pol.* **82**, 879 (1992); W. Mac *et al.*, *ibid* **87**, 492 (1995).

[4] K. Gas *et al.*, *J. Magn. Magn. Mater.*, submitted (2021), arXiv:2101.05705.

Large exciton binding energies in vdW layered magnet MnPS₃ and related systems

M. Birowska¹, Paulo E. Faria Junior², J. Fabian² and J. Kunstmann³

¹University of Warsaw, Faculty of Physics, Pasteura 5, 02-093 Warsaw, Poland

²Institute for Theoretical Physics, University of Regensburg, 93040 Regensburg, Germany

³Theoretical Chemistry, Technische Universität Dresden, 01062 Dresden, Germany

Transition metal dichalcogenides (TMDs) continue to provide an excellent platform for investigating optical properties in the 2D realm mainly due to two aspects: they are stable in air and their excitonic binding energies are giant, about 0.5 eV. Moreover, there is a fascinating connection between spin and valleys, easily addressed by circularly polarized light.

In this work, we present a comprehensive theoretical investigations of the optical properties of the van der Waals layered magnet MnPS₃, which is one important example from the large family of transition metal phosphorus trichalcogenides (MPX₃) [1,2]. This family shares the two aspects with TMDs: monolayer MPX₃ are stable in air and we predict that their excitonic binding energies are even greater than in TMDCs, being more than 1 eV [3]. However, MPX₃ bring along an entirely new ingredient: magnetism. In fact, these materials are antiferromagnets, allowing one to both study and use magnetism and optics, and their interplay, in a single stable material. There is no precedence of such a platform in the realm of conventional materials.

Our findings are based on the extensive first principle calculations and versatile formalism of the Bethe-Salpeter equation, that is able to capture the two-body approach of the excitonic properties. We also highlight the role of the magnetic orderings in electronic and optical properties. In particular, the strong impact of the magnetic ordering on the binding energy of excitons in the monolayer limit is demonstrated, as well as its substantial influence on effective mass of the carriers. Hence, the dependence of the excitonic energies on magnetic ordering is proposed as a tool for investigating the antiferromagnetic structure of these material. In addition, our results revealed that the magnetic state of the monolayer samples is sensitive to the polarization of light.

The study was accomplished thanks to the funds allotted by the National Science Centre, Poland within the framework of the research project 'SONATA12' no. UMO-2016/23/D/ST3/03446. Financial support from the Deutsche Forschungsgemeinschaft (DFG, German Research Foundation) under Project-ID 314695032 (SFB1277) is acknowledged by P.E.F.J. and J.F. and under Project-ID 317551441 by J.K. Access to computing facilities of TU Dresden ZIH for the project "TransPheMat", PL-Grid Polish Infrastructure for Supporting Computational Science in the European Research Space, and of the Interdisciplinary Center of Modeling (ICM), University of Warsaw are gratefully acknowledged.

[1] R. Brec, *Solid State Ionics* vol. **22**, p. 3-30 (1986).

[2] B. L. Chittari *et al.* *Phys. Rev. B* **94**, 184428 (2016).

[3] M. Birowska, P.E.F. Junior, J. Fabian, J. Kunstmann, *Phys. Rev. B* **103**, L121108 (2021).

Influence of substrate misorientation on emission and waveguiding properties of blue (In,Al,Ga)N laser-like structure studied by synchrotron radiation microbeam X-ray diffraction

A. Kafar,^{2,1} A. Sakaki,³ R. Ishii,¹ S. Stanczyk,^{2,4} K. Gibasiewicz,² Y. Matsuda,¹
D. Schiavon,^{2,4} S. Grzanka,^{2,4} T. Suski,² P. Perlin,^{2,4} M. Funato,¹ and Y. Kawakami¹

¹Kyoto University, Kyoto 615-8510, Japan

²Institute of High Pressure Physics PAS, Sokolowska 29/37, 01-142 Warsaw, Poland

³Nichia Corporation, Tokushima 774-8601, Japan

⁴TopGaN Ltd., Sokolowska 29/37, 01-142 Warsaw, Poland

III–N material system offers a rather unique possibility of bandgap engineering by the change of substrate misorientation. Sarzyński *et al.* [1], demonstrated that InGaN alloy composition sharply depends on surface miscut, leading to the variation of In content between 7% and 14%. In the present work we go along the same direction but we show that we can engineer the local surface misorientation to form a needed lateral, In content profile within one wafer or even within one chip. Such an approach can be used for fabrication of specialized devices [2,3] but also as an advanced experimental platform [4].

The goal of this study [5] is to examine in details how the substrate misorientation angle influences the structural parameters of the epitaxial layers (a design including layers imitating waveguide and cladding layers below the active region). Thanks to the use of synchrotron radiation microbeam X-ray diffraction (SR-XRD), we were able to study the whole structure along a misorientation profile in a range of angles between 0.5° to 2.8°. The 40 x 40 μm test structure with misorientation profile was fabricated using multilevel photolithography and dry-etching. The local structural parameters were measured by synchrotron radiation microbeam X-ray diffraction, with the sampling area of below 1 x 1 μm. We directly obtained the relation between the misorientation and indium content in the quantum well, showing the induced change of the composition from 9% to 18%. By using a micro-beam we were able to obtain high spatial resolution images. We also show a good agreement of local PL emission wavelength with simulation of transition energy based on SR-XRD data and estimated Stokes shift. We observe that the substrate misorientation influences also the InGaN waveguide and AlGaN cladding composition. However, our calculation of the optical confinement factor of a full laser diode structure indicates that good light guiding properties should be preserved in the whole misorientation range studied here. This proves the usefulness of misorientation modification in applications like broadband superluminescent diodes or multicolour laser arrays.

[1] M. Sarzynski, M. Leszczynski, M. Krysko, J.Z. Domagała, R. Czernecki, and T. Suski, *Crystal Research and Technology* **47**, 321 (2012).

[2] M. Sarzyński, T. Suski, G. Staszczak, A. Khachapuridze, J.Z. Domagała, R. Czernecki, J. Plesiewicz, J. Pawłowska, S.P. Najda, M. Boćkowski, P. Perlin, and M. Leszczyński, *Applied Physics Express* **5**, 021001 (2012).

[3] A. Kafar, S. Stanczyk, M. Sarzynski, S. Grzanka, J. Goss, I. Makarowa, A. Nowakowska-Siwinska, T. Suski, and P. Perlin, *Photon. Res.* **5**, A30 (2017).

[4] A. Kafar, R. Ishii, K. Gibasiewicz, Y. Matsuda, S. Stanczyk, D. Schiavon, S. Grzanka, M. Tano, A. Sakaki, T. Suski, P. Perlin, M. Funato, and Y. Kawakami, *Optics Express* **28**, 22524 (2020).

[5] A. Kafar, A. Sakaki, R. Ishii, S. Stanczyk, K. Gibasiewicz, Y. Matsuda, D. Schiavon, S. Grzanka, T. Suski, P. Perlin, M. Funato, and Y. Kawakami, *Photonics Research* (2021).

Toward single photon emitters – new concepts in nitride optoelectronic devices

M. Chlipala, H. Turski, M. Siekacz, G. Muziol, K. Nowakowski-Szkudlarek,
A. Feduniewicz-Żmuda and C. Skierbiszewski

Institute of High-Pressure Physics PAS, ul. Sokołowska 29/37, 01-142 Warsaw, Poland

Nitride semiconductors are widely known for its application in high-efficiency light sources and power devices. But its unique properties can be also used as a platform for solid-state, single-photon emitters and detectors. This type of devices operate at cryogenic temperature whereas standard structures are not suitable for such extreme conditions where piezoelectric fields and high ionization energy of Mg acceptor in GaN lead to increased diode operation voltage and low injection efficiency [1]. High resistivity of p-type layers in standard LEDs can be exemplified by poor current spreading, as shown in Fig. 1a.

To overcome these challenges, we use a low resistance tunnel junctions (TJ) with a Ge-Mg highly doped layers [2] on which an inverted LED is grown [3] (an LED where order of p and n type layers is inverted in comparison to standard LED). Such setup overcomes a problem with low injection efficiency at cryogenic temperatures [1] and allows for the use of low resistance n-type cap layer on top of the device. Thickness of this n-type cap can be greatly reduced by the increase in doping concentration. This is realized by replacing standard Si dopant with Ge, which is known to lead to better crystal quality at extremely high concentrations [4].

In this work we present a unique GaN-based LED construction utilizing bottom tunnel junction and ultra-thin - 20 nm thick $\text{In}_{0.02}\text{GaN}$ cap doped with Ge that allows for uniform current spreading as presented in Fig. 1b. Samples were grown on bulk GaN substrate along [0001] direction using plasma-assisted molecular beam epitaxy.

It is shown that proposed structure is a feasible platform for further integration with superconductors, e.g. niobium nitride, which can be epitaxially grown within the same material system. Short distance between superconducting material and the active region should allow for cooper pair injection into the LED what was shown for GaAs emitter [5].

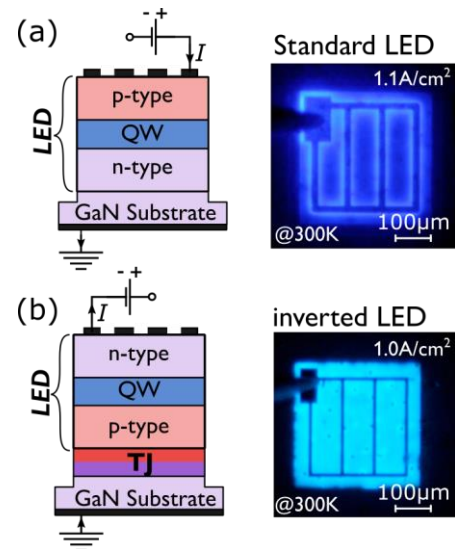


Fig. 1 Schematic structure with photo of processed device: (a) standard LED, (b) inverted LED with thin cap.

Acknowledgments: This work is carried out within Foundation for Polish Science co-financed by the European Union under the European Regional Development Fund (POIR.04.04.00-00- 210C/16-00, POIR.04.04.00-00-5D5B/18-00); Polish National Science Centre (2015/17/B/ST7/04091, UMO-2018/31/B/ST5/03719, UMO-2019/35/N/ST7/04182).

- [1] M. Chlipala et al., Opt. Express, vol. 28, no. 20, p. 30299 (2020)
- [2] Zak, M. et al., Phys. Rev. Appl. 15, 1–13 (2021)
- [3] Turski, H., Bharadwaj, S., Xing, H. and Jena, D. J., Appl. Phys. 125, 1–23 (2019)
- [4] Fritze et al., Appl. Phys. Lett. 100, (2012).
- [5] Panna, D. et al., Nano Lett. 18, 6764–6769 (2018)

Towards Deep-UV Lasers Diodes by MBE

Len van Deurzen¹, Ryan Page², Kazuki Nomoto³, Jimy Encomendero³, Vladimir Protasenko³, Huili (Grace) Xing^{2,3} and Debdeep Jena^{1,2,3}

¹*Department of Applied and Engineering Physics, Cornell University, Ithaca, USA*

²*Department of Materials Science and Engineering, Cornell University, Ithaca, USA*

³*Department of Electrical and Computer Engineering, Cornell University, Ithaca, USA*

High-power, semiconductor UV-C (200-280 nm) emitters are desirable as they are an energy-efficient and compact tool with diverse applications. These include quantum computing and communication, pathogen detection and sterilization, water purification, gas sensing, photolithography, and spectroscopy, to name a few. The realization of UV-C Laser Diodes (LD) based on the AlGaIn material system has proven challenging as these wide-bandgap semiconductors exhibit low carrier mobilities, very high dopant activation energies and asymmetries between electron and hole transport. This makes it a challenge to achieve population inversion and sufficient gain by electrical injection. Since lasing occurs when the gain of the LD equals the optical losses, the minimization of the optical losses is of paramount importance. In general, the total optical loss can be described by the sum of intrinsic material loss and cavity loss. In this work, we quantify the effects of mirror slant and roughness on the cavity loss and apply a combined dry and TMAH-based wet etching technique to reduce these effects [1]. Furthermore, the recent development of MBE homoepitaxy on bulk AlN substrates helps keep the intrinsic losses low [2]. With these developments, we demonstrate the first optically pumped AlGaIn double heterostructure sub-300 nm laser grown by molecular beam epitaxy (MBE), exhibiting peak gain at 284 nm. Moreover, we develop Distributed Bragg Reflectors (DBRs) which can reduce the mirror loss of an ideal zero roughness and zero slant facet, which is limited by the refractive index mismatch between air and AlGaIn, even more. Pulsed electrically injected laser diodes have recently been realized by MOCVD [3-4]. With the electrically pumped continuous wave (CW) laser diode in mind, we propose multiple electronic design optimizations to improve hole injection in wide-bandgap light-emitting diodes (LEDs) and LDs. These include low-resistivity and low contact resistance p-InGaIn contacts as well as active region optimization.

The authors appreciate NSF RAISE-TAQS 1839196 for financial support; the devices were fabricated in CNF (NSF 1710298) and use shared facilities supported by MRI 1631282.

[1] Shinji Yashue et al., Jpn. J. Appl. Phys. **58** SCCC30 (2019)

[2] Y. Cho et al., Appl. Phys. Lett. **116**, 172106 (2020)

[3] Z. Zhang et al., Appl. Phys. Express, **12**, 124003 (2019)

[4] T. Sakai et al., Appl. Phys. Lett. **116**, 122101 (2020)

Carrier Dynamics in Thin Germanium-Tin Epilayers: The Issue of Below Bandgap States

E. Rogowicz¹, J. Kopaczek², J. Kutrowska-Girzycka¹, M. Myronov³, R. Kudrawiec², and M. Syperek¹

¹*Faculty of Fundamental Problems of Technology, Department of Experimental Physics, Wrocław University of Science and Technology, Wyb. Wyspiańskiego 27, 50-370 Wrocław, Poland*

²*Faculty of Fundamental Problems of Technology, Department of Semiconductor Materials Engineering, Wrocław University of Science and Technology, Wyb. Wyspiańskiego 27, 50-370 Wrocław, Poland*

³*Department of Physics, The University of Warwick, Gibbet Hill Road, Coventry, CV4 7AL, UK*

Germanium-Tin ($\text{Ge}_{1-x}\text{Sn}_x$) with a small fraction of Tin can be an interesting alternative for a gain medium for optoelectronic devices compatible with the Si-based mid-infrared silicon photonics. Despite the $\text{Ge}_{1-x}\text{Sn}_x$ -on-Si lasers, at low temperatures, have already been demonstrated, the knowledge of the material properties is still barely known. In particular, there is a lack of precise information about the nature of emitting states carrier relaxation kinetics, relaxation pathways, and accompanied physical mechanisms important for the dynamic parameters of laser devices.

Here we present an in-depth spectroscopic explore of optical properties and carrier dynamics in $\text{Ge}_{1-x}\text{Sn}_x$ epilayers with different Sn content (6-12%), by utilizing the complementary experimental techniques: Raman scattering, photoluminescence (PL), photoreflectance (PR), time-resolved photoluminescence (TRPL) and differential reflectivity (TRDR). Those methods give insights into the emission and absorption properties of the system in question and radiative and nonradiative relaxation and recombination pathways. Based on TRDR and TRPL experiments' nature, we identify: (i) two initial electron relaxation processes after photo-excitation; (ii) radiative electron-hole recombination on below-bandgap-states; (iii) non-radiative carrier recombination involving the Shockley-Read-Hall mechanism; (iv) non-radiative recombination through the surface states. In particular, the experimental results significantly increase the knowledge on carrier dynamics in the $\text{Ge}_{1-x}\text{Sn}_x$ alloy. It provides unknown up-to-date kinetic parameters of the initial stage of electron relaxation and further carrier recombination dynamics, unveiling the important role of the bandgap inhomogeneity for the relaxation dynamics, and showing the important role of the below-bandgap states that can participate in the light generation process in $\text{Ge}_{1-x}\text{Sn}_x$ epilayer[1].

[1] E. Rogowicz, J. Kopaczek, J. Kutrowska-Girzycka, M. Myronov, R. Kudrawiec, and M. Syperek, ACS Applied Electronic Materials **3**, 344–352 (2021).

Exciton g-factors of van der Waals heterostructures from first principles calculations

Tomasz Woźniak¹, Paulo E. Faria Junior², Gotthard Seifert³, Andrey Chaves⁴
and Jens Kunstmann³

¹ Wrocław University of Science and Technology, Wrocław, Poland

² Universitaet Regensburg, Germany

³ Technische Universitaet Dresden, Germany

⁴ Universidade Federal do Ceará, Fortaleza, Brazil

External fields are a powerful tool to probe optical excitations in materials. The linear energy shift of an excitation in a magnetic field is quantified by its effective g-factor. Here we show how exciton g-factors and their sign can be determined by converged first principles calculations. We apply the method to monolayer (1L) excitons in semiconducting transition metal dichalcogenides (TMDs) and to interlayer excitons in MoSe₂/WSe₂ heterobilayers and obtain excellent agreement with recent experimental data. The precision of our method allows to assign measured g-factors of optical peaks to specific transitions in the band structure and also to specific regions of the samples. This revealed the nature of various, previously measured interlayer exciton peaks. We further show that, due to specific optical selection rules, g-factors in van der Waals heterostructures are strongly spin and stacking-dependent. The presented approach can potentially be applied to a wide variety of semiconductors [1].

The method was successfully applied to bigger excitonic complexes: trions, their phonon replicas and biexcitons in 1L WS₂. It also overcomes the currently used simple models, yielding g-factors of individual electrons and holes in perfect agreement with their experimental values [2].

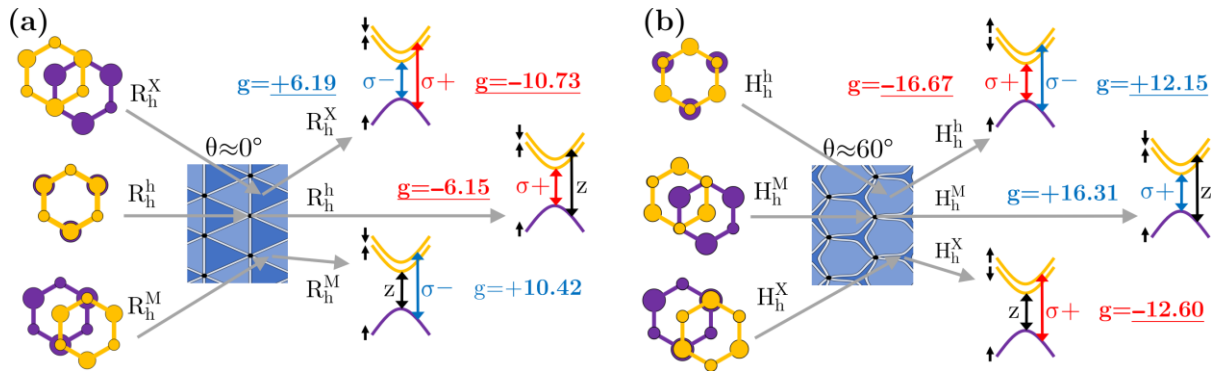


Figure 1: Exciton g-factors for high-symmetry stacking configurations in (a) 0° and (b) 60° MoSe₂/WSe₂ heterobilayer

[1] T. Woźniak, P. E. Faria Junior, G. Seifert, A. Chaves, J. Kunstmann, *Phys. Rev. B* **101**, 235408 (2020).

[2] M. Zinkiewicz, T. Woźniak, T. Kazimierzczuk, P. Kapuściński, K. Oreszczuk, M. Grzeszczyk, M. Bartoš, K. Nogajewski, K. Watanabe, T. Taniguchi, C. Faugeras, P. Kossacki, M. Potemski, A. Babiński, M. R. Molas, *Nano Lett.* **21**, 6, 2519–2525 (2021).

Classical Huang-Rhys Description of Luminescence for a Carbon Related Defect in BN

Aleksandra K. Dąbrowska, **Krzysztof Pakuła**, Mateusz Tokarczyk,
Johannes Binder, Roman Stępniewski, Andrzej Wyszomolek

*Institute of Experimental Physics, Faculty of Physics, University of Warsaw,
ul. Pasteura 5, 02-093 Warsaw, Poland*

Boron nitride (BN) in the sp^2 – hybridized structure combines the properties of classic nitrides (extraordinary resistance to external conditions and wide bandgap) with the two – dimensional nature [1]. Such a combination renders hBN suitable for use in a wide range of applications (i.e. deep UV light source, insulating barrier in van der Waals heterostructures). The Metal Organic Vapour Phase Epitaxy (MOVPE) is one of the most promising growth methods in terms of the production of large-scale, uniform boron nitride with a relatively high growth rate, compatible for use in commercial devices. Therefore, first it is necessary to understand the nature of the point-like defects in BN and gain control over their occurrence.

The MOVPE growth of BN is carried out on sapphire substrates with triethylboron (TEB) and ammonia as precursors of boron and nitrogen, respectively. The high growth rates cause increased disorder of the sp^2 – BN [2]. This allows to obtain thick material, eligible to study the

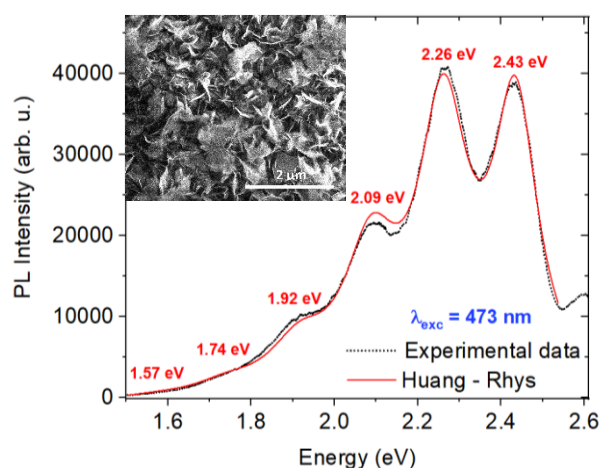


Figure 1 Photoluminescence spectra (excited by 473 nm laser line) with Lorentzian peak fits with relative intensities described by the Huang-Rhys model. Inset: SEM (Scanning Electron Microscopy) image showing the surface morphology of the sample.

nature of point- like defects which are still barely known. Some point defects show characteristic intra-center emission, which allows for their identification. In this communication we focus on carbon-related defects. The studied sample (Fig. 1) was grown at a relatively low growth temperature (1050°C), under high pressure (800 mbar) and comparatively low V/III ratio (25). The photoluminescence spectra (PL) consists of a zero phonon line at 2.43 eV with its phonon replicas and can be described by the Huang – Rhys model (Fig. 1) [3]. It means that in this spectral range there is a signal from only one entity. We will present the Huang – Rhys parameters obtained from the fitting, providing

information about the electron – phonon coupling for the carbon-related defects in our BN layers.

A thorough analysis and the association of defects with specific bands in PL spectra will enable gaining the total control on their presence and concentration also in epitaxial, continuous layers.

[1] K.S. Novoselov et al., *Science* 353.6298, aac9439 (2016)

[2] K. Pakuła et al., arXiv 1906.05319 (2019)

[3] K. Huang, A. Rhys, *Proc. R. Soc. Lond.* A204, 406–423 (1950)

Acknowledgement: This work has been partially supported by the National Science Centre under grant no. 2019/33/B/ST5/02766

Deep UV Photoluminescence of MOCVD grown Boron Nitride

K. P. Korona, K. Pakuła, A. K. Dąbrowska, J. Binder, R. Stępniewski, A. Wysmołek,

*Institute of Experimental Physics, Faculty of Physics, University of Warsaw,
ul. Pasteura 5, 02-093 Warsaw, Poland*

Boron nitride (BN) is a wide band-gap semiconductor with energy gap about 6 eV. In spite of lately observed wide interest in BN properties, there are still many discrepancies in reports on its photoluminescence (PL) spectra. In the present work we aim to elucidate some of the intriguing features of the PL of h-BN by means of a joint experimental and theoretical study.

The experimental part was performed mostly on the boron nitride layers grown on sapphire substrates by metal-organic chemical vapor deposition (MOCVD) using triethylboron (TEB) and ammonia (NH₃). The layers grown at about 1050°C and about 1310°C were investigated. The samples were undoped or doped with silicon (in order to obtain n-type) or magnesium (in order to obtain p-type). We also measured an industrial-grade sample for a comparison.

The photoluminescence was excited with the 215 nm (5.8 eV) light generated as fourth harmonic of the Ti:Sapphire laser line. Micro-PL spectroscopy was performed with the mirror objective. Time-resolved PL (TRPL) was measured with a streak camera and with quartz optics.

In the photoluminescence a donor-acceptor (or DX) emission at 230 nm (5.4 eV) was observed at helium temperature in samples grown at 1310°C (BN:Si, BN:Mg). The 5.4-eV line is close to the BN band gap so it can be of excitonic origin. Additionally, in such samples broad bands of PL can be observed in the mid-gap region about 330 nm and 400 nm (marked as D330 and D400 in Fig. 1). We do not observe any influence of the doping on the observed spectra.

On the other hand, in sample grown at 1050°C (LT BN) some sharp lines at range of 300 nm (4.1 eV) and 380 nm (3.2 eV) were measured (marked as CC300 and CC380 in Fig.1).

The CC300 and CC380 emission spectra consisted of few sharp lines with nearly identical lifetimes (about 0.7 ns). The detailed analysis reveals that the extra lines are a series of phonon replicas. Based on the theoretical results we postulate that the 300-nm and 380-nm lines can be assigned to pairs of carbon impurities. The carbon is present in our samples due to use of organic precursor TEB during growth. The TEB/NH₃ ratio is higher in the samples grown at 1050°C.

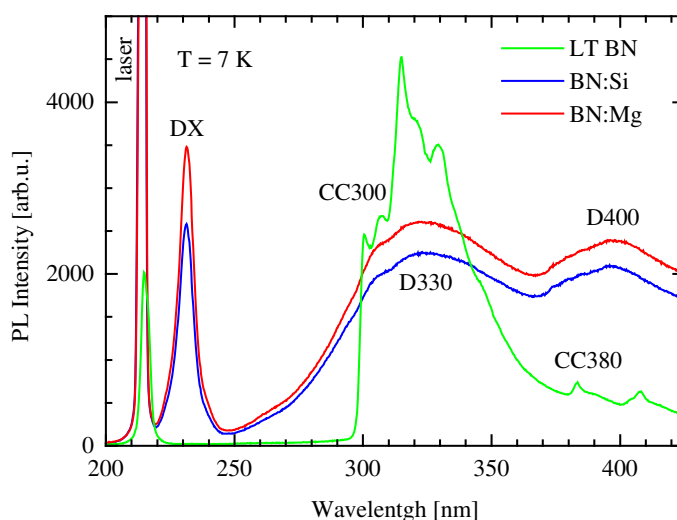


Fig. 1.

Photoluminescence spectra of BN samples: pure, doped with Mg and Si.

Detailed studies on the influence of dielectric environment on exciton and trion properties in monolayer and bilayer MoTe₂

E. Zięba ¹, J. Kutrowska-Girzycka ¹, P. Mrowiński ¹, M. Florian ², C. Gies ², S. Tongay ³, K. Watanabe ⁴, T. Taniguchi ⁴, C. Schneider ⁵, and M. Syperek ¹

¹ *Laboratory for Optical Spectroscopy of Nanostructures, Faculty of Fundamental Problems of Technology, Wrocław University of Science and Technology, Wrocław 50-370, Poland*

² *Institute für Theoretische Physik, Universität Bremen, Germany*

³ *Arizona State University, Tempe, Arizona 85281, USA*

⁴ *Advanced Materials Laboratory, National Institute of Materials Science, 1-1 Namiki, Tsukuba 305-0044, Japan*

⁵ *Institute of Physic, Carl von Ossietzky University of Oldenburg, Germany*

Molybdenum ditelluride (MoTe₂) belongs to a family of widely studied transition-metal dichalcogenides with several well recognizable members: MoS₂, MoSe₂, WS₂, and WSe₂. However, the properties of MoTe₂ are still not very well known. MoTe₂ is an indirect gap semiconductor when crystallizes in the multi-layered 2H form. This property holds even when the material is three monolayers-thin. Transition to the direct bandgap material occurs when 2H-MoTe₂ is thinned down to a bi-layer (BL) or a monolayer (ML). The ML and BL 2H-MoTe₂ direct-gap energy is established to ~1.10 eV (1125 nm) and ~1.05 eV (~1200 nm) at room temperature, respectively. Therefore, it makes the material attractive for light-emitting devices operating in the near-infrared spectral range. Since the excitonic interaction largely determines the direct gap energy, it opens the way for tuning the excitonic bandgap of 2H-MoTe₂ by altering the interparticle interaction through the material encapsulation in different dielectric environments.

This report presents detailed optical studies of mechanically exfoliated ML and BL 2H-MoTe₂ exposed to a technologically relevant dielectric environment potentially important for the fabrication of hybrid MoTe₂/classical semiconductor/insulator optical devices. Optical properties of MoTe₂ are evaluated by high-spatially-resolved photoluminescence, differential reflectivity, photo-modulated reflectivity, and Raman studies at cryogenic and room temperature. Materials combination includes either typical ones: ML and BL 2H-MoTe₂ encapsulated in PMMA/air, SiO₂/air, hBN/air, SiO₂/hBN, hBN/hBN, Si/air, and Si/hBN interfaces, and less known: Si₃N₄/air, 4H-SiC/air, GaP/air, InP/air, GaAs/air, Si₃N₄/hBN, 4H-SiC/hBN, InP/hBN, and GaAs/hBN. All of the interfaces can be characterized by an effective electric permittivity ϵ_{eff} spanning the range of ~(2.0-9.85). It allows for broad control over the electric field screening of interacting particles confined to MoTe₂ manifested in shifting the emission energy of basic excitations, namely exciton (X) and trion (T). We find that the dielectric screening, accompanied by the renormalization of a quasi-particle bandgap, only slightly affects the X emission energy (E_X), showing its decreasing of about a few meV with increasing the ϵ_{eff} . A slightly stronger trend is observed for the trion for which the emission energy (E_T) can decrease by ~10 meV with increasing the ϵ_{eff} . These observations are reflected in the tuning range of the trion binding energy: $E_{b,T} = E_X - E_T$. For ML MoTe₂, the $E_{b,T}$ can be tuned in the range of ~(26-22 meV), exhibiting clear descendancy with the ϵ_{eff} . The same trend is obeyed for BL MoTe₂, however, the $E_{b,T}$ is tuned within the range of ~(20-15 meV).

Dielectric properties of transition metal trichalcogenides MPX_3 .

A. Skolasińska¹ and M. Birowska¹

¹University of Warsaw, Faculty of Physics, Pasteura 5, 02-093 Warsaw, Poland

2D semiconducting crystals such as widely examine TMDs materials are known to strongly absorb light. The great potential of 2D materials for future optoelectronic applications requires a detailed study of their electronic and optical properties. The dielectric constant, which determine the polarization of the media is a crucial parameter in solid state physics. The fundamental material properties such as bandgap, conductivity, optical absorption are of critical importance in transport and optoelectronic applications. In addition, the dielectric screening is particularly relevant for determining the exciton binding energies.

The recent studies have shown that the $MnPS_3$ exhibit large exciton binding energy [1]. The $MnPS_3$ is a representative system of the transition metal phosphorus trichalcogenides compounds (MPX_3 , where M are transition metals $M=Ni, Mn, Fe$ etc. and chalcogen atoms $X=S, Se$), which is a large family of the antiferromagnetic semiconductors [2]. Here, we examine the compounds of MPX_3 to determine the dielectric constants and 2D polarizabilities, in the framework of the density functional theory within the Independent Particle approach (IP). Our results reveal that the in-plane 2D polarizabilities are approximately two times lower (e.g. $MnPS_3$, $NiPS_3$ equal to 3.3\AA , 3.9\AA , respectively) than widely examine TMD's (e.g. for MoS_2 equals to 6.6\AA), which might have a consequence in obtaining large exciton binding energies. We also discuss the role of the magnetic ordering, Hubbard U parameter on the dielectric screening and the ionic contribution to the static dielectric constant.

The study was accomplished thanks to the funds allotted by the National Science Centre, Poland within the framework of the research project 'SONATA12' no. UMO-2016/23/D/ST3/03446. Access to computing facilities of TU Dresden ZIH for the project "TransPheMat", PL-Grid Polish Infrastructure for Supporting Computational Science in the European Research Space, and of the Interdisciplinary Center of Modeling (ICM), University of Warsaw are gratefully acknowledged.

[3] M. Birowska, P.E.F. Junior, J. Fabian, J. Kuntsmann, *Phys. Rev. B* **103**, L121108 (2021).

[2] B. L. Chittari *et al.* *Phys. Rev. B* **94**, 184428 (2016).

Dark Excitons In Monolayer WS₂

Malgorzata Zinkiewicz¹, Artur O. Slobodeniuk², Tomasz Kazimierczuk¹,
Piotr Kapuściński^{3,4}, Kacper Oreszczuk¹, Magdalena Grzeszczyk¹, Miroslav Bartoš^{3,5},
Karol Nogajewski¹, Kenji Watanabe⁶, Takashi Taniguchi⁷, Clément Faugeras³,
Piotr Kossacki¹, Marek Potemski^{1,3}, Adam Babiński¹ and Maciej R. Molas¹

¹ Institute of Experimental Physics, Faculty of Physics, University of Warsaw, Poland.

² Department of Condensed Matter Physics, Charles University in Prague, Czech Republic

³ LNCMI, CNRS-UGA-UPS-INS-EMFL, Grenoble, France

⁴ Department of Experimental Physics, Wrocław University of Science and Technology, Poland

⁵ Central European Institute of Technology, Brno University of Technology, Czech Republic

⁶ Research Center for Functional Materials, NIMS, Tsukuba, Japan

⁷ International Center for Materials Nanoarchitectonics, NIMS, Tsukuba, Japan

We have investigated dark exciton complexes in a monolayer of WS₂ encapsulated in hexagonal BN (hBN) by low temperature and polarization resolved magneto-photoluminescence experiments. The in-plane component of the magnetic field is brightening dark states (see Fig. 1). In line with previous studies on WSe₂ [1], we identify the Coulomb exchange interaction coupled neutral dark (X^D) and grey (X^G) excitons through their polarization properties. The X^{D/G} line is red-shifted by 40 meV from the bright excitonic transition (X^B) peak and the energy separation between the X^G and X^D emissions is equal to 530 μeV. Another brightened in magnetic field line is the dark trion (T^D) redshifted by 57 meV from the X^B. Contrary to dark excitons, dark trions do not show any fine structure nor linear polarization due to the absence of coupling between dark trions in the two valleys. Applying

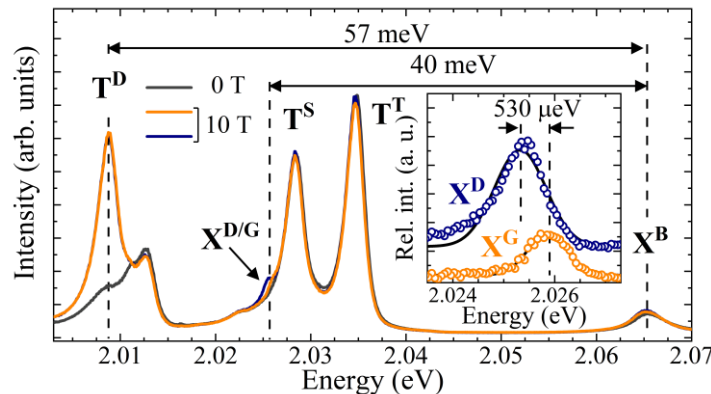


Figure 1: Low-temperature PL spectra measured on a WS₂ ML encapsulated in hBN flakes at B = 0 T and at B_{||} = 10 T. Grey curve represents unpolarized detection, while the blue and orange curves correspond to the detection of two linear polarizations aligned parallel and perpendicular to the direction of magnetic field, respectively. The inset shows the relative intensities of the grey (X^G) and dark (X^D) exciton emissions defined as (PL_{B=10 T} - PL_{B=0 T})/PL_{B=0 T} [2].

the magnetic field in both perpendicular and parallel configurations with respect to the monolayer plane, we have determined the g-factor of dark trions to be $g \sim -8.6$. Time resolved measurements indicate that the decay time of dark trions is close to 0.5 ns, which is more than two orders of magnitude larger than that of bright trions in the same monolayer. What is more, we have found that this system is an *n*-type doped semiconductor as the dark trions dominate the emission spectrum and they present much higher brightening rate with respect to dark excitons, which is in contrast to previous results obtained in WSe₂.

[1] M. R. Molas, et al., *Physical Review Letters* **123**, 096803 (2019).

[2] M. Zinkiewicz, et al., *Nanoscale* **12**, 18153 (2020).

Excitons in Transition Metal Dichalcogenide Heterostructures

K. Sadecka¹, M. Bieniek^{1,2}, A. Wójs¹, P. Hawrylak²

¹ *Department of Theoretical Physics, Wrocław University of Science and Technology,
Wybrzeże Wyspiańskiego 27, 50-370 Wrocław, Poland*

² *Department of Physics, University of Ottawa, Ottawa, Ontario, Canada K1N 6N5*

Single layers of transition metal dichalcogenides (TMDs) MX_2 ($\text{M} = \text{Mo}, \text{W}$; $\text{X} = \text{S}, \text{Se}, \text{Te}$) are novel semiconductor research platforms enabling exploration of many fundamental physical phenomena. These include, e. g., low energy massive Dirac fermions, valley degrees of freedom which allow for selective excitation with circularly polarized light and strong electron-electron interactions leading to excitons with binding energy ~ 500 meV [1], robust charged exciton states [2,3] and broken symmetry valley- and spin-polarized phases [4]. TMDs are also the basic “blocks” to the construction of van der Waals heterostructures [5]. Such systems, built from atomically thin layers of MX_2 crystals, enable the formation of excitons composed of electrons and “holes” in distinct layers producing long-lived interlayer excitons with very strong binding energies [6,7] and interlayer many body complexes [8]. It is also possible to farther advance means of manipulation of properties of TMD van der Waals heterostructures with mutual twisting of layers [9].

In the following work the electronic and excitonic properties of TMD heterostructure $\text{MoSe}_2 / \text{WSe}_2$ will be described using a combination of density functional theory, tight-binding approximation and Bethe-Salpeter equation. We start with determining exciton fine structure due to type-II spin-split band arrangement, considering both A/B, spin bright/dark and intra-/inter- layer exciton series. In next step we study properties of electron and hole Bloch wavefunctions in tight-binding approximation, especially Berry curvature and its effect on the excitonic spectrum renormalization and topological splitting of the $2p$ -bound exciton states.

- [1] M. Bieniek, L. Szulakowska, and P. Hawrylak, *Phys. Rev. B* **101**, 125423 (2020).
- [2] J. Jadcak, L. Bryja, J. Kutrowska-Girzycka, P. Kapuściński, M. Bieniek, Y. S. Huang, and P. Hawrylak, *Nature communications* **10**, 107 (2019).
- [3] J. Jadcak, J. Kutrowska-Girzycka, M. Bieniek, T. Kazimierczuk, P. Kossacki, J. J. Schindler, J. Debus, K. Watanabe, T. Taniguchi, C. H. Ho, A. Wójs, P. Hawrylak, and L. Bryja, *Nanotechnology* **32**, 145717 (2021).
- [4] L. Szulakowska, M. Cygorek, M. Bieniek, and P. Hawrylak, *Phys. Rev. B* **102**, 245410 (2020).
- [5] A. K. Geim, and I. V. Grigorieva, *Nature* **499**, 419 (2013).
- [6] P. Rivera, K. L. Seyler, H. Yu, J. R. Schaibley, J. Yan, D. G. Mandrus, W. Yao, and X. Xu, *Science* **351**, 6274 (2016).
- [7] E. Calman, M. M. Fogler, L. V. Butov, S. Hu, A. Mishchenko, and A. K. Geim, *Nature communications* **9**, 1 (2018).
- [8] L. A. Jauregui, A. Y. Joe, K. Pistunova, D. S. Wild, A. A. High, Y. Zhou, G. Scuri, K. De Greve, A. Sushko, C.-H. Yu, T. Taniguchi, K. Watanabe, D. J. Needleman, M. D. Lukin, H. Park, and P. Kim, *Science* **366**, 6467 (2019).
- [9] E. M. Alexeev, D. A. Ruiz-Tijerina, M. Danovich, M. J. Hamer, D. J. Terry, P. K. Nayak, S. Ahn, S. Pak, J. Lee, J. I. Sohn, M. R. Molas, M. Koperski, K. Watanabe, T. Taniguchi, K. S. Novoselov, R. V. Gorbachev, H. Suk Shin, V. I. Fal’ko, and A. I. Tartakovskii, *Nature* **567**, 81–86 (2019).

Charge Transport in MBE-grown MoTe₂ Bilayers With Enhanced Stability Provided by AlO_x Capping

Z. Ogorzałek ¹, B. Seredyński ¹, S. Kret ², A. Kwiatkowski ¹, K. Korona ¹,
M. Grzeszczyk ¹, J. Mierzejewski ¹, D. Wasik ¹, W. Pacuski ¹, J. Sadowski ^{1,2,3}
and M. Gryglas-Borysiewicz ¹

¹ Faculty of Physics, University of Warsaw, Pasteura 5, Warsaw, Poland,

² Institute of Physics, Polish Academy of Sciences, al. Lotnikow 32/46, Warsaw, Poland,

³ Department of Physics and Electrical Engineering, Linnaeus University, Kalmar, Sweden

MoTe₂ is a transition metal dichalcogenide (TMD), which has been intensively studied in the last few years. It exists in several crystalline phases among which the semimetallic T_d and semiconducting 2H exhibit numerous intriguing physical properties. It is well known however, that MoTe₂ shows significant sensitivity to air, which makes ex-situ experiments, involving sample preparation and processing, very challenging. [1-3] The question of stability is especially important in the case of ultra-thin, single and few-layer samples, which provide access to the most interesting physics.

In this paper we address the problem of low stability of MoTe₂ and propose a very efficient protective capping, that stabilizes transport properties of the layers. A molecular beam epitaxy technique has been used to grow ultra-thin MoTe₂ films in 2H-semiconducting phase on large area GaAs (111)B substrates. A transmission electron microscopy study reveals the high quality of the MoTe₂ films. Directly after the growth, MoTe₂ films have been in-situ capped with a thin (3 nm) layer of Al, which oxidizes after exposure to ambient conditions. This oxide serves as a protective layer to the underlying MoTe₂ and it is thin enough to make good-quality electrical contacts. Wide range temperature resistivity studies showed that charge transport in MoTe₂ is realized by hopping with an anomalous hopping exponent of $x \simeq 0.66$, reported also previously for ultra-thin, metallic layers. We demonstrate that this approach provides a significant improvement of the MoTe₂ stability. Upon exposure to pure nitrogen and air atmospheres, the resistivity of unprotected sample changes by more than 900%, whereas the protected sample shows electrical stability at the level of 1% over one week and 5% in the timescale of several months. [4]

[1] H. Diaz et al., *2D Materials* **2** (2015)

[2] M. Yamamoto et al., *J. Phys. Chem.* **117** (2013)

[3] G. Mirabelli et al., *J. Appl. Phys.* **120**, 125102 (2016)

[4] Z. Ogorzałek et al., *Nanoscale* **12**, 16535-16542 (2020)

Exploring Electronic Properties of Functionalized 2D MBenes -Graphene Like 2D Boron Sheets.

Varun G. Nair^{1,2}, K. Kotur¹, Agnieszka. M. Jastrzębska² and Magdalena Birowska¹

¹ University of Warsaw, Faculty of Physics, Pasteura 5, 02-093 Warsaw, Poland

² Warsaw University of Technology, Faculty of Materials Science and Engineering, 02-507 Warsaw, Wołoska 141, Poland

The two-dimensional (2D) materials have received increasing attention due to their wide variety of application in different fields. The 2D materials such as the layers of transition metal borides called MBenes are comparatively new [1, 2]. Similarly, like MXenes materials, which have been widely studied so far [3], MBenes can be chemically exfoliated from their bulk counterparts (MAB phases). The MAB phases are the orthorhombic crystals of the form MA_2B , M_2AlB_2 , M_3AlB_2 , M_3AlB_4 , and M_4AlB_6 .

In this communication we present a comprehensive *ab initio* studies of 2D MBenes structures in the framework of the Density Functional Theory (DFT) using VASP software. We examine the orthorhombic and hexagonal structures with various concentration of surface functionalization groups: -OH, -H, -O. We discuss the issue of the structural phase transition. We examine both magnetic FeB and nonmagnetic MoB MBenes layers. Our results reveal that the pure systems are metallic, however, for particular concentration and arrangement of the surface groups, the materials turn to exhibit semiconducting behavior. In addition, an impact of the number of the layers on the electronic properties is also considered.

The study was accomplished thanks to the funds allotted by the National Science Centre, Poland within the framework of the research project 'OPUS 18' no. UMO-2019/35/B/ST5/02538. Access to computing facilities of PL-Grid Polish Infrastructure for Supporting Computational Science in the European Research Space, and of the Interdisciplinary Center of Modeling (ICM), University of Warsaw are gratefully acknowledged.

[1] Zhonglu Guo, Jian Zhou, and Zhimei Sun, *Journal of Materials Chemistry A* **5** (45), 23530-23535 (2017)

[2] Mohammad Khazaei, Junjie Wang, Mehdi Estili, Ahmad Ranjbar, Shigeru Suehara, Masao Arai, Keivan Esfarjani, and Seiji Yunoki, *Nanoscale* **11** (23), 11305-11314 (2019)

[3] Yury Gogotsi and Babak Anasori, *ACS Nano* **13** (8), 8491-8494 (2019)

Optical properties of transition metal trichalcogenides MPX₃: a first principle study of 2D magnets

M. Rybak¹, T. Woźniak¹, P. F. Junior², P. Scharoch¹ and M. Birowska³

¹*Faculty of Fundamental Problems of Technology, Wrocław University of Science and Technology, Wybrzeże Wyspiańskiego 27, 50-370 Wrocław, Poland*

²*Institute for Theoretical Physics, University of Regensburg, 93040 Regensburg, Germany*

³*University of Warsaw, Faculty of Physics, Pasteura 5, 02-093 Warsaw, Poland*

Two-dimensional (2D) crystals have been recently extensively studied owing to their unique optoelectronic properties [1]. The family of 2D materials has grown considerable with new additions, such as transition metal trichalcogenides (TMTs) [2]. These materials exhibit wide range of bandgaps and intrinsic magnetism, presenting an unique opportunity to integrate optical functionalities with magnetism. The recent theoretical reports have demonstrated that MnPS₃ can be inferred indirectly using different polarization of light and exhibits a giant excitonic binding energy [3], pointing the possibility of usage in room-temperature optoelectronic devices.

Here, we present a comprehensive theoretical results of the optical properties of the series of antiferromagnetic MPX₃ monolayers (M=Mn, Ni, Fe, Co, and X=S,Se), in the framework of the density functional theory (DFT) within the GGA+U approach and spin-orbit interaction included (SOI). In particular, our results reveal that the effective mass of holes and electrons are smaller for the MPSe₃ compounds than MPS₃ materials and strongly depends on the Hubbard U. Moreover, the inclusion of the SOI does not affect the band edges and their curvatures, and hence, the effective masses. In the case of the AFM-Neel magnetic ordering, the inclusion of the SOI causes an in-equivalency of the pair of valleys (K⁺,K⁻), resulting in gaps difference at K⁺ and K⁻ up to 130 meV for U=5eV for MnPSe₃ structure. In addition, the 2D polarizabilities are up to 40 % greater in the case of MPSe₃ compounds than MPS₃ materials, and are much lower than corresponding values for widely examine TMD's. Finally, for the direct transitions we determine the optical selection rules revealing that the systems MnPS₃, MnPSe₃ and FePS₃ are optically active at K valleys.

The study was accomplished thanks to the funds allotted by the National Science Centre, Poland within the framework of the research project 'SONATA12' no. UMO-2016/23/D/ST3/03446. Access to computing facilities of TU Dresden ZIH for the project "TransPheMat", PL-Grid Polish Infrastructure for Supporting Computational Science in the European Research Space, and of the Interdisciplinary Center of Modeling (ICM), University of Warsaw are gratefully acknowledged.

[1] K. F. Mak, J. Shan, *Nat. Photonics* **10**, p. 216–226 (2016).

[2] B. L. Chittari *et al.* *Phys. Rev. B* **94**, 184428 (2016).

[3] M. Birowska, P.E.F. Junior, J. Fabian, J. Kuntzmann, *Phys. Rev. B* **103**, L121108 (2021).

Electric Field Modulation of GaN Transmittance in Terahertz Range

R. M. Balagula¹, L. Subačius¹, J. Jorudas¹, P. Prystawko², and I. Kašalynas¹

¹Center for Physical Sciences and Technology, Vilnius, LT-10257, Lithuania

²Institute of High Pressure Physics PAS, Warsaw, 01-142, Poland

Compact tunable sources of terahertz (THz) radiation remain a goal in many research fields. One of the options is to design a THz emitter based on a transit-time resonance effect in polar semiconductors. This effect can be treated as quasi-periodic electric-field-induced movement of electrons transforming an electron distribution function in momentum space into a needle-type shape. It is promoted in polar materials where the interaction between electrons and phonons is high, for example, GaN, InP. As of now the only direct experimental observation of the emission related to streaming effect has been achieved in millimeter-wave range in n-type InP crystal [1]. The observation of emission at the frequencies of several THz was theoretically predicted in GaN with Monte-Carlo simulations [2]. Recent measurements of hot-electron noise temperature behaviour were used to indirectly observe the periodic streaming motion in two-dimensional electron gas in GaN/AlGaN heterostructures [3]. The transit-time resonance effect can be observed also by indirect measurement of THz transmission (reflection) of incident radiation [4]. In this work we investigated the transmission of THz beam polarized along or orthogonally to the electric field direction with particular attention on fast signal modulation with applied electric field.

A 10 μm thick *n*-type doped GaN epilayer was grown on a semi-insulating GaN substrate. The Hall experiments, conducted on Van der Paw samples at room temperature, revealed the carrier density and mobility values of about $1 \times 10^{16} \text{ cm}^{-3}$ and $1000 \text{ cm}^2/\text{V}\cdot\text{s}$, respectively. Ohmic contacts were formed to apply pulsed electric field to the sample in a lateral direction. Current-voltage characteristics (*I/V*) were measured using the pulse width and repetition rate of several microseconds and tens of Hz, respectively, to prevent heating of the lattice. The superlinear section at low-to-moderate electric field regions, attributed to impurity breakdown, and the sublinear section in high electric fields were observed in our samples. A field dependence of electron mobility and concentration were investigated under assumption of full impurity ionization both at room temperature and in high electric fields. The transmission, reflection, and absorption spectra were modeled for the structure using transfer matrix method and measured in THz and MIR ranges using THz-TDS and FTIR spectrometers, respectively. Modulation of THz signals under pulsed electric field excitation of the GaN crystal was measured for two polarizations of probing radiation at selected frequencies of monochromatic THz source and fixed temperatures. The obtained results indicate a possibility of observation of the field-induced effects in polar semiconductors, related to orientation of electron distribution along electric field lines.

This work has received funding from European Social Fund (project No 09.3.3-LMT-K-712-19-0184 under the measure "Development of Competences of Scientists, other Researchers and Students through Practical Research Activities") under grant agreement with the Research Council of Lithuania (LMTLT).

- [1]. L.E. Vorob'ev, et al., *JETP Lett.*, vol. 73, pp. 219-222, 2001.
- [2]. P. Shiktorov, et al., *Phys. Status Solidi*, vol. 5, pp. 236-239, 2008.
- [3]. M. Ramonas, et al., *Appl. Phys. Lett.*, vol. 128, pp. 055702, 2020.
- [4]. G.I. Syngayivska and V.V. Korotyeyev, *Ukr. J. Phys.*, vol. 58, pp. 40-55, 2013.
- [5]. V.A. Shalygin, et al., "*J. Appl. Phys.*", vol. 106, p. 123523, 2009.

Structural and electrical analysis of the "buffer-free" AlGaIn/GaN on SiC heterostructure

J. Jorudas¹, P. Prystawko², M. Dub^{2,3}, A. Selskis¹, M. Skapas¹, P. Sai^{2,3},
M. Sakowicz^{2,3}, S. Romyantsev^{2,3}, W. Knap^{2,3}, I. Kašalynas¹

¹Center for Physical Sciences and Technology (FTMC), Saulėtekio 3, 10257 Vilnius, Lithuania

²Institute of High Pressure Physics PAS, ul. Sokołowska 29/37, 01-142, Warsaw, Poland

³CENTERA Laboratories, Institute of High Pressure Physics PAS, ul. Sokołowska 29/37, 01-142 Warsaw, Poland

Aluminum gallium nitride/gallium nitride (AlGaIn/GaN) high electron mobility transistor (HEMT) structures have been widely used in high power and high-frequency applications up to the THz frequency range. In order to reduce the density of threading dislocations and to provide an electrically isolating layer the standard HEMT structures usually contain thick acceptor doped GaN buffer. Recently developed "buffer-free" AlGaIn/GaN heterostructures on SiC substrate without the usage of thick GaN allow to avoid buffer-associated trapping effects and improve thermal management[1]–[3]. In this work, the structural and electrical properties of these heterostructure layers are investigated and compared with standard HEMT structures.

The heterostructure layers were grown on a 4" diameter, 500-μm-thick semi-insulating SiC substrate. The growth protocol consisted of a 2.4-nm GaN cap, a 20.5-nm Al_{0.25}Ga_{0.75}N barrier, and a 255-nm GaN channel deposited on a 62-nm high-quality AlN nucleation layer (NL) on SiC. The sheet resistance (R_{sh}) of the conductive two-dimensional electron gas (2DEG) channel was $380 \pm 10 \Omega/\square$. The structural and morphological analysis were performed under transmission electron microscope (TEM) and atomic force microscope (AFM). For example, AFM measurements revealed that the characteristic RMS roughness was as small as $S_q = 0.56 \text{ nm}$ over the scan area of $1.5 \mu\text{m}^2$. TEM pictures demonstrated high structural quality of the layers and high quality of the interface between AlN NL and SiC substrate and sharp interface between Al_{0.25}Ga_{0.75}N barrier, and GaN channel layers. To determine electrical properties, test devices including Schottky barrier diodes, HEMTs and various test components were fabricated on heterostructures processing Ti/Al/Ni/Au and Ni/Au as for ohmic and Schottky contacts, respectively. Hall measurements using Van der Pauw devices revealed a thermally stable electron density at $N_{2DEG} = 1 \times 10^{13} \text{ cm}^{-2}$ but with mobility values varying from $\mu = 1.7 \times 10^3 \text{ cm}^2/\text{V s}$ to $\mu = 1.0 \times 10^4 \text{ cm}^2/\text{V s}$ at 300 K and 77 K, respectively. Moreover, recent study on the electrical and noise properties of Schottky barrier diodes and HEMTs, developed of this "buffer-free" AlGaIn/GaN material, has revealed the improved thermal stability and relatively low trap density[4], [5]. These results together in correlation with good structural characteristics of this novel material make it suitable for high-frequency and high-power applications.

The work was supported by the Research Council of Lithuania under Polish-Lithuanian initiative DAINA through the "TERAGANWIRE" project (grant No. S-LL-19-1).

- [1] J.-T. Chen *et al.*, *Appl. Phys. Lett.*, **113**, 4 (2018).
- [2] H. Chandrasekar *et al.*, *IEEE Electron Device Lett.*, **39**, 10 (2018).
- [3] G. J. Riedel *et al.*, *IEEE Electron Device Lett.*, **30**, 2 (2009).
- [4] P. Sai *et al.*, *Appl. Phys. Lett.*, **115**, 18 (2019).
- [5] J. Jorudas *et al.*, *Micromachines*, **11**, 12 (2020).

AlGa_{0.2}N composition correction under variable ammonia flow and pressure conditions in MOVPE reactor

K. Moszak^{1,2}, W. Olszewski^{1,3}, D. Majchrzak^{1,2}, D. Pucicki^{1,4}, J. Osiecki¹,
J. Serafińczuk^{1,3}, D. Hommel^{1,4}

¹ Łukasiewicz Research Network – PORT Polish Center for Technology Development, Stabłowicka 147, 54-066 Wrocław, Poland

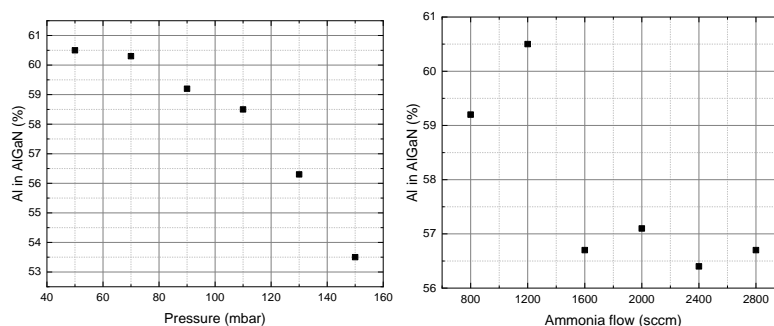
² Institute of Low Temperature and Structure Research PAS, Okólna 2, 50-422 Wrocław, Poland

³ Institute of Experimental Physics, University of Wrocław, Maksa Born'a 9, 50-204 Wrocław, Poland

⁴ Department of Nanometrology, Wrocław University of Science and Technology, Janiszewskiego 11/17, 50-372 Wrocław, Poland

Aluminium gallium nitride (AlGa_{0.2}N) epitaxially grown layers with a high concentration of aluminium are successfully used in many kinds of optoelectronic devices e.g. deep ultraviolet light-emitting diodes (DUV-LEDs) [1]. The complexity of the nowadays device structures often makes the growth more complicated, including fast and often changes of parameters growth of following layers. Precise control of AlGa_{0.2}N composition in a successive layer of the device is crucial for its proper operation. Therefore AlGa_{0.2}N composition must be controlled, independent of the changing of the remaining precursor ratio, on the total flow of ammonia always supplied in excess and also independent on the current pressure in the reactor. Any uncontrolled deviation of aluminium concentration in AlGa_{0.2}N layers can affect the series resistance of the device, optical losses due to light reabsorption, electrical contacts characteristics, luminescence characteristics and many others.

In this work, we present the study of the AlGa_{0.2}N composition deviation under variable ammonia flow and pressure conditions. The MOVPE growth was proceed in 3x2' FT-CCS reactor on sapphire wafers. The sets of the AlGa_{0.2}N/AlN heterostructures were grown in stable temperature conditions (1072-1078°C). The characteristic of the pressure dependence of AlGa_{0.2}N composition was studied in the pressure range from 50 mbar to 150 mbar (Fig.1). In this pressure range, besides the 7% change in the composition of the AlGa_{0.2}N layer change of the growth rate (from 0,20 to 0,14 nm/min) was observed as well. The ammonia flow rate was varied from 800 to 2800 sccm and the difference in composition (4%) and also in growth rate (from 0,23 to 0,22 nm/min) of AlGa_{0.2}N were noticed. The AlGa_{0.2}N growth rate was determined by in-situ reflectance measurements. HRXRD and AFM measurements were carried out for both attempts to compare the structural quality of the samples and determine the Al percentage. As a result of the study, characteristics were obtained which take into consideration corrections to maintain the growth of the layers under optimal conditions and to obtain the desired composition of the deposited layers.



[1] H. Hirayama, *et al.*, *Phys. Stat. Sol.*, **206**(6), (2009)

DFT based modeling of point defect diffusion across the $\text{In}_{0.125}\text{Ga}_{0.875}\text{N}/\text{GaN}$ and $\text{In}_{0.25}\text{Ga}_{0.75}\text{N}/\text{GaN}$ interfaces

R. Hrytsak^{1,2}, P. Kempisty¹, M. Leszczynski¹, and M. Sznajder²

¹ Institute of High Pressure Physics, Polish Academy of Sciences, Warsaw, Poland

² College of Natural Sciences, Institute of Physics, University of Rzeszow, Poland

Point defects such as impurities or vacancies are common source of non-radiative recombination centers in semiconductor optoelectronic devices. Their presence in the active regions (quantum wells-QWs) of the light emitting diodes (LEDs) strongly influences optical properties of these emitters. In the case of InGaN QWs used in blue/green LEDs many efforts have been done to increase their internal quantum efficiency by e. g., reducing the point defect density, improving the GaN surface morphology, manipulating the strain state of QW's, or preventing decomposition of QW's caused by migration of indium atoms and formation of metallic clusters, what is detrimental to luminescence of LEDs [1]. Recently, it has been shown experimentally that point defects (most probably gallium vacancies) induce decomposition of InGaN quantum wells (QWs) at high temperatures [2].

In the present paper, by means of SIESTA program, we performed DFT modeling of point defects migration through the $\text{In}_x\text{Ga}_{1-x}\text{N}/\text{GaN}$ ($x=0.125, 0.25$) heterointerfaces in order to find the preferred directions of such migration and to check possibilities for accumulation of certain defects, what can support experimental findings of paper [2]. We studied a motion of nitrogen, gallium, and indium vacancies (V_N , V_{Ga} , V_{In}) in various charge states, as well as complexes consisting of substitutional metal atom and metal vacancy. The $\text{In}_x\text{Ga}_{1-x}\text{N}/\text{GaN}$ interface was represented by means of a superlattice model with the growth direction along hexagonal c axis. The GaN substrate with a lateral unit cell 4×4 was represented by means of 6 double Ga-N monolayers, while the InGaN material having 6 double Ga(In)-N mixed layers was strained to the lateral lattice constant of GaN. Inside each metal layer of InGaN material substitutional In atoms were placed regularly into lattice sites. Next, by means of procedure described in [3] we calculated heights of the energy barriers related to the migration of the studied defects, utilizing the Nudged Elastic Band (NEB) method.

We have found that there is an energetic "hierarchy" of barriers for the migration of individual defects along c axis of the $\text{In}_x\text{Ga}_{1-x}\text{N}/\text{GaN}$ heterointerface, the lowest migration barrier exhibits indium vacancy V_{In} , the next one is the barrier related to the migration of gallium vacancy V_{Ga} , and the highest barrier is observed for the nitrogen vacancy V_N . With the increasing concentration of indium atoms in the $\text{In}_x\text{Ga}_{1-x}\text{N}$ structure a preferred migration direction of the charged indium vacancies V_{In}^{3-} is observed, i.e., from the interface to the interior of the $\text{In}_{0.25}\text{Ga}_{0.75}\text{N}$ material. A charged $\text{In}_{Ga}V_{Ga}^{3-}$ complex overcomes lower potential barriers near the $\text{In}_{0.125}\text{Ga}_{0.875}\text{N}/\text{GaN}$ and $\text{In}_{0.25}\text{Ga}_{0.75}\text{N}/\text{GaN}$ interfaces than those of single V_{Ga}^{3-} vacancy. The same concerns charged nitrogen vacancy V_N^{3+} formed near the indium dopant atom's sublattice, while crossing the respective interfaces. The formation and migration of charged indium vacancy V_{In}^{3-} and the $\text{In}_{Ga}V_N^{3+}$ complex in the preferred directions lead to an increased concentration of indium atoms in the vicinity of the interface, what can be a physical reason for the decomposition of quantum wells at the $\text{In}_x\text{Ga}_{1-x}\text{N}/\text{GaN}$ interface, starting from the first quantum well.

[1] Z. Li, J. Liu, M. Feng *et al.*, *Appl. Phys. Lett.* **103**, 152109 (2013).

[2] M. Grabowski, E. Grzanka, S. Grzanka *et al.*, *Sci. Rep.* **11**, 2458 (2021).

[3] R. Hrytsak, P. Kempisty, E. Grzanka, *et al.*, *Comput. Mater. Sci.*, **186**, 110039 (2021).

Tunnel junction for III-Nitride devices with inverted polarization

M. Żak, H. Turski, G. Muziol, M. Siekacz, K. Nowakowski-Szkudlarek, M. Chlipala and C. Skierbiszewski

Institute of High Pressure Physics PAS, ul. Sokołowska 29/37, Warsaw, Poland

III-Nitrides optoelectronic devices are mainly grown on the c-plane Ga-polar substrates. Such structures are characterized by low injection efficiency due to the undesired built-in piezoelectric field in the active region. High injection efficiency is characteristic to the structures grown on the N-polar substrates, but such growth is much more demanding. On the other hand, tunnel junction (TJ) can be stacked with III-nitride optoelectronic devices to form n-p-n light emitting structure with low on-resistance [1]. Such TJ can also be grown first on the Ga-polarity of n-type GaN substrate, to provide a platform for p-n device in which the built-in piezoelectric fields are inverted. Such approach can effectively mimic the N-polar devices [2].

For TJs grown on the top of the structure, the piezoelectric field and electric field caused by dopants have the same sign and both increases tunneling probability [1]. In the case of TJ buried below LED, the piezoelectric field inside the TJ is subtracted from this electric field caused by doping, thus total tunneling current is decreased. On the other hand, when material inside the TJ is changed from InGaN to AlGaN the piezoelectric field enhances the tunneling probability [3]. Nevertheless, the higher bandgap and effective masses of carriers in AlGaN, have a negative impact on the tunneling process.

In this work we theoretically investigate properties of TJ dedicated to devices with inverted polarity with previously developed tunneling model [1]. The interplay between piezoelectric field and doping is analyzed for varies composition of symmetrically doped AlGaN and InGaN sandwiched between p- and n-type GaN doped at the level of 5×10^{19} at/cm³. On Fig. 1 we present an initial calculation of the voltage drop appearing on TJ at 1 kA/cm² for InGaN and AlGaN alloys as a function of thickness of these layers. We see that with Mg and Si doping at level of 10^{20} at/cm³, the benefits from smaller energy bandgap and effective masses of InGaN alloys overcomes unfavorable direction of built-in piezoelectric field. The theoretical predictions will be discussed in the light of experimental data obtained with TJ grown by plasma-assisted molecular beam epitaxy.

Acknowledgments: This work was supported partially by TEAM-TECH POIR.04.04.00-00-210C/16-00 and HOMING POIR.04.04.00-00-5D5B/18-00 projects of the Foundation for Polish Science co-financed by the European Union under the European Regional Development Fund and the Polish National Centre for Research and Development Grants LIDER/29/0185/L-7/15/NCBR/2016 and LIDER/35/0127/L-9/17/NCBR/2018 and National Science Center Poland within grant No. 2019/35/D/ST3/03008.

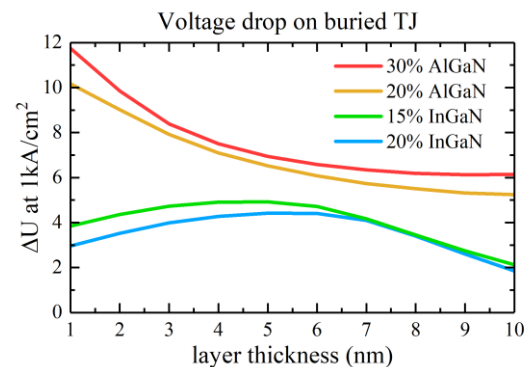


Fig. 1. The voltage drop on buried tunnel junction n-GaN/n⁺-(Al,In)GaN/p⁺-(Al,In)GaN/p-GaN as a function of total thickness of AlGaN or InGaN layers. The AlGaN and InGaN is symmetrically doped at 10^{20} at/cm³, while GaN at 5×10^{19} at/cm³.

- [1] M. Żak et al., *Phys. Rev. Appl.* **15**, 024046 (2021).
- [2] H. Turski et al., *ECS J. Solid State Sci. Technol.* **9**, 015018 (2020).
- [3] K. Lee et al., *Appl. Phys. Lett.* **117**, 061104 (2020).

Size dependence of Internal Quantum Efficiency (IQE) in nitride micro-LEDs with tunnel junction grown by PAMBE

J. Slawinska^{*1}, C. Skierbiszewski¹, M. Siekacz¹, G. Muziol¹, M. Żak¹, M. Hajdel¹, K. Nowakowski-Szkudlarek¹, A. Feduniewicz-Zmuda¹

¹*Institute of High Pressure Physics, Polish Academy of Sciences, Warsaw, Poland*

^{*}email: julia@unipress.waw.pl

In recent years nitride LEDs have been broadly employed in general illumination and backlight units due to their higher luminous efficacy and longer lifetime compared to conventional light sources. Depending on the chip size μ LEDs find various application like smartwatches or smartphones displays with high brightness. Although the operating principle for conventional broad-area LEDs and μ LEDs remains unchanged, the processing of a μ LEDs involves additional step. It generates new challenges.^[1]

The innovative method of μ LEDs fabrication is presented. The light emission area was defined by size of the tunnel junction (TJ) embedded inside diode. The epitaxial structures presented here were grown entirely by plasma assisted molecular beam epitaxy (PAMBE) on (0001) bulk GaN crystals. The PAMBE grown LED structure emitting light at 450 nm was capped with TJ (40 nm) and 100 nm n-type GaN. The emission size of μ LEDs arrays was defined by shallow He⁺ implantation (300 nm) or reactive ion etching (RIE) of n-type GaN and TJ region. The ion implantation and RIE deteriorate p-type conductivity and significantly increases the TJ resistance in the areas outside μ LEDs. The regrowth of 200 nm of high conductive n-type GaN enhances the current spreading at the top of the arrays of μ LEDs and allow to apply the side contacts to device. We demonstrate that the array of μ LEDs emit light only in TJ regions which were masked during ion implantation or RIE.^[2]

The electroluminescence of μ LEDs arrays with μ LEDs diameter from 20 μ m down to 2 μ m were investigated. We found that the Internal Quantum Efficiency (IQE) decreases as diameter of μ LEDs is reduced. In conventional μ LEDs size dependent decrease of IQE was justified by creation of defects on the walls of quantum wells (while deep etching to define μ LEDs size) causing increase of non-radiative recombination. In the case of our μ LEDs with TJ, the quantum well is untouched during fabrication (shallow etching). Although size dependent decrease of IQE can be observed. Nonetheless this effect can have a different justification. Details will be discussed.^[3]

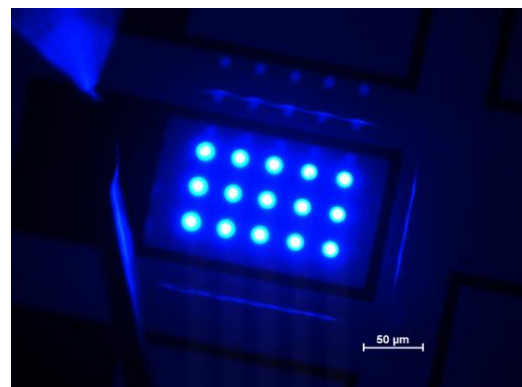
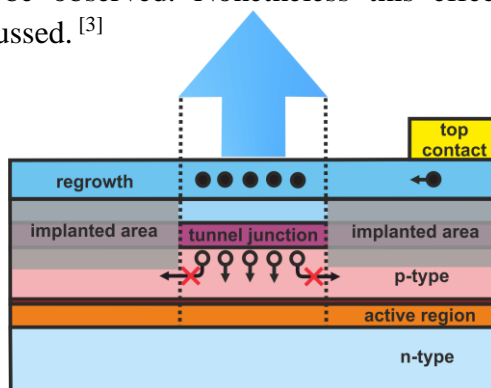


Fig. 1: Concept of implanted microLED with tunnel junction.

Fig. 2: Electroluminescence of 10 μ m microLED arrays

[1] T.Wu et al., Appl. Sci. 8, 1557 (2018)

[2] C. Skierbiszewski et al., Appl. Phys. Express 11, 034103 (2018)

[3] J.Kou et al., Optics Express 27, 358049 (2019)

Acknowledgements: This work was supported by TEAM-TECH POIR.04.04.00-00-210C/16-00 Project of the

Foundation for Polish Science cofinanced by the European Union under the European Regional Development Fund

Porous GaN for cladding layers in nitride edge emitting laser diodes

**M. Sawicka¹, N. Fiuczek¹, G. Muziol¹, M. Hajdel¹, A. Feduniewicz-Żmuda¹,
K. Nowakowski-Szkudlarek¹, M. Żak¹, P. Wolny¹, H. Turski¹, M. Siekacz¹ and
C. Skierbiszewski¹**

¹ *Institute of High Pressure Physics PAS, Sokołowska 29/37, Warsaw, Poland*

One of the challenges in nitride laser diodes fabrication is the optimal design of a cladding layer that provides sufficient refractive index contrast to prevent light leakage to GaN substrate. On one hand, thick AlGaIn layers are required because of a relatively low refractive index contrast between GaN and AlN and on the other hand, thick layers are undesired because they pose a risk of relaxation by cracking. Several different material solutions to this problem have been proposed. One of them is InAlN of 18%In that is in-plane lattice matched to GaN [1], but its epitaxy is a challenge of its own. Second, recently proposed solution is porous GaN [2]. The advantages of porous GaN, apart from no issues with strain, are low refractive index, n , and its high tunability with porosity because it is in fact a composite of air and GaN, where $n_{\text{air}} = 1$ of $n_{\text{GaN}} = 2.5$. Therefore, porous GaN can be used for claddings instead of AlGaIn to avoid the issues with strain and more effectively act as a cladding layer.

This work presents the electrochemical etching of GaN:Si layers as a method to obtain porous material. Si doping level and applied bias are the key parameters to control pore size and porosity value [2]. We demonstrate porous GaN used for cladding layers in nitride edge emitting laser diodes. The structures are grown on bulk GaN (0001) substrates by plasma-assisted molecular beam epitaxy (PAMBE) and then undergo dedicated processing in order to introduce porosity in the bottom cladding, as presented in Figure 1.

We will compare refractive index profiles and expected near-field patterns of laser diodes with different material solutions in the bottom claddings: AlGaIn, InAlN and porous GaN. We will also present perspectives for the development of nitride laser diodes with porous layers.

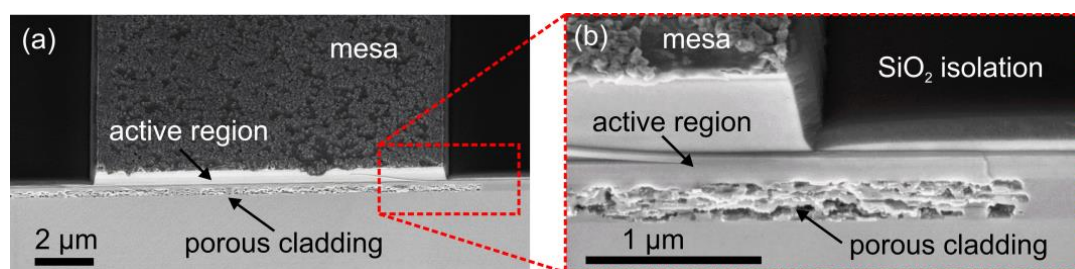


Figure 1. SEM images of a cleaved mirror of a laser diode structure with porous bottom cladding fabricated by electrochemical etching of highly doped GaN:Si.

This work was supported partially by National Science Center Poland within grant no. 2019/35/D/ST5/02950 and is part of POIR.04.04.00-00-4463/17-00 project of the Foundation for Polish Science co-financed by the European Union under the European Regional Development Fund

- [1] A. Castiglia et al. Applied Physics Letters, 94 (2009)
- [2] G. Juan et al., Proc. of SPIE Vol. 9748, 97480Q (2016)
- [3] M. Sawicka et al., Nanoscale 12, 6137 (2020)

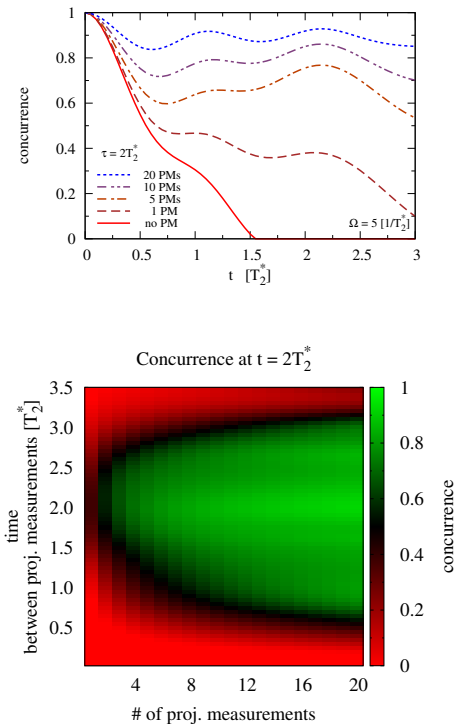
Retardation of Quantum Correlation Decay of Two Spin Qubits by Quantum Measurements

Igor Bragar

Institute of Physics, Polish Academy of Sciences, al. Lotników 32/46, Warszawa, Poland

We study a system of two electron spins each interacting with its small nuclear spin environment (NSE), which is a prototype system of two quantum dot (QD) spin qubits, where number of nuclear spins can be up to a million. In such a system it is possible to initialise, to coherently manipulate, to entangle and to read out electron spins only, the NSEs of QDs are beyond of direct experimentalists' control [1, 2].

The two electron spins subsystem (TESSS) initially being in an entangled state in course of time evolution loses its coherences and quantum correlations due to the Fermi contact hyperfine coupling with NSEs. If one looks at the density matrix of the whole system $\hat{\rho}(t)$, it becomes evident that quantum correlations (coherences) initially present solely in TESSS do not simply disappear, but changes into the quantum correlations between TESSS and its NSEs. With connection to that one may propose a way to counteract decay of entanglement in TESSS by performing some manipulations with TESSS (the subsystem to which experimentalists have an access), e.g. repeatable quantum projective measurements (PMs) of TESSS. Unlike in quantum Zeno effect, the goal of proposed manipulations is not to freeze TESSS in its initial state and to preclude any time evolution of the state by infinitely frequent quantum measurements. Instead of that, performing a few cycles of free evolution of the system for a some time τ followed by a quantum measurement of TESSS with subsequent postselection of TESSS state (the same as the initial one) produces quantum correlations in NSEs and also restores the quantum correlations in TESSS. By numerical calculation of the system evolution (full density matrix $\hat{\rho}(t)$) we show that in contrast to a fast decay of TESSS entanglement on timescale $\approx T_2^*$ (shown in Fig. 1 of [3] or [4]), performing a few cycles of evolution of initially entangled two electron spins interacting with their NSEs followed by quantum measurement performed on TESSS gradually build up coherences in the entire system and the rest decay of quantum correlations of TESSS may be significantly slowed down for specific cycle durations τ and numbers of the performed cycles (see Fig. 1).



- [1] D. Kim, S. G. Carter, A. Greulich, A. S. Bracker, and D. Gammon, *Nature Phys.* **7**, 223–229 (2011).
- [2] K. De Greve, D. Press, P. L. McMahon, and Y. Yamamoto, *Rep. Prog. Phys.* **76**, 092501 (2013).
- [3] P. Mazurek, K. Roszak, R. W. Chhajlany, and P. Horodecki, *Phys. Rev. A* **89**, 062318 (2014).
- [4] I. Bragar and L. Cywiński, *Phys. Rev. B* **91**, 155310 (2015).

Figure 1: Plot: time evolution of entanglement (concurrence) of TESSS initially being in the Bell state $\hat{\rho}(0) = |\psi_-\rangle\langle\psi_-|$. Map: concurrence of TESSS calculated for $\hat{\rho}(t = 2T_2^*)$. Electron Zeeman splitting $\Omega = 5 [1/T_2^*]$. NSEs consist of 5 spins $\frac{1}{2}$ each.

Multi-band envelope-function theory of fine structure splitting in semiconductor nanostructures

Mateusz Krzykowski* and Paweł Machnikowski

Department of Theoretical Physics, Wrocław University of Science and Technology,
Wybrzeże Wyspiańskiego 27, 50-370 Wrocław, Poland

In this contribution, we study the exciton fine structure splitting (FSS) using multi-band envelope-function theory, explicitly accounting for band-mixing of carrier states localized in semiconductor nanostructures. We expand the exchange interaction Hamiltonian into short-range (SR) and long-range (LR) contributions and conduct thorough analysis, splitting them further in the terms of Laplace expansion (for SR) and multipole expansion (for LR). Compared to the single-band theory [1, 2], which accounts only for the coupling between heavy hole and conduction bands, our model includes all the relevant terms depending on the band-mixing. This allowed us to account for features present in experimental data not accounted for by the single-band model.

We study the model by simulating a self-assembled, lens-shaped InGaAs quantum dot (QD). Strain and piezoelectric field are calculated in the continuous medium approximation. Electron and hole envelope functions are obtained using 8-band $\mathbf{k}\cdot\mathbf{p}$ theory, which explicitly accounts for band-mixing. More details about the model can be found in [3]. We calculate exciton states using configuration interaction based on single-state envelope functions.

In this work we demonstrate the importance of band-mixing for FFS. This approach not only introduces dark exciton splitting (DS), completely absent in the single-band model, but also significantly modifies bright exciton spilling (BS) as well as bright-dark exciton splitting (BDS). For example the monopole LR term, strongly dependent on the band-mixing, introduces a significant contribution of $\approx 15\%$ to the BDS with reverse sign in relation to the leading term present in the single-band model. We also study the effects of d -shell admixture to the valence band.

We study the FSS as a function of QD elongation and external fields. This choice of parameters is motivated by the fact that the presence or absence of DS and BS depends on the symmetry of the system. Due to piezoelectric effect and QD asymmetry in growth direction we observe slight dark and bright exciton splittings even in circular QDs, but these effects are small compared to elongated systems. We also compare our results for axial electric field with recent results [4] and find that due to the interplay between different contributions to the exchange interaction it is practically impossible to completely cancel dark nor bright exciton splittings.

[*] Electronic address: mateusz.krzykowski@pwr.edu.pl

- [1] T. Takagahara, *Phys. Rev. B* **47**, 4569 (1993).
- [2] E. Kadantsev and P. Hawrylak, *Phys. Rev. B* **81**, 45311 (2010).
- [3] K. Gawarecki, *Phys. Rev. B* **97**, 235408 (2018).
- [4] M. Zieliński, *Phys. Rev. B* **102**, 245423 (2020).

Spread of Correlations in Highly Disordered System with Long-Range Coupling

K. Kawa, P. Machnikowski

Wrocław University of Science and Technology, 50-370, Wrocław, Poland

In recent years, much effort has been devoted to investigating the existence of the Lieb-Robinson [1] boundary on speed for non-relativistic quantum systems in models with interactions decreasing with some power of the distance between atoms, $\propto 1/r^\mu$ [2-5]. Such models correspond to physical systems such as systems of trapped ions, Rydberg atoms, ultracold atoms, or superconducting qubits. Limited velocity of propagation in such a systems was proved mathematically [4] for $\mu > 2d + 1$ (beyond some particular cases, where μ can be even smaller [5]).

We study the evolution of correlations arising after a local quench, i.e., rotation of one spin in a ferromagnetic spin chain. The coupling between the spins is long-range, decreasing as a power law of distance, $\propto 1/r^\mu$. In addition, the spins experience a random potential with a large standard deviation (strong disorder regime). In a strongly disordered system, only the direct coupling to the initially excited atom becomes relevant. This "central atom model" allows us to find an approximate solution to the full model. The correlation at a given node increases in three phases (see Fig. 1(b)). First, there is an increase with the square of time, then, at some point in time (inversely proportional to the strength of the disorder) there is a change in the growth trend to linear over time. Finally, there is a saturation of correlation for time proportional to the inverse of the coupling to the central node. It is possible to find the time for which a given correlation value is reached (see Fig. 1(c)). In this way, we can determine how the correlation "wave front" propagates. Because of two growth phases (before saturation occurs) the wave front changes its time dependence from $r(t) \propto t^{1/\mu}$ to $r(t) \propto t^{1/2\mu}$. A special case is $\mu = 1$, where propagation is initially a ballistic motion (i.e. light cone emerges) and then it becomes standard diffusion. For $\mu > 1$ propagation is always sub-ballistic and it indicates the propagation velocity decreasing in time.

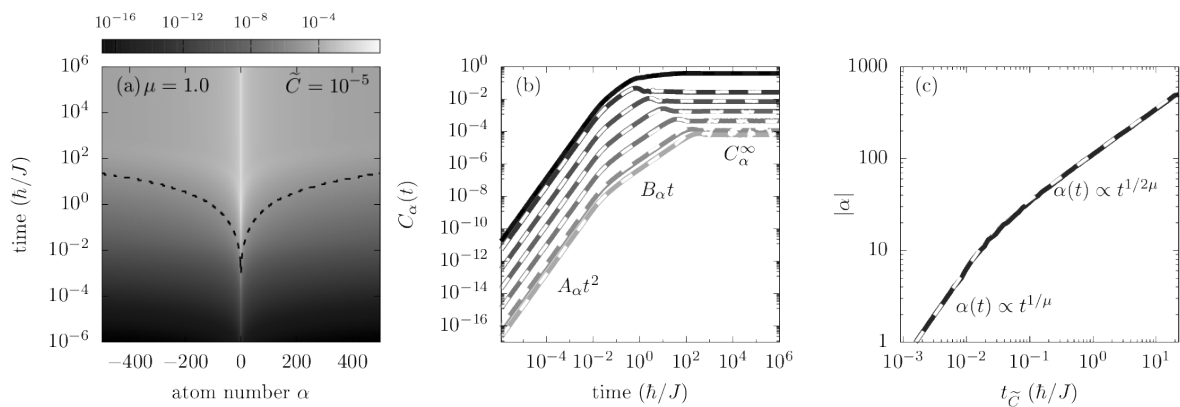


Figure 1

- [1] E. H. Lieb and D. W. Robinson, *Commun. Math. Phys.* **28**, 251 (1972)
- [2] C. F. Chen and A. Lucas, *Phys. Rev. Lett.* **123**, 250605 (2019).
- [3] L. Colmenarez and D. J. Luitz, *Phys. Rev. Research* **2**, 043047 (2020).
- [4] T. Kuwahara, K. Saito, *Phys. Rev. X* **10**, 031010 (2020).
- [5] M. C. Tran et al., *Phys. Rev. X* **10**, 031009 (2020).

An atomic scale study of isoelectronic dopant pairs in GaAs using X-STM and DFT

T.J.F. Verstijnen¹, D. Tjeertes¹, A. Rice², K. Alberi², M.E. Flatté^{3,1} and P.M. Koenraad¹

¹ Department of Applied Physics, Eindhoven University of Technology, P.O. Box 513, 5600 MB Eindhoven, The Netherlands,

² National Renewable Energy Laboratory, Golden, CO 80401, [USA](#),

³ Department of Physics and Astronomy, University of Iowa, Iowa City, Iowa 52242, [USA](#)
Corresponding author: t.j.f.verstijnen@tue.nl

Isoelectronic doping of GaAs with Bi can be used to generate longer wavelength devices on GaAs substrates. The Bi dopants lower the size of the band gap of GaAs by shifting up the valence band maximum (VBM). Due to this shift of the VBM and spin-orbit split-off band (SO), the Auger recombination losses are also suppressed. Incorporating large amounts of Bi dopants in GaAs is difficult, however, due to the low Ga-Bi reactivity and the strong tendency of Bi to segregate. One way of influencing the Bi incorporation in GaAs is co-doping of the material with N. Another reason for co-doping the material with N dopants is the fact that N doping of GaAs lowers the size of the band gap by lowering the conduction band maximum (CBM). This means that in a co-doped region, both the electrons and holes are confined, which enhances recombination.

Here the interaction between Bi and N dopants in GaAs is studied using cross-sectional scanning tunneling microscopy (X-STM) and density functional theory (DFT). Specifically, the occurrence of the various nearest neighbor (NN) pairs are studied in order to better understand the interaction between the dopants. Using DFT, both bulk and growth surface simulations of GaAs doped with Bi and/or N are performed. The bulk calculations predict Bi-Bi and N-N anti-clustering and Bi-N clustering. Through dopant pair counting of the observed Bi-Bi pairs found in X-STM measurements of GaAs:BiN it is concluded however that a large amount of first NN Bi-Bi pairs is present in GaAs:Bi. Another observation from these measurements is that a relatively low amount of fourth NN Bi-Bi pairs is present in GaAs:Bi. Simulations of Bi-Bi pairs in the (001) growth surface of GaAs show that these first NN Bi-Bi pairs are likely to be formed during the growth. Since the first and fourth NN Bi-Bi pair visible in our X-STM measurements are both situated on top of the (001) growth surface, the fourth NN Bi-Bi pairs are likely converted into first NN Bi-Bi pairs during the growth of the material.

A search for potentially valuable thermoelectric materials over 18-electron half-Heusler alloys

Kaja Bilińska, Maciej J. Winiarski

*Institute of Low Temperature and Structure Research, Polish Academy of Sciences,
Okólna 2, 50-422 Wrocław, Poland*

According to the interest in the 18-valence-electron half-Heusler (hH) compounds and recent investigations of their thermoelectric properties [1-3], a search of wide spectrum for hH semiconductors was performed [4]. The elements considered here do follow the periodic table groups: III (Sc, Y, La, Ga, In), IV (Ti, Zr, Hf), V (V, Nb, Ta), VIII (Fe, Ru, Os), X (Ni, Pd, Pt), XIV (Ge, Sn, Pb), and XV (As, Sb, Bi). The structural and electronic properties of over 150 cubic hH phases formed by these elements were investigated within the density functional theory (the GGA and modified Becke-Johnson GGA approaches) in the following schemes: III-X-XV (e.g. ScNiSb), IV-X-XIV (e.g. HfNiSn), IV-IX-XV (e.g. HfCoSb), V-IX-XIV (e.g. NbCoSn), V-VIII-XV (e.g. NbFeSb).

Among over 150 hH alloys, some compounds with metal character and few topological insulators were predicted, including one novel TI (LuPdAs). Finally, 50 new semiconductor 18-electron hH systems were found, wherein 24 followed the '10 $k_B T$ rule'. One may assume that the novel 24 18-electron hH phases following the '10 $k_B T$ rule' are promising materials for further investigations of thermoelectric characteristics.

Calculations were performed in Wrocław Center for Networking and Supercomputing (Project no. 158).

- [1] M. J. Winiarski, K. Bilińska, D. Kaczorowski, K. Ciesielski, *Journal of Alloys and Compounds*, 762, 901-905, **2018**.
- [2] M. J. Winiarski, K. Bilińska, *Intermetallics*, 108, 55-60, **2019**.
- [3] M. J. Winiarski, K. Bilińska, *Acta Physica Polonica A*, 138, 533-538, **2020**.
- [4] K. Bilińska, M. J. Winiarski, *not yet published*

The magnetic properties of the iron phthalocyanine molecule on the Ti₂C MXenes layer

Aleksei Koshevarnikov¹, Tomi Ketolainen¹, Jacek A. Majewski¹

¹*Faculty of Physics, University of Warsaw, ul. Pasteura 5, Warsaw, Poland*

Transition metals - phthalocyanines (TMPc's) are perspective molecules forming on suitable substrates hybrid systems that potentially could be implemented as active parts of spintronic devices. The choice of substrate affects the magnetic properties of TMPc's. MXenes, novel 2D materials, were not studied yet as substrate part of such hybrid systems. Here, we report the results of theoretical studies of the iron phthalocyanine (FePc) molecule on the Ti₂C surface. Special attention is paid to the issues of structural optimization and magnetic characteristics of this complex. Various magnetic configurations of this system are considered. The ability of the surface to assume stable ferromagnetic and antiferromagnetic states and the orientation change of the FePc magnetic moment give rise to four different configurations of the system exhibiting various properties. The significant ferromagnetic interaction between the iron atom and the upper titanium layer plays important role in the reorientation of the iron atom magnetic moment. We also analyze a model of the system in which the FePc molecule is in a quintet state (the ground state of an isolated molecule is a triplet). All calculations have been performed using density functional theory employing the plane waves and pseudopotentials as implemented in the Quantum Espresso numerical package.

Acknowledgement: This research has been supported by the NCN grant OPUS-12 (UMO-2016/23/B/ST3/03575) and OPUS-16 (UMO-2018/31/B/ST3/03758).

Self-consistent and External Electric Field Calculations for Crystal Phase Quantum Dots

Martyna Patera¹, Piotr T. Róžański¹, and Michał Zieliński¹

¹*Institute of Physics, Faculty of Physics, Astronomy and Informatics, Nicolaus Copernicus University in Toruń, Grudziądzka 5, 87-100 Toruń, Poland*

Crystal phase quantum dots are type II systems in which electrons are confined in a small section of zinc blende material, whereas holes are delocalized in a surrounding wurtzite nanowire. The transition between zinc blende and wurtzite phases defines the potential that binds excitons [1]. In this work, we present preliminary results of excitonic calculations for these nanostructures, which account for the influence of an external electric field. Solving this problem is a formidable challenge for many reasons. From a modeling point of view, these are demanding numerical calculations involving one million of atoms or more. In fact, a state-of-the-art approach [2,3] in which the empirical tight-binding method is coupled directly with the configuration interaction method fails in this case. This is due to the fact that the single particle states obtained from the tight-binding method form a poor basis for the following many-body calculation. Our solution of this problem is to use a multi-configurational self-consistent approach, in which the electron-hole interactions are accounted for prior to applying the electric field. This approach allowed us to efficiently and accurately treat the effect of an external electric field on excitonic spectra. However, this approach is not limited to crystal phase quantum dots, but may also find applications in atomistic modeling of other nanostructures, such as transition metal dichalcogenide layers or phosphorous multi-dopant systems in silicon.

- [1] M. Bouwes Bavinck, K. D. Jöns, M. Zieliński, G. Patriarche, J.-C. Harmand, N. Akopian, and V. Zwiller, *Nano Lett.* **16**, 1081 (2016).
- [2] M. Zieliński, M. Korkusiński, and P. Hawrylak, *Phys. Rev. B* **81**, 085301 (2010).
- [3] M. Zieliński, *Phys. Rev. B* **86**, 115424 (2012).

DMRG and Monte Carlo Studies of CrI₃ Phase TransitionsBartosz Rzepkowski¹, Michał Kupczyński¹, Paweł Potasz², Arkadiusz Wójs¹¹*Department of Theoretical Physics, Faculty of Fundamental Problems of Technology, Wrocław University of Science and Technology, PL-50370 Wrocław, Poland*²*Institute of Physics, Faculty of Physics, Astronomy and Informatics Nicolaus Copernicus University, ul. Grudziadzka 5, 87-100 Toruń, Poland*

The monolayer of CrI₃ has been reported to exhibit the ferromagnetic order, with a Curie temperature of 45 K and off-plane easy axis, which has attracted much attention in the community of condensed matter physics. Here we study the nature of phase transitions in the XXZ Hamiltonian on a honeycomb lattice, which can effectively model CrI₃, with two parameters, λ - symmetric exchange anisotropy and D - the single ion anisotropy. In our analysis we use the Density Matrix Renormalization Group method (DMRG) and compare results with classical models predictions. These results are presented in Fig. 1. The main conclusion is that prediction of the magnetic ordering of the Hamiltonian's ground state agrees within an entire range of a parameter space.

Using classical Monte Carlo simulations we estimate the Curie temperature for CrI₃ (for a parameter set marked with a red star in Fig. 1), by finding the peak of magnetic susceptibility (given in Fig. 2), and obtain the value $T_c = 49.7$ K, which is close to the experimental result of 45 K.

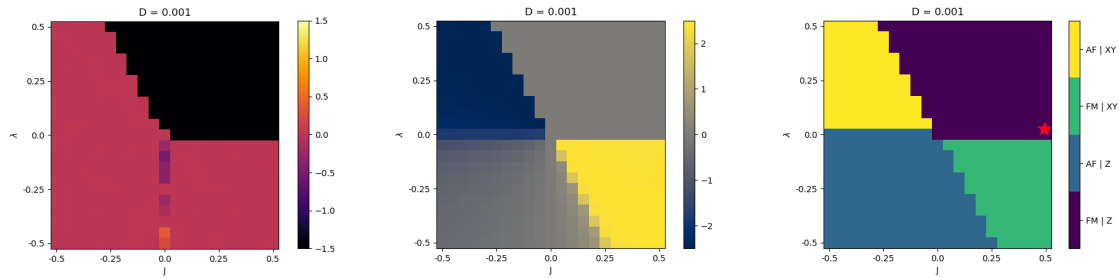


Figure 1: (left) The average value of spin in the off-plane axis. (middle) The average correlation between neighbouring spins in the XY plane. (right) Classical phase predictions.

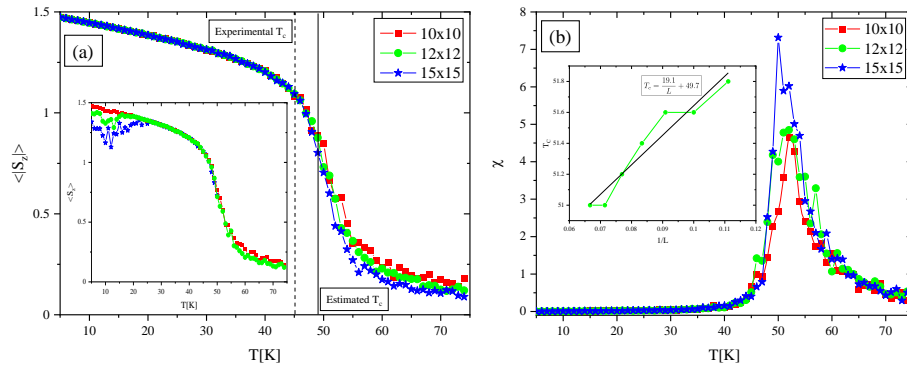


Figure 2: (a) Relationship between $\langle |S_z| \rangle$ and T . (b) Magnetic susceptibility as a function of temperature. Inset: Scaling of the T_c .

Shift electric current induced by energy relaxation of hot carriers in quantum wells

G. V. Budkin¹ and S.A. Tarasenko¹

¹*Ioffe Physical-Technical Institute, Polytekhnicheskaya 26, Saint-Petersburg 194021, Russia*

We report on the theoretical study of the “phonogalvanic effect” where electric current arise as a result of energy relaxation of hot electrons. We demonstrate that the violation of thermal equilibrium between the electron and phonon subsystems in a semiconductor quantum well with a sufficiently low symmetry leads to the generation of a direct electric current. Microscopically, the current emerges due to the displacement of the wave packets of Bloch electrons in the real space during the emission or absorption of phonons, which tend to restore thermal equilibrium in the system. In contrast to the well-known Seebeck thermoelectric effect, which requires a temperature gradient, the phonogalvanic current emerges also at homogeneous electron gas heating.

A detailed microscopic model is developed for the deformation mechanisms of electron-phonon interaction in narrow-gap quantum wells based on semiconductors with the zinc-blende structure, such as HgTe quantum wells. Electronic states for narrow-gap quantum wells are described in Bernevig-Hughes-Zhang model. We consider a two-dimensional electron gas in a quantum well structure, which is initially heated compared to the phonon bath. Frequent electron-electron collisions thermalize the electron gas so that it can be described by the effective temperature that is above the lattice temperature. We demonstrate that the processes of phonon emission or absorption in zinc-blend quantum wells lead to the the in-plane shift of the Bloch electrons in the real space. We calculate the shifts of the electrons involved in the quantum transitions in the framework of the density matrix taking into account both the contribution stemming from the phase gradients and the contribution determined by the Berry connection [1]. We show that, in the course of energy relaxation, the shifts of electrons have a preferable direction if the structure is grown along low-symmetry direction, although the phonons are emitted in all directions. Directional electron shifts lead to the direct electric current, which is generated until the electron temperature reaches the lattice temperature and thermal equilibrium between electrons and phonons is restored. The dependencies of shift currents on the Fermi level are obtained for HgTe quantum wells of various thicknesses grown along low-symmetry crystallographic directions.

[1] G. V. Budkin and S. A. Tarasenko *New J. Phys.* **22**, 013005 (2020).

Excitonic complexes in monolayers of transition metal dichalcogenides

Maciej R. Molas

Institute of Experimental Physics, Faculty of Physics, University of Warsaw, Warsaw, Poland

Monolayers (MLs) of semiconducting transition metal dichalcogenides (S-TMDs) MX_2 , where $\text{M} = \text{Mo}$ or W and $\text{X} = \text{S}, \text{Se}, \text{or Te}$, are direct band gap semiconductors with minima of the conduction band (CB) and maxima of the valence band (VB) located at the inequivalent K^\pm points of their hexagonal Brillouin zone (BZ). The strong spin-orbit interaction and lack of inversion symmetry result in the splitting of the VB (Δ_v) and the CB (Δ_c) extrema. Whereas the former splitting is of the order of a few hundred s of millielectronvolts, the latter equals only a few tens of millielectronvolts and can be positive or negative. Consequently, two subgroups of MLs can be distinguished: “*bright*” (the excitonic ground state is optically active or bright) comprising MoSe_2 and MoTe_2 , and “*darkish*” (the excitonic ground state is optically inactive or dark) composed of MoS_2 , WS_2 , and WSe_2 .

In my talk I will give a concise overview on excitonic complexes apparent in S-TMD monolayers. The first part of the lecture will cover the brief introduction to the properties of S-TMDs. Particularly, differences between “*bright*” and “*darkish*” MLs will be discussed in terms of optical transitions. In the second part, I will demonstrate that, in S-TMD MLs the s -type Rydberg series of excitonic states follows a simple energy ladder: $\varepsilon_{ns} = -Ry^*/(n + \delta)^2$. The effective Rydberg energy in the formula, Ry^* is very close to the Rydberg energy scaled by the dielectric constant of the medium surrounding the ML and by the reduced effective electron-hole mass, whereas the ML polarizability is accounted for only by δ .

The main part of my talk will be devoted to the study of emission lines apparent in the low-temperature photoluminescence spectra of n -doped WS_2 ML embedded in hexagonal BN layers. Results of measurements in external magnetic fields and first-principles calculations will be reviewed. It will be demonstrated that apart from the neutral exciton line, all observed emission lines are related to the negatively charged excitons. Consequently, emissions due to both the bright (singlet and triplet) and dark (spin- and momentum-forbidden) negative trions as well as the phonon replicas of the latter optically-inactive complexes are identified. The semidark trions and negative biexcitons are also distinguished. On the basis of their experimentally extracted and theoretically calculated g -factors, three distinct families of emissions are identified due to exciton complexes in WS_2 : bright, intravalley-, and intervalley-dark. The g -factors of the spin-split subbands in both the conduction and valence bands are also determined.

2D materials and their hybrids: pathway toward new phenomena

P.J. Kowalczyk¹, I. Lutsyk¹, D.A. Kowalczyk¹, M. Rogala¹, P. Dabrowski¹,
P. Krukowski¹, M. Piskorski¹, W. Kozłowski¹, E.M. Lacinska², A. Wyszomolek², R.
Stepniowski², J. Binder², R. Udovityska³, J. Jung³, J. Ulanski³, J. Baranowski⁴,
S.A. Brown⁵, G. Bian⁶ and Z. Klusek†¹

¹ Department of Solid State Physics, University of Lodz, Poland

² Faculty of Physics, University of Warsaw, Poland

³ Department of Molecular Physics, Lodz University of Technology, Poland

⁴ Lukaszewicz-Microelectronics and Photonics Institute, Poland

⁵ Department of Physics and Astronomy, University of Canterbury, New Zealand

⁶ Department of Physics and Astronomy, University of Missouri, USA

Since its official discovery in 2004 graphene is one of the most studied two-dimensional (2D) materials. Its discovery initiated search for other "one-layer-thick" materials in particular among layered solids held by van der Waals (VdW) forces. In consequence other monoatomic 2D materials were discovered like stanene, germanene, borophene, phosphorene and later α -bismuthene (α -Bi) and α -antimonene (α -Sb) [1]. Investigations of number of 2D layered compounds was also initiated with transition metal dichalcogenides (TMDCs) and hexagonal boron nitride (hBN) as one of most interesting representatives. Soon after the idea of hybrid structures i.e., artificial thin structures composed of two or more layers of different 2D materials was born. Recently it was shown that in two twisted layers of graphene unexpected physical phenomena i.e., superconductivity is observed. This discovery initiated number of studies on twisted homo - and heterostructures of 2D materials.

In our research we concentrate on experimental characterization of 2D materials and their hybrids. In particular we investigate graphene, 1T-TaS₂, MoTe₂, hBN, we also developed synthesis techniques of single layers of α -Sb [1], α -Bi [2], MoO₃ [3]. Each of these materials has unique properties by itself including large carrier mobility in graphene, large spin-orbit coupling in TaS₂, formation of Weyl fermions on bulk surface of MoTe₂, large band gap for hBN, 2D topological states at edges of α -Sb [1], superlubricity and Dirac cones formation due to nonsymmorphic symmetries in α -Bi [2] and unexpectedly large work function for MoO₃ [3]. Our efforts concentrate on combining these unique phenomena by building hybrid structures and investigation of their properties. In particular we managed to increase work function of graphene above 5 eV (by either 1L of MoO₃ or thin film of Re₂O₇) which allowed us to build working graphene based OLED. We also constructed TaS₂/graphene hybrids and showed substantial charge transfer and formation of moire patterns which might lead to development of twistronics in this unique system.

This work is supported by National Science Center, Poland under projects: 2015/19/B/ST3/03142, 2016/21/B/ST5/00984, 2018/31/B/ST3/02450, 2018/30/E/ST5/00667, 2019/32/T/ST3/00487, 2019/35/B/ST5/03956, 2020/38/E/ST3/00293

[1] T. Maerkl, P. J. Kowalczyk, M. Le Ster et.al., *2D Materials* **5**, 11002 (2017).

[2] P. J. Kowalczyk, S. A. Brown, T. Maerkl et.al., *ACS Nano* **14**, 1888 (2020).

[3] D. A. Kowalczyk, M. Rogala, K. Szalowski et al., *2D Materials* **8**, 25005 (2021).

Fine structure of *K*-excitons in multilayers of MoS₂ and MoSe₂

M. Bhatnagar ¹, N. Zawadzka ¹, Ł. Kipczak ¹, M. Grzeszczyk ¹, K. Watanabe ²,
T. Taniguchi ³, A. Babiński ¹ and M. Molas ¹

¹ Institute of Experimental Physics, Faculty of Physics, University of Warsaw, Poland

² Research Center for Functional Materials, NIMS, Tsukuba, Japan

³ International Center for Materials Nanoarchitectonics, NIMS, Tsukuba, Japan

Semiconducting transition metal dichalcogenides (S-TMDs) have recently attracted considerable attention due to their unique electronic structures and optical properties. As S-TMDs monolayers (1 MLs) possess a direct band gap located in the K^\pm points of the Brillouin zone (BZ), an indirect band gap located in the range outside the K^\pm points is apparent in multilayers (N-MLs). Particularly, due to the hybridization of electronic states at the K^\pm points of the BZ in 2H-stacked N-MLs, new excitonic resonances, so-called interlayer excitons, have been observed in MoS₂ and MoSe₂ N-MLs encapsulated in hexagonal BN (hBN) flakes [1,2].

We investigate high quality multilayers of MoS₂ and MoSe₂ embedded between hBN flakes with the aid of reflectance contrast experiment (RC) performed at low temperature ($T=5$ K). Apart from the usually reported intralayer A (X_A) and B (X_B) excitons, a series of additional resonances is observed in the RC spectra of N-MLs, see Figure. For MoS₂ N-MLs, the number of the observed transitions in the vicinity of the A exciton scales with the number of layers, *i.e.* two (X_A and IE) for 2 ML, three (X_A , IE and IE*) for 3 ML and four (X_A , IE, IE* and $X_{A'}$) for 4 ML. In contrast, only two resonances (X_A and IE) are observed for N-MLs of MoSe₂. We associate this difference with the spin-orbit splitting in the valence band, which equals about 150 meV and 190 meV for MoS₂ and MoSe₂, respectively. The IE and IE* resonances are related to the interlayer excitons. The former complex consists of an electron localized in a single layer and a hole, which is delocalized between the two neighbouring layers. The latter one is composed of an electron localized in a single layer and a hole delocalized over all layers forming N-MLs [3]. We probe the observed transitions in N-MLs of MoSe₂ through helicity-resolved RC measurements in magnetic fields applied perpendicular to the layer plane. The effect of the magnetic field on the splitting of the intra-layer and inter-layer excitons is shown with experimentally extracted g-factors to unambiguously assign the observed peaks to transitions involving intralayer and interlayer excitons.

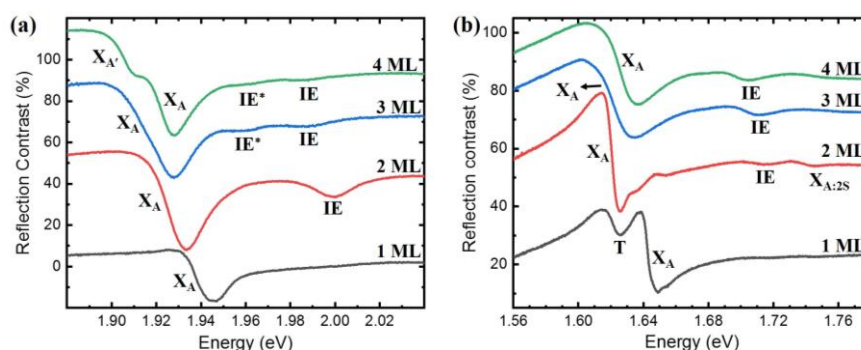


Figure: The low-temperature RC spectra of (a) MoS₂ and (b) MoSe₂ thin layers. Intra-layer and interlayer excitonic transitions have been marked for both cases.

[1] A. O. Slobodeniuk, *et al.*, *2D Materials* **6**, 025026 (2019).

[2] J. Horng, *et al.*, *Physical Review B* **97**, 241404(R) (2018).

[3] N. Leisgang, *et al.*, *Nature Nanotechnology* **15**, 901 (2020).

Rydberg series of dark excitons and spin-orbit splitting of the conduction band in WSe₂ monolayer

P. Kapuściński^{1,2}, A. Delhomme¹, D. Vaclavkova¹, A. O. Slobodeniuk³,
M. Grzeszczyk⁴, M. Bartos⁵, K. Watanabe⁶, T. Taniguchi⁷,
C. Faugeras¹ and M. Potemski^{1,4}

¹ *Laboratoire National des Champs Magnétiques Intenses, CNRS-Univ. Grenoble Alpes-UPS-
INSA-EMFL, 25, avenue des Martyrs, 38042 Grenoble, France*

² *Department of Experimental Physics, Wrocław University of Technology,
Wybrzeże Wyspiańskiego 27, 50-370 Wrocław, Poland*

³ *Department of Condensed Matter Physics, Faculty of Mathematics and Physics,
Charles University, Ke Karlovu 5, Praha 2 CZ-121 16, Czech Republic*

⁴ *Institute of Experimental Physics, Faculty of Physics, University of Warsaw,
ul. Pasteura 5, 02-093 Warszawa, Poland*

⁵ *Central European Institute of Technology, Brno University of Technology,
Purkyňova 656/123, 612 00 Brno, Czech Republic*

⁶ *Research Center for Functional Materials, National Institute for Materials Science,
1-1 Namiki, Tsukuba 305-0044, Japan*

⁷ *International Center for Materials Nanoarchitectonics,
National Institute for Materials Science, 1-1 Namiki, Tsukuba 305-0044, Japan*

Monolayers of transition metal dichalcogenides (TMD) from group VI, such as tungsten diselenide, are recently extensively studied group of semiconducting materials with multi-valley electronic band structure and a direct optical band gap, strong light-matter coupling and existence of robust excitonic complexes. However, despite of decades of intense research on these materials, the knowledge of electronic bands of even the best-studied TMD monolayers remains often quite approximate.

One parameter of the band structure that is not yet known is the amplitude of the spin-orbit coupling (Δ_c) at the edge of their conduction bands. This parameter is of great importance because it greatly influences the interpretation of the basic results of optical and transport experiments, often reported in the study of TMD structures. It has been estimated from various theoretical calculations, but so far has not been derived in an experiment, as being usually only one among other entangled components (e.g., the strength of Coulomb interaction) contributing to the extracted characteristic energies.

In this report, we derive the amplitude of the spin-orbit coupling in WSe₂ monolayer by comparing energy the ladders of bright (optically active, spin-allowed) and dark (inactive, spin-forbidden) exciton Rydberg series, with the latter appearing in the photoluminescence spectrum only in high in-plane magnetic fields thanks to the magnetic brightening effect. These bright and dark excitons differ mainly in the band where the bound electron comes from - the upper or lower subbands of the spin-orbit separated conduction band, respectively. By uncovering the rich Rydberg series of both bright and dark excitonic states, which correspondingly extrapolate to "bright" and "dark" single particle bandgaps, we are able to extract their difference - the amplitude of the spin-orbit coupling $\Delta_c=14$ meV. It is worth noting that this value is much lower than commonly assumed, which calls for revision of theoretical calculations of electronic bands in TMD monolayers.

Upconversion photoluminescence processes in monolayer WSe₂ and MoSe₂

Leszek Bryja¹, Joanna Kutrowska- Girzycka¹, Martyna Majak¹,
Jakub Lubczyński¹, Ching- Hwa Ho², Joanna Jadczak¹

¹ Department of Experimental Physics, Wrocław University of Science and Technology,
Wrocław, Poland

² Graduate Institute of Applied Science and Technology, National Taiwan University of Science and Technology, Taipei 106, Taiwan

The monolayer transition metal dichalcogenides (TMDs) emerge as an outstanding platform to study electron- electron and electron- phonon interaction [1, 2]. They host variety of intra- and inter- valley neutral and charged excitonic complexes, which are either optically active or inactive due to the conservation of a spin or a momentum. The higher number of excitonic features positioned energetically below the bright direct exciton have been observed in the low temperature emission spectra of W-based structures mainly due the dark exciton band lying at lower energy than the bright band.

They have been identified as bright singlet and triplet trions, neutral and charged bright biexcitons, spin-forbidden dark exciton, dark trions and momentum-indirect dark excitons activated by scattering with defects or phonons.

Here, we demonstrate an observation of momentum- dark excitons in temperature- dependent upconversion photoluminescence (UPC PL) in hBN- encapsulated WSe₂ monolayers. The two momentum- dark excitons I₁ and I₂ (located in different valleys K-Λ and K-K') show up in the excitonic UPC PL spectra as intensity enhancements 34 and 45 meV below the bright exciton (Fig.1a-f), correspondingly, which is in line with recent theoretical calculations [3]. We show that the observation of momentum- dark excitons in the upconversion emission process requires special conditions related to the electron doping as well as the temperature. Moreover, in the UPC PL spectra we observe prominent resonances at energies corresponding to the biexciton and both the spin- singlet and-triplet trions (Fig. 1e-f). The revealing of the fine trion structure in the UPC PL sheds a new light on previous studies of monolayer WSe₂, where only the triplet trion- exciton coupling was observed. For comparison we perform similar experiments in hBN- encapsulated mono-

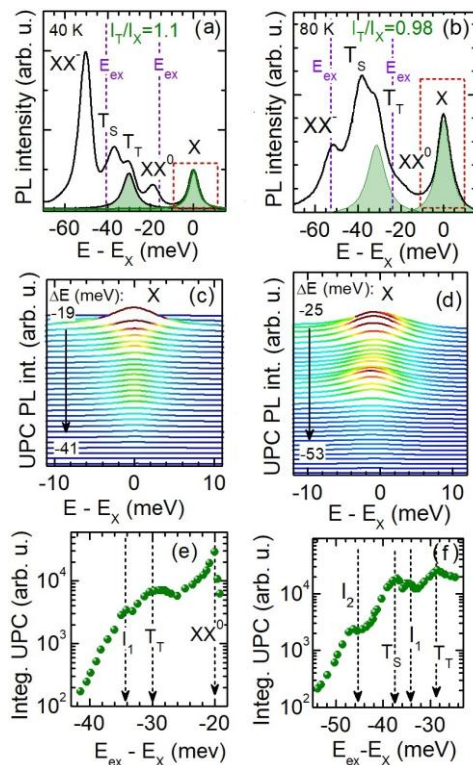


Fig. 1 (a-b) The PL spectrum of WSe₂ at 40 and 80 K, respectively. (c-d) The evolution of the UPC PL spectra as function of energy gain ($\Delta E = E_{ex} - E_X$). (e-f) Integrated UPC PL intensity of the exciton X as a function of ΔE .

layer MoSe₂, where the dark exciton band lying at higher energy than the bright band. By increasing the temperature from 7 to 120 K we probe phonon- mediated exciton- trion interaction as the normal PL intensity of the singlet trion gradually decreases.

[1] J. Jadczak et al., *Nature Communications* **10**, 107 (2019).

[2] J. Jadczak et al., *Materials* **14**, 399 (2021).

[3] S. Brem et al., *Nano Lett.* **20**, 4 (2020).

Bright Quantum Dot Single-Photon Emitters at Telecom Bands Heterogeneously Integrated with Si

Pawel Holewa ^{1,2}, Aurimas Sakanas ¹, Ugur Meriç Gür ³, Pawel Mrowiński ²,
Anna Musiał ², Niels Gregersen ¹, Elizaveta Semenova ^{1,4}, Marcin Syperek ²

¹ DTU Fotonik, Technical University of Denmark, DK-2800 Kgs. Lyngby, Denmark

² Laboratory for Optical Spectroscopy of Nanostructures, Faculty of Fundamental Problems of Technology, Wrocław University of Science and Technology, Wrocław, Poland;

³ DTU Electrical Engineering, Technical University of Denmark, Kgs. Lyngby, Denmark

⁴ NanoPhoton-Center for Nanophotonics, Technical University of Denmark, Kgs Lyngby, Denmark

Self-assembled semiconductor quantum dots (QD) are well-controllable and highly-flexible solid-state sources of single-photons. The information encoded in a quantum state of a photon can be utilized in a variety of the quantum information processing schemes [1]. However, up to date QD-based non-classical single-photon emitters operating in the long-wavelength telecom bands (>1460 nm) were investigated separately from the Si platform despite their great potential for heterogeneous integration with the silicon-based quantum photonic chips.

Here, we demonstrate a novel, robust, cost-effective, and industry-compatible approach for achieving a single-photon emitter based on an InAs/InP quantum dot heterogeneously integrated with the Si platform [2]. We show that by simplifying the device architecture and employing a metallic mirror beneath the emitter instead of a monolithic Bragg reflector, obtained photon extraction efficiency from the emitter reaches 10% with room for further improvement, which is a very competitive measure for the up-to-date solutions. The device architecture and its fabrication procedure led to single-photon generation purity above 98% at the liquid helium temperature and triggered operation mode and 75% at 80 K.

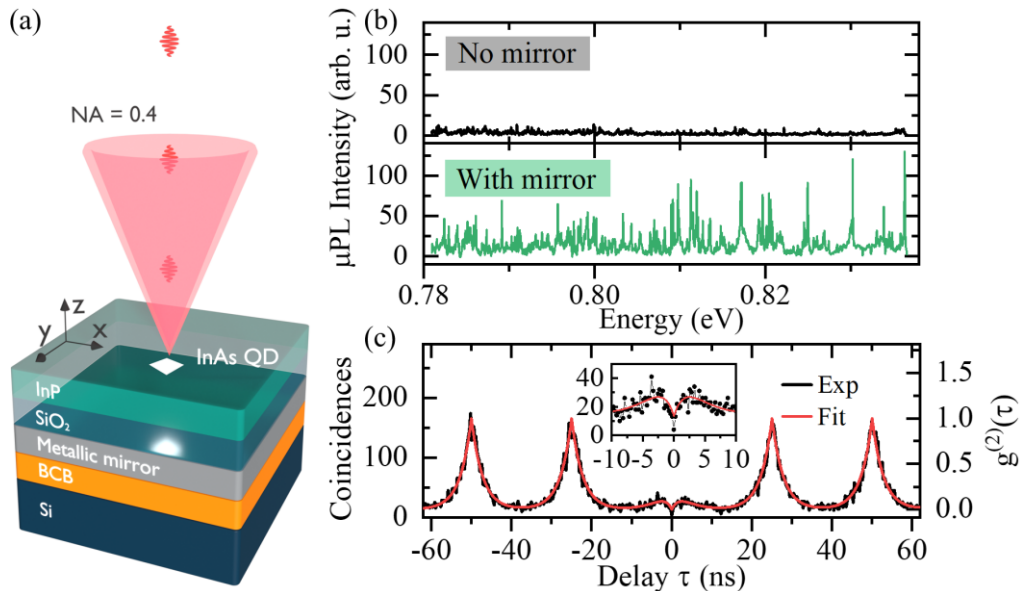


Figure 1 (a) Fabricated structure (InAs/InP QDs integrated with the Si wafer), (b) Comparison of μ PL spectra for the QDs over the mirror and for the reference structure, (c) Autocorrelation of the exemplary single line emitting at $1.54 \mu\text{m}$ under pulsed laser excitation.

[1] P. Senellart, G. Solomon, A. White, *Nat. Nanotechnol.*, **12**, 11 (2017)

[2] P. Holewa *et al.*, arxiv:2104.07589

Bright Single-Photon Emitters with a CdSe Quantum Dot and Multimode Tapered Nanoantenna for the Visible Spectral Range

M.V. Rakhlin¹, S.V. Sorokin¹, D.R. Kazanov¹, I.V. Sedova¹, T.V. Shubina¹,
S.V. Ivanov¹, V. Yu. Mikhailovskii² and A.A. Toropov¹

¹ Ioffe Institute, 26 Polytekhnicheskaya str., St. Petersburg, 194021, Russia

² Saint-Petersburg State University, 7/9 Universitetskaya nab., St. Petersburg, 199034, Russia

In the last decades, a lot of attention has been paid to development of the sources of quantum light such as single-photon emitters possessing non-classical photon statistics and sources of entangled pairs of single photons. These devices are key elements for the systems of quantum cryptography, information teleportation, and quantum computing. Self-organized single quantum dots (QDs) based on wide-gap II-VI compounds, grown by epitaxial techniques (usually by molecular beam epitaxy), are considered as promising candidates for creation of the room-temperature single photon sources due to exceptionally large binding energy of excitons and biexcitons. So far, single-photon emission at elevated temperatures has been demonstrated for the structures with CdSe/Zn(S,Mg)Se [1] and CdTe/ZnTe [2] epitaxial QDs and room temperature operation has been achieved under both optical [3] and electrical [4] pumping. The fabrication of intense II-VI single-photon sources is, nevertheless, hampered by a difficulty with growth of monolithic cavity structures suitable for increasing extraction efficiency of the single-QD emission.

In this work, we report on single-photon emitters for the green-yellow spectral range, which comprise a CdSe/ZnSe quantum dot placed inside a semiconductor tapered nanocolumn acting as a multimode nanoantenna. Despite the presence of many optical modes inside, such a nanoantenna is able to collect the quantum dot radiation and ensure its effective output. We demonstrate periodic arrays of such emitters, which are fabricated by focused ion beam etching from a II-VI/III-V heterostructure grown using molecular beam epitaxy. With non-resonant optical pumping, the average count rate of emitted single photons exceeds 5 MHz with the second-order correlation function $g^{(2)}(0) = 0.25$ at 220 K [5]. Such single photon emitters are promising for secure free space optical communication lines.

M.V. Rakhlin thanks the Council for Grants of the President of the Russian Federation.

- [1] K. Sebal, P. Michler, T. Passow, D. Hommel, G. Bacher, A. Forchel, *Appl. Phys. Lett.* **81**, 2920 (2002).
- [2] C. Couteau, S. Moehl, F. Tinjod, J. M. Gerard, K. Kheng, H. Mariette, J.A. Gaj, R. Romestain, *Appl. Phys. Lett.* **85**, 6251 (2004).
- [3] O. Fedorych, C. Kruse, A. Ruban, D. Hommel, G. Bacher, T. Kmmell, *Appl. Phys. Lett.* **100**, 061114 (2012).
- [4] W. Quitsch, T. Kmmell, A. Kruse, D. Hommel, G. Bacher, *Phys. Status Solidi C* **11** 1256 (2014).
- [5] M. Rakhlin, S. Sorokin, D. Kazanov, I. Sedova, T. Shubina, S.V. Ivanov, V. Mikhailovskii, A. Toropov, *Nanomaterials* **11**, 916 (2021).

Controlling the energy and timing of single photons by acoustic modulation of a quantum dot

Daniel Wigger¹, Matthias Weiß^{2,3}, Michelle Lienhart²,
Maximilian Nägele^{2,3}, Kai Müller^{4,3}, Jonathan J. Finley^{4,3},
Tilmann Kuhn⁵, Hubert J. Krenner^{5,2,3}, and Paweł Machnikowski¹

¹Wrocław University of Science and Technology, 50-370 Wrocław, Poland

²Augsburg University, 86159 Augsburg, Germany

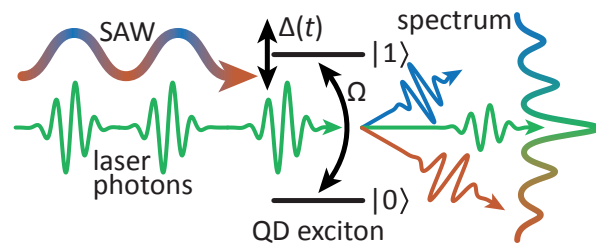
³Nanosystems Initiative Munich (NIM), 80799 München, Germany

⁴Technische Universität München, 85748 Garching, Germany

⁵University of Münster, 48149 Münster, Germany

When considering resonant light scattering experiments on a single quantum dot (QD) excitons interesting physics emerge. In this context many studies focus on two distinct cases: (i) The strong coupling case is often realized by a high Q cavity and small optical intensities. This regime of light matter coupling is usually identified by a double peak structure in the light scattering spectrum stemming from the vacuum Rabi splitting. (ii) In the strong driving case an intense laser is used that generates a characteristic triple peak structure, the so-called Mollow triplet. This effect does not require a particularly efficient light-matter coupling. In the case of low coupling strength and weak optical driving operating in the single photon limit, the light scattering spectrum does not significantly deviate from the initial laser.

The situation changes drastically when the QD is additionally interfaced with an phononic field, in our case a surface acoustic wave (SAW). The deformation potential coupling between phonon and QD exciton leads to harmonic modulations $\Delta(t)$ of the exciton's transition energy if a single monochromatic SAW is acting on the QD.



The laser photons scattered from the exciton now develop a comb-like spectrum, whose peak spacing is precisely given by the frequency of the SAW field as schematically depicted in the figure. We model the detected resonance fluorescence signal in this system by a semi-classical approach and calculate the two-time correlation function via quantum regression. Direct comparison between theory and experiment exhibits excellent agreement. We find that the intensities of the phonon sidebands also adapt the dynamics of the SAW by showing a periodic beating [1]. Applying a slight energy detuning between the laser and the exciton transition we have access to tune both, the time-integrated spectral intensities and the relative timing of the intensities of different sidebands. By simultaneously generating two SAWs with frequencies ω_{SAW} and $2\omega_{\text{SAW}}$ we demonstrate that the photon scattering spectrum can also be controlled by wave mixing processes that depend crucially on the relative phase between the two acoustic fields [2]. An additional minute detuning via $2\omega_{\text{SAW}} \rightarrow 2\omega_{\text{SAW}} + \delta_{\text{SAW}}$ again leads to intensity modulations of the sidebands determined by δ_{SAW} . Only limited by the electronic control of the experiment these beats can reach down to a few μHz , i.e., periods of a few hours.

[1] D. Wigger, M. Weiß, et al., *in preparation*.

[2] M. Weiß, D. Wigger, et al., *Optica* **8**, 291–300 (2021).

Deterministically fabricated and tunable quantum dot single-photon source emitting in the telecom O-band

N. Srocka,^a P. Mrowiński,^b J. Große,^a M. von Helversen,^a M. Schmidt,^a T. Heindel,^a S. Rodt,^a and S. Reitzenstein^a

^a *Institut für Festkörperphysik, Technische Universität Berlin, Hardenbergstraße 36, 10623 Berlin, Germany*

^b *Laboratory for Optical Spectroscopy of Nanostructures, Department of Experimental Physics, Wrocław University of Science and Technology, Wybrzeże Wyspiańskiego 27, Wrocław, Poland*

Deterministically fabricated and tunable quantum dot (QD) single-photon sources emitting in the telecommunication O-band ($\sim 1.3 \mu\text{m}$ wavelength) are of high practical importance for the implementation of quantum communication networks [1]. We demonstrate a device based on epitaxially grown (MOCVD) InGaAs/GaAs QDs whose emission is redshifted to the telecom O-band via strain reducing layer approach [2]. The quantum device is realized via flip-chip processing in combination with thermocompression bonding of the QD heterostructure and a piezoelectric crystal and layer-by-layer wet etching process to obtain a thin semiconductor membrane with the QD active layer attached to the piezo crystal. Next, photonic mesa structures with deterministically integrated QDs are fabricated by low-temperature cathodoluminescence (CL) scanning and in-situ electron-beam lithography [3].

We characterized our deterministic QD devices first with by micro-photoluminescence (μPL) using quasi-resonant pulsed excitation to determine the purity and the indistinguishability of emission yielding $g(2)(0) < 0.03$ at 10 K and visibility of 16 % (96% post-selected). We achieved broadband (40 nm) photon-extraction efficiency which is in reasonably good agreement with numeric results predicting an efficiency of 9% [4]. The lower experimental photon-extraction efficiency mainly attributed to a non-ideal internal quantum efficiency of maximal 85% for the present QDs. Next, we investigated the tunability and spectral stability of emission by using a strain field induced by external strain tuning via the piezo element. We found two similar quantum dot photon mesa structures to demonstrate that we are capable of tuning two CX states of different QD-mesas to resonance and stabilize their wavelength by a closed-loop PID control system [5]. Our technological achievements and experimental findings are very promising for the implementation of two-photon interference experiment of remote QDs which is crucial for developing long-distance quantum communication networks with the use of fiber optics technology.

- [1] H. J. Kimble, Nature 453, 1023 (2008).
- [2] V. M. Ustinov et al Appl. Phys. Lett. 74, 2815 (1999).
- [3] M. Gschrey et al., Nat. Commun. 6, 7662 (2015).
- [4] N. Srocka et al., Appl. Phys. Lett. 116, 231104 (2020).
- [5] N. Srocka et al., Appl. Phys. Lett. 117, 224001 (2020).

Magneto-optical properties of a CdTe Quantum Dot with a single ion of Vanadium

K. E. Połczyńska, T. Kazimierczuk, P. Kossacki and W. Pacuski

Faculty of Physics, University of Warsaw, Pasteura 5, Warsaw, Poland

The application of quantum technologies such as spintronics, solotronics or quantum computing is highly promising when it comes to miniaturization in modern technology. In order to achieve effective devices, there is a need to investigate the spin properties of impurity interacting with the semiconductor lattice and confined carriers. Zero-dimensional semiconductor structures such as epitaxial quantum dot (QD) is a model system to probe fundamental interactions in condensed matter. For example, QDs can be used to examine the spin of a single magnetic ion [1,2,3].

Vanadium is a transitional metal with a nuclear spin $\frac{7}{2}$ and 3 electrons on the d shell. It exhibits spin $\frac{3}{2}$ in V^{2+} configuration [4] leading to two possible fundamental states with spin projection $\pm\frac{3}{2}$ or $\pm\frac{1}{2}$. Particular spin configuration is expected to depend on the strain of the crystal lattice in a QD.

In this work we examine self-assembled CdTe QDs doped with V, in ZnTe barrier, fabricated using molecular beam epitaxy. We observed a single QD including a single vanadium dopant and measured magneto-optical properties of such a system. According to numerical modeling based on experimental data (shown in the fig. 1), we conclude that V in this case exhibit spin $\frac{1}{2}$, which makes our system a realization of a qubit.

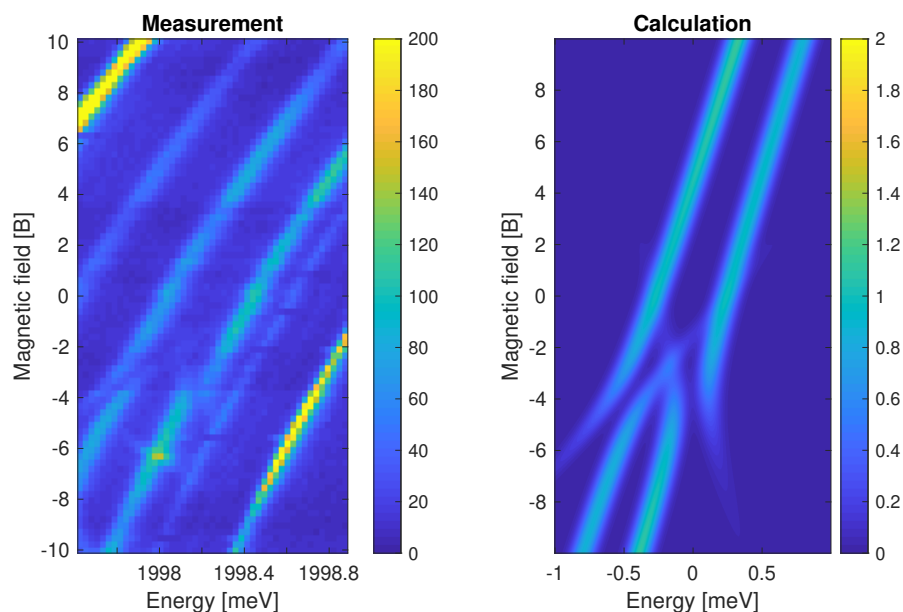


Figure 1: Microphotoluminescence spectrum and calculation of the neutral exciton of the QD with a single vanadium dopant.

- [1] L. Besombes et al, *Phys. Rev. Lett* **93**, 207403 (2004).
- [2] J. Kobak et al, *Nature Communications* **5**, 3191 (2014).
- [3] T. Smoleński et al, *Nature Communications* **7**, 10484 (2016).
- [4] M. Herbich et al, *Phys. Rev. B* **59**, 2726 (1999).

Charge Separation in Blends of Newly Synthesized C60 Fullerene Derivatives and P3HT

Maciej Krajewski¹, Piotr Piotrowski², Wojciech Mech¹, Krzysztof P. Korona¹, Jacek Wojtkiewicz¹, Marek Pilch¹, Andrzej Kaim², Aneta Drabińska¹, Maria Kamińska¹

¹ University of Warsaw Faculty of Physics, Pasteura 5, Warsaw, Poland

² University of Warsaw Faculty of Chemistry, Pasteura 1, Warsaw, Poland

Organic solar cells (OSCs) have experienced a lot of attention in the last decade. The active layer of the OSC contains a blend of donor and acceptor materials. Conductive polymers, such as P3HT or PTB7, are most often used as donors, while the fullerene derivatives PC61BM or PC70BM serve usually as acceptors. Power conversion efficiency (PCE) of solar cells is strongly correlated with the effectivity of the charge separation process [1], so understanding of charge transfer mechanisms is essential for the further development of OSCs. In our study, four newly synthesized fullerene C60 derivatives with various aromatic substituents (thiophene or pyrene moieties, both in symmetrical and asymmetrical configurations), and their blends with P3HT were chosen to investigate the charge transport processes in the active layer. Two experimental techniques were applied: light-induced Electron Spin Resonance (LESR) along with time-resolved photoluminescence (TRPL). Additional characterization by means of UV/VIS spectroscopy was combined with DFT/TDDFT calculations, showing good consistency of experimental and theoretical results. During illumination, the reference blend of PC61BM:P3HT exhibits exceptionally intense separation of electron and hole that is evident in the LESR spectrum as two distinct lines [2]. The intensities of these two lines provide information about the number of the steady-state photoexcited and separated electrons and holes, which should correlate with the PCE. LESR measurements of all blends with the synthesized fullerene derivatives also showed two characteristic lines, indicating charge transfer within them. Interestingly, the asymmetrical molecules (i.e. with only one aromatic substituent) exhibited much stronger LESR signal, making them more suitable for photovoltaic applications.

TRPL technique was applied to trace the photo-carriers behavior inside the active layer. Observation of photoluminescence quenching provides information on charge separation effectivity and the characteristic lifetime of photoexcited carriers. Studies showed that the most effective PL quenching is present in blends of P3HT and fullerene derivatives with one aromatic substituent. At the same time, the blends with symmetrical fullerene derivatives (with two aromatic substituents) and P3HT did not exhibit any significant PL attenuation. Therefore, it can be concluded that the most dominant relaxation mechanism inside them is radiative recombination.

In the final step, we prepared OSCs with active layers made of P3HT and the newly synthesized fullerene derivatives. It was found that the best performance is obtained in cells with fullerene derivatives showing the two distinct LESR lines and fast PL quenching. However, even the best PCE values for the new fullerene derivatives were still lower than for the reference cell (0.17% vs. 2.23%), most probably due to their low solubility. Nevertheless, the correlation of carrier separation effectivity, as observed in LESR and PL/TRPL measurements, with the PCE of the respective solar cells was clearly visible.

Acknowledgments: Research was co-funded by project TECHMATSTRATEG1/347431/14/NCBR/2018 (NCBiR).

[1] F. Laquai, et al., *Macromol. Rapid Commun.*, vol. 36, pp. 1001–1025, 2015

[2] C. Deibe, et. al, *Adv. Mater.*, vol. 22, no. 37, pp. 4097–4111, 2010

Optical spectroscopy of excitons in the atomically thin topological insulator Bismuthene

P. Holewa¹, P. Wyborski¹, L. Dusanowski^{1,2}, R. Stühler³, A. Consiglio⁴, D. Di Sante⁴, W. Hanke⁴, C. Schneider^{2,5}, S. Höfling², R. Claessen³, and M. Syperrek¹

¹ *Laboratory for Optical Spectroscopy of Nanostructures, Faculty of Fundamental Problems of Technology, Wrocław University of Science and Technology, Wyb. Wyspiańskiego 27, 50-370 Wrocław, Poland*

² *Physikalisches Institut, Universität Würzburg, Am Hubland, D-97074 Würzburg, Germany*

³ *Physikalisches Institut and Würzburg-Dresden Cluster of Excellence ct.qmat, Universität Würzburg, 97074 Würzburg, Germany*

⁴ *Institut für Theoretische Physik und Astrophysik, Universität Würzburg, D-97074 Würzburg, Germany*

⁵ *Institut für Physik, Universität Oldenburg, D-26111 Oldenburg, Germany*

Optical spectroscopy of atomically thin materials has enhanced our understanding of the physics of collective excitations in low-dimensional semiconductors. A substantial increase of Coulomb correlations in single-layered two-dimensional crystals leads to the observation of new many-body states, including Rydberg series neutral excitons and stable charged exciton complexes. In addition, the crystal symmetry and the presence of heavy metal atoms strongly imprint the excitonic bandstructure, affecting the relevant energy scales and inducing topological phenomena manifested in the presence of Berry curvature for electrons and holes at the band edges. For example, the most widely studied members of a single-layered transition-metal dichalcogenide family (WS₂, WSe₂, MoS₂, MoSe₂, MoTe₂) are topologically trivial. However, two candidates for atomically thin topological insulator have appeared in recent years, namely 1T'-WTe₂ and Bi arranged to the honeycomb lattice on a SiC substrate [1]. Here, the latter one is particularly interesting. The heavy Bi atoms induce a giant spin-orbit coupling responsible for the opening of a substantial topological bandgap (~0.67 eV, indirect) in the material, which is accessible by optical spectroscopy in the near-infrared spectral range.

This communication shows the room-temperature results of the high-spatially-resolved photo-modulated reflectivity experiment performed on epitaxially grown Bismuthene on a SiC substrate. A single layer of Bi atoms forms a superstructure in honeycomb geometry. Our study reveals the emergency of strong optical resonances within the electronic bandgap of Bismuthene with the fundamental optical transition observed at ~1.19 eV. The resonances are ascribed as excitonic features associated with the excitonic transitions in the vicinity of the K/K' valley of the Brillouin zone. The optical spectra were confronted with the results of scanning tunnelling spectroscopy and ab initio G₀W₀ calculations, including electronic Coulomb correlations, and shows that the exciton binding energy in this atomically thin topological insulator can be as high as ~100 meV.

[1] F. Reis, G. Li, L. Dudy, M. Bauernfeind, S. Glass, W. Hanke, R. Thomale, J. Schäfer, R. Claessen, *Science* 357, 287 (2017).

Index of authors

- Adamus Z. MoP4.3, TuP3.3, TuP3.6, TuP4.5, WeO2
Adhikari A. MoP2.1, MoP2.4, WeP2.1
Agarwal Prof.Amit. MoP3.6
Alberi K. ThP3.5
Aleszkiewicz M. TuP3.5, WeO2, WeP3.6
Aleszkiewicz M.A. WeP4.4
Alexander Lau A.L. MoP3.3
Alves E. MoP2.2, WeP2.2
Amatti M. MoP2.8
Ambroziak R. TuP4.2
Amouyal Y. WeP4.6
Andrearczyk T. MoP3.8
Anwar A.R. TuP2.4
Arciszewska A. TuP4.5
Arciszewska M. MoP3.1
Autieri C. MoP3.4
Autieri Dr.Carmine. MoP3.6
Avdienko P.S. TuP4.3
Avdonin A. MoP3.1, TuP4.5
Babiński A. TuP1.2, WeO7, WeP1.3, WeP4.7, ThP1.5, FrO1
Baj M. WeP3.5
Balagula R.M. TuP4.6, ThP2.1
Ballarini D. MoO6, TuO7, WeO5
Bansil A. MoP3.6
Baranowski J. MoO5, TuP2.1, FrI2
Baranowski M. WeP1.10
Baranowski P. MoP1.5, TuP4.7, WeP4.2
Bardyszewski W. MoP4.5, WeO4
Barquinha P. MoI2
Bartoš M. ThP1.5
Bartos M. FrO2
Bauer G. WeO3
Benyoucef M. MoP1.3
Bhatnagar M. FrO1
Bian G. FrI2
Biegańska D. MoP4.8, TuO8
Bieniek M. TuP1.5, TuP1.9, ThP1.6
Bilińska K. ThP3.6
Binder J. MoO1, MoO3, MoO4, MoO5, TuP1.3, WeP1.1, WeP1.2, WeP1.7, ThP1.1, ThP1.2, FrI2
Birowska M. TuP1.4, WeP1.4, ThO2, ThP1.4, ThP1.8, ThP1.9
Blais A. S5
Bockowski M. TuP2.10
Bogaczewicz R.A. MoP1.1
Bogucki A. MoO2, MoP1.6, WeP4.5
Bogusławski P. MoP2.3, TuO5
Bohdan A. MoP4.9
Borysiewicz M.A. MoP4.4, WeP2.5
Bożek R. MoO1, MoO2, WeP1.1, WeP3.5
Bożek RB. WeP1.8
Bragar I. MoP1.2, ThP3.1
Branquinho R. MoI2
Brodowska B. MoP3.1
Brown S.A. FrI2
Brunner K. WeO1
Bryja L. FrO3
Brzezicki W. WeO2, WeP3.3, WeP3.7
Buczko R. WeO3, WeP3.2
Budkin G.V. ThP3.10
Budniak A.K. WeP4.6
Burakowski M. MoP1.8
But D. B. MoO8, MoP2.5, TuO4, TuP1.1, TuP2.8
Caha O. WeO3
Calvo-Gallego J. MoO7
Carlos E. MoI2
Carmine Autieri C.A. MoP3.3
Chaves A. ThO7
Chernikov A. WeP1.10
Chernyadiev A.V. MoP2.5
Chlipala M. ThO4, ThP2.5
Chusnutdinow S. MoP1.5, TuP4.4, WeP4.2, WeP4.8
Ciechan A. MoP2.3
Claessen R. FrO10
Clericò V. MoO7
Comaron P. TuO7
Consiglio A. FrO10
Cora I. WeP2.5
Courtade E. TuO3
Crooker S.A. TuO3
Cuono G. MoP3.3, MoP3.6
Cywiński G. MoO8, TuO4, TuP1.1, TuP2.8
Cywiński Ł. MoP1.2, ThP3.2
Dąbrowska A.K. MoO1, MoO3, TuP1.3, WeP1.1, WeP1.2, WeP1.7, ThP1.1, ThP1.2
Dąbrowski A. WeP3.1
Dabrowski P. FrI2
Dad S. MoO9
Das K. TuP2.5

de Luca M. TuO2
 Deilmann T. TuI2
 Delgado-Notario J.A. MoO7
 Delhomme A. FrO2
 Demchenko I.N. MoP2.8
 Deng H. TuI3, TuP3.6
 Dhavse R. WeP4.3
 Di Sante D. FrO10
 Diduszko R. MoP3.4
 Dietl T. MoP3.6, WeO2
 Diez E. MoO7
 Dłużewski P. MoP2.2, TuO1, WeP2.8
 Domagała J. WeO2
 Drabińska A. MoO4, FrO9
 Drózd P.A. TuP2.2
 Dub M. MoO8, ThP2.2
 Dusanowski Ł. FrO10
 Dvoretzky S. TuO4
 Dybko K. MoP3.4, MoP3.5, WeP3.1, WeP3.4, WeP4.1, ThO1
 Dyksik M. WeP1.10
 Dynowska E. MoP2.2
 Dziawa P. MoO9, MoP3.5
 Dzięczek D.D. TuP4.1
 Edathumkandy Y.K. TuP2.5
 Encomendero J. ThO5
 Estrecho E. MoP4.8, WeO6
 Fabian J. ThO2
 Faraz Sadia.Muniza. WeP2.9
 Faria Junior P.E. ThO2, ThO7
 Fās T. WeP4.6
 Faugeras C. ThP1.5, FrO2
 Faye D. WeP2.2
 Fedorchenko I. TuP3.6
 Feduniewicz-Żmuda A. TuP2.3, ThO4, ThP2.6, ThP2.7
 Figielski T. MoP3.8
 Fijalkowski K.M. WeO1
 Filipiak M. TuP1.1, TuP2.2, TuP2.8
 Finley J.J. FrO6
 Finzel K. WeP1.10
 Firsov D.D. TuP4.3
 Fiuczek N. TuP2.3, ThP2.7
 Flågan S. TuO2
 Flatté M.E. ThP3.5
 Florian M. ThP1.3
 Fogarassy Z. WeP2.5
 Fortunato E. MoI2
 Fuchs G.D. S3
 Funato M. ThO3
 Furman M. TuO6, TuO7
 Gaca J. TuP2.1
 Galicka M. WeO3, WeP4.8
 Gas K. TuP2.10, WeP3.6, WeP4.1, ThO1
 Gawraczyński J. WeP4.7
 Georgiev R. WeP4.2
 Gheewala S.M. WeP4.3
 Ghosh B. MoP3.6
 Ghosh S. WeO6
 Gibasiewicz K. ThO3
 Gies C. ThP1.3
 Gmitra M. WeP1.5
 Godlewski M. WeP2.4
 Golias E. WeO3
 Golnik A. MoP1.6, WeP4.5
 Gong M. ThO5
 Goryca M. TuO3, TuP1.6, WeP1.8
 Goscinski K. WeP4.8
 Gosk J. MoP2.9
 Gould C. WeO1
 Grabecki G. MoP3.4, WeP3.1
 Grandjean N. ThI2
 Graszka K. TuP3.6, TuP4.5
 Gregersen N. FrO4
 Gregoratti L. MoP2.8
 Grendysa J.G. WeP4.4
 Grochot A. TuP2.10
 Grodzicki M. TuP2.6
 Grosse J. FrO7
 Gryglas-Borysiewicz M. MoO4, WeP3.4, WeP3.5, WeP4.1, ThP1.7
 Grzanka S. ThO3
 Grzeszczyk M. MoO2, TuP1.2, TuP1.8, WeO7, WeP1.3, WeP4.7, ThP1.5, ThP1.7, FrO1, FrO2
 Gür U.M. FrO4
 Guzewicz E. MoP2.1, MoP2.4, MoP2.8, WeP2.7, WeP2.8, WeP4.8
 Gwozdz K. WeP4.8
 Hahn T. WeO8
 Hajdel M. ThP2.6, ThP2.7
 Hanke W. FrO10
 Haras M. MoO8, TuO4
 Hartl M. WeO1
 Hawrylak P. TuP1.5, ThP1.6
 Heindel T. FrO7

Heuser T. MoP1.4
 Ho Ch.H. FrO3
 Höfling S. MoP1.9, TuO8, FrO10
 Holewa P. MoP1.8, FrO10, FrO4
 Hommel D. TuP2.6, ThP2.3
 Howarth J. TuP1.6, WeO9
 Hruban A. MoP3.4, WeP3.1
 Hrytsak R. ThP2.4
 Hussain G.H. MoP3.3
 Hyart T. TuP3.7, WeO2, WeP3.7
 Ikamas K. MoP2.5
 Inabez-Insa J. WeP4.7
 Ishii R. ThO3
 Islam Msc.Rajibul. MoP3.6
 Ivanov S.V. FrO5
 Ivaschenko V. TuP2.7
 Ivonyak Y. TuO4
 Iwanowski P. MoP3.4, WeP3.1
 Iwański J. MoO1, MoO3, TuP1.3, WeP1.1
 Iwinska M. TuP2.10
 Jabeen F. MoP1.9
 Jadczyk J. FrO3
 Jakiela R. MoP2.4, TuO1, WeP2.3, WeP2.6, WeP3.1
 Jakubczyk T. TuO2
 Jarosz D.J. WeP4.4
 Jasiński J. WeP1.10
 Jasinski J.B. WeI3
 Jastrzębska A.M. TuP1.4, ThP1.8
 Jastrzębski J. TuP1.9
 Jaworowski B. TuP3.4
 Jena D. ThO5
 Jorudas J. TuP4.6, ThP2.1, ThP2.2
 Jukam N.J. TuP4.1
 Jung J. FrI2
 Jureczko P. WeP1.9
 Kachorovskii V.Yu. TuP2.2
 Kacman P. WeO3
 Kafar A. ThO3
 Kaim A. FrO9
 Kaminska A. ThI3
 Kaminska M. MoP4.9
 Kamińska M. WeO5, FrO9
 Kamminga M. WeP1.10
 Kapuściński P. ThP1.5, FrO2
 Karczewski G. MoP1.10, MoP1.5, TuP4.4, TuP4.7,
 WeP4.2
 Karpińska K. MoP3.5, TuP4.4
 Karpińska M. WeP1.10
 Kašalynas I. TuP4.6, ThP2.1, ThP2.2
 Kasprzak J. WeO8
 Kaszub W. MoO4
 Kavak H. MoP4.1
 Kawa K. ThP3.4
 Kawakami Y. ThO3
 Kazakov A. TuP3.3, WeO2, WeP3.6, WeP4.4
 Kazanov D.R. FrO5
 Kazimierczuk T. MoO2, MoP1.10, MoP1.7, TuP1.6,
 WeO8, WeO9, WeP1.6, WeP4.5,
 ThP1.5, FrO8
 Kędziora M. MoP4.6, TuP4.2
 Kempt R. WeP1.10
 Ketolainen T. ThP3.7
 Khaliq A. MoP3.1
 Khranovskyy Volodymyr. WeP2.9
 Kierdaszuk J. MoO4
 Kilanski L. MoP3.1
 Kipczak Ł. WeO7, WeP1.3, FrO1
 Kirilenko D.A. TuP4.3
 Klembt S. TuO8
 Klusek Z. FrI2
 Kłopotowski Ł. WeP1.10
 Knap W. MoO7, MoO8, TuO4, TuP1.1, TuP2.2, TuP2.8,
 TuP4.8, ThP2.2
 Kochan D. WeP1.5
 Koenraad P.M. ThP3.5
 Kołaciński C. MoP2.5
 Kołtąj K. TuP4.2
 Kołodziej J. MoP3.4, TuP3.6, TuP3.8, WeP3.6
 Kołodziejczyk J. TuP1.10
 Komkov O.S. TuP4.3
 Kończykowski M. TuP3.6
 Kopaczek J. ThO6
 Kopalko K. MoP2.4, WeP2.8
 Korczak J. TuP4.4, WeP4.1
 Korona K.P. MoP4.9, TuP2.1, ThP1.2, ThP1.7, FrO9
 Kors A. MoP1.3
 Koshevarnikov A. ThP3.7
 Kossacki P. MoO2, MoP1.10, MoP1.6, MoP1.7,
 TuP1.2, TuP1.6, TuP1.8, WeO8, WeO9,
 WeP1.6, WeP4.5, ThP1.5, FrO8
 Kossut J. MoP1.10
 Kotur K. WeP1.4, ThP1.8
 Kowalczyk D.A. FrI2
 Kowalczyk L. MoP3.5

Kowalczyk P.J. FrI2	Lifshitz E. WeP4.6
Kowalski B.J. MoP3.4, TuP3.6, WeP3.6, WeP4.8	Lioubtchenko D. TuP1.1
Kowalski G. MoO1, MoO3, TuP1.3, WeP1.1	Lis M. TuP3.2
Kozak A. TuP2.7	Lisauskas A. MoP2.5
Kozanecki A. MoP2.2, TuO1, WeP2.2, WeP2.3, WeP2.6	Liu N. WeO1
Kozdra S. WeP1.2	Lubczyński J. FrO3
Kozłowski W. FrI2	Ludwiczak K. MoO1
Krajczewski J. TuP4.2	Ludwig A.L. TuP4.1
Krajewska A. MoO4, MoO8, TuP1.1	Lutsyk L. FrI2
Krajewski M. FrO9	Lynnyk A. MoP2.9
Krajewski T.A. WeP2.8	Lysak A. TuO1, WeP2.1, WeP2.3, WeP2.6
Kraśnicki W. MoP1.6	Łempicka K. WeO5
Kravchuk T. WeP2.5	Łepkowski S.P. TuP2.4
Krenner H.J. FrO6	Łopion A. MoP1.6, WeP4.5
Kret S. MoO2, MoO9, TuP4.7, WeP3.4, WeP3.5, ThO1, ThP1.7	Łuka G.-. WeP2.8
Krishtopenko S.S. TuO4	Łusakowska E. MoP3.5
Król M. MoP4.6, MoP4.7, TuO6, TuO7, WeO4, WeO5	Łusakowski A. MoP3.4, TuO5, WeP3.1, WeP3.6
Królicka A. WeP4.1, ThO1	Łusakowski J. TuO4, TuP4.8
Kruck T.K. TuP4.1	Machnikowski P. MoP1.1, WeO8, ThP3.3, ThP3.4, FrO6
Krukowski P. FrI2	Magalhaes S. MoP2.2, WeP2.2
Krusin-Elbaum L. TuP3.6	Majak M. FrO3
Krzykowski M. ThP3.3	Majchrzak D. TuP2.6, ThP2.3
Krzywda J.A. ThP3.2	Majewski J.A. TuP1.10, ThP3.7
Kuc A. WeP1.10	Maletinsky P. TuO2
Kucharek J. TuP1.7	Mandal P. WeO1
Kucharek J.K. WeP1.8	Mandal P.S. WeO1, WeO3
Kudelski A. TuP4.2	Marchewka M.M. WeP4.4
Kudrawiec R. ThO6	Marchwiany M. TuP1.4
Kuhn T. WeO8, FrO6	Marco L.De. WeO5
Kula P. MoP4.6, MoP4.7, WeO4, WeO5	Marie X. TuO3
Kulinowski K. WeP4.9	Martins R. MoI2
Kunstmann J. ThO2, ThO7	Mathew J.A. WeP2.6
Kupczyński M. MoP3.7, TuP3.4, ThP3.9	Matsuda Y. ThO3
Kurowska B. WeP2.8	Matuszewski M. MoO6, TuO6, TuO7, WeO4, WeO5
Kurpas M. WeP1.9	Maude D.K. WeP1.10
Kutrowska-Girzycka J. ThO6, ThP1.3, FrO3	Mazur R. MoP4.6, MoP4.7, WeO4, WeO5
Kwiatkowska E. MoP4.9	Mech W. FrO9
Kwiatkowski A. WeP4.1, ThP1.7	Meziani Y.M. MoO7
Lábár J. WeP2.5	Michałowski P.P. TuP2.6, WeP1.2
Lacinska E.M. FrI2	Mierzejewski J. ThP1.7
Lagoudakis P.G. WeO4	Mikhailov N.N. TuO4
LewandkóW R. MoP2.7	Mikhailovskii V.Yu. FrO5
Li J. TuO3	Mikulicz M. MoP1.3
Liang M. WeP1.10	Minikayev R. MoP3.5, WeP3.4, WeP4.1
Lienhart M. FrO6	Mirek R. TuO6, TuO7
Liew T.C.H. TuO7, WeO6	Mishra A. TuP3.7

Mishra S. MoP2.1, MoP2.4
 Molas M. FrO1
 Molas M.R. TuP1.2, WeO7, WeP1.3, WeP4.7, ThP1.5, FrI1
 Molenkamp L.W. WeO1
 Moll P.J. S1
 Morawiak P. MoP4.6, MoP4.7, WeO4, WeO5
 Morawiec K. TuO1
 Morpurgo A. S4
 Moszak K. TuP2.6, ThP2.3
 Mrowiński P. ThP1.3, FrO4, FrO7
 Muhammad Z. TuP3.5
 Müller K. FrO6
 Musiał A. MoP1.3, MoP1.4, MoP1.8, MoP1.9, FrO4
 Muszyński M. MoP4.6, TuP4.7
 Muziol G. ThO4, ThP2.5
 Muzioł G. ThP2.6, ThP2.7
 Myronov M. ThO6
 Nägele M. FrO6
 Nair V.G. ThP1.8
 Nguyen Minh Nguyenn. WeP3.7
 Nogajewski K. MoO2, WeO8, WeP1.6, ThP1.5
 Nomoto K. ThO5
 Nowakowski-Szkudlarek K. TuP2.3, ThO4, ThP2.5, ThP2.6, ThP2.7
 Nowicki P. TuP4.8
 Ogorzałek Z. MoP1.7, WeP3.4, WeP3.5, ThP1.7
 Oliwa P. MoP4.5, MoP4.7, WeO4
 Olkowska-Pucko K. TuP1.2, WeP1.3
 Olszewski W. TuP2.6, ThP2.3
 Olszowska N. MoP3.4, TuP3.5, TuP3.6, TuP3.8, WeP3.6
 Opala A. MoO6, TuO6, TuO7
 Oreszczuk K. MoO2, MoP1.7, TuP1.6, WeO9, WeP1.6, ThP1.5
 Orlowski B.A. WeP4.8
 Osiecki J. ThP2.3
 Ostrovskaya E.A. MoP4.8, WeO6
 Otón E. MoP4.6
 Otsuji T. MoO7
 Özdal T. MoP4.1
 Ozga M. MoP2.4, WeP2.4
 Pacuski W. MoO1, MoO2, MoO9, MoP1.6, MoP1.7, MoP4.10, TuO6, TuO7, TuP1.7, WeP1.6, WeP1.8, WeP3.5, WeP4.5, ThP1.7, FrO8
 Page R. ThO5
 Pakuła K. ThP1.1, ThP1.2
 Panico R. MoO6
 Paradowska K.M. WeP2.3
 Park K. TuP3.6
 Pasek W.K. MoP3.7
 Pashnev D. TuP4.6
 Pasternak I. MoO5, MoO8
 Paszkowicz W. MoP2.4
 Patel P.N. WeP4.3
 Patera M. ThP3.8
 Pavlov K. TuP1.1
 Pawlak M.P. TuP4.1
 Pawłowski J. TuP1.9
 Perlikowski I. MoP4.1
 Perlin P. ThO3
 Perwez W. TuP2.9
 Pfeiffer L.N. MoP4.8, WeO6
 Piecek W. MoP4.6, MoP4.7, WeO4, WeO5
 Pieczarka M. MoP4.8, TuO8, WeO6
 Pieniżek A. WeP2.2
 Piętak K. MoO4, TuP2.1
 Piętka B. MoP4.5, MoP4.6, MoP4.7, TuO6, TuO7, WeO4, WeO5
 Pietrzyk M.A. MoP2.2, MoP2.6, TuO1, WeP2.2
 Pilch M. FrO9
 Piotrowska S. MoP4.7
 Piotrowski P. FrO9
 Piskorski K. MoP4.4
 Piskorski M. FrI2
 Placzek-Popko E. WeP2.3
 Plochocka P. WeP1.10
 Plucinski L. WeI1
 Płachta J. MoP1.10, MoP1.5
 Podemski P. MoP1.9
 Polaczynski J. WeO2
 Polaczyński J. MoP3.5, TuP3.3, TuP4.4, WeP4.4
 Połczyńska K.E. MoO2, MoP1.6, MoP1.7, WeO8, WeP4.5, FrO8
 Popko E. MoP2.6
 Porada O. TuP2.7
 Potasz P. ThP3.9
 Potemski M. MoO2, TuP1.6, TuP1.8, WeO8, WeO9, WeP1.6, ThP1.5, FrO2
 Prem S. MoP3.2
 Prystawko P. MoO8, TuP2.2, TuP2.8, ThP2.1, ThP2.2
 Przewłoka A. MoO4, MoO8
 Przedziecka E. MoP2.1, MoP2.4, TuO1, WeP2.1, WeP2.2, WeP2.3, WeP2.6

Przybylinska H. TuP2.10
 Przybytek J. TuO4
 Pucicki D. ThP2.3
 Puźniak R. MoP2.9
 Quandt D. MoP1.4, MoP1.8
 Rącz A. WeP2.5
 Radecka M. WeP4.9
 Rader O. WeO3
 Rakhlin M.V. FrO5
 Rechcińska K. MoP4.7, WeO4
 Rechciński R. WeO3, WeP3.2
 Rehman A. TuP1.1
 Reissig Louisa. MoP4.2
 Reithmaier J.P. MoP1.3
 Reitzenstein S. MoP1.4, MoP1.8, FrO7
 Reszka A. MoP3.5, TuP2.9, TuP3.6, TuP4.5, WeP4.1
 Rice A. ThP3.5
 Robert C. TuO3
 Rodek A. MoO2, MoP1.7, TuP1.6, TuP1.8, WeO8,
 WeO9, WeP1.6
 Rodt S. MoP1.4, MoP1.8, FrO7
 Rogala M. FrI2
 Rogowicz E. ThO6
 Rogoża J. MoO5, WeP1.7
 Rosmus M. MoP3.4, TuP3.5, TuP3.8, WeP3.6
 Różański P. T. ThP3.8
 Rozbiegała E.B. MoO4, TuP2.1
 Rudniewski R. MoP4.3, TuP3.3, TuP3.5, WeP4.4
 Rumyantsev S. MoO8, TuP1.1, TuP2.8, ThP2.2
 Rybak M. ThP1.9
 Rzepkowski B. ThP3.9
 Sadecka K. TuP1.9, ThP1.6
 Sadowski J. MoO2, MoO9, MoP3.8, WeP3.5, ThP1.7
 Sai P. MoO8, TuP2.8, ThP2.2
 Sajkowski J.M. MoP2.1, MoP2.2, WeP2.2, WeP2.3,
 WeP2.6
 Sakaki A. ThO3
 Sakanas A. FrO4
 Sakowicz M. MoO8, TuP2.8, ThP2.2
 Saleem Y. TuP1.5
 Salvador-Sánchez J. MoO7
 Samadi S. WeP3.2
 Sánchez-Barriga J. WeO3
 Sankowska I. TuO1
 Sanvitto D. MoO6, TuO7, WeO5
 Sarwar M. WeP2.7
 Sawicka M. TuP2.3, ThP2.7
 Sawicki K. MoP4.10
 Sawicki M. TuP2.10, WeP3.6, WeP4.1, ThO1
 Schiavon D. ThO3
 Schifano R. WeP2.8
 Schmidt M. FrO7
 Schneider C. TuO8, ThP1.3, FrO10
 Schreyeck S. TuP4.4, WeO1
 Ściesiek M. MoP4.10
 Sedova I.V. TuP4.3, FrO5
 Seifert G. ThO7
 Sęk G. MoP1.3, MoP1.4, MoP1.8, MoP1.9
 Selskis A. ThP2.2
 Semenova E. FrO4
 Serafińczuk J. ThP2.3
 Seredyński B. MoO2, MoO9, TuO6, TuO7, WeP3.5,
 ThP1.7
 Shafiq A.S. TuP4.1
 Shamim Md.Kashif. MoP4.2
 Sharma Seema. MoP4.2
 Shields B. TuO2
 Shree S. TuO3
 Shubina T.V. FrO5
 Sidorchak P. WeP3.4
 Siekacz M. TuP2.3, ThO4, ThP2.5, ThP2.6, ThP2.7
 Simma M. WeO3
 Simon P. TuP3.7
 Singh Arpana. MoP4.2
 Singh Bahadur MoP3.6
 Sitek J. MoO5
 Sitnicka J. TuP3.6, TuP4.5
 Skapas M. ThP2.2
 Skierbiszewski C. TuP1.8, TuP2.3, ThO4, ThP2.5,
 ThP2.6, ThP2.7
 Skolasińska A. ThP1.4
 Skompska M. MoP4.9
 Skupiński P. TuP3.6, TuP4.5
 Sławinska J. ThP2.6
 Slobodeniuk A.O. ThP1.5, FrO2
 Slynko E.I. MoP3.1
 Slynko V.E. MoP3.1
 Sławińska J. TuP1.8
 Słowikowski M. TuP2.2, TuP2.8
 Smertenko P.S. WeP2.8
 Smirnov S. TuP1.1
 Smulko J. TuP1.1
 Śnieżek D. MoP4.3
 Snoke D.W. MoP4.8, WeO6

Sobanska M. TuP2.9
 Sobczak K. TuP3.6, TuP4.5
 Sobol T. TuP3.1
 Sochacki T. TuP2.10
 Sokołowski M. TuP1.4
 Sorokin S.V. TuP4.3, FrO5
 Spisak B.J. WeP4.9
 Spitzer N.S. TuP4.1
 Springholz G. WeO2, WeO3
 Srocka N. MoP1.4, MoP1.8, FrO7
 Stachowicz M. MoP2.2, WeP2.2, WeP2.6
 Stanczyk S. ThO3
 Stawicki P. TuO6
 Stefaniuk T. WeO5
 Steger M. MoP4.8, WeO6
 Stelmaszczyk K. TuP2.8
 Stępniewski R. MoO1, MoO3, MoO5, TuP1.3, WeP1.1, Toropov A.A. FrO5
 WeP1.7, ThP1.1, ThP1.2, FrI2
 Stier A.V. TuO3
 Stonio B. TuP1.1
 Story T. MoP3.5, TuO5, TuP4.4, WeP3.6, WeP4.1,
 ThO1
 Strak P. TuO1
 Strittmatter A. MoP1.4, MoP1.8
 Strupiński W. MoO5
 Stühler R. FrO10
 Subačius L. ThP2.1
 Suchomel H. TuO8
 Suffczyński J. MoP4.10, TuO6, TuO7, WeP4.6
 Sukach A. TuP2.7
 Sulich A. MoP2.4
 Surrente A. WeP1.10
 Suski T. ThO3
 Sutter E. ThI4
 Sutter P. ThI4
 Sybilski P. MoP2.1, TuO1, WeP2.1, WeP2.3, WeP2.4
 Syperek M. MoP4.8, TuO8, ThO6, ThP1.3, FrO10, FrO4
 Szade J. TuP3.1
 Szałowski K. WeP1.5
 Szczytko J. MoP4.5, MoP4.6, MoP4.7, TuO6, TuO7,
 WeI2, WeO4, WeO5
 Szofa M. TuO4, TuP2.2, TuP4.8
 Szot M. MoP3.5, TuP4.4
 Sztenkiel D. TuP2.10, TuP2.5
 Szymon R. MoP2.6, TuP2.9
 Szymura M. MoP1.5, WeP4.2
 Tajwar Zarreen. WeP2.9
 Taliashvili T. MoP3.5
 Taniguchi T. MoI1, MoO2, MoO7, TuO3, TuP1.2,
 TuP1.6, TuP1.8, WeO8, WeO9, WeP1.6,
 ThP1.3, ThP1.5, FrO1, FrO2
 Tarasenko S.A. ThP3.10
 Tarkowski T. TuP4.8
 Tatarczak P. MoO3, TuP1.3
 Taube A. MoP4.4
 Teppe F. TuO4
 Tetyorkin V. TuP2.7
 Tjeertes D. ThP3.5
 Tkachenko L. MoO5
 Tkachuk A. TuP2.7
 Tokarczyk M. MoO1, MoO3, MoP4.9, TuP1.3, TuP3.6,
 WeP1.1, WeP3.5, ThP1.1
 Tongay S. ThP1.3
 Trif M. MoP3.2, TuP3.7
 Tronowicz B. TuP1.7
 Truscott A.G. MoP4.8, WeO6
 Tuomisto F. TuI1
 Turowski B. TuP3.3, TuP3.5, WeO2, WeP3.6
 Turski H. TuP2.3, ThO4, ThP2.5, ThP2.7
 Tworzydło J. TuP3.2
 Tyszka K. TuO6, TuO7
 Udovyt'ska R. FrI2
 Ulanski J. FrI2
 Ulyashin Alexander. WeP2.9
 Umansky V. TuP4.8
 Ungier P. MoP4.3
 Urbanowicz A. TuP4.6
 Urbaszek B. TuO3
 Vaclavkova D. FrO2
 van Deurzen L. ThO5
 Varykhalov A. WeO2, WeO3
 Velázquez-Pérez J.E. MoO7
 Verstijnen T.J.F. ThP3.5
 Volnianska O. MoP2.8
 Volobuev V.V. TuP3.3, TuP3.5, WeO2, WeO3, WeP3.6,
 WeP4.4
 von Helversen M. FrO7
 Vyborny K. ThI1
 Wadge A.S. MoP3.4
 Wahab Qamar.ul. WeP2.9
 Wania Rodrigues A. TuP1.5, TuP1.9
 Warburton R.J. TuO2
 Wasik D. WeP3.4, ThP1.7

Wasilewski Z.R. MoI3	Wróbel J. MoP3.8, MoP4.3, TuP4.8
Wasiluk M. MoP1.3	Wroński P.A. MoP1.9
Watanabe K. MoO2, MoO7, TuO3, TuP1.2, TuP1.6, TuP1.8, WeO8, WeO9, WeP1.6, ThP1.3, ThP1.5, FrO1, FrO2	Wurdack M. WeO6
Weiß M. FrO6	Wyborski P. MoP1.9, FrO10
West K. MoP4.8, WeO6	Wysmołek A. MoO1, MoO3, MoO4, MoO5, TuP1.3, WeP1.1, WeP1.2, WeP1.7, ThP1.1, ThP1.2, FrI2
Wieck A.W. TuP4.1	Wysokinski M. MoP3.2
Wierzbicka A. MoP2.2, MoP2.6, TuO1, TuP2.9, WeP2.1, WeP2.3	Wzorek M. MoP4.4
Wigger D. WeO8, FrO6	Xing H.G. ThO5
Wincukiewicz A. MoP4.9, WeO5	Yahniuk I. TuO4, TuP4.9
Winiarski M.J. ThP3.6	Yakimova Rositsa. WeP2.9
Winnerlein M. WeO1	Yavorskiy D. TuO4, TuP2.2, TuP4.8
Wiśniewski A. MoP3.4, WeP3.1	Ye J. WeP1.10
Wiśniewski P. TuP2.10	Yu Z.Y. WeP4.4
Witkowski B.S. WeP2.1, WeP2.4, WeP2.7	Yurgens V. TuO2
Witowski A.M. MoP3.5, TuP4.4	Zajkowska W. MoO9, WeP2.8, WeP3.5
Wójcicka A. MoP4.4, WeP2.5	Żak M. ThP2.5, ThP2.6, ThP2.7
Wojciechowski T. MoP4.3, TuP3.5, WeO2, WeP3.1, WeP3.6	Zaleszczyk W. MoP4.3, TuP3.5
Wojciechowski T.W. WeP4.4	Zaleszczyk W.Z. WeP4.4
Wójcik A. WeP1.2	Zardo I. TuO2
Wójcik M. TuP4.7	Zawadzka N. WeO7, FrO1
Wojnar P. MoP1.10, MoP1.5, TuP4.7, WeP4.2	Zdrojek M. MoO5
Wojnar T. MoP1.10	Zeller P. MoP2.8
Wójs A. ThP1.6, ThP3.9	Zhang N. WeP1.10
Wojtkiewicz J. FrO9	Zhydachevskyy Y. WeP2.6
Wojtowitz T. MoP1.10, MoP1.5, MoP3.5, MoP4.3, TuP3.3, TuP3.5, TuP4.7, WeO2, WeP3.1, WeP3.4, WeP3.6, WeP4.2	Zięba E. ThP1.3
Wojtowitz T.W. WeP4.4	Zięba M. MoP3.5, WeP3.6
Wolny P. TuP2.3, ThP2.7	Ziegler J. WeP1.10
Wołkanowicz W. MoP3.5, WeP3.4	Zielińska A. MoP1.4
Wołoś A. TuP3.6, TuP4.5	Zieliński M. S2, ThP3.8
Wosiński T. MoP3.8	Zielony E. MoP2.6, MoP4.1, TuP2.9
Woźniak T. WeO7, WeP4.7, ThO7	Zinkiewicz Ł. MoP1.7, TuP1.8
Wozniak W. MoP2.4	Zinkiewicz M. ThP1.5
	Złotnik S. MoO4, TuP2.1
	Zuber J.A. TuO2
	Zytkiewicz Z.R. TuP2.9